Diffusion-Reaction Modeling, Non-linear Dynamics, Feedback, Bifurcation and Chaotic Behavior of the Acetylcholine Neurocycle and Their Relation to Alzheimer's and Parkinson's Diseases

by

Ibrahim Hassan Mustafa

A thesis
presented to the University of Waterloo
in fulfillment of the
thesis requirement for the degree of
Doctor of Philosophy
in
Chemical Engineering

Waterloo, Ontario, Canada, 2010

Author's Declaration

I hereby declare that I am the sole author of this thesis. This is a true copy of the thesis, including any required final revisions, as accepted by my examiners.

I understand that my thesis may be made electronically available to the public.

Abstract

The disturbances and abnormalities occurring in the components of the Acetylcholine (ACh) neurocycle are considered one of the main features of cholinergic sicknesses like Parkinson's and Alzheimer's diseases. A fundamental understanding of the ACh neurocycle is therefore very critical in order to design drugs that keep the ACh concentrations in the normal physiological range.

In this dissertation, a novel two-enzyme-two-compartment model is proposed in order to explore the bifurcation, dynamics, and chaotic characteristics of the ACh neurocycle. The model takes into consideration the physiological events of the choline uptake into the presynaptic neuron and the ACh release in the postsynaptic neuron. In order to approach more realistic behavior, two complete kinetic mechanisms for enzymatic processes pH-dependent are built: the first mechanism is for the hydrolysis reaction catalyzed by the acetylcholinesterase (AChE) and the other is for the synthesis reaction catalyzed by the cholineacetyltransferase (ChAT). The effects of hydrogen ion feed concentrations, AChE activity, ChAT activity, feed ACh concentrations, feed choline concentrations, and feed acetate concentrations as bifurcation parameters, on the system performance are studied. It was found that hydrogen ions play an important role, where they create potential differences through the plasma membranes. The concentrations of ACh, choline and acetate in compartments 1 and 2 are affected by the activity of AChE through a certain range of their concentrations, where the activity of AChE is inhibited completely after reaching certain values. A detailed bifurcation analysis over a wide range of parameters is carried out in order to uncover some important features of the system, such as hysteresis, multiplicity, Hopf bifurcation, period doubling, chaotic characteristics, and other complex dynamics.

The effects of the feed choline concentrations and the feed acetate concentrations as bifurcation parameters are studied in this dissertation. It is found that the feed choline concentrations play an important role and have a direct effect on the ACh neurocycle through a certain important range of the parameters. However, the feed acetate concentrations have less effect. It is concluded from the results that the feed choline is a more important factor than the feed acetate in ACh processes.

The effects of ChAT activity and the choline recycle ratio as bifurcation parameters, on the system performance are investigated. It was found that as the ChAT activity increases, ACh concentrations in compartments 1 and 2 increase continuously. The effect of the choline recycle ratio shows that choline reuptake plays a very critical role in the synthesis of ACh in compartment 1, where it supplies the choline as a substrate for the synthesis reaction by ChAT. The concentrations of ACh, choline and acetate in compartments 1 and 2 are affected by the choline recycle ratio through a certain range

of the choline recycle ratio; then, they become constant as the choline recycle ratio increases further. It is concluded from our results that choline uptake is the rate limiting step in the ACh processes in both compartments in comparison to ChAT activity. Based on partial dissociation of the acetic acid in compartments 1, and 2 of the ACh cholinergic system, the two-parameter continuation technique has been applied to investigate the pH range to be closer to physiological ranges of pH values. In addition, static/dynamic solutions of the ACh cholinergic neurocycle system based on feed choline concentration as the main bifurcation parameter in both compartments have been investigated.

The findings of the above studies are related to the real phenomena occurring in the neurons, like periodic stimulation of neural cells and non-regular functioning of ACh receptors. It was found that ACh, choline, acetate, and pH exist inside the physiological range associated with taking into consideration the partial dissociation of the acetic acid. The disturbances and irregularities (chaotic attractors) occurring in the ACh cholinergic system may be good indications of cholinergic diseases such as Alzheimer's and Parkinson's diseases. The results have been compared to the results of physiological experiments and other published models. As there is strong evidence that cholinergic brain diseases like Alzheimer's disease and Parkinson's disease are related to the concentration of ACh, the present findings are useful for uncovering some of the characteristics of these diseases and encouraging more physiological research.

Acknowledgements

By the name of Allah, The Most Gracious, The Most Merciful ... All praise and thanks is due to Allah. He is the one who made this work possible. He is the one who gave me the strength and patience to accomplish this work.

I would like to extend my thanks and appreciation to my supervisors Profs Elkamel and Chen for helping me not to get lost during the development of this project. Both of them provided a motivating, enthusiastic, and critical atmosphere during the many discussions we had. It was a great pleasure to me to conduct this project under their supervision. I would like to express my thanks and gratitude to Prof Elnasahie and Prof Ibrahim for their valuable advice, guidance and encouragement throughout the project. I also would like to express my thanks to the Egyptian government for financial support and to the School of Graduate Studies and the Department of Chemical Engineering in the University of Waterloo. Finally, I hope to extend my heartfelt gratitude to my parents, my wife, my brothers and my sisters.

Table of Contents

List of Figures

Chapter (2):

Chapter (3):

Chapter (4):

Chapter (5):

Chapter (6):

Appendices:

List of Tables

Notations

$[H^+]$	hydrogen ions concentration (kmol/m^3
$[OH^-]$	hydroxyle ions concentration (kmol/m^3)
$[S_1]$	acetylcholine concentration (kmol/m^3)
$[S_2]$	choline concentration (kmol/m^3)
$[S_3]$	acetyl CoA concentration (kmol/m^3)
S_N	substrate N (catalyzed by enzyme N)
$\lfloor a \rfloor$	acetate concentration (kmol/m^3)
$[AC]$	Acetic acid concentration (kmol/m^3)
$\overline{AChE}$	concentration of acetylcholinesterase enzyme in compartment 2 (kg enzyme/m^3)
$\overline{CoA}$	concentration of coenzyme A in compartment 1 (kg enzyme/m^3)
$\overline{ChAT}$	concentration of cholineacetyltransferase in compartment 1 (kg enzyme/m^3)
$\overline{ACoA\ synthase}$	concentration of Acetyl CoA Synthase in compartment 1 (kg enzyme/m^3
K_{s1}, K_{h1}	kinetic constants for the cholineacetyltransferase catalyzed reaction (kmol/m^3)
K_{s2}, K_h	kinetic constants for the coenzyme A catalyzed reaction (kmol/m^3)
K_{s3}, K_{i3}, K_{hh3}	kinetic constants for the acetylcholinesterase catalyzed reaction (kmol/m^3)
K_W	equilibrium constant for water (kmol^2/m^6)
α'_{H^+}	membrane permeability for hydrogen ions (m/s)
α'_{OH^-}	membrane permeability for hydroxyl ions (m/s)
α'_{S_1}	membrane permeability for acetylcholine (m/s)
α'_{S_2}	membrane permeability for choline (m/s)
α'_{S_3}	membrane permeability for acetyl CoA (m/s)
α'_A	membrane permeability for acetate (m/s)
α'_{AC}	membrane permeability for acetic acid (m/s)
A_M	area of membrane separating compartments 1 and 2 (m^2)
q	volumetric flow rate (m^3/s)

$R_{W(j)}$	rate of water formation in compartment j (kmol/m^{3}s)
$R_{(j)}$	rate of reaction in compartment j (kmol/m^{3}s)
R	recycle flow rate ratio
$V_{(j)}$	volume of compartment j (m^3)
E_N	enzyme N
P_N	reaction product N (produced by S_N catalyzed by (E_N)
V_R	V_1/V_2

List of Abbreviations

AChE	Acetylcholinesterase
ChAT	Cholineacetyltransferase
CoA	Coenzyme A
ACh	Acetylcholine
CSTR	continuous stirred tank reactor
HB	Hopf bifurcation
SB	Static bifurcation
PLP	Periodic limit point
PD	period doubling
P_i	periodicity i of the periodic orbit
TRB	Torus bifurcation

Subscripts

1	Compartment 1
2	Compartment 2
f	Feed condition

Legend for Figures

———	stable steady state branch
---------	unstable steady state branch
●●●●●●●	stable periodic branch
ooooooo	unstable periodic branch

Chapter 1
Introduction

1.1 Background

Acetylcholine (ACh) is the first neurotransmitter that was mentioned as early as 1921 (Loewi 1921). It plays a central role in fundamental processes such as learning, memory, sleep (Bartus & Beer 1982, Aigner & Mishkin 1986) and muscle contraction in mammals [Combes et al.(2003), Jones et al., (2002)]. Understanding of the mechanisms for ACh regulation would provide some fundamental knowledge on the regulatory characteristics of the transmitter in the molecular processes of the chemical transmission. The regulatory mechanisms are obviously based on regulation of the enzymatic reactions for synthesis and degradation of transmitters.

The electrochemical transmission of nervous signals is usually accompanied by the metabolic regulation of neurotransmitters at the synapse (Berl et al., 1975; Zimmermann, 1988). In order to keep the transmission activity, the biosynthesis of the ACh in the nerve endings and its removal from the synaptic cleft by hydrolysis, uptake and diffusion processes should be regulated in parallel with the release and processing. In order to supply enough and balanced products of metabolic pathways to resist different disturbances in the cellular metabolism, feedback control mechanisms is generally functioned (Stadtman 1970), and these control mechanisms operate basically for intimate regulations of the metabolites fluxes (Kacser and Burns 1973).

Neurotransmitters generally are exposed to important disturbances due to their release and uptake of end products. Therefore, the feedback control mechanism is essentially for adjusting the metabolic systems. Since the electrochemical transmission of the ACh is known as a dynamic phenomenon and the involved fluxes of metabolites can be recognized as well, the feedback control mechanisms and the controlling roles of the fluxes in the mechanisms can be explained clearly based on the dynamic analysis of the responses of the metabolic systems to the transmitter release.

The ACh neurocycle system consists of two compartments separated by a permeable membrane. The presynaptic neuron ending is the first compartment in which the biosynthesis reaction of ACh occurs catalyzed by the enzyme of cholineacetyltransferase (ChAT) by the acetyl-CoA and choline substrates. In the synaptic cleft as the other compartment, the ACh molecules are released from the first compartment to interact with the ACh receptor causing the signal transmission and a fast hydrolysis reaction into choline and acetate occurs and is catalyzed by the enzyme of

acetylcholinesterase (AChE). Each compartment is open with relevant influxes and effluxes. The reaction products are reused in other metabolic reactions where CoA is utilized for production of Acetyl-CoA and choline is reuptaken from the synaptic cleft to the presynaptic neuron for resynthesis of ACh. The synthesis reaction occurs according to the following equation:

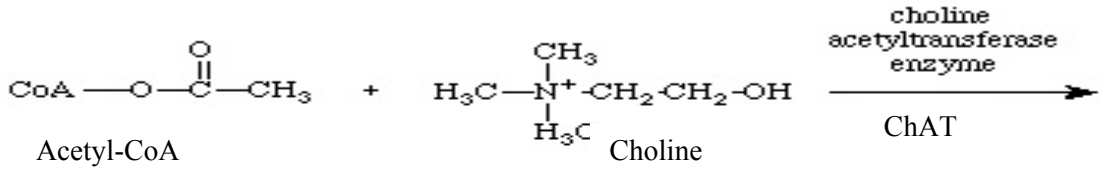

Acetyl-CoA Choline

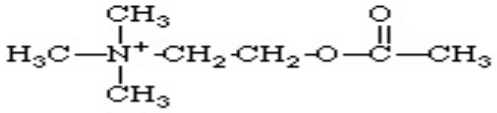

ACh

Since the behavior of neurotransmitter mechanisms represents a great challenge for understanding cholinergic diseases such as Parkinson's and Alzheimer's diseases, it is very important to understand the cholinergic system behavior. In this dissertation, mathematical tools such as bifurcation analysis, well established nonlinear dynamics, and computer simulation are applied for modeling and prediction of complex behavior of the ACh neurocycle behavior.

The method of bifurcation analysis and computer simulation are now established as an effective procedure for dynamic analysis and have been applied to obtain much knowledge of the dynamic behavior of metabolic pathways [Garfinkel (1975); Hayashi and Sakamoto (1986)]. Based on the regulating kinetic mechanisms of the enzymatic reactions, mathematical models can be established, and then the entire time course under different initial conditions and system environments and various flow rates of metabolites can be employed in terms of the change of system parameters by numerically integrating the rate equations [Sakamoto (1986) and Santos et al., (2006]].

Bifurcation theory is a mathematical discipline that deals with nonlinear phenomena. It investigates the stability and dynamics in non-linear systems. In bifurcation investigation a branch of solutions can be obtained by varying one parameter of the system and then the stability of the solution changes can be obtained. In the ACh cholinergic systems, numerical bifurcation analysis is well established with several software packages available like MATCONT [Dhooge et al., (2003)] and AUTO [Doedel et al., (2002)].

According to Chaos theory, chaos can be defined as the disorder of a system where it opposes relevant rules; this definition is consistent with the concept of instability of dynamical systems

discovered primarily by the French physicist: Henri Poincare in the early 20th century. Chaos theory points to an apparent unpredictability. Edward Lorenz found that chaotic systems are very sensitive conditions and could perform the first experiment related to chaotic systems at 1960 [Abarbanet et al., (1996)]. Chaos theory started with some of ideas related to irregularities in the universe such as arrhythmic beats of a human heart and fluid turbulence, then it has developed with wide ideas and can be described by the term complexity as shown by Gleick [Abarbanet et al., (1996); Sprott et al., (1993)].

1.2 Scope and objectives

This dissertation is concerned with the dynamic behavior and the regulatory mechanism in ACh neurocycle system and the functioning of chemical transmission. Some dynamic aspects and kinetic regulatory mechanisms in the ACh neurocycle at the synapse are studied. In this dissertation a mathematical model is constructed to represent the fundamental processes in chemical transmission and dynamic analysis bifurcation and computer simulation are performed to reveal the dynamic aspects of regulation of ACh level in the presynaptic and postsynaptic terminals for signal transmission and the regulatory function of ChAT and AChE enzymes.

The dynamic behavior of this ACh neurocycle system during nervous signal transmission is first examined for release of various amounts of ACh under the condition of constant influx rates of the substrates. A feedback mechanism for flux control is thus applied as a regulatory control action for adjusting ACh synthesis and hydrolysis and dynamic analysis is performed to explain characteristics of the ACh regulations mechanisms. The scope of the dissertation will cover the following stages:

- The first stage is building two complete kinetic mechanisms for enzymatic processes hydrogen proton (which is relevant to pH) dependent and substrates dependent: The first mechanism is for synthesis of ACh in the presynaptic terminal from choline and acetyl Co-A catalyzed by the enzyme ChAT and the other is for hydrolysis of ACh in the postsynaptic cleft into choline and acetate by the enzyme AChE. These mechanisms are based on understanding the nature of interactions between both compartments and lead to deriving reasonable rate equations and describe synthesis and hydrolysis reactions accurately. In general, in this dissertation, the synthesis and hydrolysis of ACh are analyzed on the level of single vesicles, rather than at that of the whole nervous system.

- The second stage is building the dynamic process models where a complete neurocycle of the ACh is simulated as a simplified feedback two enzyme/two-compartment system. Each compartment is described as a constant flow, constant volume, isothermal, continuous stirred tank reactor (CSTR), and constant choline recycle ratio. The presynaptic and postsynaptic cells are represented by these two compartments separated by a permeable membrane assuming that all the events are homogeneous in all vesicles, and using the proper dimensionless state variables and parameters. Using dynamic mole balances for the chemical species involved in the enzymatic neurocycle of the neurotransmitter we obtain a set of differential equations to describe the system. Nonlinearity of this set of highly non-linear balance equations gives us preliminary insight into the bifurcation and chaotic behavior of this complex biological system. At high product concentration product inhibition is not considered because of the assumption of being compartments 1 and 2 as a CSTR, so each product will transport through both compartments [Athel et al., (2001)].
- The third stage is studying bifurcation behavior using the feed parameters, enzyme activities and choline recycle ratio as bifurcation parameters and dynamics simulations are carried out for different parameter values. Therefore, many dynamic characteristics are obtained by studying the Poincare map and monitoring the periodic and chaotic behaviors.
- The fourth stage is to use the two-parameter continuation technique based on partial dissociation of acetic acid in addition to a well established kinetic scheme and appropriate kinetic data to investigate the effect of pH transients on the dynamic and static solutions of the ACh cholinergic neurocycle system based on feed choline concentration as the main bifurcation parameter.

The main objectives of this dissertation are as follows:

1) Obtaining reasonable kinetic rate equations by building two complete kinetic mechanisms for enzymatic processes pH-dependent for ACh: The first is for the ACh synthesis in the presynaptic terminal from choline and acetyl Co-A by the enzyme ChAT and the other is for the hydrolysis of ACh in the postsynaptic cleft into choline and acetate by the enzyme AChE.
2) Describing the metabolic processes of the ACh neurocycle by building the dynamic process models considering the physiological phenomena such as the choline uptake from the synaptic cleft to the presynaptic neuron where a complete neurocycle of the ACh as a neurotransmitter is simulated as a simplified feedback two enzyme/two-compartment system.

3) Investigating the bifurcation behavior using the feed parameters such as feed ACh, feed choline, feed acetyl Co-A and feed hydrogen ions in addition to ChAT activity and AChE activity enzymes and choline recycle ratio as bifurcation parameters and performing dynamics simulations at different parameter values and obtaining dynamic characteristics by studying the Poincare maps and monitoring the periodic and chaotic behaviors and studying the interaction between these findings and Alzheimer's and Parkinson's diseases.
4) Studying the dynamical behavior and investigating the parameters and initial conditions values which achieve point, periodic and chaotic attractors in addition to estimating the routes to fully developed chaos.
5) Investigating the rate limiting step and estimating the most important factors in the ACh processes from the parametric study.
6) Investigating the effect of partial dissociation of acetic acid using a well established kinetic scheme and kinetic data on the dynamic and static solutions of the ACh cholinergic neurocycle system based on feed choline concentration as the main bifurcation parameter.

1.3 Thesis Structure

The thesis is composed of 7 chapters. The introductory chapter contains a brief background of the ACh processes, scope and objectives of the research.

Chapter 2 presents two kinetic mechanisms: the first is for the synthesis reaction catalyzed by ChAT and the other is for the hydrolysis reaction catalyzed by AChE through non-linear feedback model. Chapter 2 studies the effect of hydrogen ion feed concentrations, AChE activity, and ACh feed concentrations, as bifurcation parameters, on the system performance. Chapter 3 demonstrates how the substrates of feed choline concentrations and feed acetate concentrations, as bifurcation parameters affect on ACh neurocycle and which of them is the rate limiting factor. Chapter 3 covers the model prediction for the effect of different feed parameters on dynamic behaviors and the different attractors in both compartments. Chapter 4 explains the effect of ChAT activity and choline recycle ratio on the performance of ACh neurocycle and it answers with Chapter 5 the question what the rate limiting step in ACh processes is and what their interaction with Alzheimer's and Parkinson's diseases is. In Chapter 5, we investigate the application of two parameters continuation method on bifurcation for ACh neurocycle

considering partial dissociation of acetic acid based on feed choline concentration as the main bifurcation parameter. Chapter 6 presents a description of the kinetic and parameter constants used in the thesis. In addition, a sensitive analysis of the most important parameters used in theses is undertaken in Chapter 6. Chapter 7 highlights summary, conclusions, and contributions of the thesis and suggestions for future work. Chapters 2, 3, 4 and 5 are arranged in publication format, each with its individual abstract, introduction, techniques, results and discussion as well as conclusion.

Chapter 2

Non-Linear Feedback Modeling and Bifurcation of the Acetylcholine Neurocycle and its Relation to Alzheimer's and Parkinson's Diseases

This chapter is based on the paper published (Mustafa et al., (2009a). In this chapter two-enzyme-two-compartment model is proposed in order to explore the bifurcation, dynamics, and chaotic characteristics of the acetylcholine (ACh) neurocycle. The model takes into consideration the physiological events of the choline uptake into the presynaptic neuron and choline release in the postsynaptic neuron. The effects of hydrogen ion feed concentrations, acetylcholinesterase (AChE) activity, and feed ACh concentrations, as bifurcation parameters, on the system performance are studied. It is found that hydrogen ions play an important role, where they create potential differences through the plasma membranes. The concentrations of ACh, choline and acetate were affected to be affected by the activity of AChE through a certain range of their concentrations, where the activity of AChE was inhibited completely after reaching certain values. A detailed bifurcation analysis over a wide range of parameters is carried out in order to uncover some important features of the system, such as hysteresis, multiplicity, Hopf bifurcation, period doubling, chaotic characteristics, and other complex dynamics. These findings are related to the real phenomena occurring in the neurons, like periodic stimulation of neural cells and non-regular functioning of ACh receptors. The results of this model are compared to the results of physiological experiments and other published models. As there is strong evidence that cholinergic brain diseases like Alzheimer's disease (AD) and Parkinson's disease are related to the concentration of ACh, the present findings are useful for uncovering some of the characteristics of these diseases and encouraging more physiological research.

Keywords: Bifurcation, Acetylcholinesterase, Cholineacetyltransferase, Acetylcholine, Choline, Acetate, Neurocycle, Hydrogen ions, Parkinson's disease, Alzheimer's disease, Dynamic behavior, Chaos.

2.1 Introduction

Acetylcholine (ACh) serves as the transmitter of nerve impulses at cholinergic synapses. In humans and homoeothermic animals, ACh influences synaptic transmission of neuromuscular junction from motor nerves to skeletal muscles, from preganglionic parasympathetic and sympathetic

fibers to neurons in the autonomic ganglia. ACh plays a vital role in the memory excitations and such vital functions such as learning, thinking, sleep and cognition. It is released from the presynaptic neurons in various concentrations. After ACh is released from the presynaptic neuron, it is received by ACh cholinergic receptors (AChr), located in the postsynaptic membrane, to induce chemical and electrical signals. Consequences of events are resulted leading to inhibition and excitation of postganglionic cells [Quinn et al., 1995, Tucek 1978]. There are two substrates required for the biosynthesis of ACh: choline and acetyl coenzyme A (acetyl-CoA). There are two enzymes: the first one is the enzyme choline acetyltransferase (ChAT) which catalyzes the biosynthesis of ACh in the presynaptic neurons; the other is the enzyme acetylcholinesterase (AChE) which catalyzes the hydrolysis of ACh in the synaptic cleft.

It is clear that the presynaptic neurons require three substances: ChAT, acetyl-CoA and choline. Acetyl-CoA is the only substance which is synthesized directly in the presynaptic terminals. ChAT is supplied from the cell bodies of cholinergic neurons by the mechanism of axonal transport (Tucek 1978). However, choline is the only product which is synthesized outside of the presynaptic neurons. It is supplied from the extracellular fluid and degradation of ACh (Tucek 1978).

As shown in Figure (2-1), a complete neurocycle of ACh constitutes a coupled two-enzyme system with the following two simultaneous events (Guyton and Hall, 2000): Firstly, in the presynaptic neuron, ChAT catalyzes the synthesis reaction from choline and acetyl CoA substrates, then ACh is stored in the vesicles which transport through the cytoplasm of the neuron to be fused with the presynaptic membranes to give the opportunity for ACh release in the synaptic cleft (Guyton and Hall, 2000; Tucek, 1978). Secondly, as soon as ACh has been received by the postsynaptic receptors and finished its excitation job, the hydrolysis reactions catalyzed by the acetyl cholinesterase (AChE) to form choline and acetic acid starts (Tucek, 1985).

Because choline cannot be synthesized inside brain, brain depends on other resources for getting choline. There are two sources for choline in the fluid existing in the environment outside neurons inside the brain: the first one is the free choline of the blood plasma and the second one is the brain cells, where it has been released from choline containing compounds (Tucek 1985).

Tucek (1978) explained the fraction of free choline in the plasma required for the biosynthesis of ACh in the brain. This fraction is estimated based on species where ACh is synthesized. For instances, in rats, free choline represents 12%, in rabbits 50 %, and 80 % in mice (Tucek 1978). Choline produced in synaptic gaps by the hydrolysis of ACh is re-utilized for the synthesis of ACh in

presynaptic nerve endings (Tucek 1978). Therefore, choline recycled plays an important role in the synthesis of ACh.

Because hydrogen protons are released in the enzymatic reactions, the pH is declined. Koch (1986) showed that because the density of the negative ion charges in the membrane is low, the pH becomes lower. Friboulet et al., 1981 illustrated that once ACh neurotransmitter compounds are thrown in a certain concentration inside a side of the synthesized AChE membrane, an electric potential difference is appeared.

Friboulet et al., (1981) showed that a hysteresis and multiplicity behavior of stationary action potential is appeared since the enzyme function is influenced by varying substrate concentrations. Furthermore, the appeared hysteresis behavior is developed for a certain range of parameters due to the hydrogen protons production which will cause itself an auto- catalytic influence in addition to the presence of diffusion effects (Shen and Larter, 1994; Friboulet et al., 1981).

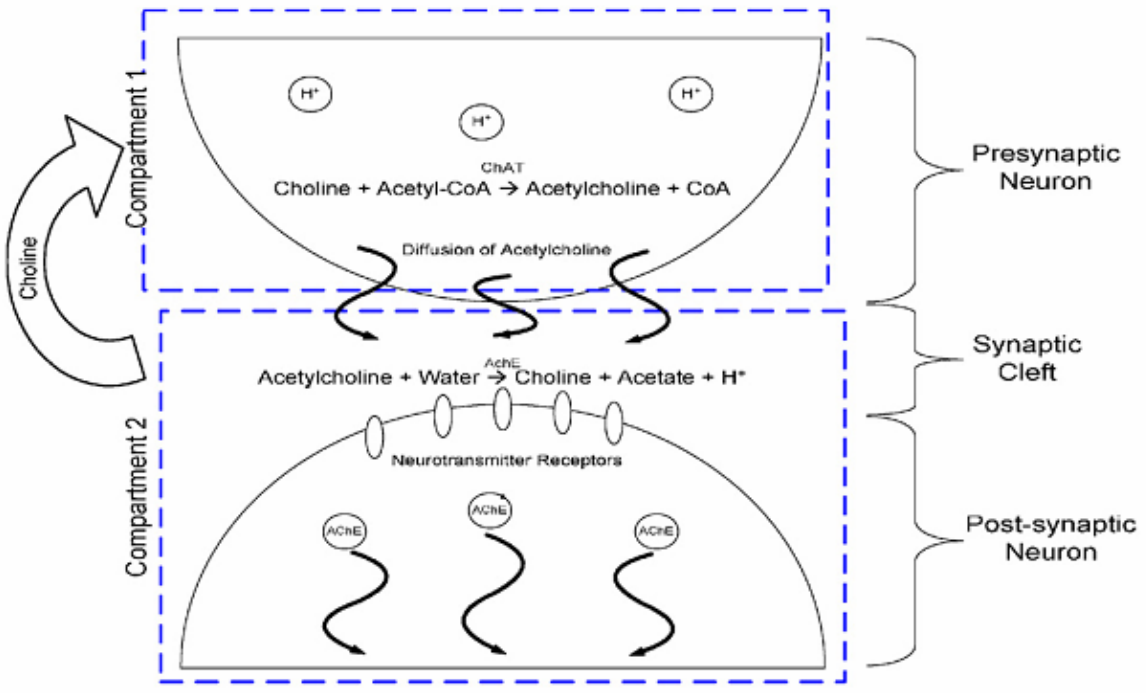

Figure 2- 1: Schematic of synaptic neurons and cleft

Elnashaie et al. (1995a), and Ibrahim and Elnashaie (1997) investigated the neurocycle of the ACh utilizing a two-compartment model with AChE as the only enzyme. Complex static and dynamic behaviors including bifurcation, instability, chaos and hyperchaos have been estimated. Mahecha-

Botero et al. (2004) investigated a complete but simplified neurocycle for the ACh as a neurotransmitter in an AChE/ChAT system and found that complex dynamic bifurcations, hysteresis, multiplicity, period doubling and period halving, as well as period adding and period subtracting dominated the dynamics of the system. Garhyan et al., (2006) presented a building of a diffusion-reaction model utilizing kinetic data to simulate the in vivo behavior of AChE and ChAT of the cholinergic ACh system to explore the bifurcation and chaotic behavior of this enzyme system simulating the ACh neurocycle in the brain.

In this chapter, two kinetic mechanisms are proposed: one is for the synthesis of ACh by the enzyme ChAT and the other is for the hydrolysis of ACh by the enzyme AChE. The mathematical expressions for both reactions are derived to obtain reasonable rate equations. These models try to analyze the synthesis and hydrolysis of ACh at the level of a single vesicle, rather than the whole nervous system. Consequently, the problems of ACh turnover such as action potential problems, and interaction between ACh and postsynaptic receptors in the brain have not been included in the present investigation. Nevertheless many of the dynamic phenomena discovered by Holden and Fan (1992a; 1992b; 1992c) and Fan and Holden (1993) using the three-dimensional non-phenomenological action potential model are also obtained using the present phenomenological model.

In this chapter we employ novel diffusion-reaction models but improve upon previous investigations by Elnashaie and coworkers (Elnashaie et al., 1995, Mahecha- Botero et al., 2004, Garhyan et al., 2006). We build novel kinetic mechanisms to get more reasonable and precise kinetic synthesis and hydrolysis rate equations by considering realistic kinetic schemes. The model is built based on new considerations such as ChAT synthesis and AChE hydrolysis reactions in the first compartment and other physiological considerations such as the recycle effects of choline from the synaptic cleft to the presynaptic neurons.

2.2 Formulation of the diffusion-reaction two-enzyme /two compartment model

Figure 2.1 shows as simplified manner describing the diffusion- reaction two-enzyme two-compartment system of the ACh cholinergic neurocycle. Figure 2.2 clarifies the two compartments of ChAT/AChE system. The first compartment represents the presynaptic terminal, and the second compartment represents the synaptic cleft and the postsynaptic neuron. Every compartment is assumed to be a continuous stirred tank reactor (CSTR), isothermal, constant volume, constant flow,

and the two compartments are divided by a permeable membrane. The ionization of the acetic acid is assumed to be completely in order to simplify the solution of the model. All events and reactions are supposed to be in homogenous systems. All state variables and parameters are described in the dimensionless form. All assumptions can be described in details as follows:

Model Assumptions:

In this section, we list all assumptions used in the work. All hypotheses and assumptions are clarified and the reasoning behind them is justified:

1) Compartment 1 represents the presynaptic terminal neuron where ACh is synthesized from choline and acetyl CoA as substrates and catalyzed by the enzyme ChAT. However, compartment 2 consists of two main parts: the postsynaptic neuron and the synaptic cleft where both parts are lumped together into one homogeneous compartment representing a unified compartment which is compartment 2 instead of 3 or 4 or 5 compartments because both the synaptic cleft and the post-synaptic neurons are harmonized and interactive. This in addition for the purpose of avoiding the expected complexity and difficulty in solving the model and analyzing the results when the dimensionality is too high.

2) The concentrations of substances in compartment 2 represent the average concentrations in both the synaptic cleft and the post-synaptic neuron.

3) Each compartment is assumed to be homogenous; this means we neglect the internal mass transfer limitations between the cytoplasm and the synaptic vesicles in compartment 1 and the diffusion between ACh and the postsynaptic receptors in compartment 2.

4) Both compartments are assumed to be separated by a completely permeable membrane.

5) No product inhibition in both compartments. However, the synthesis reaction catalyzed by the enzyme ChAT in compartment 1 is assumed to be inhibited by the choline substrate as the limiting substrate and acetyl CoA. In addition, compartment 2 is assumed to be inhibited by ACh as the substrate.

6) The transport of substances from compartment 1 to compartment 2 is via passive diffusion, however, the transport of choline from compartment 2 to compartment 1 is via facilitated diffusion.

7) Changes in hydrogen proton concentrations in compartments 1 and 2 causing an autocatalytic effect between compartments 1 and 2 and is represented with a concentration gradient as the driving force for the transport from compartment 1 to compartment 2. The effects of potential differences occurred because of the unequal distribution of salts such as Na, K and Cl are ignored.

8) The system is isothermal, thus no effect with variation of temperature.

9) The dissociation of acetic acid is ignored in chapters 3, 4, and 5, and is taken into consideration at equilibrium as shown in chapter 5.

10) Both volumes of compartment 1 and 2 are assumed to be constant and equal V_1 and V_2 respectively.

11) Because compartment 1 includes the size of the presynaptic terminal and compartment 2 represents both the synaptic cleft and the surface of the postsynaptic neurons. Thus, compartment 1 is assumed to be larger than compartment 2 with the ratio $V_R=V_1/V_2$.

12) The recycle ratio is taken from Tucek et al (1990, 1985 and 1978); where choline produced from the hydrolysis of ACh in compartment 2 supplies choline with a high percent around 40-80% of the required choline for the synthesis reactions catalyzed by ChAT in compartment 1.

13) Each of the feed stream of axonal feed ACh (S_{1f}), the feed stream of plasma choline and choline produced from the release of phospholipids (S_{2f}), the feed stream of acetyl CoA coming from mitochondria (S_{3f}), and the feed stream of hydrogen protons coming from the metabolic reactions and ionization of water (h_f), are collected together in a constant flow rate (q) to meet the choline recycle stream before entering the presynaptic neuron.

14) Both the feed flow rate to compartment 1 and the exit flow rate from compartment 2 are assumed to be constant at q (m^3/sec).

15) The diffusion and reaction events occurring in both contacted cholinergic neurons are explained by the two-enzyme two-compartment model.

In compartment 1, ACh is formed according to the following reaction catalyzed by ChAT:

$$R_{(1)}: \quad Choline + Acetyl - CoA \xrightarrow{ChAT} Acetylcholine + CoA \qquad (2.1)$$

In compartment 2, ACh is degraded according to the following reaction catalyzed by AChE

$$R_{(2)}: \quad Acetylcholine + Water \xrightarrow{AChE} Choline + Acetate + H^+ \qquad (2.2)$$

Each reaction $R_{(1)}$ or $R_{(2)}$ is assumed to be hydrogen ions based and substrate inhibited as shown in Appendix (A). This leads to a non-monotonic dependence of the reaction rates on the substrates and pH. The rates can be formulated by employing previous assumptions and basic biokinetics knowledge as explained in the following section. The details of the derivation are given in appendix (A) and appendix (B). Appendix B provides a derivation of the dynamic model equations and the necessary dimensionalization. All state variables, parameters, and rate equations are in the dimensionless form

as given in Table 2.1. The system is 8 dimensions, where there are non-linear eight ordinary differential equations.

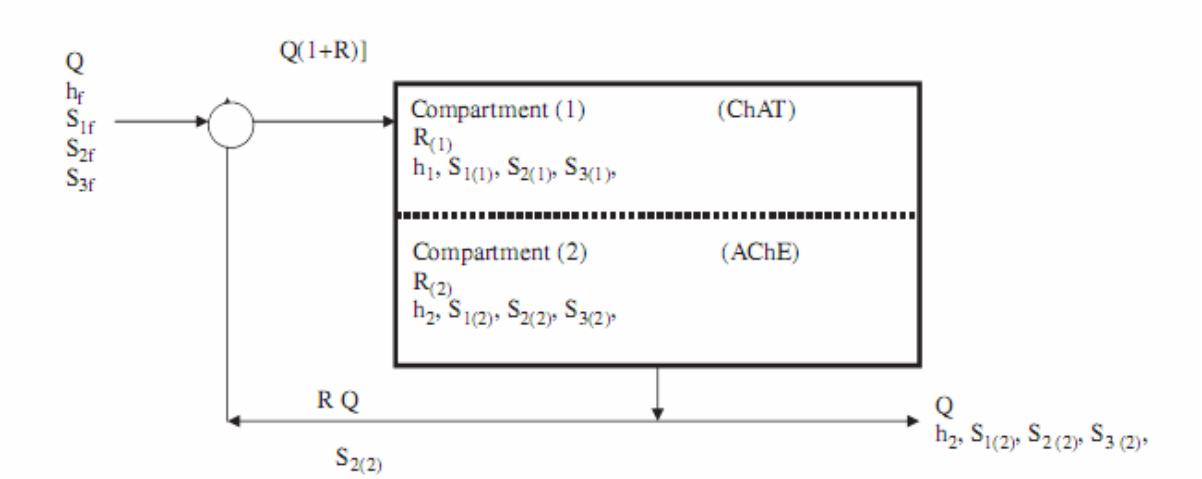

Figure 2- 2: The two-enzyme/ two-compartment model

Table 2-1: Dimensionless forms of the ordinary differential equations of the eight state variables

Item	Compartment	Differential equation
Hydrogen protons	1	$\frac{dh_{(1)}}{dT} = h_f - \gamma_1 \left(\frac{1}{h_f}\right) - \alpha_H \left(h_{(1)} - h_{(2)}\right) + \alpha_{OH}\gamma_1 \left(\frac{1}{h_{(1)}} - \frac{1}{h_{(2)}}\right)$
	2	$\frac{dh_{(2)}}{dT} = V_R(\alpha_H \left(h_{(1)} - h_{(2)}\right) - \alpha_{OH}\gamma_1 \left(\frac{1}{h_{(1)}} - \frac{1}{h_{(2)}}\right) - \left(h_{(2)} - \frac{\gamma_1}{h(2)}\right) + \frac{B_2}{k_{h1}} r(2))$
Acetylcholine	1	$\frac{ds_{1(1)}}{dT} = s_{1f} - \alpha_{s1}\left(s_{1(1)} - s_{1(2)}\right) + \frac{B_1 r(1)}{K_{s1}}$
	2	$\frac{ds_{1(2)}}{dT} = V_R(\alpha_{s_1}\left(s_{1(1)} - s_{1(2)}\right) - s_{1(2)} - \frac{B_2 r(2)}{K_{s1}})$
Choline	1	$\frac{ds_{2(1)}}{dT} = s_{2f} + R * s_{2(2)} - \alpha_{S2_1}\left(s_{2(1)} - s_{2(2)}\right) - \frac{B_1}{S_{2refernce}} r(1)$
	2	$\frac{ds_{2(2)}}{dT} = V_R(\alpha_{S2}\left(s_{2(1)} - s_{2(2)}\right) - (1+R) * s_{2(2)} + \frac{B_2}{S_{2reference}} r(2))$

Acetate	1	$\frac{ds_{3(1)}}{dT} = s_{3f} - \alpha_{S3}\left(s_{3(1)} - s_{3(2)}\right) - \frac{B_1}{S_{3refernce}} r(1)$
	2	$\frac{ds_{3(2)}}{dT} = V_R\left(\alpha_{S3}\left(s_{3(1)} - s_{3(2)}\right) - s_{3(2)} + \frac{B_2}{S_{3refernce}} r(2)\right)$
Rate of synthesis ($r_{(1)}$)	1	$r_{(1)} = \frac{\theta_1 s_{21} s_{31}}{\theta_2 / h_1 (h_1 + 1 + \delta h_1^2) + \theta_3 s_{31} + \theta_4 s_{21} + \theta_5 s_{21} s_{31}}$
Rate of hydrolysis ($r_{(2)}$)	2	$r_{(2)} = \frac{s_{12}}{s_{12} + 1/h_2 (h_2 + 1 + \delta h_2^2) + \alpha s_{12}^2}$

2.3 Proposed Mechanisms for Enzymatic Processes of ACh

Figures A_1 and A_2 shown in appendix A and appendix B represent full mechanisms for the pH-dependent substrate-inhibited enzyme hydrolysis and synthesis reactions, respectively. We present below the rates r_1 and r_2 for the synthesis and hydrolysis reactions. The details of the derivations are given in Appendix (A).

Rate of Synthesis (r_1)

From Figure (A_2) and appendix (A) the final dimensionless reaction rate equation in terms of dimensionless variables and parameters for the synthesis reaction catalyzed by the enzyme ChAT is given by:

$$r_1 = \frac{\theta_1 s_{21} s_{31}}{\theta_2 / h_1 (h_1 + 1 + \delta h_1^2) + \theta_3 s_{31} + \theta_4 s_{21} + \theta_5 s_{21} s_{31}} \qquad (2.3)$$

Rate of Hydrolysis (r_2)

From Figure A_1 and appendix (A) the final dimensionless reaction rate equation in terms of dimensionless variables and parameters for the hydrolysis reaction catalyzed by the enzyme AChE is given by:

$$r_2 = \frac{s_{12}}{s_{12} + 1/h_2 (h_2 + 1 + \delta h_2^2) + \alpha s_{12}^2} \qquad (2.4)$$

Thus the two-enzyme/two-compartment model is described by the set of eight ordinary non-linear differential equations in Table 2-1 with the rate eqs (2.3, and 2.4). This highly non-linear set of

equations is used for the detailed dynamic investigation undertaken in this work. The model equations are in terms of 8 state variables namely: $h_{(1)}, h_{(2)}, s_{1(1)}, s_{1(2)}, s_{2(1)}, s_{2(2)}, s_{3(1)}$ and $s_{3(2)}$ and 25 parameters (Tables 2.2 and 2.3). Because of the lack of experimental data for human brain this investigation is limited to the use of carefully chosen parameters (Hersh and Peet, 1977; Mahecha-Botero et al., 2004; Garhyan et al., 2006; Elnashaie et al., 1984, 1985). All values of the parameters (with respective references) used in this investigation are given in Table 2.3.

Table 2-2: Dimensionless state variables, parameters, and other terms.

Dimensionless State Variables	
$h_{(j)} = \dfrac{[H^+]_{(j)}}{K_{h1}}$	Dimensionless hydrogen ion concentration in compartment j
$s_{1(j)} = \dfrac{[S_1]_{(j)}}{K_{s1}}$	Dimensionless acetylcholine concentration in compartment j
$s_{2(j)} = \dfrac{[S_2]_{(j)}}{[S_2]_{reference}}$	Dimensionless choline concentration in compartment j
$s_{3(j)} = \dfrac{[S_3]_{(j)}}{[S_3]_{reference}}$	Dimensionless acetate concentration in compartment j
Dimensionless Membrane Permeabilities	
$\alpha_{H^+} = \dfrac{\alpha'_{H^+} A_M}{q}$	$\alpha_{OH^-} = \dfrac{\alpha'_{OH^-} A_M}{q}$
$\alpha_{S_1} = \dfrac{\alpha'_{S_1} A_M}{q}$	$\alpha_{S_2} = \dfrac{\alpha'_{S_2} A_M}{q}$
$\alpha_{S_3} = \dfrac{\alpha'_{S_3} A_M}{q}$	
Dimensionless Kinetic Parameters for AChE Catalyzed Reaction	
$\gamma_1 = \dfrac{K_W}{K_{i1}}$	
Dimensionless Kinetic Parameters for ChAT Catalyzed Reaction	

$\theta_1 = Et(S_{2ref})S_{3ref}$	$\theta_2 = \frac{K_2 K_1}{K_2^{\setminus}}$	$\theta_3 = \frac{S_{3ref} K_1}{K_2^{\setminus}}$	$\theta_4 = \frac{S_{2ref}}{K_3 K_2^{\setminus}}$
$\theta_5 = \frac{(S_{2ref})S_{3ref}}{K_2^{\setminus}}$			
Other Terms Used in Dimensionless Form			
$V_R = \frac{V_{(1)}}{V_{(2)}}$	$T = \frac{qt}{V_{(1)}}$	$B_1 = \frac{V_1 V_{M1} \overline{ChAT}}{q}$	$B_2 = \frac{V_2 V_{M2} \overline{AChE}}{q}$

Table 2- 3: Values of the kinetic Parameters

:**Parameter**	**Value**	**Reference**
θ_1	5.2(0.1)	Hersh & Peet (1977)
θ_2	12	Hersh & Peet (1977)
θ_3	1000	Hersh & Peet (1977)
θ_4	5	Hersh & Peet (1977)
θ_5	1	Hersh & Peet (1977)
α	0.5	Garhyan et al., (2006), Elnashaie et al., 1983a; Elnashaie et al., 1983b; Elnashaie et al., 1984; Elnashaie et al., 1995; Ibrahim et al., 1997)
δ	1	Garhyan et al., (2006), Elnashaie et al., 1983a; Elnashaie et al., 1983b; Elnashaie et al., 1984; Elnashaie et al., 1995; Ibrahim et al., 1997)
$K_a(k_h)$	$1.066*10^{-6}$ kMole/m^3(μMole/mm^3)	Garhyan et al., (2006), Elnashaie et al., 1983a; Elnashaie et al., 1983b; Elnashaie et al., 1984; Elnashaie et al., 1995; Ibrahim et al., 1997)
K_{s1}	$5.033*10^{-7}$ kMole/m^3(μMole/mm^3)	Garhyan et al., (2006), Elnashaie et al.,

		1983a; Elnashaie et al., 1983b; Elnashaie et al., 1984; Elnashaie et al., 1995; Ibrahim et al., 1997)
S_{2ref}	1.0×10^{-4} kMole/m^3(μMole/mm^3)	Guyton and Hall, (2000)
S_{3ref}	1.0×10^{-6} kMole/m^3(μMole/mm^3)	Guyton Hall, (2000)
B_1	5.033×10^{-5} kMole/m^3(μMole/mm^3)	Garhyan et al., (2006)
B_2	5.033×10^{5} kMole/m^3(μMole/mm^3)	Garhyan et al., (2006)
α_{H^+}	2.25	Elnashaie et al., (1984)
α_{OH^-}	0.5	Elnashaie et al., (1984)
α_{S_1}	1	Elnashaie et al., (1984)
α_{S_2}	1	Elnashaie et al., (1984)
α_{S_3}	1	Elnashaie et al., (1984)
V_R	1.2	Elnashaie et al., (1984)
pH_f	8.2	Guyton, 2000
s_{1f}	15	Garhyan et al., (2006)
s_{2f}	1.15	Garhyan et al., (2006)
s_{3f}	3.9	Garhyan et al., (2006)
γ_1	0.01	Garhyan et al., (2006), Elnashaie et al., 1983a; Elnashaie et al., 1983b; Elnashaie et al., 1984; Elnashaie et al., 1995; Ibrahim et al., 1997)
R	0.8	Tucek (1978)

2.4 Solution Techniques and Numerical Tools

The results of bifurcation diagrams for the system were obtained using XPPAUT and AUTO 2000, a bifurcation and continuation software for ordinary differential equations. Both static and dynamic bifurcations can be performed by this software package (Ermentrout 2002). The dynamics

results such as phase planes and time traces were obtained via FORTRAN programme. For the chaotic behavior, we used one- dimensional Poincare map to investigate the intersections in one direction between a hyperplan surface (Which is chosen at certain value of a state variable) and trajectories. (Garhyan et al., 2006; and Strogatz 1994). From discrete points of intersections, we are able to construct the bifurcation diagram of Poincare. Then we can investigate the dynamics behavior of the chaotic attractors. This is performed using IMSL libraries which contain DGEAR subroutine. Step size is chosen automatic based on the stiff differential equations during the investigations of the dynamics. Sometimes we used matlab to ensure the solution quality. The Poincare diagram is plotted using a program employed by Ibrahim et al., (2002) [Garhyan et al., 2006; Elnashaie et al., 1984)].

2.5 Physiological Validation Values

To validate the results of the system with physiological and experimental results and with other models of previous investigators during the investigations of the change the system parameters, we should compare our system behavior with the following physiological values of ACh, choline, acetate, and pH. These values depend on experimental review and other models like that used by Garhyan et al., 2006 and Mahecha- Botero et al., (2004). The concentration are given in (kmol/m^3)
Human brain pH in a feline model is found in the range of 6.95-7.35. (Zauner and Muizelaar, 1997), and pH in a human brain was found by (Rae et al., 1996) in the range 6.95 - 7.15. Free ACh in rat brain was found around 0.22×10^{-5} kmol/m^3 and total ACh was in found around 1.77×10^{-5} kmol/m^3. Tucek, 1990 and Garhyan et al., 2006 showed that in guinea pig cerebral cortex the range was 0.31×10^{-5} (free ACh) to 1.67×10^{-5} kmol/m^3 (total ACh).

Wessler et al., (2001) Mahecha- Botero (2004) reported that ACh concentration in human placenta in the range of 3.0×10^{-5} to 55.5×10^{-5} kmol/m^3. Mahecha- Botero (2004) showed that in the isolated rings of rat pulmonary artery ACh was measured to be in the range of 0.001×10^{-5} to 3.0×10^{-5} as pointed to (Kysela and Torok, 1996). Mahecha- Botero (2004) and Garhyan et al. (2006) reported that choline concentration in mouse rat brain is about 1.15×10^{-4} kmol/m^3. This range was confirmed by Tucek (1978) and choline concentration in human plasma is in the range of 0.01×10^{-4} to 0.7×10^{-4} kmol/m^3 (Chay and Rinzel, 1981; Mahecha – Botero (2004) and Garhyan et al., (2006)).

2.6 Results and Discussion

The diffusion-reaction biosystem bifurcation and chaotic behavior is extensively investigated using three bifurcation parameters: (A) feed hydrogen ions concentration (h_f), (B) AChE enzyme activity measure (B_2), and (C) feed ACh concentration (s_{1f}). All of these parameters are in the dimensionless form.

2.6.1 Feed Hydrogen Ions Concentration (h_f)

The feed hydrogen ions concentration is expressed as the dimensionless value h_f when it is used as a bifurcation parameter and the corresponding value of the pH feed will be given in ACh region; while the hydrogen ions concentration is reported as a state variable in terms of pH. The feed hydrogen ions are defined as the hydrogen ions coming to the nerve ending as a product of metabolic reactions occurring outside the presynaptic terminal. For example, the metabolic synthesis of acetyl CoA and metabolic reactions associated with ATP produce hydrogen ions. The concentrations of these feed hydrogen ions (h_f) will influence pH of the ACh neurocycle. h_f is an independent bifurcation parameter and will be investigated. Figures 2.3 and 2.4 show the bifurcation diagrams using the hydrogen ions feed concentration as the bifurcation parameter.

In Figure 2.3(a) the bifurcation diagram is shown for a wide range of this bifurcation parameter ($0 < h_f < 0.02$) corresponding to ($7.6961 < pH_f < 14$). As shown in the Figure 2-3(a); the ACh concentration in compartments 1 $\left(s_{1(1)}\right)$ increases in the range [$0 < h_f < 0.00373281$] from 4.7 to 5.35 (in the dimensionless form), then $\left(s_{1(1)}\right)$ decreases in the range ($0.00373281 < h_f < 0.0065611$) to 3.88, then it increases again in the range ($0.0065611 < h_f < 0.0077$) to the value 4.17 after that $\left(s_{1(1)}\right)$ remains constant. Figure 2-3(c) proceeds in a similar fashion to Figure 2-3(a), where the choline concentrations in compartment (1) $\left(s_{2(1)}\right)$ in the range [$0 < h_f < 0.00373281$] decreases from 3.2205 to 3.217 (dimensionless) then $\left(s_{2(1)}\right)$ increases in the range [$0.00373281 < h_f < 0.0065611$] to 3.234 then it decreases again in the range [$0.0065611 < h_f < 0.0077$] to the value 3.232 after that in the range [$0.0077 < h_f$], $\left(s_{1(1)}\right)$ remains constant with increasing of h_f.

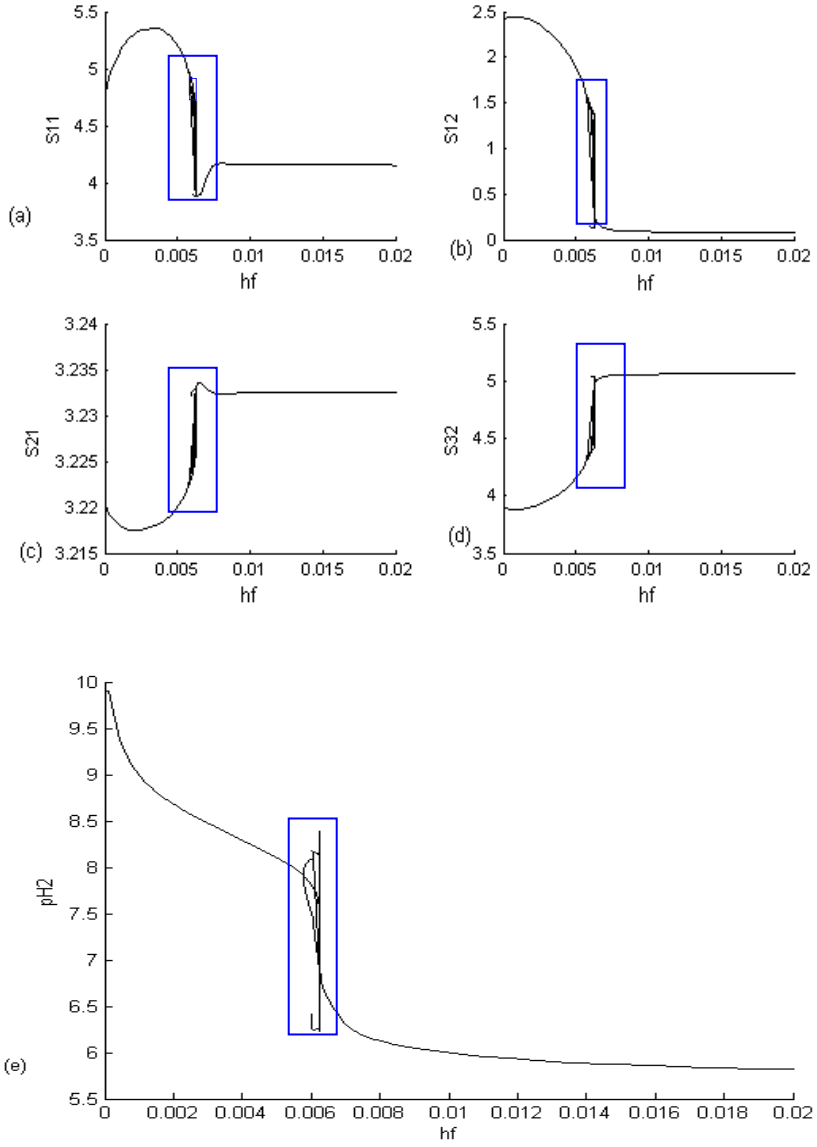

Figure 2- 3: Bifurcation diagram hydrogen ions concentration (hf) as the bifurcation parameter: Overall diagrams:

(a) effect on ACh in compartment (1) ($s1_{(1)}$); (b) effect on ACh in compartment (2) ($s1_{(2)}$); (c) effect on choline concentration in compartment (1) ($s2_{(1)}$); (d) effect on acetate concentration in compartment (2) ($s3_{(2)}$); and (e) effect on pH concentration in compartment (2) (pH(2)).

Figure 2.3(b) shows the ACh concentration in compartment 2 $(s_{1(2)})$ increases in the range [0 < h_f < 0.001182] from 2.41 to 2.44 (in the dimensionless form), then $(s_{1(2)})$ decreases in the range [0.001182 < h_f < 0.007] to 0.1227, after that $(s_{1(2)})$ remains constant with the increasing of h_f. The acetate concentration in compartment (2) $(s_{3(2)})$ is shown in Figure 2.3(d) where $(s_{3(2)})$ decreases in the range [0<h_f<0.001182] from 3.90 to 3.889 (in dimensionless form), then decreases in the range [0.001182<h_f<0.007] to 5.038, after that $(s_{3(2)})$ remains constant with increasing h_f. Figure 2-3(e) shows that the $pH_{(2)}$ decreases continually from 9.75 to 5.69 in the range [0<h_f<0.02]then it remains constant as h_f increases in the range [0.0077 < h_f].

A possible explanation for the effect of h_f is that when feed hydrogen ions concentration increases in the range [0.0077 < h_f], the synthesis reaction catalyzed by ChAT is stopped completely, so this leads to a reduction of the concentration of ACh in compartment 1 $(s_{1(1)})$and in compartment 2 $(s_{1(2)})$ as well, but both choline and acetate concentrations are increasing due to accumulation not consumption. These results are in accordance with the experimental results of Iwamoto et al., (2006) who showed that at high hydrogen ions concentration (low pH), the permeation of human choline from the synaptic vesicles is inhibited. Iwamoto et al., (2006) showed also that the choline uptake is inactivated at low pH (here high concentration of h_f) and enhanced and becomes activated at high pH. Figure 2-4 shows enlargements of the very narrower bifurcation regions denoted by rectangles in Figure 2-3. Six interesting regions are distinguished as follows:

(1) **The first region**: (h_f >0.006263; pH_f < 8.2004). In this region a unique stable stationary steady state is exhibited in the ACh cholinergic system as shown in Figures 2-4; Figures 2-4(a) shows that $(s_{1(1)})$ decreases from 3.905 to 3.89 in the range [0.006254<h_f<0.006258]. While in Figure 2-4(b), $(s_{1(2)})$decreases from 0.291849 to 0.280188. Figure 2-4(c) shows that $(s_{2(1)})$ increases from 3.233 to 3.23392. In Figure 2-4(d), $(s_{3(2)})$increases from 4.95 to 4.9931 in the same range of h_f. $pH_{(2)}$ decreases from 6.97 to 5.85, through the same range of h_f.

(2) **The second region**: (0.006252<h_f < 0.006263; [8.20036 < pH_f < 8.201124). In this region, the phenomenon of bistability is appeared. It is observed that both point and periodic attractors coexist with unstable periodic attractors (appeared as empty circles) separating them. The significance of the bistability is that the system can approach to both attractors (either point or periodic) at the same value

of the bifurcation parameter h_f based on the initial conditions. In this region as h_f decreases to 0.006252 the first Hopf bifurcation HB_1 occurs. HB_1 is defined as a "subcritical Hopf bifurcation" because a branch of unstable periodic orbits (appeared as empty circles) appears with a stable stationery branch at this point forming a separatrix between the basins of the attraction of the stable steady states. Figure 2-4(e) shows that $pH_{(2)}$ oscillates between 6.25 and 8.13. In this region chaos may be developed via the well known Feigenbaum (1980) PD route. The first PD point is at h_f =0.006263

(3) The third region: ($0.006007 < h_f < 0.006263$; $5.57657 < pH_f < 5.5945$). This region contains a unique stable periodic branch (appeared as full circles), giving rise to sustained oscillations where the system demonstrates oscillatory behavior. Simulations for this oscillatory behavior are given as time traces and phase planes showing the behavior of a stable periodic orbits as the only system attractor as will be discussed later in Figures 2- 9 and 2-10.

(4) **The fourth region:** ($0.00598 < h_f < 0.006007$; $8.2185 < pH_f < 8.2204$). This region contains a both a stable periodic branch and an unstable periodic branch. The only attractor in this region is periodic, where the second period doubling PD arises at h_f=0.006007.

(5) **The fifth region** ($0.00578 < h_f < 0.\ 0.00598$; $8.2204 < pH_f < 8.2352$). This region has two unstable periodic branches. In this region, there is no one definite attractor. Where the system can approach to the periodic attractor in the right direction giving rises to oscillations with a fast decreasing amplitude or can approach to the stable steady state in the left direction leading to the second Hopf bifurcation point (HB_2), which appears at $h_f = 0.00578$. As shown in Figure 2-4 (a) the ACh concentration in compartment (1) $\left(s_{1(1)}\right)$ oscillates between 4.3 and 4.99 corresponding to $2.5165*10^{-6}$ and $2.51*10^{-}$ ($kmol/m^3$) corresponding to a low ACh concentration, while $s_{1(2)}$ oscillates between 0.76 and 1.765 corresponding to $0.383*10^{-6}$ and $0.89*10^{-6}$ ($kmol/m^3$) corresponding to a very low ACh concentration. $pH_{(2)}$ is between 6.7 and 7.25 (Figure 2-4 (e)) which is close to the expected physiological values. Figure 2-4(c) shows that the choline concentration in compartment (1) $\left(s_{2(1)}\right)$ has very soft oscillations between $3.229 * 10^{-4}$ and $3.2247*10^{-4}$ ($kmol/m^3$).

(6) **The sixth region** ($0.0055 < h_f < 0$ corresponding to 0.00578; $8.2352 < pH_f$). A unique stable steady-state attractor is the only attractor appeared in this region. This region corresponds to $pH_{(2)}$ between 7.85 and 8.01 as shown in Figure 2-4(e). Figure 2-4(a) shows that $s_{1(1)}$ is between $2.403 *10^{-6}$

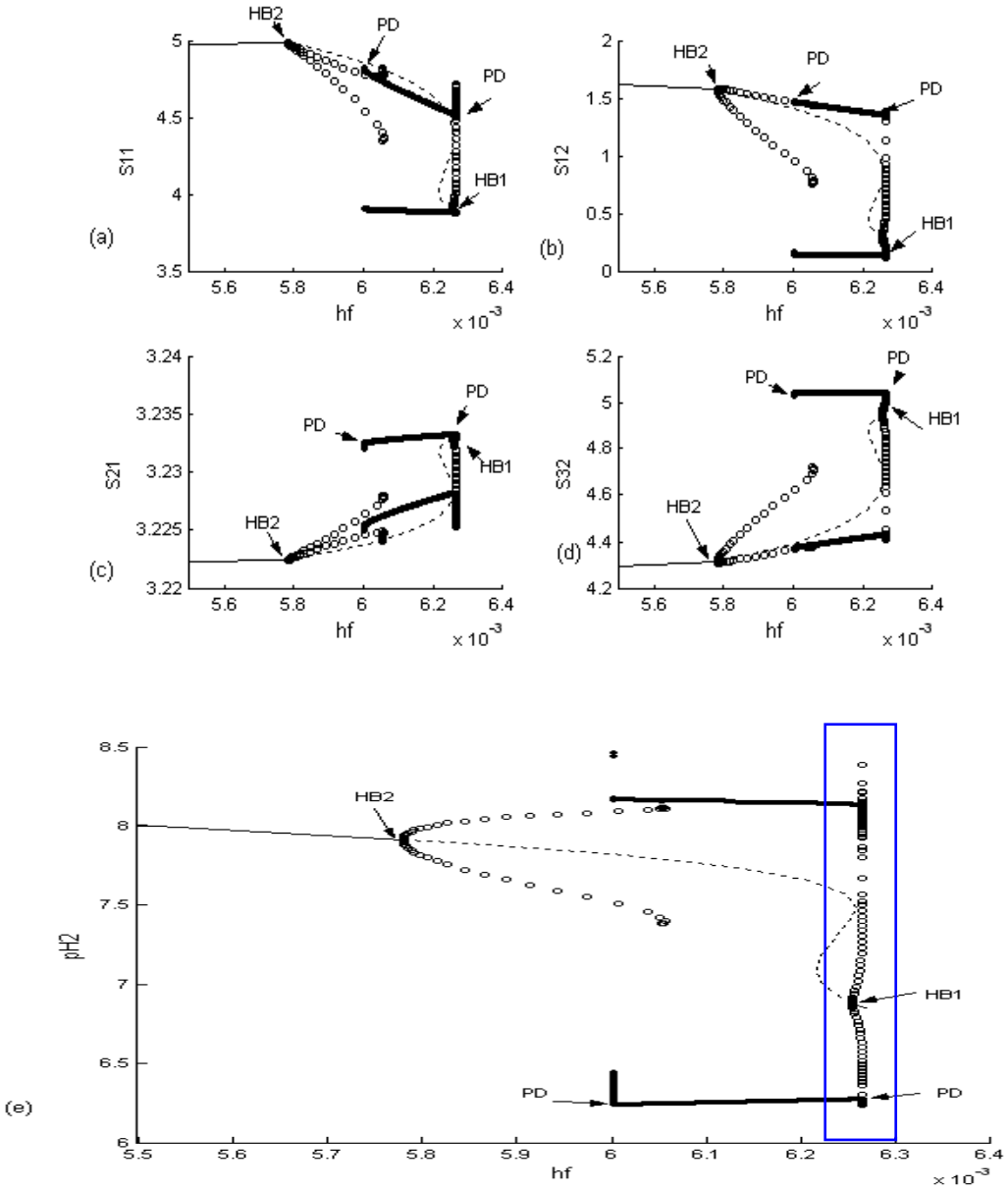
(a)
S11
HB2
PD
PD
HB1
hf
x 10^-3
(b)
S12
HB2
PD
PD
HB1
hf
x 10^-3
(c)
S21
PD
PD
HB1
HB2
hf
x 10^-3
(d)
S32
PD
PD
HB1
HB2
hf
x 10^-3
(e)
βH2
HB2
HB1
PD
PD
hf
x 10^-3

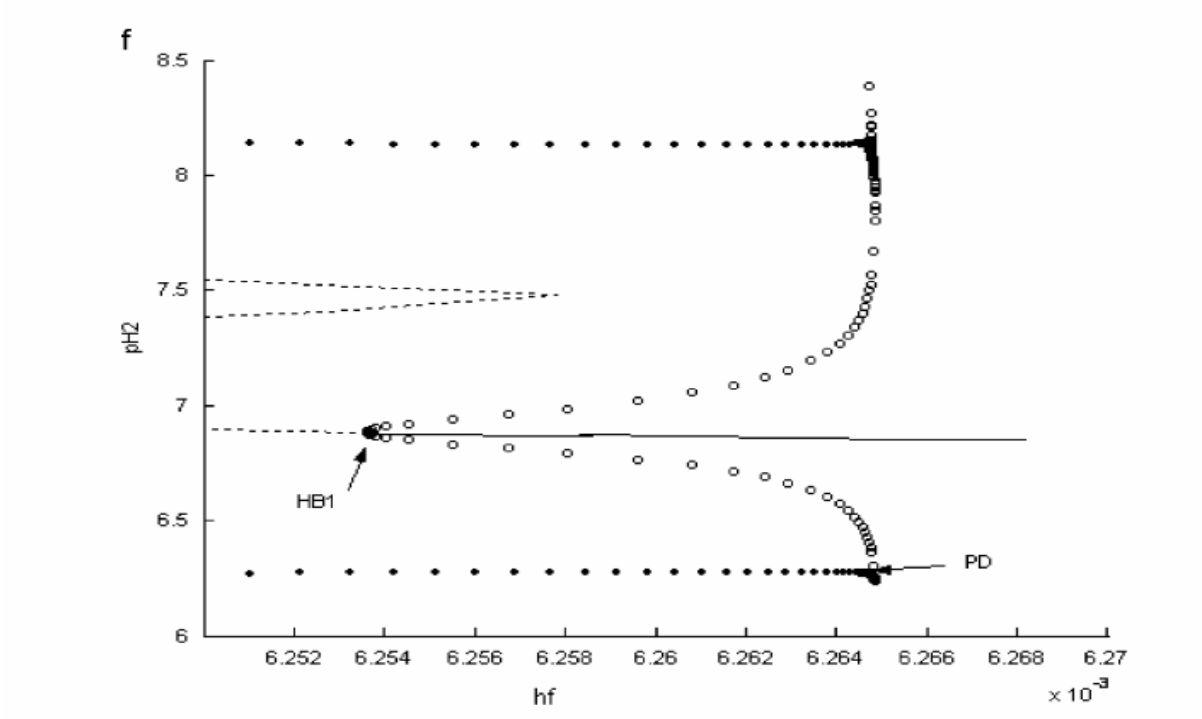

Figure 2- 4: Bifurcation diagram: h_f (hydrogen ions concentrations) as the bifurcation parameter Enlargement for the boxes in Figure 2-3: (stable:—, unstable: -----), periodic branch (stable •, unstable ○): (a) enlargement of the box in Figure 2-3(a); (b) enlargement of the box in Figure 2.3 (b); (c) enlargement of the box in Figure 2.3 (c); (d) enlargement of the box in Figure 2.3 (d); (e) enlargement of the box in Figure 2.3 (e); and (f) enlargement of the box in Figure 2.4 (e);

and $2.7*10^{-6}$ (kmol/m^3) while $s_{1(2)}$ oscillates between $0.86*10^{-6}$ and $1.21*10^{-6}$ (kmol/m^3) as shown in Figure 2-4 (b) $s_{2(1)}$ is between $3.222*10^{-4}$ and 3.2174 and $3.2247*10^{-4}$ (kmol/m^3) with little possible physiological range as shown in Figure 2-4(c). In Figure 2-4 (d) $s_{3(2)}$ oscillates between $4.31*10^{-6}$ and $4.34*10^{-6}$ (kmol/m^3).

If we compare our results to those of Mahecha- Botero et al. (2004), we find that the range of the state variables values appears to be larger than those of Mahecha- Botero et al. For example ACh concentration in compartment (1) $\left(s_{1(1)}\right)$ varies in the range ($3.85< s_{1(1)} <5.38$); as shown in Figure 2-4 (a), however, Mahecha- Botero et al., (2004) predicted a change in the range ($1.25< s_{1(1)} <2$) only. Also the choline concentration in our results ($s_{2(1)}$) is about 3 times that in the results of Mahecha- Botero et

al., (2004) These discrepancies may be explained by the fact that the recycle of choline from the second compartment to the first compartment is considered in our model but not taken into consideration by Mahecha- Botero et al., (2004). In addition, the rate of synthesis reaction is more reasonable and more precise than that used by Mahecha- Botero et al., (2004) or by Garhyan et al., (2006). In our model, we observe oscillations at low feed concentrations of feed hydrogen ions ($0.00578053 < h_f < 0.00625361$), while the model of Mahecha- Botero et al. (2004) failed to do so. Our results are in accordance with those of Shen and Larter (1994). It can be suggested that the oscillatory behavior is resulted due to many reasons; the fist one is the autocatalytic effect which occurs because of the enzymatic reaction – pH dependent and leads to oscillatory behavior. Another factor leading to the complexity is the substrate inhibition and nonlinearity appearing the kinetic rate equations. The third reason for appearing the complexity is the choline recycle, where the feed back of information and choline recycle can be one of the main reasons leading to increase the oscillatory behavior. This can be helpful in explaining the oscillatory behavior in our model because our system of two compartment/diffusion model is also pH dependent, and it can be inhibited by the substrate (choline) in the first compartment or by ACh as substrate in the second compartment. Furthermore; Shen and Larter (1994) confirmed the important role of the bell-shaped pH dependence of the AChE enzyme activity in the catalysis mechanism. H^+ protons are a product of the enzymatic reactions if an ester is a substrate, and this is occurring in the ACh reactions. Finally, at low h_f (high pH) values, the system will be autocatalytic and characterized by oscillatory behavior.

2.6.2 AChE Enzyme Activity (B_2)

AChE enzyme is the enzyme responsible for the hydrolysis of ACh in compartment (2) into choline and acetate after the interaction between ACh and postsynaptic receptors. It is involved in the nervous transmission. Therefore; it is very important to investigate the effect of the activity of AChE enzyme (B_2) on the ACh neurocycle system. Wecker et al., (1978) investigated the effect of AChE inhibition on the synthesis of ACh and choline content in separated brain areas in animals using paraxon as a cholinesterase inhibitor. They found that AChE activity has been inhibited by about 90 % in the regions of hippocampus, cerebral cortex, and striatum. ACh concentrations increased to 125%, 150%, and 150% of control values, respectively. Furthermore, free choline reduced to 75% of the control values in the same regions by the same inhibitor paraxon [Wecker et al., (1978)]. Garhyan et al., (2006) and Mahecha- Botero et al., (2004) indicated that there is a strong relation between the cholinergic diseases such as Alzheimer's and Parkinson's diseases and the disturbances in the activity of AChE enzyme (B_2).

The bifurcation parameter (B_2) is taken like that used by Garhyan et al., 2006 and three parameters. $B_2 = \frac{V_2 V_{M2} \overline{AChE}}{q}$ Where V_{M2} is the maximum rate of the ACh hydrolysis that incorporates kinetic constants that dominate the final reaction step, V_2 = volume of compartment 2, $\overline{AChE}$ = AChE concentration in compartment 2, and q = the flow rate. The activity of AChE enzyme (B_2) is a function of the AChE concentrations. The bifurcation parameter (B_2) will be investigated in two cases. Both cases are investigated with new physiological phenomena taken in consideration such as choline recycle ratio from the synaptic cleft to the presynaptic neuron and the synthesis kinetic mechanism in the first compartment. Then the results will be compared with physiological results and with other models such as the models belonging Garhyan et al., (2006) and Mahecha- Botero et al., (2004). The first case explains the multiplicity phenomena which is called static bifurcation at the high values of the AChE enzyme activity. In the second case, the dynamic bifurcation at the low values of the AChE enzyme activity will be analyzed. These cases are discussed in details below.

(A) Case (1): Static Bifurcation

In this case the activity of AChE enzyme (B_2) will be investigated as the main bifurcation parameter at certain values of the feed ACh ($s_{1f} = 50$) which is equivalent to 2.52 *10^{-5} kmol/m^3 representing a high value on the basis of physiological measurement to investigate the ability of AChE enzyme to degrade the high concentration of ACh. Feed pH_f=6.17 which represents a weak acidic ACh environment which is very close to the physiological range. The rest of the parameters are taken as mentioned in Table 2-3. As shown in Figure 2-5, the hysteresis phenomenon dominates the system. There are 3 main regions will be explained as follows:

1. **Region 1**: In the region $(B_2 \succ 1.82 \times 10^{-4})$ kmol/m^3.

In this region the AChE activity works in a high efficient way to degrade the ACh concentration in compartment 2. $(s_{1(2)})$. Figure 2-5(b) shows that $(s_{1(2)})$ is kept in the range $s_{1(2)} = 0.003379 - 2.94$ corresponding to 1.7×10^{-9} and 0.15×10^{-5} kmol/m^3, respectively. Figure 2-5(a) shows that $(s_{1(1)})$ is kept in the range $s_{1(1)} = 54.74 - 51.92$ corresponding to 2.76×10^{-5} and 2.61×10^{-5} kmol/m^3, respectively. Both choline concentration in compartment (1) $s_{2(1)}$

and acetate concentration in compartment (2), $s_{3(2)}$, remain around 3.66 and 28.9 corresponding to 3.66×10^{-4} and 28.9×10^{-6} kmol/m^3, respectively. The explanation of the current results is that there is a competition between the diffusion process of ACh from compartment 1 to compartment 2 and the enzymatic processes catalyzed by the enzymes AChE and ChAT. Because the enzyme AChE works at the highest efficiency, we will find the enzymatic processes are much faster than the diffusion processes. This is much clear in the concentration of ACh in compartment 2 which is too small around in comparison to the concentration of ACh in compartment 1 which is around 52.

Because hydrogen ions concentration is a product of the hydrolysis reaction in compartment 2, $pH_{(2)}$ will take the same behavior of $s_{3(2)}$. As seen in Figure 2-5(e), $pH_{(2)}$ has its lowest value which is $pH_{(2} = 4.57$. This because acetic acid is ionized completely as assumed in the model into hydrogen protons and acetate.

In comparison to the results of Mahecha- Botero et al., (2004) and Garhyan et al., (2006), ACh in compartment (1) and (2), and choline concentration in compartment (1) and acetate concentration in compartment (2) , here, are higher than that in their model. This is because the choline recycle principle was not taken into consideration in their model where the choline produced from the postsynaptic neuron is the main source for the choline required for ACh synthesis in the presynaptic neuron or compartment (1). In addition; the rate of synthesis of ACh which is proposed as shown in the Appendices is more efficient than used their work.

2. **Region 2**: $\left(0.899\times10^{-4} \le B_2 \le 1.82\times10^{-4}\right)$ kmol/m^3

In this range of AChE activity, a phenomenon appeared between static bifurcation points (SB_1 and SB_2) where there are two stable steady state and unstable steady state (known as saddle points) separating them. This phenomenon is known as hysteresis. The system exhibits steady state multiplicity without oscillations. The presence of the multiplicity region will have its effects on the behavior of the system to respond to external disturbances that may move the system into this multiplicity region [Elnashaie (1977), Garhyan et al., (2006)]. Static bifurcation is usually involved in multiplicity of steady states. Because hysteresis forces the system to exist in a wide range of the state variables, it will help the system to respond clearly when the bifurcation parameters change slightly away from the static bifurcation. As shown in Figure 2-5(d) when the bifurcation parameter (B_2) changes less than 0.899×10^{-4} , acetate

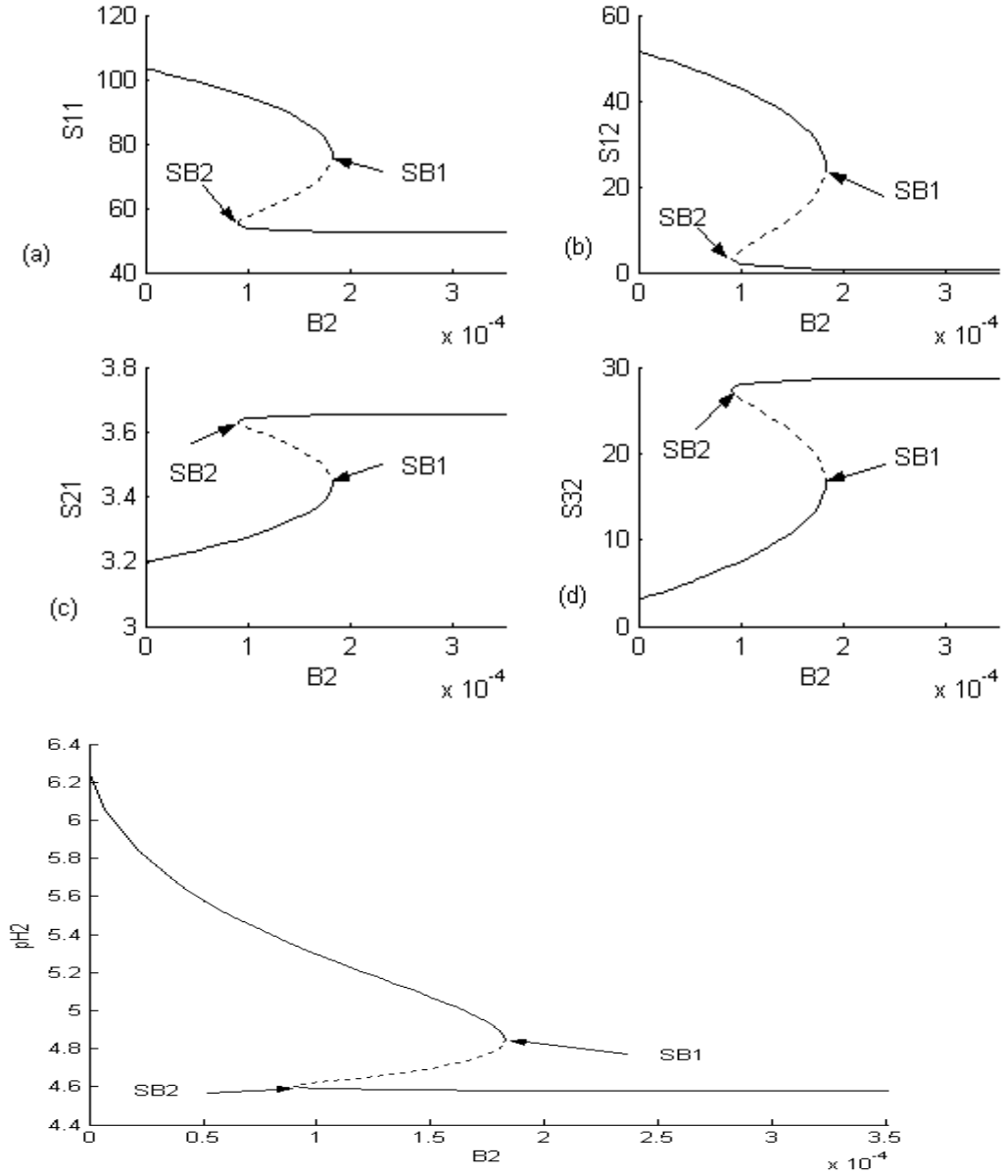

Figure 2- 5: Bifurcation diagram at s_{1f}=50, h_f=0.62682: B_2 (linked to enzyme activity) as the bifurcation parameter: (stable: —, unstable: ----------): (a) effect on ACh in compartment (1) ($s_{1(1)}$); (b) effect on ACh in compartment (2) ($s_{1(2)}$), c) effect on choline concentration in compartment (1) ($s_{2(1)}$), (d) effect on acetate concentration in compartment (2) ($s_{3(2)}$), and (e) effect on pH concentration in compartment (2) ($pH_{(2)}$)

concentration will decrease suddenly from 29×10^{-6} kmol/ m^3 to 7×10^{-6} kmol/ m^3 and the same for pH in compartment 2, where pH_2 increases from 4.6 to 5.5 suddenly as shown in Figure 2-5(f). The hysteresis or multiplicity phenomenon helps the system to gain the flexibility property to respond to any external physiological changes, such as the inhibition of AChE by beta amyloid peptide aggregates or the medications used for treating Alzheimer's disease which is based on inhibiting AChE to increase the ACh concentrations. If we compared the results to that got by Mahecha- Botero et al., (2004) and Garhyan et al., (2006), the hysteresis phenomena appeared in the range $\left(0.39766\times10^{-4} \le B_2 \le 0.85\times10^{-4}\right)$ kmol/m^3 which is smaller than our range. In addition, the ACh concentration in compartment (2) $\left(s_{1(2)}\right)$ in their model was in the range 1.4814×10^{-6} and 2.18×10^{-5} kmol/m^3 which is closer to ours and the $pH_{(2)}$ which is out of the expected physiological range and it was varying between 4.6 and 5.35 so it is also close to the range of ours.

3. **Region 3**: the range $\left(0 \le B_2 \le 0.899\times10^{-4}\right)$ kmol/m^3.

In this very small range of B_2, we find that the system is characterized by only point attractors or stable stationery state. Figure 2-5(a) shows that $s_{1(1)}$ varies between 96 and 104 corresponding to 48.32×10^{-6} and 52.35×10^{-6} kmol/m^3 which is out of the physiological range according to Tucek (1978) , because we will find the rate of enzymatic processes is lower than the rate of diffusion. $s_{1(2)}$ confirms the explanation where it changes in the range 2.18×10^{-5} - 2.63176×10^{-5} kmol/m^3 as shown in Figure 2-5 (b). $pH_{(2)}$ remains outside of the physiological range because of the fully dissociation of acetic acid assumption as shown in Figure 2-5(e) where it changes in the range 5.35-6.24. In comparison to and Garhyan et al., (2006), pH is in the range 6 and 8.24 and the ACh in the range 2.1646×10^{-5} and 2.506×10^{-5} kmol/m^3, which is close to our range.

Case (2): Dynamic Bifurcation

Dynamic bifurcation is very important because it will help to learn how the ACh cholinergic system responds to the low values of the AChE enzyme activity, and how it changes with time. Dynamic bifurcation will clarify how state variables behave with the complexity. The dynamic bifurcation is investigated as shown in Figure 2- 6 at s_{1f} =1.4 corresponding to 0.12 x10^{-5} kmol/m^3 which is the lowest value in the range given by Tucek (1978). The range given by Tucek (1978) and (1985) is

[0.12×10^{-5} to 1.77×10^{-5}] kmol/m^3. The dynamic bifurcation diagrams shown in Figure 2-6 exist in a small range of the AChE enzyme activity (B_2) which is ($3.5\times10^{-5} \le B_2 \le 5\times10^{-5}$) kmol/m^3.

Based on the type of the qualitative behavior Figure 2-6 can be divided into 3 regions (AB, BC and CD). There are two Hopf bifurcations (HBs). The first one (HB_1) appears at the point B where the AChE enzyme activity $B_2= 4.91\times10^{-5}$ kmol/m^3, and the second HB_2 appears at the point C where $B_2= 3.93\times10^{-5}$ kmol/m^3. The main regions can be divided into two regions based on the type of the qualitative behavior of the dynamic ACh system:

i) Stable Steady State (Point Attractor)

This type of solution is represented by two regions: (AB) and the region (CD)

1. **Region AB**: B_2 in the range $\left(4.91\times10^{-5} \le B_2 \le 5.0\times10^{-5}\right)$ kmol/m^3

- First of all in the range ($B_2 \ge 5.0\times10^{-5}$) the system is characterized by only one type of solution which is point attractor which is stationary behavior. As shown in Figure 2-6 the ACh concentration in both compartments: $s_{1(1)}$ and $s_{1(2)}$ are small in comparison to their values in different ranges of B_2 where the enzyme AChE works with high capacity. Figure 2-6(a) shows that $s_{1(1)}$ is between 3.897 and 3.91 corresponding to 1.961×10^{-6} and 1.97×10^{-6} kmol/m^3. However, $s_{1(2)}$ changes in the range of 0.280188 to 0.303586 corresponding to 0.141×10^{-6} and 0.153×10^{-6} kmol/m^3 as shown in Figure 2-6(b). Both $s_{2(1)}$ and $s_{3(2)}$ which are choline and acetate concentration increase at high values as shown in Figure 2-6(c) and Figure 2-6(d), respectively. Figure 2- 6(e) shows that $pH_{(2)}$ has its lowest value $pH_{(2)}$ = 6.84 (maximum hydrogen ions concentration) in this region because of the highest concentration of H^+ ions due to the fully ionization of acetic acid, then in comparison to the physiological values, $pH_{(2)}$ does not agree with them.
- Second, B_2 in the range $\left(4.91\times10^{-5} \le B_2 \le 4.99\times10^{-5}\right)$ kmol/m^3. As the AChE activity decreases until the point B, HB1 appears **at** $B_2 = 4.91\times10^{-5}$ kmol/m^3. Mathematically HB_1 is appeared when the real parts of a pair of complex conjugate eigenvalues become negative, causing the system to undergo a bifurcation. In the the range: $\left(4.93\times10^{-5} \le B_2 \le 4.99\times10^{-5}\right)$, Period doubling (PD) appears at $B_2 = 4.99\times10^{-5}$ as shown in Figure 2-6. In comparison to model of Mahecha- Botero et al., (2004), PD at $B_2 = 1.7784\times10^{-5}$ which is smaller than the previous range

because our system is more stable than their system. However, in the range : $\left(4.91\times10^{-5} \le B_2 \le 4.93\times10^{-5}\right)$ kmol/m^3, the system is characterized by the behavior of bistability which means that both types of solution stationery and periodic solutions coexist at the same values of the bifurcation parameter B_2. The bistability usually appears around HB_1 where instable periodic orbits separated stationery (stable steady state) and the stable periodic orbits. So that HB_1 is called subcritical hopf bifurcation. In this range of B_2 which causes bistability, it is observed that $s_{1(1)}$ changes between 3.897 and 4.74 corresponding to 1.961×10^{-6} and 2.39×10^{-6} kmol/m^3 as shown in Figure 2-6(a) and $pH_{(2)}$ changes between 6.3 and 7.4, which is a region close to the expected physiological pH values according to Tucek (1990) (Figure 2-6(e)). It is observed that ACh levels in both compartments in this range change in a range close to the physiological range. As shown in Figure 2-6(a) and Figure 2-6(b).

2. **Region CD**: $\left(B_2 \le 3.93\times10^{-5}\right)$ kmol/m^3

In this region, the system is characterized by only a stationery state. The physiological values in this region correspond to range of $pH_{(2)}$ around 7.75 which is close to the range of Mahecha- Botero et al., (2004) as shown in(Figure 2-6(e)). In Figure 2-6(a), $s_{1(1)}$ reaches the maximum value at very low values of B_2, where $s_{1(1)}$ = 5.32 corresponding to (2.67×10^{-6} kmol/m^3) which is the highest value in Figures 2- 6(a). Figure 2- 6(b) shows that $s_{1(2)}$ reaches its maximum value (1.66×10^{-6} kmol/m^3) as the reaction that consumption by AChE is almost stopped in this region. However, in the model of Mahecha- Botero et al., (2004), the maximum value of $s_{1(2)}$ reaches its (1.258×10^{-6} kmol/m^3).

In Figure 2-6(c), $s_{2(1)}$ reaches the lowest value (3.22×10^{-4} (kmol/m^3) as the reaction that produces it almost stops. This value of $s_{2\,(1)}$ is higher than that in the model of Mahecha- Botero et al., (2004), as discussed before because the choline consumed in the presynaptic neuron which is compensated by recycling the choline produced by hydrolysis reactions was not taken into consideration by Mahecha- Botero et al., (2004), Therefore, the range of the dynamics of the results of Mahecha- Botero et al (2004) is larger than ours where HB_1 and HB_2 appear in the results of Mahecha- Botero et al., (2004), in the range ($1.82\times10^{-5} \le B_2 \le 4.43\times10^{-5}$) (kmol/m^3) and HB_1 and HB_2 appear at B_2= 1.82×10^{-5}, and 4.43×10^{-5} respectively; however, our model shows that HB_1 and HB_2 appear in the range ($3.93\times10^{-5} \le B_2 \le 4.91\times10^{-5}$).

.

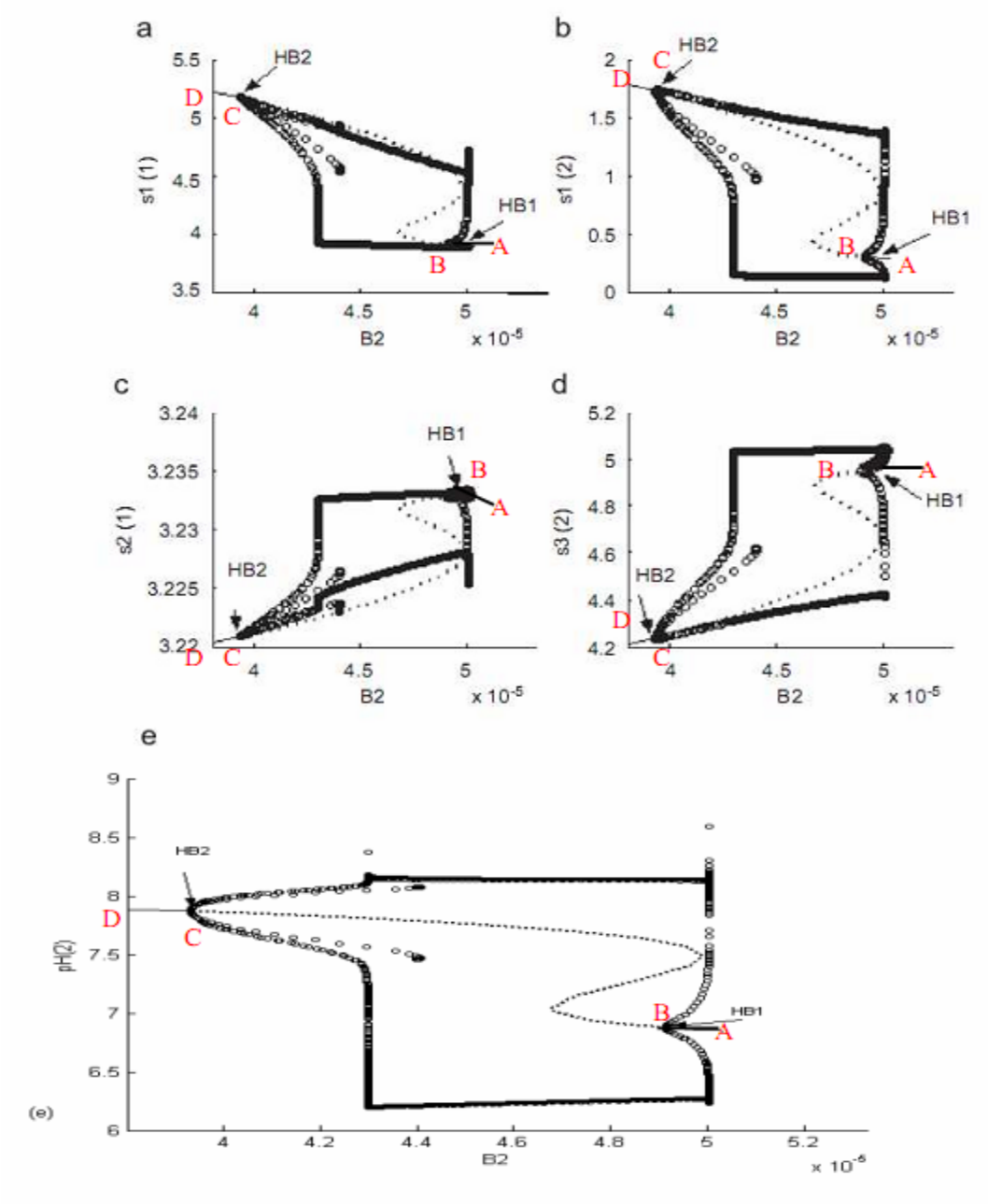

Figure 2- 6: Bifurcation diagram at s_{1f}=2.4, B_2 (linked to enzyme activity) as the bifurcation parameter: stable: —, unstable: ----------), periodic branch (stable: •, unstable ◦)

(a) Effect on ACh in compartment (1) ($s_{1(1)}$); (b) effect on ACh in compartment (2) ($s_{1(2)}$); (c) effect on choline concentration in compartment (1) ($s_{2(1)}$), (d) effect on acetate concentration in compartment (2) ($s_{3(2)}$), and (e) For pH in compartment 2 ($pH_{(2)}$)

3. **Region CD**: $\left(3.93\times10^{-5} \le B_2 \le 4.91\times10^{-5}\right)$ kmol/m^3.

In this region, the oscillatory behavior is the only attractor and there is no stable steady state attractor as shown in Figure 2-6. In this range of B_2, $pH_{(2)}$ oscillates in the range 6.15-8.2 as illustrated in (Figure 2-6(e)) which is close to the expected physiological pH values. In Figure 2-6(b), $s_{1(2)}$ changes between 5.033×10^{-7} and 8.81×10^{-7} kmol/m^3 corresponding to very low ACh concentration. The results in this range of B_2 is smaller than the results of Gahyran et al., (2006) and Mahecha- Botero et al., (2004), which is $\left(1.78\times10^{-5} \le B_2 \le 4.26\times10^{-5}\right)$ kmol/m^3 because our system is more stabilized than their system due to the consideration of choline uptake. The results are in accordance qualitatively with the experimental results done by Santos et al., (2006). One of the main explanations to the complexity phenomena is the competition between both enzymatic reactions (which are characterized by high non-linearity and pH dependent and substrate inhibition) and diffusion processes).

2.6.3 Feed ACh Concentration $\left(s_{1f}\right)$

Figure 2-7 illustrates the bifurcation diagrams with $\left(s_{1f}\right)$ as the main bifurcation parameter. In synaptic neurons there are two sources for the ACh content: the first is that synthesized by ChAT in the presynaptic neuron, and the other is that the mobile ACh in the nerve which is synthesized in other neurons and transported through the axons and represents about 20% of the total ACh content (Tuck, 1978). The feed ACh concentration (S_{1f}) here represents the ACh concentration synthesized in other neurons and transported to the presynaptic neurons by the mechanism of axonal transport.

A) Case 1: Static Bifurcation Analysis

1) Region 1: $\left(31.8 \le s_{1f} \le 100\right)$

In this region, the system is characterized by only a stationery state. Due to the high concentration of s_{1f} in this region, the rate of enzymatic processes will be slower than the rate of diffusion processes. The rate of hydrolysis reaction catalyzed by the AChE occurs in the second compartment may be inhibited by the excess levels of ACh. The concentration of ACh in compartment (1) is the resultant of that in the feed flow (s_{1f}) and that produced by the synthesis reaction catalyzed by the enzyme ChAT in compartment (1).

The range of $(31.8 \le s_{1f} \le 100)$ is corresponding to $(0.19*10^{-5} \le s_{1f} \le 5.033*10^{-5})$ kmol/m^3. This is a region of high feed ACh concentration causing substrate inhibition. Figure 2-7(a) shows that $s_{1(1)}$ is between 59.5 and 200 corresponding to 2.99×10^{-5} and 10.07×10^{-5} kmol/m^3. In Figure 2-7(b) $s_{1(2)}$ is between 25.94 and 99.4 corresponding to 1.31×10^{-5} and 5×10^{-5} kmol/m^3. $pH_{(2)}$ is between 5.75 and 8 (Figure 2-7(e)) and $s_{2(1)}$ is almost constant where it varies in the range (3.32×10^{-4} - 3.47×10^{-4}) kmol/m^3 (Figure 2-7(c)). The range of ACh concentration in compartment 1 in this region is larger than that of Garhyan et al., (2006) and Mahecha- Botero et al., (2004). Because the rate of synthesis of ACh in compartment 1 is higher than their rate of synthesis because they ignored the physiological phenomena occurring in the system that in compartment (2)

2) Region 2: $(24.34 \le s_{1f} \le 31.8)$.

In this range the hysteresis or multiplicity phenomenon appears as s_{1f} decreases to $s_{1f} = 31.8$ where the first static bifurcation point (SB_1). In this range there are two stable steady state solutions separated by unstable steady state solutions (which are called saddle node). The multiplicity dominates the system between the two static bifurcation points where the second static bifurcation appears at $s_{1f} = 24.34$ as illustrated in (Figure 2-7). The hysteresis phenomenon has a vital significance where it reflects the flexibility of the system to external disturbances as the shortage or excessive mobile ACh transported by axonal transport (s_{1f}) close to the static bifurcation points. For example, (Figure 2-7(b)) illustrates that the ACh concentration in compartment 2 ($s_{1(2)}$) changes suddenly from $s_{1(2)} = 2.55$ to $s_{1(2)} = 26.67$ as the ACh feed concentration is slightly increased from SB_1 which exists at $s_{1f} = 31.8$. This hysteresis phenomenon gives the ACh cholinergic a freedom to move through a big range of the state variables. For instance, Figure 2-7(b) illustrates that there are steady state solutions coexisting at $s_{1f} = 28$. Two of these three solutions, the system can approach where both of them are stable at $s_{1(2)} = 1.23$ and $s_{1(2)} = 21$. However; the third solution is unstable where the system cannot approach which is $s_{1(2)} = 5.64$. This region of multiplicity is equivalent to a range of feed ACh

concentration between 1.23×10^{-5} and 1.6×10^{-5} kmol/m^3 which fits well the expected physiological range. Figure 2-7(a) shows that the ACh concentration in compartment 1 ($s_{1(1)}$) is between 1.82×10^{-5} and 1.897×10^{-5} kmol/m^3 and ($s_{1(2)}$) varies in the range $(0.128-0.585)\times10^{-5}$ kmol/m^3. This range is expected to fit the physiological behavior as well. In Mahecha- Botero et al., (2004) and Garhyan et al., (2006) results, the hysteresis phenomenon occurs through a range of s_{1f} is from 1.902×10^{-5} to 3.02×10^{-5} kmol/m^3 which is larger than our range. However; the range of ($s_{1(2)}$) is similar to that of Garhyan et al., (2006) because the variation in the range of the rate of ACh hydrolysis is limited.

3) **Region 3**: $(2.4 \le s_{1f} \le 24.34)$.

In this range, the stationery state is the only solution or the point attractor is the only attractor. Figure 2- 7(a) shows that ($s_{1(1)}$) is between 27.4 and 3.89 corresponding to 1.38×10^{-5} and 0.196×10^{-5} kmol/m^3 and Figure 2- 7(b) shows that ($s_{1(2)}$) is between 0.21 and 0.82 corresponding to 0.011×10^{-5} and 0.045×10^{-5} kmol/m^3. $s_{2(1)}$ varies between 3.43 and 3.233 corresponding to 3.43×10^{-4} and 3.233×10^{-4} kmol/m^3 as shown in Figure 2- 7(c). Figure 2- 7(e) shows that $pH_{(2)}$ varies between 5 and 6.85. This region has a unique stable steady state as shown in Figure 2- 7. The physiological values of the feed ACh concentration (s_{1f}) are between 0.121×10^{-5} and 1.23×10^{-5} kmol/m^3 which are within the range of the physiological values and fit the expected biological behavior. Physiological values of other state variables also correspond to the physiological values reported in literature. For example, ACh concentration in compartment 1 ($s_{1(1)}$) changes between 0.196×10^{-5} and 1.897×10^{-5} and in compartment 2 ($s_{1(1)}$) changes in the range $(1.41-5.85)\times10^{-5}$ kmol/m^3 as illustrated in (Figures 2- 7(a and b)).

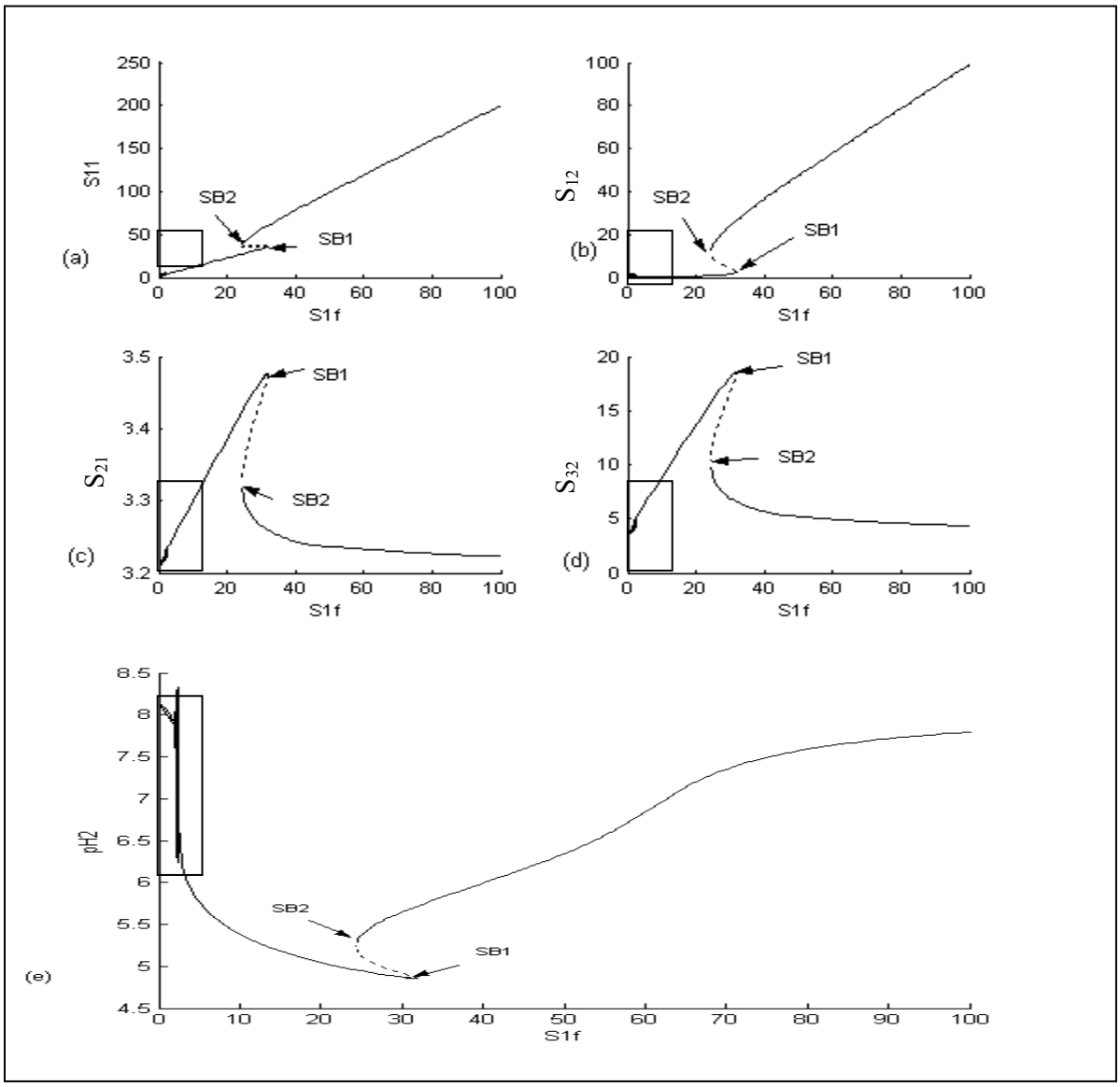

Figure 2- 7: Bifurcation diagrams: feed ACh concentration (s_{1f}) as bifurcation parameter

(stable: —, unstable: ----------) , (a) overall bifurcation diagram for ACh concentration in compartment 1($s_{1(1)}$), (b) overall bifurcation diagram for ACh concentration in compartment 2($s_{1(2)}$),

(c) overall bifurcation diagram for choline concentration in compartment 1($s_{2(1)}$),

(d) overall bifurcation diagram for acetate concentration in compartment 2($s_{3(2)}$), and

(e) overall bifurcation diagram for pH in compartment 2($pH_{(2)}$).

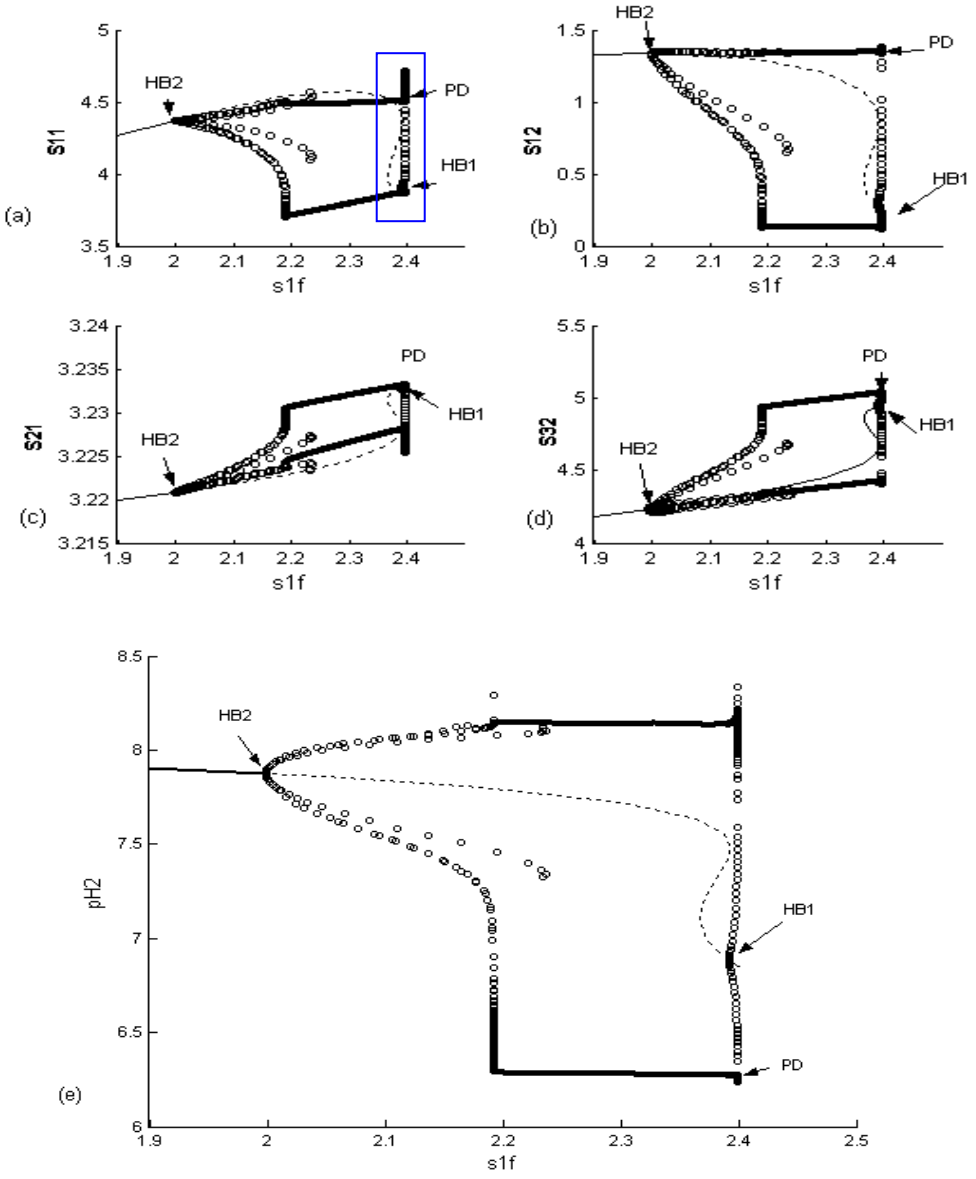
(a)
S11
HB2
PD
HB1
s1f
(b)
S12
HB2
PD
HB1
s1f
(c)
S21
PD
HB1
HB2
s1f
(d)
S32
PD
HB1
HB2
s1f
(e)
pH2
HB2
HB1
PD
s1f

(f)

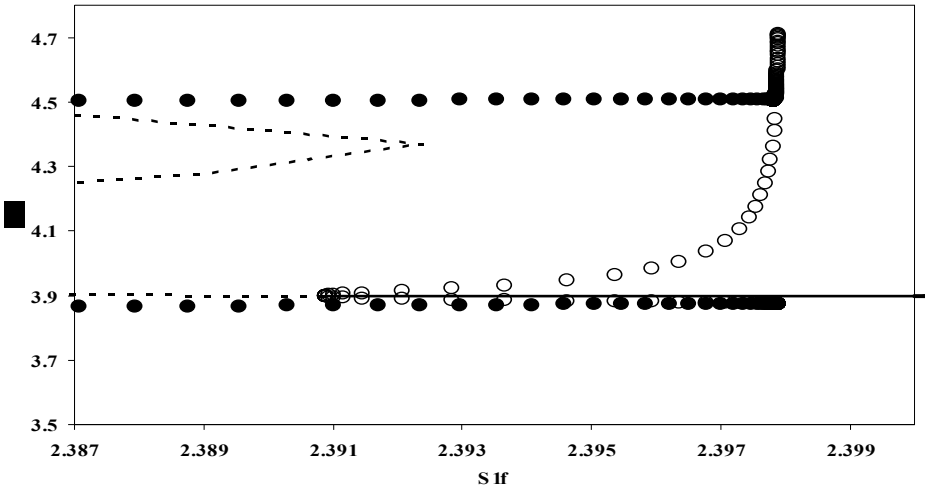

Figure 2- 8: Bifurcation diagrams: feed ACh concentration (s_{1f}) as bifurcation parameter
(stable: —, unstable: --------), periodic branch (stable: •, unstable○)

(a) enlargement of the box in Figure 2- **7(a), (b) enlargement of the box in** Figure 2- **7(b),**
(c) enlargement of the box in Figure 2-**7(c), (d) enlargement of the box in** Figure 2- **7(d), and**
(e) enlargement of the box Figure 2- **7(e), (f) enlargement of the box in** Figure 2- **7(a)**

B) Case 2: Dynamic Bifurcation Analysis

In this case the complex behavior of the system will be investigated at the lower values of the mobile feed Ach concentration where $(s_{1f} \leq 2.4)$. The system can be decided into the following set of regions:

1) **Region 1**: $(2.39 \leq s_{1f} \leq 2.4)$

In this range as shown in Figure 2-8, the first Hopf bifurcation (HB_1) appears at $s_{1f} = 2.398$. It is observed that bistability phenomenon occurs around HB_1. Both point attractors (stable steady state) and periodic attractor coexist at the same values of s_{1f} as illustrated in Figure 2-7(f).

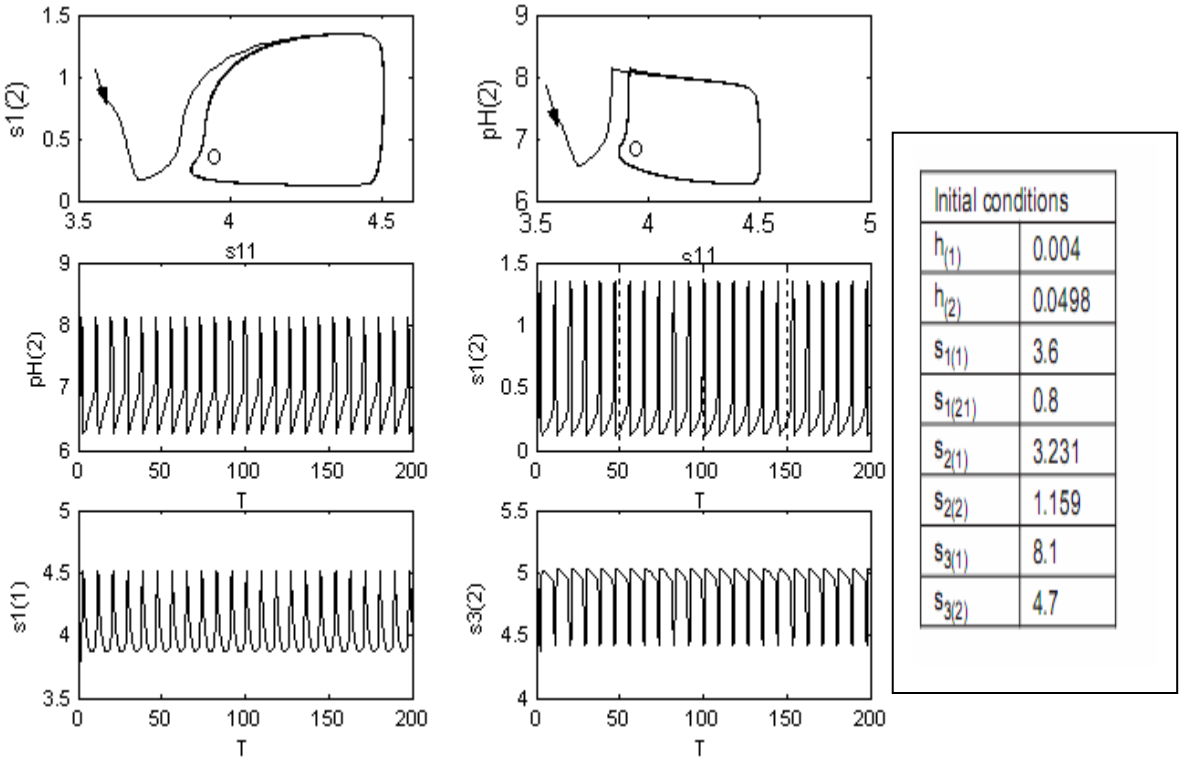

Figure 2- 9: Dynamic characteristics: stable: —, unstable: ---------), phase plane (stable: •, unstable ◦)

(a) phase plane for ACh in compartment 2 ($s_{1\,(2)}$) vs. the ACh in compartment 1 ($s_{1\,(1)}$)

(b) phase plane for pH in compartment 2 ($pH_{\,(2)}$) vs. the ACh in compartment 1 ($s_{1\,(1)}$)

(c) time traces of pH in compartment 2 ($pH_{\,(2)}$), (d) time traces of ACh in compartment 2 ($s_{1\,(2)}$), (e) time traces of ACh in compartment 1 ($s_{1\,(1)}$), and (f) Time traces of acetate in compartment 2($s_{3\,(2)}$)

.

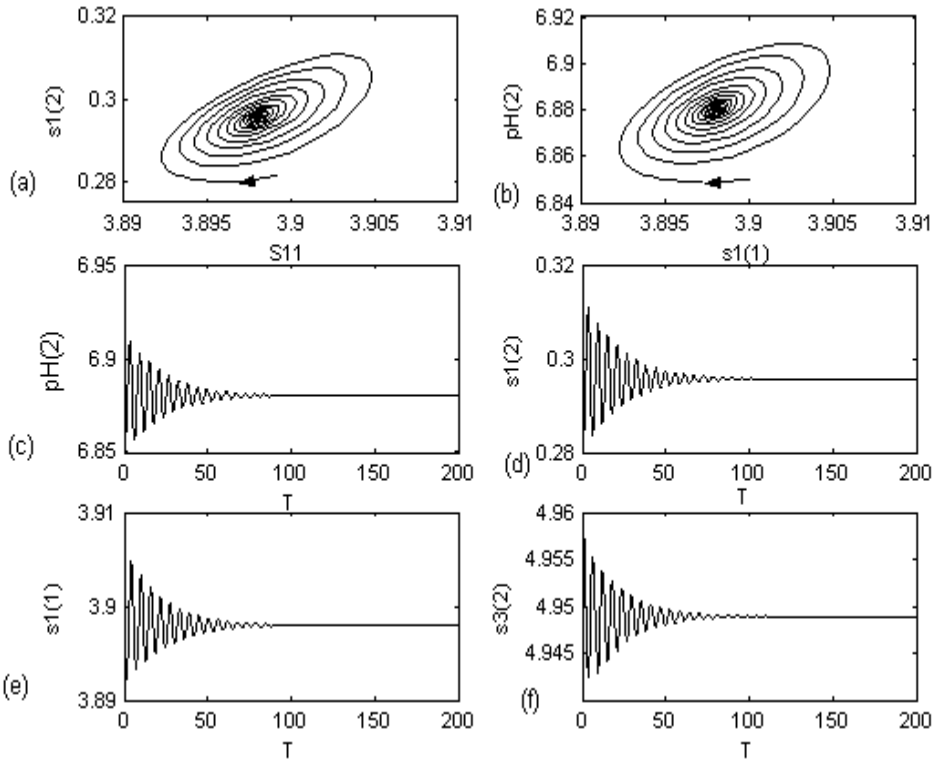

Initial conditions	
$h_{(1)}$	0.003796824
$h_{(2)}$	0.14058
$s_{1(1)}$	3.8971322
$s_{1(21)}$	0.280188
$s_{2(1)}$	3.233
$s_{2(2)}$	1.1606
$s_{3(1)}$	8.2517318
$s_{3(2)}$	4.9606

Figure 2- 10: Dynamic characteristics: stable: —, unstable: -----), phase plane (stable: •, unstable ◦)

(a) phase plane for ACh in compartment 2($s_{1\,(2)}$) vs. the ACh in compartment 1($s_{1\,(1)}$)

(b) phase plane for pH in compartment 2 ($pH_{(2)}$) vs. the ACh in compartment 1 ($s_{1\,(1)}$)

(c) time traces of pH in compartment 2 ($pH_{(2)}$), (d) time traces of ACh in compartment 2 ($s_{1\,(2)}$), (e) time traces of ACh in compartment 1 ($s_{1\,(1)}$), and (f) time traces of acetate in compartment 2 ($s_{3\,(2)}$)

There are unstable periodic orbits (appeared as (empty closed circles) separate both solutions. This bistability leads to the condition, that at the same value of s_{1f} slightly different initial conditions lead to different types of attractors (Figure 2-9 and Figure 2-10). The first initial condition (Figure 2-10) leads to stable steady state (a point attractor) ; while the second initial condition (Figure 2-9) leads to a periodic attractor. The physiological values correspond to a range of feed ACh concentration between 0.12×10^{-5} and 0.1203×10^{-5} kmol/m^3 which is a region of low ACh concentration. The pH in compartment 2($pH_{(2)}$) is close to the physiological expected range where it is between 6.25 and 8.5. This region with low ACh concentration is thus characterized by the presence of bistability. The

PD occurs at s_{1f}=2.393 close to the first Hopf bifurcation point HB_1, however in Mahecha- Botero et al., (2004) and Garhyan et al., (2006) model it is close to the second Hopf bifurcation point HB_2.

2. Region 2: $\left(2.196 \le s_{1f} \le 2.39\right)$.

The system in this range demonstrates oscillatory behavior where the periodic attractor is the only attractor existing in this range as shown in (Figure 2-8(a, b, c, d and e)). Figure 2- 9(a, b, c, d and e) shows the oscillatory behavior of the system, it shows the phase planes and time traces as well at the corresponding initial conditions. It is observed in Figure 2-9 that all state variables attempt to approach the periodic attractors. Figure 2-8(a) shows that ACh concentration is very low. Figure 2-9(c) illustrates that the pH in compartment 2 ($pH_{(2)}$) oscillates between 6.26 and 8.14, which are close to the expected physiological range. The range of the feed ACh concentration is between 0.1105×10^{-5} and 0.1203×10^{-5} kmol/m^3 which represent a low ACh range. Figure 2-8(c) shows that the choline concentration in compartment 1 ($s_{2(1)}$) has very small range between 3.22235×10^{-4} and 3.23285×10^{-4} kmol/m^3. Figure 2-9 and Figure 2-10 show that dynamic characteristics were performed at different initial conditions leading to different behaviors of the system. Figure 2-9 show the periodic attractors at the corresponding initial conditions. Figure 2-9(c) show that $pH_{(2)}$ changes in the range 6.277- 8.14, which are close to the expected biological pH values. The ACh in compartment 1 $s_{1(1)}$ oscillates between 4.5 and 3.9 corresponding to *2.265*10^{-6}* and 1.963*10^{-6} (kmol/m^3) corresponding to a low ACh concentration as shown in Figure 2-9(e). $s_{1(2)}$ oscillates between 0.13 and 1.47 corresponding to 6.54*10^{-8} and 7.4*10^{-7} (kmol/m^3) corresponding to a very low ACh concentration as shown in Figure 2-9(d). However $s_{3(2)}$ is close to the physiological range with soft oscillations between 4.46 and 5.01 corresponding to 4.46 *10^{-6} and 5.01 *10^{-6} (kmol/m^3) as shown in Figure 2-9(f). Figure 2-10 shows the point attractors when the initial conditions are slightly different where $pH_{(2)}$, $s_{1(2)}, s_{1(1)}$, and $s_{3(2)}$ at 6.87, 0.295, 3.897 and 4.948 respectively as shown in Figure 2-10.

3. Region 3: $\left(1.999 \le s_{1f} \le 2.196\right)$

This region corresponds to the feed ACh concentration (s_{1f}) between 0.10061×10^{-5} and 0.1094×10^{-5} kmol/m^3 which represents a very low ACh concentration. As shown in Figure 2-8 this

region has unstable periodic orbits where the periodic oscillations decrease with small amplitudes as the bifurcation parameter decreases until it reaches the second Hopf bifurcation point (HB_2) at $s_{1f} = 1.999$. In this region there is no definite equilibrium, where the system can approach the stable periodic orbits in the right directions or approach the steady state in the left direction.

(a)

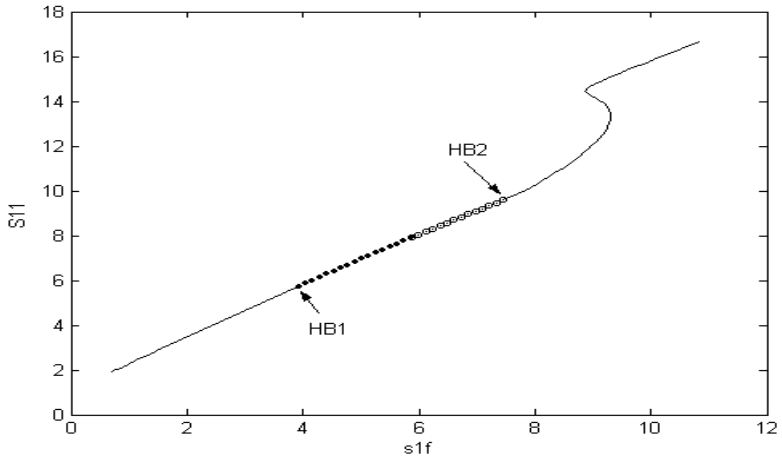

Initial conditions	
$h_{(1)}$	0.000805984
$h_{(2)}$	0.004122
$s_{1(1)}$	5.4684
$s_{1(21)}$	0.31424
$s_{2(1)}$	5.6255
$s_{2(2)}$	2.018
$s_{3(1)}$	5.09
$s_{3(2)}$	3.833

(b)

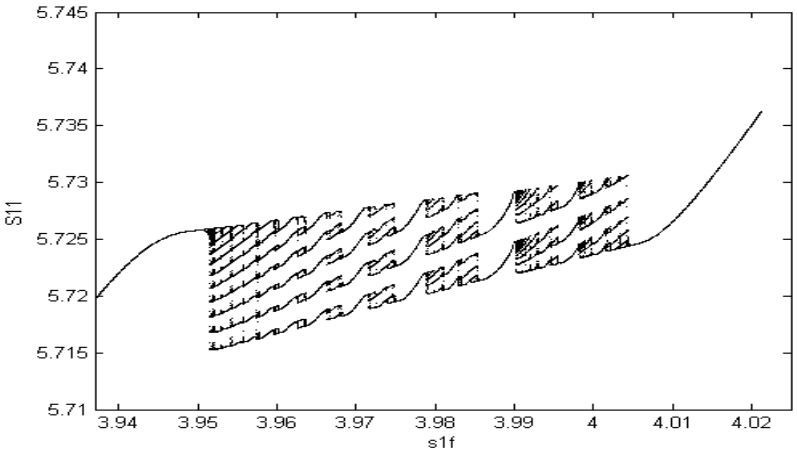

Figure 2- 11: (a) Bifurcation diagram at $s_{2f} = 2, s_{3f} = 2, h_f = 0.002, B_1 = 0.0001, B_2 = 0.002$ and the rest of the system parameters as in Table 2-3: effect of s_{1f} on $s_{1(1)}$, (b) one dimensional Poincaré bifurcation diagrams (Poincaré plane is located at $s_{1(2)} = 0.305$), $s_{2f} = 2$, $s_{3f} = 2, h_f = 0.002$, $B_1 = 0.0001$, $B_2 = 0.002$ and the rest of the system parameters a in Table 2- 3 for the corresponding initial conditions

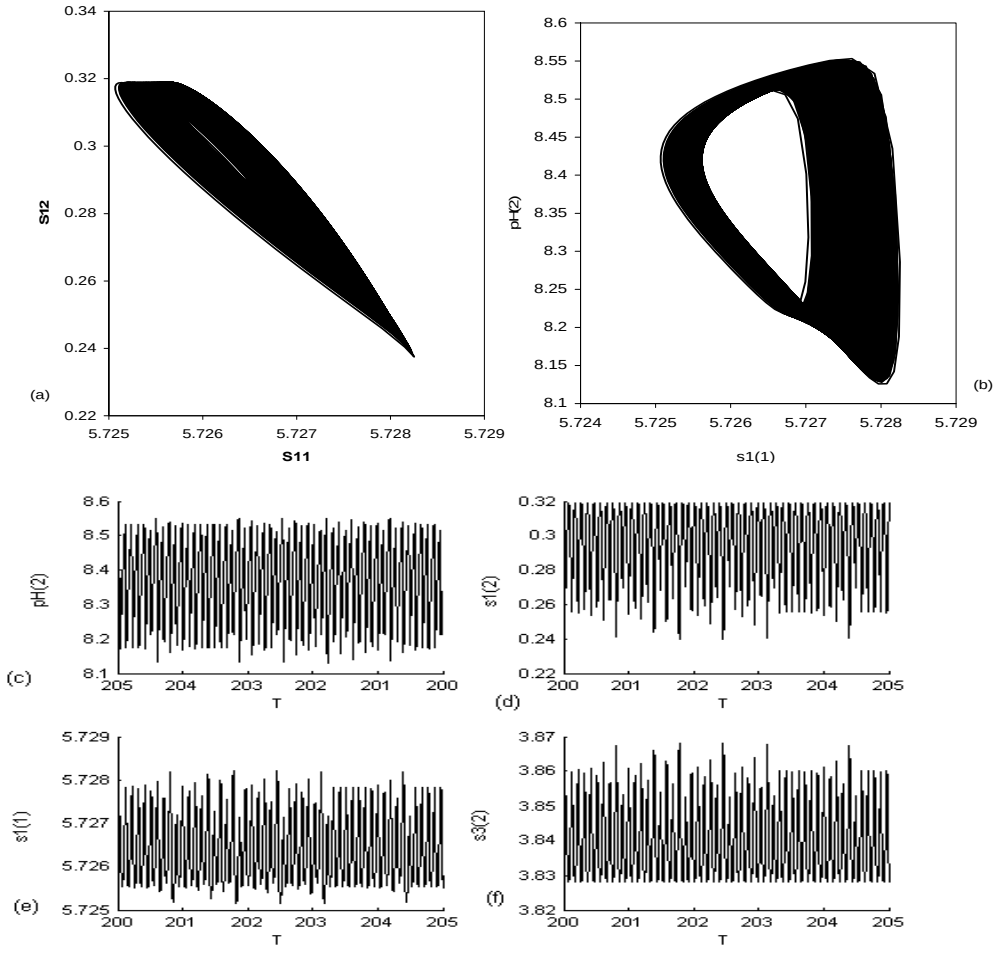

Initial conditions	
$h_{(1)}$	0.000805984
$h_{(2)}$	0.004122
$s_{1(1)}$	5.4684
$s_{1(21)}$	0.31424
$s_{2(1)}$	5.6255
$s_{2(2)}$	2.018
$s_{3(1)}$	5.09
$s_{3(2)}$	3.833

Figure 2- 12: Dynamic characteristics at $s_{1f} = 3.95135$, and $s_{2f} = 2, s_{3f} = 2$, $h_f = 0.002$, $B_1 = 0.0001$, $B_2 = 0.002$ and the rest of the system parameters in Table 2- 3 for the corresponding initial conditions:

(a) Phase plane for ACh in compartment 2($s_{1\,(2)}$) vs. the ACh in compartment 1($s_{1\,(1)}$)

(b) Phase plane for pH in compartment 2 ($pH_{\,(2)}$) vs. the ACh in compartment 1 ($s_{1\,(1)}$)

(c) time traces of pH in compartment 2 ($pH_{(2)}$), (d) time traces of ACh in compartment 2 ($s_{1(2)}$), (e) time traces of ACh in compartment 1 ($s_{1(1)}$), and (f) time traces of acetate in compartment 2 ($s_{3(2)}$)

4. **Region 4**: $\left(s_{1f} \leq 1.999\right)$

This region corresponds to feed ACh concentration lower than 0.10061×10^{-5} kmol/m^3. In this range, the stable stationary state is the only solution available in this region. Figure 2-8(a) illustrates that $s_{1(1)}$ varies in the range 4.4-1 corresponding to $\left(0.21-0.05033\right)\times10^{-5}$ kmol/m^3

Figure 2-8(e) shows that the pH in compartment 2 ($pH_{(2)}$) varies in a narrow range of 7.95 and 8.14. Figure 2-8(c) shows that the choline concentration in compartment 1($s_{2(1)}$) is lower than 3.22×10^{-4} kmol/m^3. In comparison to the results of Garhyan et al., (2006) and Mahecha- Botero et al., (2004), their dynamical behavior occurs in the range ($1.64 \leq s_{1f} \leq 2.43$) which is wider than our range which is $1.99 \leq s_{1f} \leq 2.39$).

Figure 2-11 (a) shows the static bifurcation diagram at $h_f = 0.002$, $B_2 = 0.002$ and the rest of the system parameters are shown in Table 2.3. The effect of s_{1f} as the bifurcation parameter on $s_{1(1)}$ is studied at the corresponding initial conditions, in order to investigate the fully developed chaotic behavior. In Figure 2-11(a) there are two Hopf bifurcation points, the first HB point is at $s_{1f} = 3.932$, and the other is at $s_{1f} = 7.453$. The periodic branch loses its stability giving rise to chaotic behavior at $s_{1f} = 5.87254$.

In addition, this region is characterized by the presence of fully developed chaos (Figure 2-11(b)). Chaos may develop via the well known Feigenbaum period adding route (Feigenbaum, 1980). Period adding appears when $s_{1f} = 3.95115$. In order to have a full picture about the evolution of the chaotic behavior, Pioncare abstracted the time trace and phase plan representations to a comprehensive map where a hypothetical hyperplane surface is assumed to cross the trajectory in the state space, the Pioncare map accounts only for the intersections of the plan with the trajectories. Figure 2-11(b) shows the Pioncare map of the region under consideration. It is clear that the evolution of chaotic behavior is via period adding sequence, the map is characterized also by wide regions of periodic windows of period adding. This map of Figure 2-11(b) is constructed using Pioncare plan at $s_{1(2)} = 0.305$. The periodic bifurcation sequence is characterized by period adding sequence to

chaos; this may be summarized as follows: Period one attractor – evolution of chaos via period adding– window of period two - evolution of chaos via period adding – window of period three - evolution of chaos via period adding – window of period four - evolution of chaos via period adding –

Initial conditions	
$h_{(1)}$	0.000805984
$h_{(2)}$	0.004122
$s_{1(1)}$	5.4684
$s_{1(21)}$	0.31424
$s_{2(1)}$	5.6255
$s_{2(2)}$	2.018
$s_{3(1)}$	5.09
$s_{3(2)}$	3.833

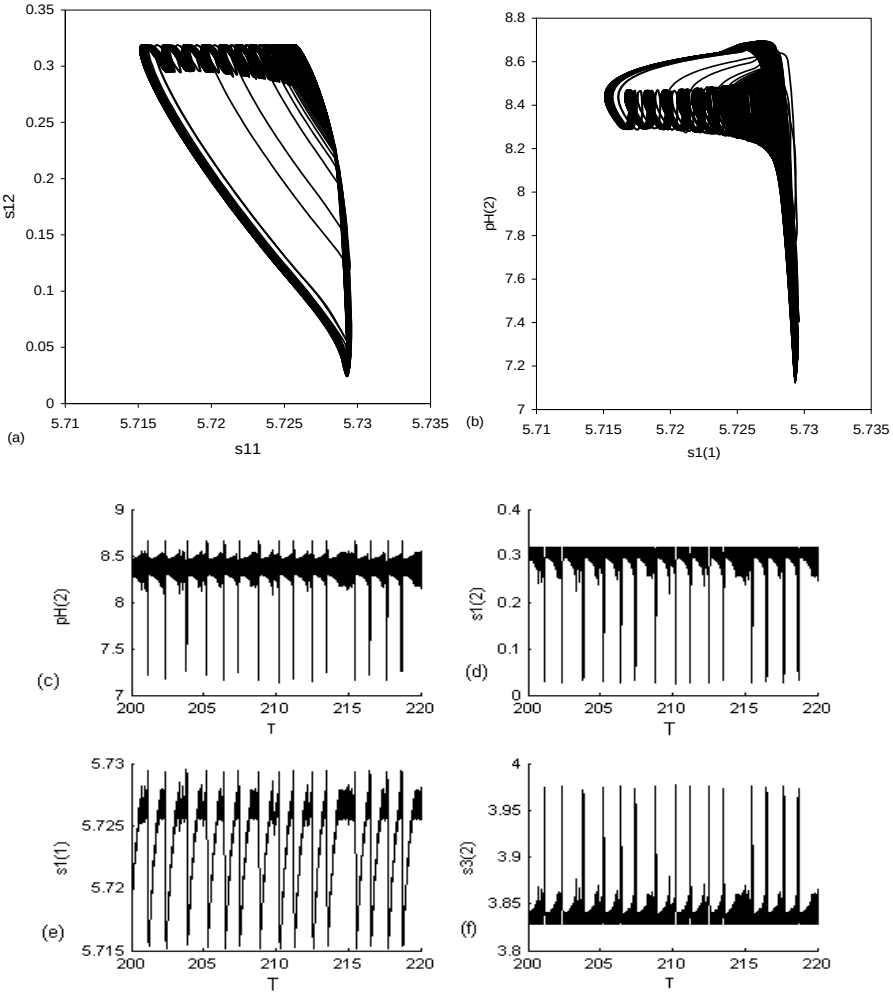

Figure 2-13: Dynamic characteristics at $s_{1f} = 3.9518$ and $s_{2f} = 2, s_{3f} = 2, h_f = 0.002$, $B_1 = 0.0001$, $B_2 = 0.002$ and the rest of the system parameters as in Table 2- 3 for the corresponding initial conditions

((a) phase plane for ACh in compartment 2($s_{1\,(2)}$) vs. the ACh in compartment 1($s_{1\,(1)}$)

(b) phase plane for pH in compartment 2 ($pH_{(2)}$) vs. the ACh in compartment 1 ($s_{1\,(1)}$)
(c) time traces of pH in compartment 2 ($pH_{(2)}$), (d) time traces of ACh in compartment 2 ($s_{1\,(2)}$), (e) time traces of ACh in compartment 1 ($s_{1\,(1)}$), and (f) time traces of acetate in compartment 2 ($s_{3\,(2)}$).

window of period five – evolution of chaos via period adding – window of period six and so on where a cascade of further period adding occurs as s_{1f} decreases until the map becomes chaotic and the attractor changes from a finite to an infinite set of points. Time traces and phase planes are shown in Figure 2-12 and in Figure 2-13 at $s_{1f} = 3.95135$ and $s_{1f} = 3.9518$ respectively as chaotic intermittency attractors. In the intermittency route, periodic oscillations dominate for certain time intervals, and then they are interrupted by bursts of erratic oscillations of finite durations (Garhyan et al (2006). Figure 2-12 illustrates that after an initial transient, the solution settles into an irregular oscillation that persists as time (T) approaches infinity.

2.7 Summary and Conclusions

Two kinetic mechanisms for both the synthesis reactions catalyzed by the enzyme ChAT and the hydrolysis reactions catalyzed by the enzyme (AChE) are proposed to obtain more reasonable rate equations for describing the synthesis and hydrolysis kinetics in the synapses and for simulating the ACh neurocycle in the brain. These rate equations are pH dependent and substrate inhibited. An eight-dimensional non-linear mathematical model (two-enzyme/two-compartment) is proposed for describing the metabolic events in the ACh neurocycle system considering the physiological reality of the choline uptake from the synaptic cleft into the presynaptic neuron. The concepts of complex nonlinear dynamics such as dynamic and static bifurcation, chaos and instability have been applied to predict and control the system performance. The proposed model and kinetic mechanisms showed that they are important for understanding the behavior of the cholinergic ACh neurocycle.

The results obtained from studying the effect of bifurcation parameters such as (the feed hydrogen ions concentrations and the AChE enzyme activity and feed ACh concentrations) assures the presence of oscillatory behavior at the low concentrations of these parameters. The ACh cholinergic system is characterized by the existence of complex dynamic phenomena such as chaotic behavior via a period adding sequence and instability around the subcritical hopf bifurcation points. It is found that the system is not influenced clearly at low pH_f. The results are in accordance with the physiological and experimental and theoretical reviews. One of the main explanations is that the high

concentrations of H^+ will inhibit choline diffusion into presynaptic membrane, another explanation is that the high concentrations may inhibit the synthesis and hydrolysis reaction and finally will cause the state variables to approach the plateau as illustrated in Figure 2-3 (a, b, c, d and e). The choline recycled from the postsynaptic neurons to be reused in the presynaptic neurons is taken into consideration and will help the system to control and regulate the levels of the state variables in both compartments. Therefore, ACh and choline concentrations in compartment (1) are higher than that of Mahecha- Botero et al., (2004) because of the choline uptake considerations and the reasonable rate equation of synthesis of ACh.

From investigating the static bifurcation of the bifurcation parameters of the activity of AChE enzyme and mobile feed ACh concentrations, it is observed that the hysteresis and multiplicity control the system. This hysteresis phenomenon reflects flexibility of the system and its capability to respond to any forcing disturbances affecting the cholinergic ACh system to be able to regulate its components to adapt to any sudden changes. The feed back mechanism of the system can work as a vital control device to control and regulate the transmission activity and the processes of the ACh in both compartments. The findings of this research can be useful to be able to understand the characteristics and the behavior of the ACh cholinergic system and discover the disturbances in the enzymatic processes occurring in the system. In addition, the relation between the neurological sicknesses like Alzheimer's and Parkinson's disease and the complex dynamics and chaotic behavior of the ACh system can be helpful for enriching more research on other disorders in living organisms.

Chapter 3

Effect of Choline and Acetate Substrates on Bifurcation and Chaotic Behavior of Acetylcholine Neurocycle and Alzheimer's and Parkinson's Diseases

This chapter is based on the paper published by Mustafa et al., (2009)b. In this chapter a novel two-enzyme/ two-compartment model is developed in order to explore the dynamics, bifurcation, and chaotic characteristics of the acetylcholine neurocycle. The model takes into consideration the physiological events of the choline uptake into the presynaptic neuron and choline release in the postsynaptic neuron. The effects of feed choline concentrations, feed acetate concentrations as bifurcation parameters are studied. It was found that feed choline concentrations play an important role and have a direct effect on the acetylcholine neurocycle through a certain important range of parameters. The feed acetate concentrations have less effect. A detailed bifurcation analysis over a wide range of parameters is carried out in order to uncover some important features of the system, such as static bifurcation, dynamic bifurcation and chaotic behavior. These findings are related to the real phenomena occurring in the neurons, like periodic stimulation of neural cells and non-regular functioning of acetylcholine receptors. The results are compared to the results of physiological experiments and other published models. As there is strong evidence that cholinergic brain diseases like Alzheimer's disease and Parkinson's disease are related to the concentration of acetylcholine, the .present findings are useful for uncovering some of the characteristics of these diseases and encouraging well directed physiological research coupled to useful mathematical modeling. It is concluded from the results in this chapter that feed choline is more important factor than feed acetate in ACh processes.

Keywords: Acetylcholinesterase Cholineacetyltransferase, Acetylcholine, Choline, Acetate, Neurocycle, Hydrogen ions, Parkinson's disease , Alzheimer's disease, Dynamic behavior, Bifurcation, Chaos.

3.1 Introduction

The neurotransmitter acetylcholine (ACh) plays a vital role in both peripheral and central nervous systems where it is responsible for physical and mental activities [Brandon et al., (2004)].

ACh is essential for the regulation of the processes of consciousness, thinking, attention, sleeping, movement and memory excitation [Brandon et al., (2004)].

The ACh neurocycle system is involved in the following main processes: Firstly, the biosynthesis of ACh occurring is performed in the presynaptic neurons and catalyzed by the enzyme Cholineacetyltransferase (ChAT); the required substrates are choline and acetyl coenzyme A (Acetyl-CoA). Secondly, ACh is released by fusion of the membranes of the presynaptic neurons with synaptic vesicles storing ACh, where it reacts with the receptors of the postsynaptic neurons to cause the electrochemical signals. Thirdly, ACh is hydrolyzed by the enzyme acetylcholinesterase (AChE) in the synaptic cleft to produce acetate and choline. Fourthly, the choline which is produced from the hydrolysis reaction is recycled from the synaptic cleft to the presynaptic neurons to be reused in the synthesis of ACh [Brandon et al., (2004)].

Acetyl-CoA is a vital substance contributing with the ATP in most of the metabolic reactions as a source of energy. It is clear that there are three substances required for syntheis of ACh: acetyl-CoA, choline, and ChAT. Acetyl-CoA is the only component of these three substances that is synthesized in the ending terminals of the presynaptic neurons (Tucek 1978). However, ChAT is synthesized in the cell bodies of cholinergic neurons and transported to the presynaptic terminals by the axonal transport mechanism; and choline is supplied from the hydrolysis of ACh and other sources in the environment outside the presynaptic neurons (Tucek 1978).

Choline required for the synthesis of ACh in the presynaptic terminals is given by the high affinity transporter from extra cellular fluid. There are two sources for choline in the environment of the brain: the first source is from the degradation of choline containing compounds existing in brain cells, and the second source is from the free choline of the blood plasma (Tucek 1985).

The content of choline can be determined by the technique of steam pulse sequence which is used for diagnosis of the irregularities in brain. Dawn et al., (2006) measured the choline concentration in the thalamus region and found it as 2.0±0.4 μ mol/g wet wt, and in the frontal lobe white matter, choline concentration was 1.9 ± 0.5 μ mol/g wet wt. Phosphatidylcholine and sphingomyelin in the extracellular fluid are considered as a basic resource of choline, where phospholipase catalyzed the degradation of phosphatidylcholine to produce free choline to be used for ACh production in the presynaptic neurons [Brandon et al., (2004); Lee et al., (1993); Zhao et al., (2001), Eugene et al., (2004)]. There is a scientific reality that the neurons in the nervous systems cannot synthesize choline in spite of its being as a vital compound for the life of neurons and very simple compound. The cells of nervous tissue can only release choline from its original compounds.

[Bussiere et al., (2001), Ballivet et al., (1996)]. In addition the surface membranes of the neurons are equipped with transporters for carrying choline from outside of the presynaptic neurons [Bussiere et al., (2001)]. The brain generally can obtain choline in the form of free choline and phospholipids via the blood stream [Glenn et al., (1983), Ballivet et al., (1996)].

Liver in living organisms represents the man source of choline [Ballivet et al., (1996)]. Choline is synthesized not as a free compound, but as the choline moiety of phosphatidylcholine [Chiao-Kang (1988), Matthies, et al., (2006)]. It is released from phosphatidylcholine mainly via the steps of lysophosphatidylcholine to glycerylphosphorylcholine then to choline [Matthies, et al., (2006)]. It can be included that the brain cannot synthesize choline itself but it can produce free choline [Tucek (1985)]. It has been found that the blood stream leaving the brain contains free choline in a concentration higher than that the blood coming to the brain [Tucek, (1978), and Tucek, (1985); Bussiere et al., (2001) and Ballivet et al., (1996)].

We thus face a very intersting situation that an organ believed to synthesize new choline in any form acts as a producer of its unesterified variety, and that the only source of this compound for brain ACh or membrane biosynthesis is the choline or choline-containing phospholipids taken up from the circulation (Tucek 1985). Because it is oberved that the brian is unable to synthesize choline, it is some kind hardly to agree with the concept of its production [Jan et al., 1981]. According to Weckler (1988), the levels of the synthesized ACh concentration depend on the range of the free choline concentration as a substrate, for example, he found that the synthesis of ACh did not change although the concentrations of free choline increased in brain rats. Furthermore, both of the concentrations of the synthesized ACh and the concentration of the released free choline reduced much when the content of the choline diet decreased.

The experimental reviews confirm that the brain cannot synthesize free choline. Alternatively it utilizes lysophosphatidylcholine as a bound choline for synthesizing ACh [Weckler (1988)]. Moreover, experimental findings indicate that the free choline of the blood plasma represents only a part of the total amount of choline which is supplied to the brain. Most of choline is supplied in a bound form such as lysophospahtetidylcholine and lipoproteins [Tucek (1985), Weckler (1988)]. In surface membranes of the cells, there are low affinity transporters for choline such as high affinity transporters [Matthies, et al., (2006)].

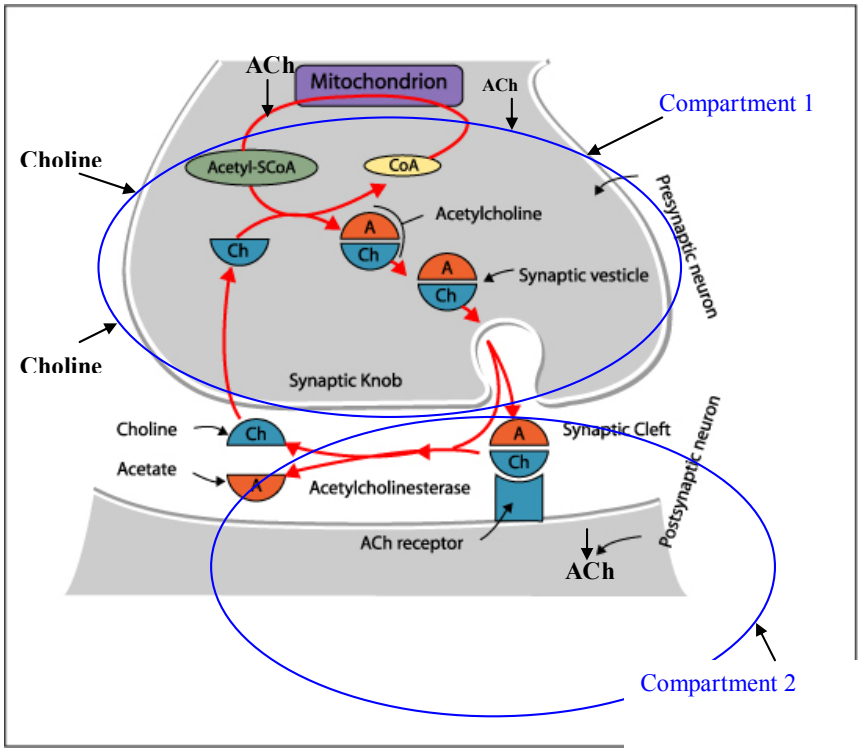

Figure 3-1: Schematic of synaptic neurons and cleft

"This image has been reproduced from AnaesthesiaUK with permission (www.AnaesthesiaUK.com)

The free choline in the blood plasma shares in a different fraction for supplying choline required for ACh synthesis based on the type of living beings. For example, Tucek (1978) showed that free choline contributes with 12% in rats, 50% in rabbits, and 80% in mice. Choline produced in synaptic gaps by the hydrolysis of ACh is re-utilized for the synthesis of ACh in presynaptic nerve endings (Tucek 1978). Therefore, choline recycled plays an important role in the synthesis of ACh and represent with around 50% of the choline utilized in the synthesis of ACh. Because the blood-brain barriers inhibit crossing plasma choline, the capillary endothelia of the brain overcomes this problem by choline carriers which work by facilitated diffusion similar to that for the neutral amino acids [Carl Faingold and Gerhard (1991)]. Although choline transports from blood to brain after the

consumption of high diet , the effluent of choline from brain to blood confirm the production of choline in brain by the hydrolysis of compounds containing choline such as phospholipids and ACh [Tucek (1985), Carl Faingold and Gerhard (1991)].

Several studies [Shawn et al., (2004), Pinthong, (2008), Mullen et al., (2007), Michel et al., (2006)] indicate that external choline in the environment outside the presynaptic terminal may play an important role for regulating the dynamics of ACh. There are a lot of arguments about the source of choline required for ACh synthesis in brain, However, it is thought that the sources exist outside the cholinergic neuron and contain three main sources: the first is choline generated from the hydrolysis of ACh, the second source is choline in the form of phospholipids and the third sources is free choline in plasma [Wecker and Dettbarn (1978), Tucek (1978); Kewitz et al., (1975); Ansell and Spanner (1975)].

Acetyl-CoA is synthesized actually in the mitochondria of the presynapic neurons. Acetyl-CoA plays an important role in the metabolic reactions. It supplies the acetyl group for catabolism of the synthetic reactions, energy production, and cell growth. However, the process of transport of acetyl CoA from inside of the mitochondria through the membranes to the cytoplasm of the presynaptic neuron is not understood [Tucek (1984); Carl Faingold and Gerhard (1991)]. Acetyl CoA is formed from acetate by the enzyme acetyl-CoA synthase. It has been found that acetate can influence the central nervous system (CNS) [Carmichael et al., (1991)]. In addition to the function of Acetyl CoA as a substrate for the synthesis of ACh, it can be used for energy generation [Yuri et al., (2003), Tucek (1978), Carmichael et al., (1991)].

Kwok et al., (1982) investigated the role of delivery of acetyl-CoA to obtain high levels of synthesied ACh in stimulated ganglia. They found that the high delivery acetyl-CoA was not affected when ACh release decreased. This leads to the strong possibility that it does not seem likely that acetyl-CoA delivery is the only factor involved in regulating ACh synthesis in ganglia [Yuri et al., (2003), Kwok et al., (1982)]. One of these factors is choline uptake from the synaptic cleft to the presynaptic neuron for ACh synthesis [Tucek (1990), Tucek, (1988); Cooper., (1994)].

To simulate the hydrolysis, excitation and synthesis processes of ACh, artificial membranes immobilized with the enzymes have been applied. Santos et al., (2006) found that an action potential difference in the form of hysteresis when they used artificial membranes immobilized with AChE and injected ACh in one side of the membranes. Because the enzymatic reactions were accompanied by production of H^+, an auto-catalytic behavior will be dominated in the system (Santos et al., (2006);

Mustafa et al., a, b (2009)). Moreover, the hysteresis of the action potential differences will exist in the form the internal pH because of the amphoteric properties of the membrane.

Elnashaie et al. (1995) studied the neurocycle of the ACh system utilizing with AChE as the only enzyme. They studied complexity phenomena including dynamic and static bifurcations and the different kinds of solutions existing in the system. Mahecha-Botero et al., (2004) investigated a simplified neurocycle for the ACh as a two compartment model in ChAT /AChE system and found that complex dynamic bifurcations, hysteresis, multiplicity, period doubling and period halving, as well as period adding and period subtracting dominated the dynamics of the system. Garhyan et al., (2006) presented the formulation of a diffusion-reaction model to simulate the behavior of AChE and ChAT coupled enzymes system. However they ignored the consideration of choline uptake in the system in the system in addition to the importance of ChAT enzyme activity in the presynaptic neurons. Hence, a lot of their results were out of the physiological range **[**Garhyan et al., (2006**),** Mahecha-Botero et al., (2004), Elnashaie et al. (1995), Elnashaie et al. (2005)]. It is not clear from previous findings whether the rate-limiting step in the overall synthesis of ACh in the human placenta is the availability of choline or acetate.

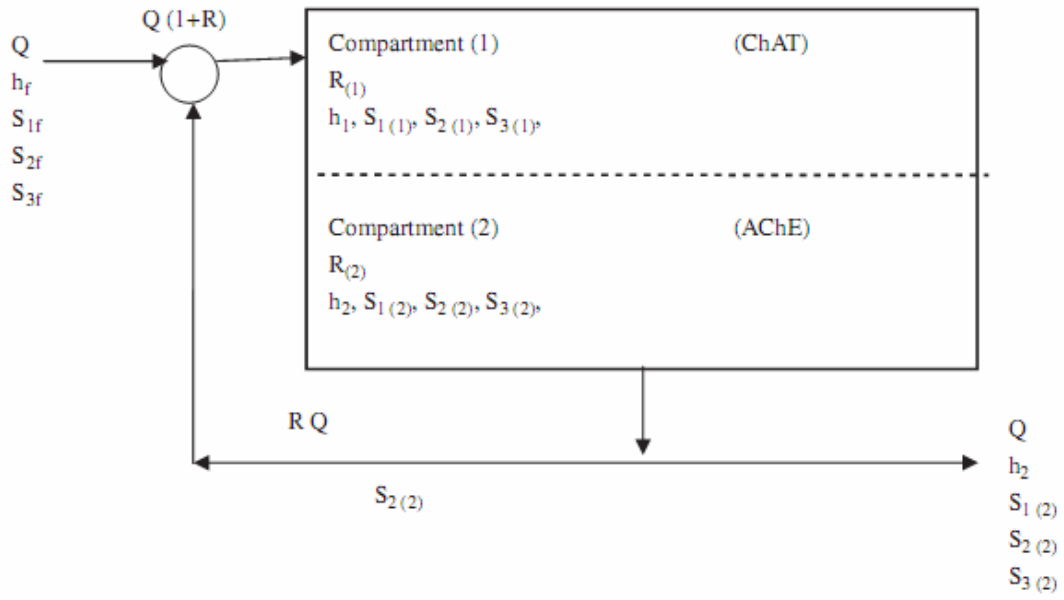

Figure 3-2: Two-enzyme/ two -compartment model

In this chapter we investigate the effect of choline and acetyl- CoA substrates on the performance of the cholinergic ACh system undertaken to increase our understanding of the

cholinergic system. We try to determine the role of each substrate and compare between them. The different solutions of the system at different feed choline and acetate concentration parameters will be analyzed. We will validate our results by comparing to physiological and experimental results and the results of previous models. We will depend on the previous two kinetic mechanisms (Mustafa et al., (2009)[a]): the first was for the synthesis of ACh by the enzyme ChAT and the other was for the hydrolysis of ACh by the enzyme AChE. We attempt to analyze the synthesis of ACh at the level of single cells, rather than the whole nervous system and try to investigate the role of feed (external) choline and acetyl CoA on the ACh processes. The present work extends up on our earlier investigation (Mustafa et al., 2009)a. Here we still employ a novel diffusion-reaction model but improve upon our previous investigation by considering realistic kinetic schemes and data for ChAT synthesis reaction, and account for the recycle effects of choline.

3.2 Formulation of the Diffusion Reaction Two-Enzyme /Two-Compartment Model

The (ChAT/AChE) enzymes system inside the neural synaptic cleft can be schematically described in a simplified manner as shown in Figure 3.1. All processes occurring in the ACh cholinergic system is treated as a two-enzyme/two-compartment system. As shown in Figure 3.1, compartment 1 represents the presynaptic neuron, and compartment 2 represents both the postsynaptic neuron and the synaptic cleft. Figure 3.1 shows that there is another stream of ACh entering compartment 1 coming by axonal transport which is called mobile ACh. The diagram shows that the choline is recycled from the synoptic cleft (compartment 2) into the presynaptic neuron terminal (compartment 1). Also Figure 3.1 shows that there are two resources of choline. The first one is produced by the hydrolysis of ACh, and then a part of it is recycled to the first compartment. The second stream is synthesized in the fluid environment outside the presynaptic neuron where choline in the latter stream comes either directly from the unbound choline in the blood plasma, or from the release of phospholipids in the brain cells (Tucek 1985). The choline produced in compartment 2 is the only component existing in the recycle stream. The physiological references such as Tucek et al., 1978 and 1985 confirmed this point where they did not refer to recycling of any other components such as ACh and acetyl CoA. As explained before, the acetyl CoA is synthesized in the mitochondria in a high quantity from pyruvate formed by the metabolism of glucose. All of these streams (The stream of axonal transport of ACh + The stream of choline synthesized in extracellular

space of compartment 1 + the stream of acetyl-CoA coming from mitochondria) are lumped in one feed stream which meets the recycle stream of choline coming from the hydrolysis of ACh to enter compartment 1 as shown in Figure 3.2. Figure 3.2 shows a simplified form of the feedback model of ACh neurocycle shown in Figure 3.1.

Figure 3.1 indicates that the ACh hydrolysis reaction, catalyzed by acetycholinesterase (AChE), occurs on ACh receptors which are located on the top of the postsynaptic neurons. Then the products of hydrolysis (Choline and Acetate) go through the synaptic cleft. We lumped those two areas together into one homogeneously stirred compartment which is compartment 2 instead of 3 or 4 or 5 compartment model because both the synaptic cleft and the post-synaptic neurons are interactive; in addition to avoid the expected complexity and difficulty to solve the model and analyze the results when the dimensionality is too high. The concentrations of components in compartment 2 represent the average concentrations in both the synaptic cleft and the post-synaptic neurons. Furthermore, we assumed that the flow rate of the feed stream to compartment 1 and that of the exit stream from compartment 2 are equal. In summary, each compartment is defined as a constant flow; constant volume, isothermal, continuous stirred tank reactor (CSTR) and the two compartments are separated by a permeable membrane. The ionization of the acetic acid is assumed to be completely in order to simplify the solution of the model. The diffusion and reaction events occurring in two contacted cholinergic neurons are explained by the two-enzyme two-compartment model. We assume that all processes occurring in the presynaptic neurons are homogeneous. We neglect the internal mass transfer process occurring between the synaptic vesicles and the surrounding cytoplasm in the presynaptic neurons.

The following rate equations explain both synthesis and hydrolysis reactions catalyzed by ChAT and AChE respectively, where $R_{(1)}$ represents the rate of synthesis and $R_{(2)}$ represents the rate of hydrolysis(Tucek (1990), Garhyan et al., (2006)) as follows:

$$R_{(1)}: \quad \text{Choline} + \text{Acetyl - CA} \xrightarrow{ChAT} \text{ACh} + \text{CoA} \qquad (1)$$

ACh is destroyed in compartment 2 by AChE by the degradation reaction as follows:

$$R_{(2)}: \quad \text{ACh} + \text{Water} \xrightarrow{AChE} \text{Choline} + \text{Acetate} + H^{+} \qquad (2)$$

Both $R_{(1)}$ and $R_{(2)}$ are considered to be substrate inhibited and pH-dependent. This leads to a non-monotonic dependence of the reaction rates on the substrates concentrations and pH. The rates can be formulated by employing certain assumptions and basic biokinetics knowledge as explained in the following section. The details of the derivation are given in our previous work (Mustafa et al., 2009)[a]. The final dimensionless forms of the ordinary differential equations of the eight state

variables are summarized in Table 3.1. The model equations are in terms of eight state variables: $h_1, h_2, s_{1(1)}, s_{1(2)}, s_{2(1)}, s_{2(2)}, s_{3(1)}$ and $s_{3(2)}$ and twenty five parameters (Tables 3.2 and 3.3). All values of the parameters and rates and differential equations are in the dimensionless form. All values of the parameters (with respective references) used in this investigation are given in Table 3.3.

3.3 Solution Techniques and Numerical Tools

The results of bifurcation diagrams for the system were obtained using XPPAUT and AUTO 2000, a bifurcation and continuation software for ordinary differential equations package (Ermentrout 2002). The software AUTO 2000 is able to perform bifurcation analysis, determining the stability of the solutions, and drawing the different solution branches. It has a lot of applications in both mathematics and engineering research areas because of its flexibility, efficiency and its multiple facilities. Both static and dynamic bifurcations can be performed by this software package (Ermentrout 2002). The eigenvalues of the differential equations determine the stability of the system. If all eigenvalues have negative real parts, the system will be stable otherwise, it will be unstable. It will undergo bifurcation, if there is an eigenvalue with zero real part. The dynamics results such as phase planes and time traces were obtained via FORTRAN programme. For the chaotic behavior, we used one- dimensional Poincare map to investigate the intersections in one direction between a hyperplan surface (Which is chosen at certain value of a state variable) and trajectories. (Garhyan et al., 2006; and Strogatz 1994). From discrete points of intersections, we are able to construct the bifurcation diagram of Poincare. Then we can investigate the dynamics behavior of the chaotic attractors. This is performed using IMSL libraries which contain DGEAR subroutine. Step size is chosen automatic based on the stiff differential equations during the investigations of the dynamics. Sometimes we used matlab to ensure the solution quality. The Poincare diagram is plotted using a program employed by Ibrahim et al., (2002) [Garhyan et al., 2006; Ibrahim et al., 1995, Elnashaie et al., 1984)].

Table 3-1: Dimensionless forms of the ordinary differential equations of the eight state variables

Item	Compartment	Differential equation
Hydrogen protons	1	$\frac{dh_{(1)}}{dT} = h_f - \gamma_1 \left(\frac{1}{h_f}\right) - \alpha_H \left(h_{(1)} - h_{(2)}\right) + \alpha_{OH}\gamma_1 \left(\frac{1}{h_{(1)}} - \frac{1}{h_{(2)}}\right)$
	2	$\frac{dh_{(2)}}{dT} = V_R(\alpha_H \left(h_{(1)} - h_{(2)}\right) - \alpha_{OH}\gamma_1 \left(\frac{1}{h_{(1)}} - \frac{1}{h_{(2)}}\right) - \left(h_{(2)} - \frac{\gamma_1}{h(2)}\right) + \frac{B_2}{k_{h1}} r(2))$
Acetylcholine	1	$\frac{ds_{1(1)}}{dT} = s_{1f} - \alpha_{s1}\left(s_{1(1)} - s_{1(2)}\right) + \frac{B_1 r(1)}{K_{s1}}$
	2	$\frac{ds_{1(2)}}{dT} = V_R(\alpha_{s_1}\left(s_{1(1)} - s_{1(2)}\right) - s_{1(2)} - \frac{B_2 r(2)}{K_{s1}})$
Choline	1	$\frac{ds_{2(1)}}{dT} = s_{2f} + R * s_{2(2)} - \alpha_{S2_1}\left(s_{2(1)} - s_{2(2)}\right) - \frac{B_1}{S_{2refernce}} r(1)$
	2	$\frac{ds_{2(2)}}{dT} = V_R(\alpha_{S2}\left(s_{2(1)} - s_{2(2)}\right) - (1+R) * s_{2(2)} + \frac{B_2}{S_{2reference}} r(2))$
Acetate	1	$\frac{ds_{3(1)}}{dT} = s_{3f} - \alpha_{S3}\left(s_{3(1)} - s_{3(2)}\right) - \frac{B_1}{S_{3refernce}} r(1)$
	2	$\frac{ds_{3(2)}}{dT} = V_R(\alpha_{S3}\left(s_{3(1)} - s_{3(2)}\right) - s_{3(2)} + \frac{B_2}{S_{3refernce}} r(2))$
Rate of synthesis ($r_{(1)}$)	1	$r(1) = \frac{\theta_1 s_{21} s_{31}}{\theta_2 / h_1 (h_1 + 1 + \delta h_1^2) + \theta_3 s_{31} + \theta_4 s_{21} + \theta_5 s_{21} s_{31}}$
Rate of hydrolysis ($r_{(2)}$)	2	$r(2) = \frac{s_{12}}{s_{12} + 1/h_2 (h_2 + 1 + \delta h_2^2) + \alpha s_{12}^2}$

Table 3-2: Dimensionless state variables, parameters and other terms

Dimensionless State Variables				
$h_{(j)} = \frac{[H^+]_{(j)}}{K_{h1}}$	Dimensionless hydrogen ion concentration in compartment j			
$s_{1(j)} = \frac{[S_1]_{(j)}}{K_{s1}}$	Dimensionless ACh concentration in compartment j			
$s_{2(j)} = \frac{[S_2]_{(j)}}{[S_2]_{reference}}$	Dimensionless choline concentration in compartment j			
$s_{3(j)} = \frac{[S_3]_{(j)}}{[S_3]_{reference}}$	Dimensionless acetate concentration in compartment j			
Dimensionless Membrane Permeabilities				
$\alpha_{H^+} = \frac{\alpha'_{H^+} A_M}{q}$	$\alpha_{OH^-} = \frac{\alpha'_{OH^-} A_M}{q}$	$\alpha_{S_1} = \frac{\alpha'_{S_1} A_M}{q}$	$\alpha_{S_2} = \frac{\alpha'_{S_2} A_M}{q}$	$\alpha_{S_3} = \frac{\alpha'_{S_3} A_M}{q}$
Dimensionless Kinetic Parameters for AChE Catalyzed Reaction: $\gamma_1 = \frac{K_W}{K_{i1}}$				
Dimensionless Kinetic Parameters for ChAT Catalyzed Reaction :				
$\theta_1 = Et(S_{2ref})S_{3ref}$	$\theta_2 = \frac{K_2 K_1}{K_2^{\backslash}}$	$\theta_3 = \frac{S_{3ref} K_1}{K_2^{\backslash}}$	$\theta_4 = \frac{S_{2ref}}{K_3 K_2^{\backslash}}$	$\theta_5 = \frac{(S_{2ref})S_{3ref}}{K_2^{\backslash}}$
Other Terms Used in Dimensionless Form:				
$V_R = \frac{V_{(1)}}{V_{(2)}}$	$T = \frac{qt}{V_{(1)}}$	$B_1 = \frac{V_1 V_{M1} \overline{ChAT}}{q}$	$B_2 = \frac{V_2 V_{M2} \overline{AChE}}{q}$	

Table 3- 3: Values of the kinetic Parameters

:**Parameter**	**Value**	**Reference**
θ_1	5.2(0.1)	Hersh & Peet (1977)
θ_2	12	Hersh & Peet (1977)
θ_3	1000	Hersh & Peet (1977)

θ_4	5	Hersh & Peet (1977)
θ_5	1	Hersh & Peet (1977)
α	0.5	Garhyan et al., (2006), Elnashaie et al., 1983a; Elnashaie et al., 1983b; Elnashaie et al., 1984; Elnashaie et al., 1995; Ibrahim et al., 1997)
δ	1	Garhyan et al., (2006), Elnashaie et al., 1983a; Elnashaie et al., 1983b; Elnashaie et al., 1984; Elnashaie et al., 1995; Ibrahim et al., 1997)
$K_a(k_h)$	$1.066*10^{-6}$ kMole/m^3(μMole/mm^3)	Garhyan et al., (2006), Elnashaie et al., 1983a; Elnashaie et al., 1983b; Elnashaie et al., 1984; Elnashaie et al., 1995; Ibrahim et al., 1997)
K_{s1}	$5.033*10^{-7}$ kMole/m^3(μMole/mm^3)	Garhyan et al., (2006), Elnashaie et al., 1983a; Elnashaie et al., 1983b; Elnashaie et al., 1984; Elnashaie et al., 1995; Ibrahim et al., 1997)
S_{2ref}	1.0×10^{-4} kMole/m^3(μMole/mm^3)	Guyton and Hall, 2000
S_{3ref}	1.0×10^{-6} kMole/m^3(μMole/mm^3)	Guyton Hall, 2000
B_1	5.033×10^{-5} kMole/m^3(μMole/mm^3)	Garhyan et al., (2006)
B_2	5.033×10^{-5} kMole/m^3(μMole/mm^3)	Garhyan et al., (2006)
α_{H^+}	2.25	Elnashaie et al., 1984
α_{OH^-}	0.5	Elnashaie et al., 1984
α_{S_1}	1	Elnashaie et al., 1984
α_{S_2}	1	Elnashaie et al., 1984
α_{S_3}	1	Elnashaie et al., 1984
V_R	1.2	Elnashaie et al., 1984
pH_f	8.2	Guyton, 2000

s_{1f}	15	Garhyan et al., (2006)
s_{2f}	1.15	Garhyan et al., (2006)
s_{3f}	3.9	Garhyan et al., (2006)
γ_1	0.01	Garhyan et al., (2006), Elnashaie et al., 1983a; Elnashaie et al., 1983b; Elnashaie et al., 1984; Elnashaie et al., 1995; Ibrahim et al., 1997)
R	0.8	Tucek (1978)

3.4 Physiological Values of the Parameters

To validate the results of the system with physiological and experimental results and with other models of previous investigators during the investigations of the change the system parameters, we should compare our system behavior with the following physiological values of ACh, choline, acetate, and pH. These values depend on experimental review and other models like that used by Garhyan et al. (2006) and Mahecha- Botero et al. (2004). The concentrations are given in (Kmol/m^3). Human brain pH in a feline model is found in the range of 6.95-7.35 [Zauner and Muizelaar(1997)] and pH in a human brain was found by (Rae et al., 1996) in the range 6.95 - 7.15. Free ACh in rat brain was found around 0.22×10^{-5} kmol/m^3 and total ACh was in found around 1.77×10^{-5} kmol/m^3. Tucek, 1990 and Garhyan et al., 2006 showed that in guinea pig cerebral cortex the range was 0.31×10^{-5} (free ACh) to 1.67×10^{-5} kmol/m^3 (total ACh) [Garhyan et al., (2006)].

Wessler et al. (2001) and Mahecha- Botero et al. (2004) reported that ACh concentration in human placenta in the range of 3.0×10^{-5} to 55.5×10^{-5} kmol/m^3. Mahecha- Botero (2004) showed that in the isolated rings of rat pulmonary artery ACh was measured to be in the range of 0.001×10^{-5} to 3.0×10^{-5} as pointed to Kysela and Torok, (1996). Mahecha- Botero (2004) and Garhyan et al. (2006) reported that choline concentration in mouse rat brain is about 1.15×10^{-4} kmol/m^3. This range was confirmed by Tucek (1978) and choline concentration in human plasma is in the range of 0.01×10^{-4} to 0.7×10^{-4} kmol/m^3 (Chay and Rinzel, 1981; Mahecha – Botero (2004) and Garhyan et al., (2006)).

The real concentration of ACh in cholinergic neurons of the brain is not known (Tucek 1978 and 1990). Despite the uncertainties associated with this estimate (the main being the proportion of cholinergic neurons in the total neuronal population of the brain), it is evident that, in the light of the present knowledge, the estimated equilibrium concentration of ACh (1.2×10^{-5} kmol/m^3) and the estimated concentration of ACh in cholinergic neurons (36×10^{-5} kmol/m^3) do not appear vastly different incompatible values. A higher concentration of ACh in presynaptic nerve endings might be achieved in two ways: by the accumulation of ACh in synaptic vesicles, and by higher concentration substrates in this part of neuron.

3.5 Results and Discussion

The diffusion-reaction biosystem bifurcation and chaotic behavior is extensively investigated using two bifurcation parameters: (A) Feed choline concentration (s_{2f}), (B) Feed acetate concentration (s_{3f}), All of these parameters are in the dimensionless form. The effects of each parameter are explained below:

3.5.1 Feed Choline Concentrations (s_{2f})

We investigate static and dynamic bifurcation due to the change of feed choline concentration. We studied the static bifurcation at a high value of the feed ACh concentrations s_{1f}=15 corresponding to 0.755 x10^{-5} kmol/m^3 as a medium value in the range of ACh in rat brain given by Tucek (1978) and the dynamic bifurcation at s_{1f}=2.4 corresponding to 0.12 x10^{-5} kmol/m^3 which is the lowest value in the range given by Tucek (1978). The range given by Tucek (1978) is $[0.12\times10^{-5}$ to $1.77\times10^{-5}]$ kmol/m^3. The bifurcation parameter (S_{2f}) is an independent parameter and represents the concentration of choline in the feed stream coming from either from the unbound choline in the blood plasma, or from the release of phospholipids in the brain cells or from both together before meeting the recycle stream. So that both of feed stream and recycle stream are independent and different.

Case (1): Static Bifurcation at s_{1f} =15 (corresponding to 0.755 x10^{-5} kmol/m^3)

Figure 3.3 shows the bifurcation diagrams with s_{2f} as the bifurcation parameter for a very wide range of values using fixed values of s_{1f} =15 and h_{1f} = 0.0062682 equivalent to pH=8.2. Only a static bifurcation in the form of hysteresis controlling system is found in this case. Figure 3.3 shows the static bifurcation through investigating the effect of changing the feed choline concentration (s_{2f}) on

the ACh concentrations (s_{11} and s_{12}) in compartments 1 and 2, choline concentration in compartment 1 (s_{21}) and acetate concentration in compartment 2 (s_{32}). Figures 5.3(a) and (b) , respectively, show that s_{11} and s_{12}, respectively, are increasing with increasing s_{2f} until certain a value of s_{2f} then s_{11} and s_{12} remain constant with further increase of s_{2f}. This is compatible with the experimental results done by Tucek (1990) and Lefresne (1973) who indicated that the content of ACh increases until it reaches a certain limiting value and then remains stable when the choline substrate concentration increases. However; s_{21} increases continuously as a function of s_{2f}. If we investigated the effect of s_{2f} on s_{22}, s_{22} will behave like s_{21} which will increase as s_{2f} increases. The ACh concentrations synthesized in both compartments 1 and 2 (s_{11}, s_{12}) are increasing with a high rate at $\left(s_{2f} \leq 13.8\right)$, however; at a high feed choline concentration $\left(13.8 \leq s_{2f}\right)$ corresponding to $\left(13.8 \text{ x } 10^{-4} \text{ kmole/m}^3 \leq s_{2f}\right)$, ACh is synthesized less efficiently from the feed choline concentration which accumulated in nervous tissue. This is in agreement with the results obtained by Schwartz et al., (1975) who indicated that at small concentrations of external choline, a big part of them was consumed to produce ACh and estimated in the range 60-75%, ; however, these valued reduced much when the external choline concentrations increased. Furthermore, our results are in agreement with the results obtained by Morel (1976) who found that when the available concentrations of choline in the cholinergic environment were plentiful, the fraction of acetate reacted with choline to produce ACh increased. Moreover, as choline was added highly, the ACh levels produced by the synthesis were unaltered. Furthermore, these results are compatible with the experimental results done by Weckler (1988) who showed that the ACh content was not affected in the presence of high concentrations of free choline released from brain cells in rats although there was a high necessity for new synthesized ACh. In addition; Weckler (1988) indicated that the capability of the brain neurons to synthesize new ACh decreased highly in the conditions of lack of available choline, where the brain cells become unable to release free choline.

Our results are in complete agreements with that done by Schwartz et al., (1975) who also found that the fraction of choline consumed to produce ACh at low external choline concentrations is higher than that at high choline concentrations. Therefore, ACh was synthesized considerably less efficiently from the excess choline which accumulated in the nervous tissue at external choline concentrations greater than about $30\text{x}10^{-4}$ kmole/m^3. In our model ACh was synthesized less efficiently when external choline concentration s_{2f} is about 25 corresponding to $25 * 10^{-4}$ kmole/m^3. From the constancy of ACh concentrations in both compartments in the presence of choline

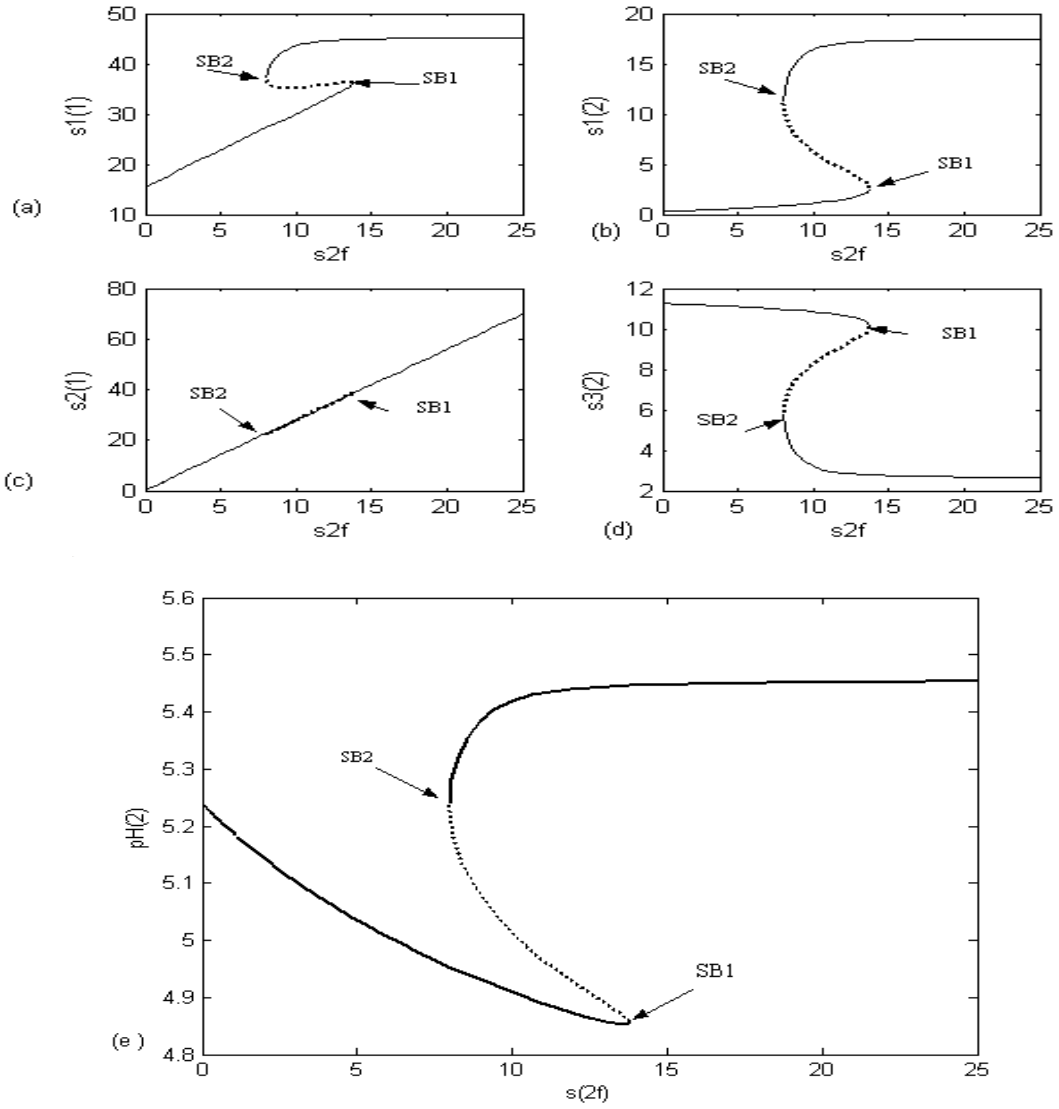

Figure 3-3: Bifurcation diagrams with choline feed concentration s_{2f} as the bifurcation parameter $(s_{1f} = 15)$ and the rest of data as shown in Table 3.3:

(a) Bifurcation diagram for ACh concentration in compartment 1(s_{11}), (b) Bifurcation diagram for ACh concentration in compartment 2(s_{12}). (c)Bifurcation diagram for choline concentration in compartment 1(s_{21}), (d) Bifurcation diagram for acetate concentration in compartment 2(s_{32}), and (e) Bifurcation diagram for pH in compartment 2 (pH_2).

concentrations higher than the critical value, i.e. $(13.8 \leq s_{2f})$ we can conclude that the release rate of ACh varied in parallel and in accordance to the incorporation rate of the feed choline (s_{2f}) to be catalyzed by the enzyme ChAT to produce ACh in compartment 1. The released transmitter in compartment 2 is compensated by synthesizing a new ACh in compartment 1. Therefore, the rate of ACh synthesis must be equivalent to the rate of transmitter release. These results confirm that the ChAT is inhibited by the excess concentrations of choline as a substrate. Another explanation is that this excess choline might be converted to an unknown material which is unable to be consumed to produce to ACh.

The results appearing in Figure 3.3 are in agreement with that obtained by Birks (1985) who showed that choline uptake from the synaptic cleft to the presynaptic neuron was the controlling factor for ACh synthesis where he has also shown that the relation between ACh synthesis and external choline fitted the Michaelis-Menten equation. Figure 5.3 (d) shows that s_{32} decreases as s_{2f} with increasing s_{2f} until certain value of s_{2f} then s_{32} remains constant with further increase of s_{2f}.

As the value of the bifurcation parameter s_{2f} increases while all other parameters are kept constant and shown in Table 3-3, different regions in the neurocycle are observed as shown in Figures 3.3 (a, b, c, d and e) as follows:

1. **Region 1**: High feed choline concentration in the region $(13.8 \leq s_{2f})$. In this region the system is characterized by a unique stable steady state and all the state variables except s_{21} change slightly while s_{21} increases continuously as shown in Figure 3.3 where s_{11} approaches a value close to 45 corresponding to 2.26 x10^{-5} kmol/m^3 and s_{12} close to 18(0.91x10^{-5} kmol/m^3) and s_{32} close to 3 corresponding to (3 x10^{-6} kmol/m^3). Figure 3.3(e) shows that pH_2 has its highest value of 5.4 which is close to the physiological values where Damsma et al., (1987) showed that the enzymatic conversion of choline and ACh was optimal between pH= 0.0 and pH= 5. However Mexel et al., (2006) showed that cortical brain pH across ranged from 5.80 to 6.95.

2. **Region 2:** $(7.9 \leq s_{2f} \leq 13.9)$

As s_{2f} is decreased, a hysteresis phenomenon occurs and a multiplicity of steady states is observed between the two static bifurcation points (SB_1 and SB_2). In this range there are two stable steady state solutions separated by unstable steady state solution (which is called saddle node). The multiplicity dominates the system between the two static bifurcation points where the second static bifurcation appears at s_{2f}=7.9. Hysteresis causes the state variables to be very sensitive in the neighborhood of the static bifurcation points. The hysteresis phenomenon has a vital significance where it reflects the

flexibility of the system to external disturbances as the shortage or plentiful feed choline concentration transported close to the static bifurcation points. For example, Figure 3.3(b) illustrates the s_{12} changes suddenly from 2.94345 to 18 corresponding to (0.15 and 0.91) x10^{-5} kmol/m^3 respectively with a slight increase in feed choline concentration near the static bifurcation point SB_1. This region fits reasonably well to the expected physiological behavior. Figure 3.3(a) shows that s_{11} varies in the range 36 to 45 corresponding to 1.8×10^{-5} and 2.26×10^{-5} kmol/m^3 while the dimensionless s_{12} varies in the range 3.5 and 18 corresponding to 1.75×10^{-5} and 9×10^{-6} kmol/m^3. Figure 3.3(e) shows that pH_2 is out of the expected physiological range and it is varying between 4.64 and 5.57. A reasonable explanation of this unexpected pH values is due to the assumption of fully ionization of acetic acid, i.e. one molecule of the acid gives a molecule of acetate ion and hydrogen ion , whereas, from 1-2% only of the acetic acid goes through ionization process. Hence, acetic acid may go through partial ionization not fully ionization process.

3. Region 3: Low feed choline concentration in the region $\left(0 \le s_{2f} \le 7.9\right)$

In this region there is a unique stable steady state. The values of the state variables in this region are close to the physiological values and follow the expected biological behavior Figure 3.3(a) shows that s_{11} vary between 15 and 27 corresponding to 7.5×10^{-6} and 13.5×10^{-6} kmol/m^3. Figure 3.3(b) shows that s_{12} varies between 0.002 and 2.98 corresponding to 0.0001×10^{-5} and 0.147×10^{-5} kmol/m^3. Figure 3.3(e) shows that pH_2 varies from 4.75 to 5.23. These results are in agreement with that of Schwartz et al., (1975) and Ismail et al., 1989. Schwartz et al., (1975) illustrated that at small concentrations of external choline, a big part of them was consumed to produce ACh and estimated in the range 60-75%; however, these valued reduced much when the external choline concentrations increased. Thus, the excessive choline which uptakes into the presynaptic neuron (compartment 1) becomes unavailable for the synthesis of ACh (Schwartz et al., (1975); Ismail et al., 1989). In our model, the ACh concentrations s_{11} increased about 67% due to increase of the s_{2f} then s_{11} became constant as s_{2f} increased.

Case (2): Dynamic Bifurcation at s_{1f}=2.4

Figure 3.4 shows the dynamic bifurcation diagrams using feed choline concentrations (s_{2f}) as the bifurcation parameter but with a different value of mobile feed substrate concentration

$(s_{1f} = 2.4)$ which represents a very low feed ACh concentrations. Figure 3.4 shows the complex behavior of the system through various stages in the neurocycle for a narrow range of the bifurcation parameter ($0.6\times10^{-4} \le s_{2f} \le 1.2\times10^{-4}$) kmol/m^3. It is clear that the system has rich dynamics phenomena at low concentration of s_{2f} where the feed choline concentrations are too small to start the synthesis reaction catalyzed by ChAT.

Figure 3.4 shows that there are three main observed regions in the bifurcation diagram, each one corresponding to a different form of qualitative behavior. There are two Hopf bifurcations (HBs). The first HB_1 appears at $s_{2f} = 0.69$ and the other HB_2 at $s_{2f} = 1.14085$. Mathematically HB point appears when the real parts of a pair of complex conjugate eigenvalues become negative, causing the system to undergo a bifurcation. HB_2 is defined as a "subcritical Hopf bifurcation" because a branch of unstable periodic orbits (appeared as empty circles) appears with a stable stationery branch at this point forming a separatrix between the basins of the attraction of the stable steady states. It is clear in this range of s_{2f} values, that the system demonstrates oscillatory behavior between the HB points. Hence, the periodic solution is the only solution available and the stationary points are not attractors anymore but repellent, and the limit cycles are the only attractors (periodic attractors) as illustrated in Figure 3.5**,** in which the behavior of state variables describe oscillatory solutions.

The oscillatory behavior in the range of feed choline concentration (range between HB_1 and HB_2) may play a vital role in the synthesis of ACh according to Santos et al., (2006). Solid bold curves represent stable steady state solutions and dashed lines represent the unstable steady states. Closed circles are used for stable orbits and the open circles for the unstable orbits. The oscillatory behavior represented by the branch between HB_1 and HB_2 (unstable zone) is also easily visualized in Figure 3.5 at s_{2f}=1.142 for ($0.914833 \le s_{2f} \le 1.14676$).

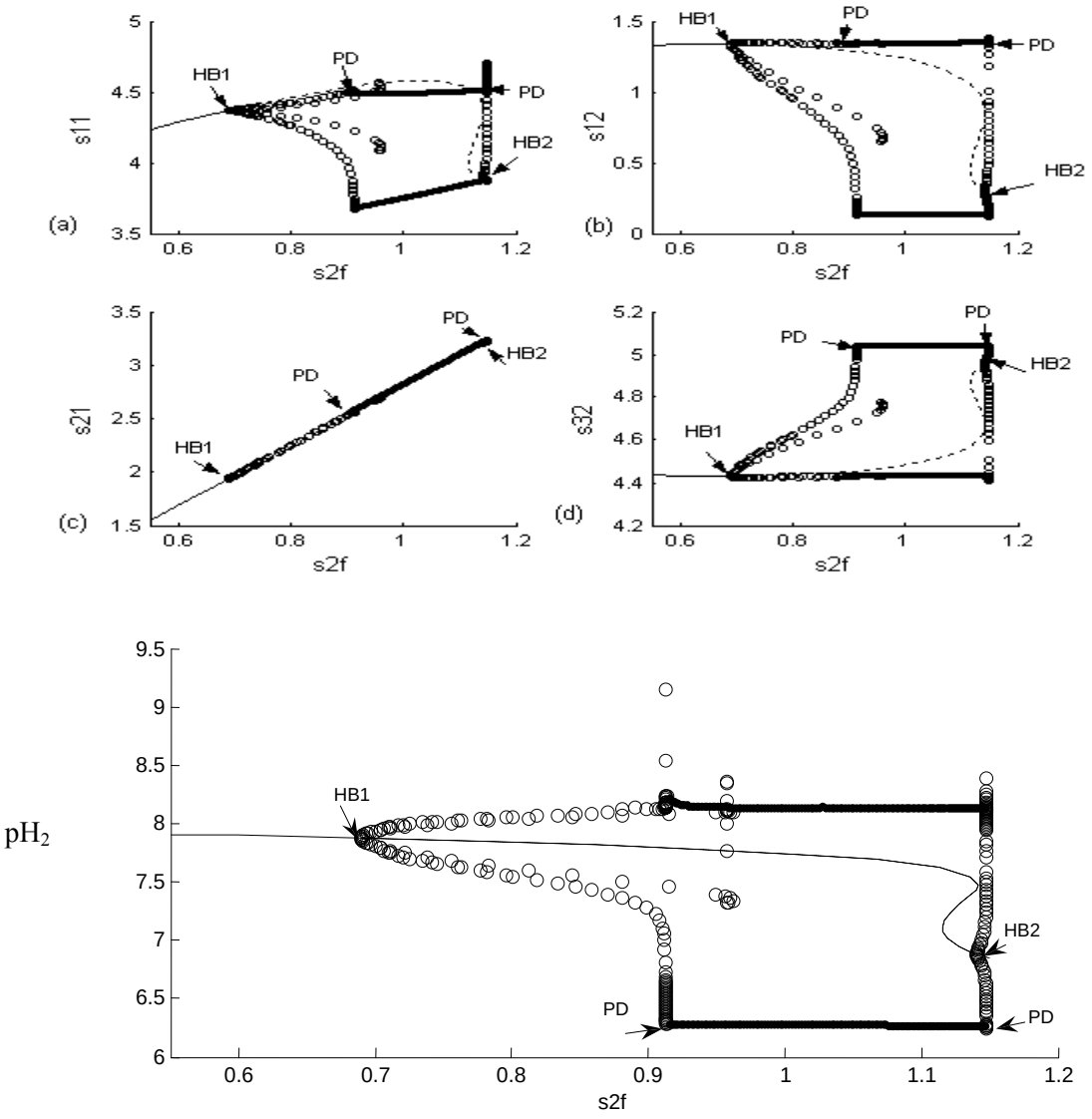

Figure 3-4: Bifurcation diagrams with choline feed concentration s_{2f} as the bifurcation parameter $(s_{1f} = 2.4)$ and the rest of data as shown in Table 3.3:

(a) Bifurcation diagram for ACh concentration in compartment 1 (s_{11}).,

(b) Bifurcation diagram for ACh concentration in compartment 2 (s_{12}).

(c) Bifurcation diagram for choline concentration in compartment 1(s_{21}),

(d) Bifurcation diagram for acetate concentration in compartment 2 (s_{32}), and

(e) Bifurcation diagram for pH in compartment 2(pH_2).

Initial conditions	
$h_{(1)}$	0.003796824
$h_{(2)}$	0.1405804
s_{11}	3.956
s_{12}	0.3
s_{21}	3.233
s_{22}	1.1606
s_{31}	8.2517318
s_{32}	4.9606

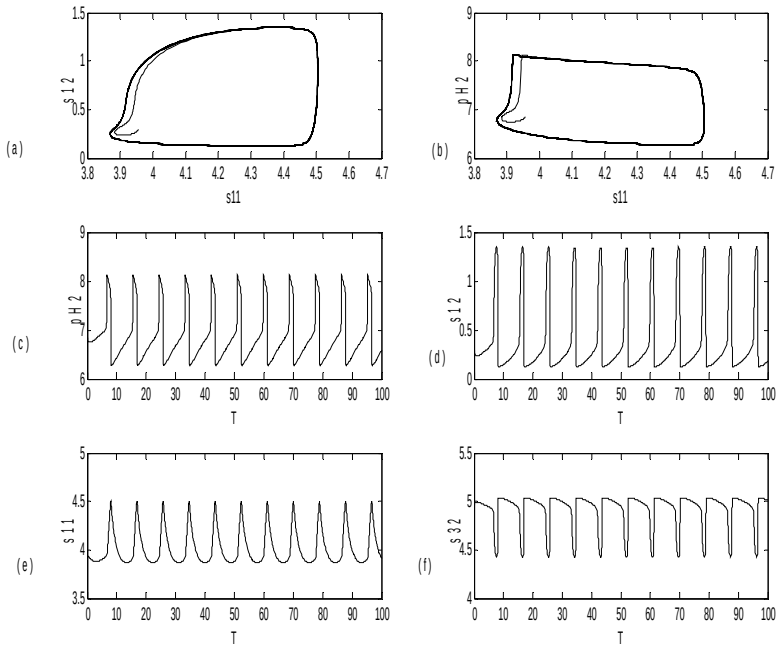

Figure 3-5: Dynamic characteristics $s_{2f} = 1.142$, s_{1f}=2.4, s_{3f}=3.9, and $h_f = 0.006268$ for different initial conditions:

(a) Phase plane for ACh in compartment 2 vs. the ACh in compartment 1.

(b) Phase plane for pH in compartment 2 vs. the ACh in compartment 1

(c) Time traces of pH in compartment 2 , (d) Time traces of ACh in compartment 2

(e) Time traces of ACh in compartment 1, and (f) Time traces of acetate in compartment 2

Initial conditions	
$h_{(1)}$	0.003796824
$h_{(2)}$	0.1405804
s_{11}	3.956
s_{12}	0.25
s_{21}	3.233
s_{22}	1.1606
s_{31}	8.2517318
s_{32}	4.9606

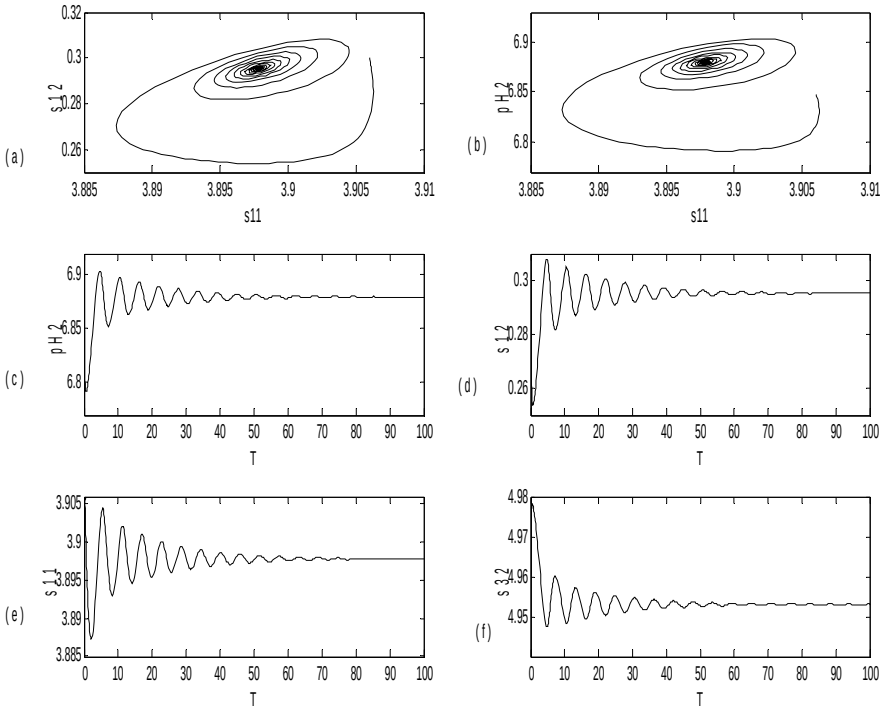

Figure 3-6: Dynamic characteristics $s_{2f} = 1.142$, s_{1f}=2.4, s_{3f}=3.9, and $h_f = 0.006268$ for the corresponding initial conditions.

(a) Phase plane for ACh in compartment 2 vs. the ACh in compartment 1.

(b) Phase plane for pH in compartment 2 vs. the ACh in compartment 1 ,

(c) Time traces of pH in compartment 2 , (d) Time traces of ACh in compartment 2

(e) Time traces of ACh in compartment 1, and (f) Time traces of acetate in compartment 2

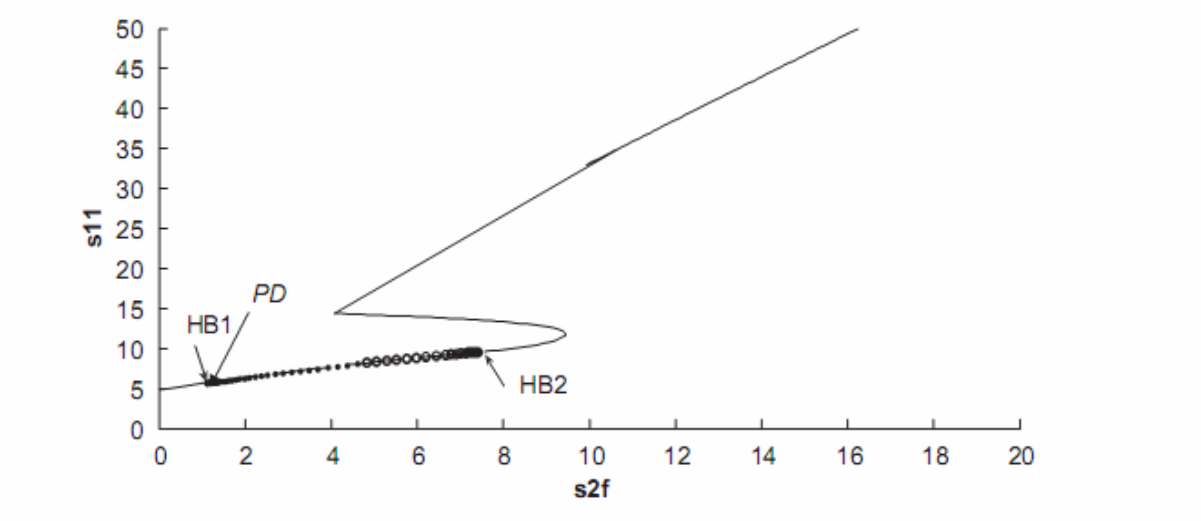

Figure 3-7: Bifurcation diagram showing the effect of s_{2f} on s_{11} at s_{1f}=4.5, s3f=2, B_1=0.0001, B_2=0.002, h_f=0.002 and the rest of parameters as shown in Table 5.3.

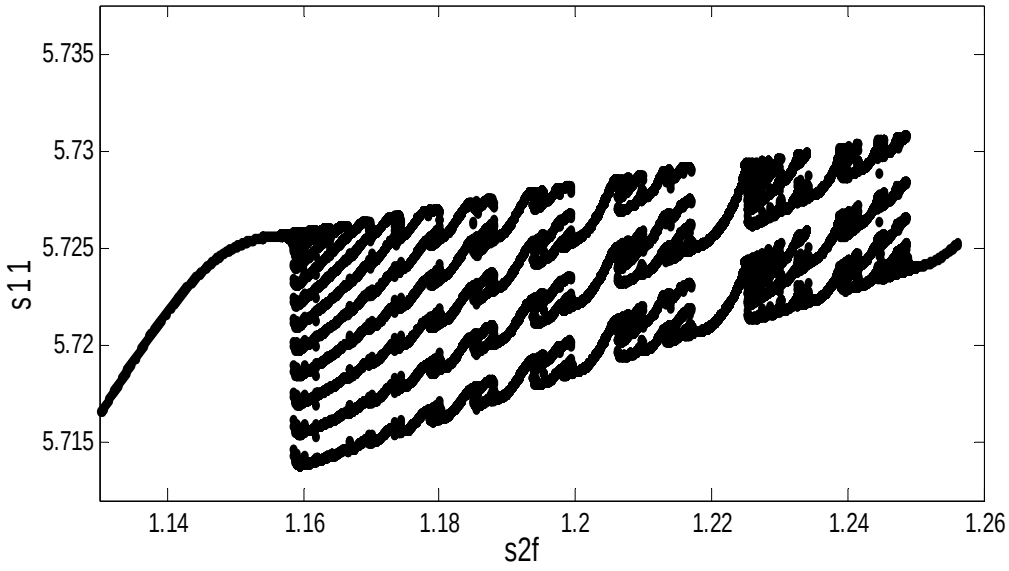

Figure 3-8: Poincare Bifurcation diagram: Poincare plane is located at s_{12} =0.3, s_{1f}=4.5, s_{3f}=2, h_f=0.002 and the rest of parameters as shown Table 5.3.

In the range ($1.14085 \le s_{2f} \le 1.14676$**) corresponding to (**$11.41 \times 10^{-5} \le s_{2f} \le 11.4676 \times 10^{-5}$**) kmole / m^3**, In this region, the phenomenon of bistability is appeared. It is observed that both point attractors and periodic attractors coexist with unstable periodic attractors (appeared as empty circles) separating them. The significance of the bistability is that the system can approach to both attractors (either point or periodic) at the same value of the bifurcation parameter s_{2f} based on the corresponding initial conditions.

Both periodic orbits and steady state stationery points exist together as shown in Figures 3.5 and 3.6. It is observed that the periodic orbits cease to exist when $s_{2f} \ge 1.14676$. The biochemical interpretation for the unstable waves in Figures 3.5 and 3.6 is that they occur as a consequence of the competition between diffusion processes from compartment 1 to compartment 2 and both enzyme reactions: the synthesis reactions catalyzed by the enzyme ChAT and the hydrolysis reactions catalyzed by the enzyme AChE.

The physiological values correspond to a range of feed choline concentration between 11.41×10^{-5} and11.4676×10^{-5}. The pH in compartment 2 (pH_2) is inside the physiological expected range where it is between 6.75 and 8.2. This region with low choline concentration is thus characterized by the presence of bistability. The period doubling (PD) points occur at s_{2f} = 0.913 and s_{2f} =1.147. The period doubling is one of the routes leading to chaos. The first initial conditions (Figure 3.5) lead to a periodic attractor, while the second initial conditions (Figure 3.6) lead to a point attractor. In addition, when initial conditions are changed in certain range, chaos will appear as will be shown in Figures 3. 8 and 3.9.

The amounts of choline and ACh associated with various times are also presented in Figure 3.6. The rate of decrease in acetate levels s_{32} is also the highest during the early portion of the period (Figure 3.6(f)), but when $T \ge 5$ (corresponding to$T \ge 62.5\mu se$), s_{32} begins to plateau around 4.96. After $T = 40$ (corresponding to 500μsec) there is no further change in the intracellular levels of acetate s_{32}. In contrast to the levels of acetate, the amount of ACh $s_{11}$and s_{12} as shown in Figures 3.6(e) and 3.6(d) increases in a high rate during the early portion of the incubation period then when $5 \le T$ began to plateau. When $40 \le T$ there was no significant change in the intracellular contents of s_{11} which approaches plateau around 3.898 (corresponding to 0.196 x 10^{-5} kmol/m^3) and s_{12} which is constant around 0.299 (corresponding to 0.015 x 10^{-5} kmol /m^3). Figure 3.6(c) shows that pH_2 increased rapidly during the early portion of the period, when $5 \le T$ pH_2 begins to plateau around 6.88. These results are in agreement with Steven and Peter (1984) who found that the rate of choline

consumption was very fast during the earlier portion of the reaction period and decreased as the reaction progressed.

In addition, our results are in accordance with Wecker and Dettbarn (1978) who indicated that the steady state concentration of ACh in discrete brain regions seems to be kept within small physiological ranges and the contents of ACh will be unaltered even choline concentrations increased. The constancy concentrations of ACh in compartment 1 may refer to the inhibition of the synthesis reactions by the excess concentration of choline.

There are different views about the available multiple origins in brain to be consumed for the synthesis of ACh, choline produced from the hydrolysis of ACh in compartment 2, plays a central role for supplying the presynaptic neurons with the required amount of choline (Wecker and Dettbarn (1978)).

Figure 3.5 shows that the amounts of choline and ACh at various times are also presented at the same values of the parameters such as Figure 3.6 but at different initial conditions. Figure 3.5 illustrates that all of pH_2, s_{11}, s_{12}, and s_{32} change periodically around the values that they arrived to plateau at in Figures 3.6.

Figure 3.7 shows the static bifurcation diagram at $h_f = 0.002$ (pH=8.69), $B_2 = 0.002$, B_1=0.0001 , and $s_{1f} = 4.5$ and the rest of the system parameters are shown in Table 3.3. The effect of s_{2f} as the bifurcation parameter on s_{11} is studied at the corresponding initial conditions, in order to investigate the fully developed chaotic behavior. In Figure 3.7 there are two Hopf bifurcation points, the first HB_1 point is at $s_{2f} = 1.094$, and the other is at $s_{2f} = 7.41$. PD appears at s_{2f}=1.25 where the periodic branch loses its stability giving rise to chaotic behavior at $s_{2f} = 1.16$ as will be shown in more details in Figure 3.7.

In addition, the region $1.16 \le s_{2f} \le 1.25$ is characterized by the presence of fully developed chaos (Figure 3.8). Chaos may develop via the well known Feigenbaum PD and period adding route (Feigenbaum, 1980) where PD appears at $s_{2f} = 1.25$. In order to have a full picture about the evolution of the chaotic behavior, Pioncare abstracted the time trace and phase plan representations to a comprehensive map where a hypothetical hyperplane surface is assumed to cross the trajectory in the state space, the Pioncare map accounts only for the intersections of the plan with the trajectories in only one direction [Just and Kantz (2000)].

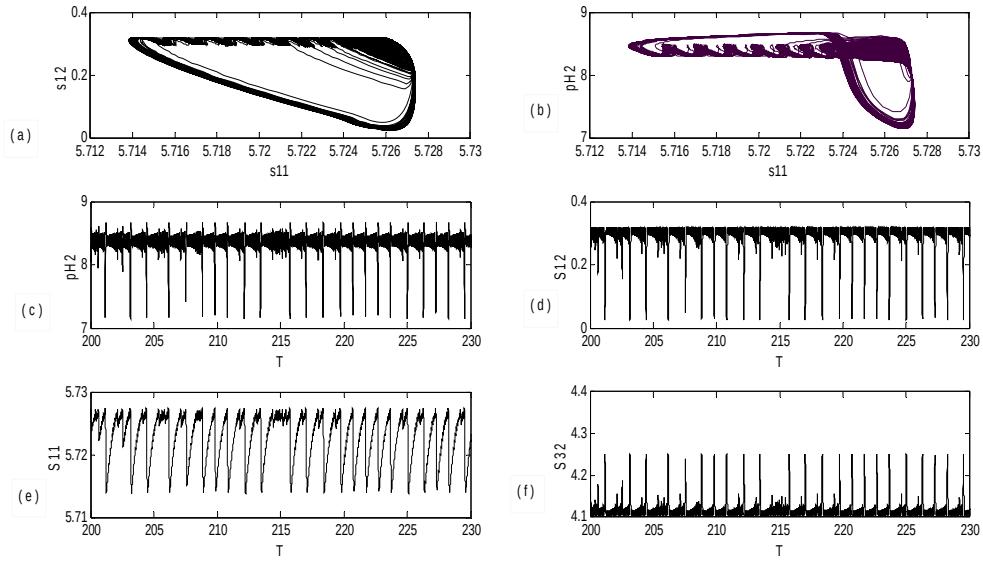

Figure 3-9: Dynamic characteristics at $s_{2f} = 1.15879999$, $s_{1f} = 4.5$, $s_{3f} = 2$, $h_f = 0.002$, $B_1 = 0.0001$, $B_2 = 0.002$ and the rest of the system parameters as shown Table 3.3

(a) Phase plane for ACh in compartment 2 vs. the ACh in compartment 1.

(b) Phase plane for pH in compartment 2 vs. the ACh in compartment 1

(c) Time traces of pH in compartment 2 , (d) Time traces of ACh in compartment 2

(e) Time traces of ACh in compartment 1 , and (f) Time traces of acetate in compartment 2

Figure 3.8 shows the Pioncare map of the region under consideration. It is clear that the evolution of chaotic behavior is via a period adding sequence. A periodic solution (limit cycle) on the phase plane appears as one point on Poincaré map. When PD takes place, period 2 appears as two points on the map, period 4 as four points, and so on. When chaos takes place, a complicated collection of points appears on Poincare map. The map is characterized also by wide regions of periodic windows of period two and period three. This map of Figure 3.8 is constructed using a Pioncare plan at $s_{12} = 0.3$. The periodic bifurcation sequence is characterized by PD sequence to chaos and periods adding sequence of periodic windows; these are summarized below:

Figure 3.8 shows that period one attractor appears at $s_{2f} = 1.25$ then evolution of chaos via PD appears as s_{2f} decreases. When the feed choline concentrations decreases to $s_{2f} = 1.23$, window of period two appears then evolution of chaos via PD follows. Window of period three at $s_{2f} = 1.21$

followed by evolution of chaos via period adding. Furthermore, when $s_{2f} = 1.2$ window of period four followed by evolution of chaos via period adding and window of period five appears at $s_{2f} = 1.19$ followed by evolution of chaos via period adding – window of period six at $s_{2f} = 1.17$ and so on where a cascade of further period adding occurs as s_{2f} decreases until $s_{2f} = 1.16$ the map becomes chaotic and the attractor changes from a finite to an infinite set of points. Time traces and phase planes are shown in Figure 3.9 and in Figure 3.10 at $s_{2f} = 1.15879999,$ and $s_{2f} = 1.158,$ respectively as chaotic attractors where it is shown that after an initial transient, the solution settles into an irregular oscillation that persists as time approaches infinity.

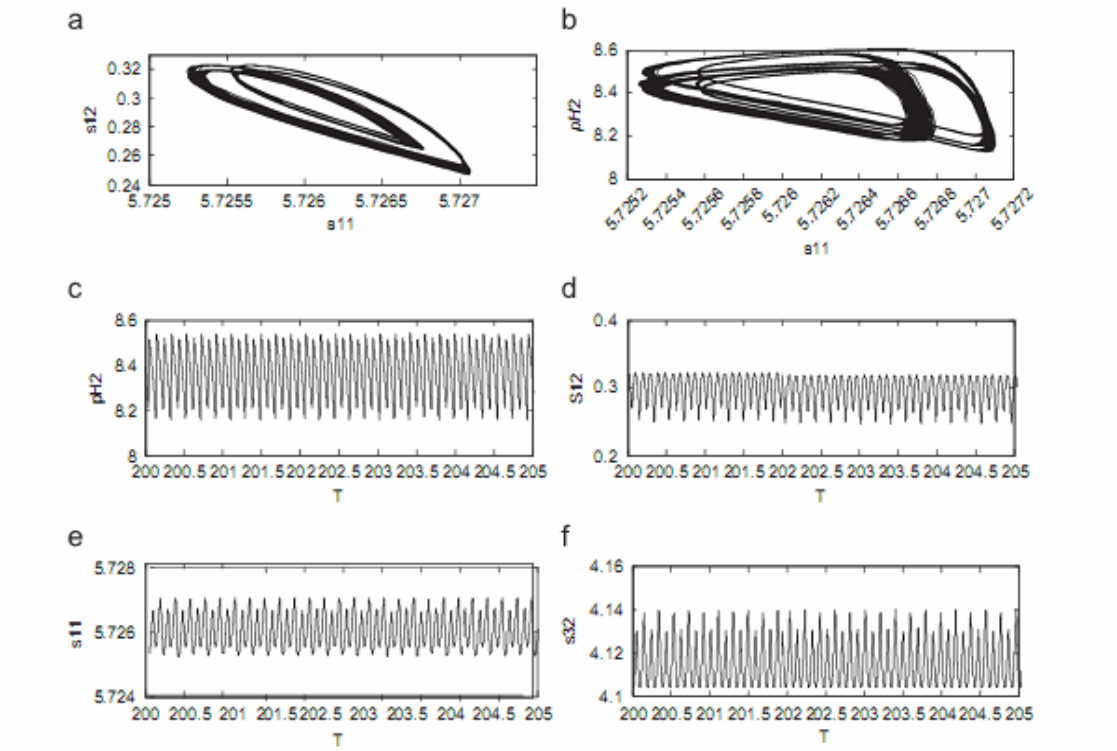

Figure 3-10: Dynamic characteristics at $s_{2f} = 1.158$, $s_{1f} = 4.5, s_{3f} = 2, h_f = 0.002,$ $B_1 = 0.0001,$ $B_2 = 0.002$ and the rest of the system parameters as shown Table 3.3.

(a) Phase plane for ACh in compartment 2 vs. the ACh in compartment 1.

(b) Phase plane for pH in compartment 2 vs. the ACh in compartment 1

(c) Time traces of pH in compartment 2 , (d) Time traces of ACh in compartment 2

(e) Time traces of ACh in compartment 1, and (f) Time traces of acetate in compartment 2

3.5.2 Feed Acetate Concentrations (s_{3f})

In the previous section it is well established that extracellular choline is returned into the presynaptic neurons to play a critical role to form the neurotransmitter ACh. The objective of the current section is to investigate the role of the feed acetate concentration and its effect on the levels of ACh, choline, and pH in both compartments. A comparison between the role of feed acetate and feed choline will be held.

We study static and dynamic bifurcations behaviors due to the change of feed acetate concentration as the bifurcation parameter. Like the previous section of the feed choline concentration, the static bifurcation is taken at high value of the feed ACh concentrations s_{1f}=15 and the dynamic bifurcation is at low value of the feed ACh concentrations s_{1f} = 2.4. The rest of parameter values are taken as shown in Table 3-3.

Case (1): Static Bifurcation Behavior at s_{1f}=15

Figure 3.11 shows the bifurcation diagrams with s_{3f} as the bifurcation parameter for a very wide range of values using a fixed value of $s_{1f} = 15.0$ and the rest of the parameters as shown in Table 3.3. It is clear as shown in Figure 3.11 that the effect of (s_{3f}) is very limited in comparison to that of (s_{2f}). For example, in Figure 3.11(a) the ACh concentration in compartment 1 (s_{11}) changes from 17.095 to 17.1071 corresponding to $8.6\text{x}10^{-6}$ and $8.61\text{x}10^{-6}$ kmol/m^3 respectively through the period of changing s_{3f} from very small concentrations (almost zero) to $s_{3f} = 30.0$ (corresponding to $s_{3f} = 30.0x10^{-6}$ kmole/m^3). Also, Figure 3.11(c) shows that the change in s_{21} is so limited and seems to be constant around 3.345. However, s_{32} increases continuously due to the incorporation of feed acetate as shown in Figure 3.11 (d). Figure 3.11 (e) shows that the change in pH_2 is also limited and stays around 5.81.

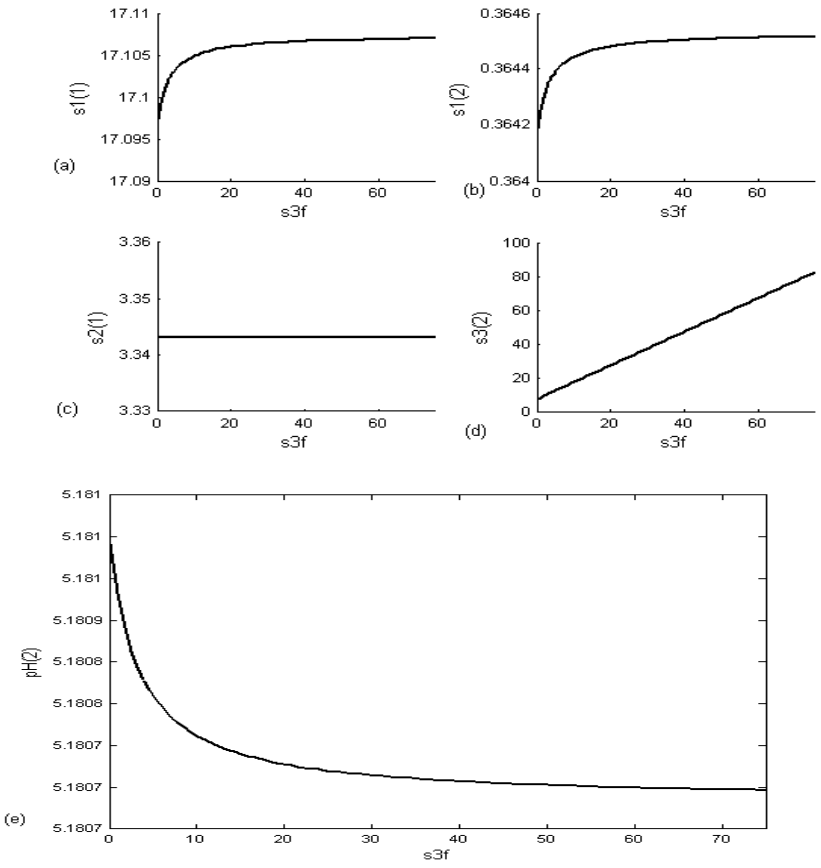

Figure 3-11: Bifurcation diagrams with acetate feed concentration s_{3f} as the bifurcation parameter $(s_{1f} = 15)$ and the rest of data as shown in Table 3.3

(a) Bifurcation diagram for ACh concentration in compartment 1(s_{11}), (b) Bifurcation diagram for ACh concentration in compartment 2(s_{12}). (c) Bifurcation diagram for choline concentration in compartment 1(s_{21}), (d) Bifurcation diagram for acetate concentration in compartment 2(s_{32})., and (e) Bifurcation diagram for pH in compartment 2 (pH_2).

These results are in agreement with the results of Morel (1976) who showed that as the feed acetate concentration increases, s_{11} increases then becomes constant when feed acetate concentrations reach $30x10^{-6}$ kmole/m^3. This means that for acetate concentrations equal to or higher than $30x10^{-6}$ kmole/m^3 , the maximal rate of incorporation is reached and they found that the total ACh was unchanged for a wide range of acetate concentrations in the incubation medium (0.01 to 30 $x10^{-6}$

kmole/m^3). One of the main reasons for this is that the limited concentration of choline is able to react with acetate to produce ACh. Another reason is the saturation of the enzyme ChAT with the excess concentration of feed acetate that transported into the presynaptic neuron. This confirmed the stability of ACh levels during the incubation. Therefore the effect of feed acetate on the incorporation of choline occurred without significant changes in the ACh content. In comparison to s_{3f}, it can be said that the feed choline concentration has more critical effect on the ACh synthesis and therefore it can be considered as the limiting substrate which is responsible for the observed maximum in ACh levels. Furthermore, our results agree with the experimental work of Kwok and Collier (1986) who investigated whether or not acetate plays a role in the supply of acetyl-CoA for ACh synthesis in the cat's superior cervical ganglion. They identified labeled ACh in extracts of ganglia. They concluded that acetate is not the main physiological acetyl precursor for ACh synthesis in this sympathetic ganglion, and that during preganglionic nerve stimulation. In their results, Kwok and Collier (1986) found that the increase of acetate concentration did not cause an increase in the synthesis of the ACh and they assured that the role of acetate in the synthesis of ACh appeared not understood. They could explain their results as the supply of acetate into the environment did not provide enough supply for acetyl-CoA to react with choline catalyzed ChAT. This gives a proper clarification for the constancy levels of ACh despite the continuous increase in acetate [Kwok and Collier (1986)].

From these findings, and our results, its can be concluded that it not enough to increase the concentrations of acetate to obtain high levels of ACh, and choline supply is the most important substrate in the ACh synthesis and it seems that feed choline (s_{2f}) is limiting for the ACh synthesis.

Case (2): Dynamic Bifurcation at s_{1f}=2.4

Figure 3.12 shows the dynamic bifurcation diagrams using feed acetate concentrations (s_{3f}) as the bifurcation parameter but with different values of feed ACh concentrations $(s_{1f} = 2.4)$ which represent very low feed ACh concentrations to study the dynamics of the ACh produced from the chemical reactions. In Figure 3.12 different stages in the neurocycle for a small range of the bifurcation parameter $(1 < s_{3f} < 4)$ corresponding to $((1x10^{-6} < s_{3f} < 4x10^{-6})$ kmol/m^3) are observed. It is clear that the system is in rich with the dynamics phenomena at low concentration of s_{3f} where the feed acetate concentrations are too small to start the synthesis reaction catalyzed by ChAT.

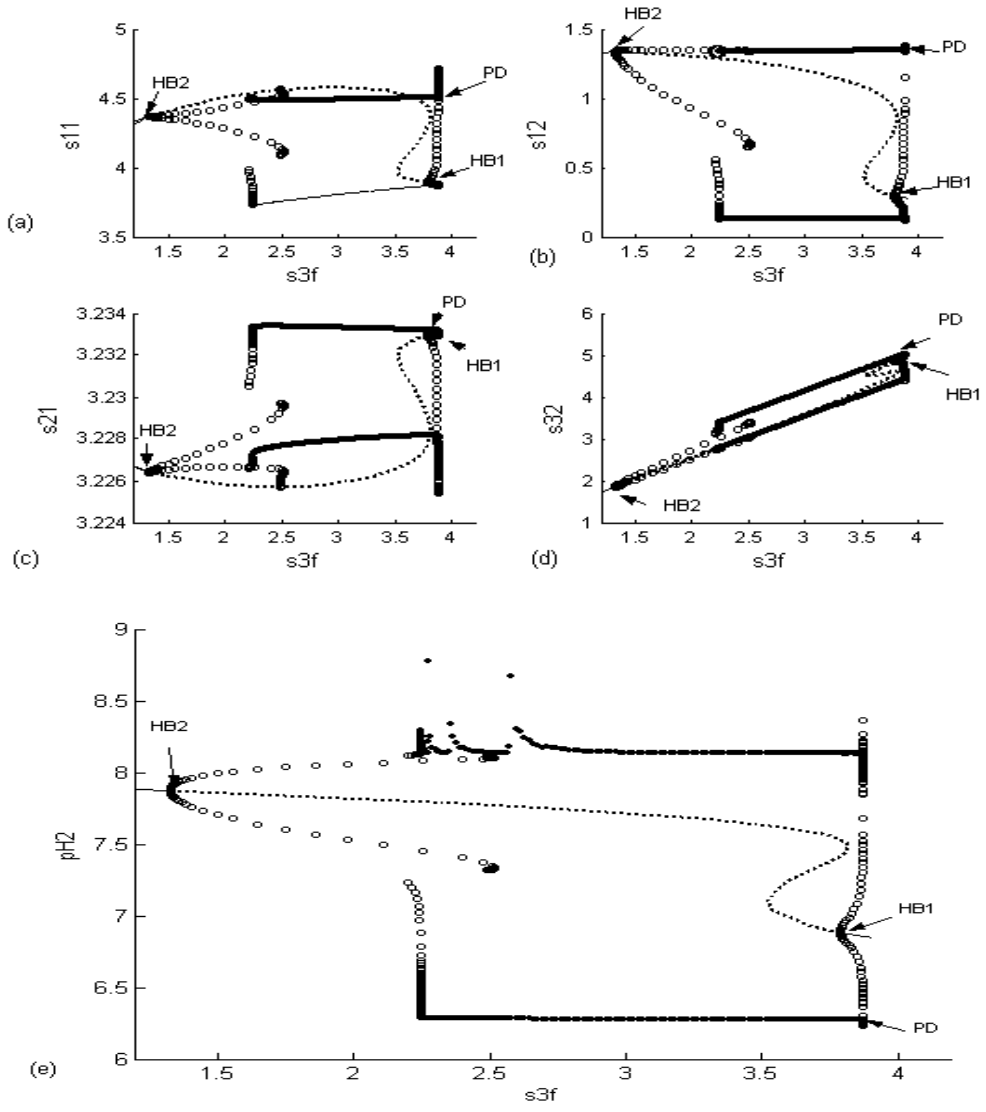

Figure 3-12: Bifurcation diagrams with acetate feed concentration (s_{2f}) as the bifurcation parameter at $(s_{1f} = 2.4)$ dimensionless and rest of data as shown in Table 3.3.

a) Bifurcation diagram for ACh concentration in compartment 1 (s_{11}), (b) Bifurcation diagram for ACh concentration in compartment 2(s_{12}), (c) Bifurcation diagram for choline concentration in compartment 1(s_{21}), (d) Bifurcation diagram for acetate concentration in compartment 2 s_{32}, and (e) Bifurcation diagram for pH in compartment 2 (pH_2).

Figure 3.12 shows that the system has a similar behavior like that in case (2) of changing of feed choline concentrations where three main regions appear in the bifurcation diagram each corresponding to a different qualitative behavior. As illustrated in Figure 3.12 there are two Hopf bifurcations (HBs): the first HB_1 at s_{3f} = 3.78656 and the other HB_2 appears at s_{3f} = 1.32614. It is clear as shown in the Figure 3.12, oscillatory behavior dominates the system between HB_1 and HB_2 where the steady state solutions (point attractor) are not an attractor and the periodic attractors are the only attractors.

In the range $(2.252 \le s_{3f} \le 3.865)$ corresponding to $(2.25\times10^{-6} \le s_{3f} \le 3.865\times10^{-6})$ kmol/m^3, the phenomena where both stable steady solutions and stable periodic solutions exist together at the same values of s_{3f} but at different initial conditions known as bistability is seen. Figure 3.12(e) shows that pH2 in the range of s3f between 2.25×10^{-6} and 3.865×10^{-6} kmol/m3 is inside the expected physiological range where it is between 6.35 and 8.3. PD point occurs at s_{3f} = 3.865 close to the first HB1 point. One of the main reasons leading to complexity is the high competition between the diffusion and the enzymatic processes in compartments 1 and 2. In addition; the recycle of choline contributes the complexity phenomena. In addition the high non-linearity of the reaction rates appeared due to the substrate inhibition and pH dependence contributes the complexity phenomena. This phenomenon is compatible with that obtained experimentally by Santos et al.(2006); Friboulet and Thomas (1982 and 1985).

3.6 Summary and Conclusions

In this chapter, the effects of both feed choline and acetate substrate concentrations on a coupled ChAT/ AChE enzymes system were investigated considering the choline reuptake into the presynaptic neuron. It is found that as the feed choline concentrations increase, ACh levels in both compartments increase gradually until $(s_{2f} = 25.6)$ where ACh is synthesized less efficiently when $(s_{2f} \ge 25.6)$. Hence, the release of ACh in compartment 2 varies in parallel to the incorporation of the choline in compartment 1 to produce ACh. The released ACh can be compensated by synthesizing new ACh in compartment 1 (s_{11}). Therefore, the rate of ACh synthesis must be equal to the rate of transmitter release. This is in agreement with the results obtained by Schwartz et al., (1975).

At low concentrations of the feed choline concentrations, it is found that the system exhibits complex dynamics bifurcation including chaotic behavior via a period doubling and period adding sequence in the range ($1.14085 \le s_{2f} \le 1.14676$). A bistability behavior is observed where periodic and point attractors coexist with an unstable periodic orbit as the separatrix separating the domains of attraction of the periodic and point attractors. Both steady state and periodic solutions coexist at the same value of s_{2f} in the previous range but at different conditions as shown in Figures 3.5 and 3.6. It can be concluded that the availability of choline into presynaptic neuron (compartment 1) at low external concentrations plays an effective role in synthesis of the transmitter. In addition, ACh was synthesized considerably less efficiently from the excess choline which accumulated in nervous tissue at external concentrations greater than about 30 $x10^{-4}$ kmole/m^3.

The results are analyzed based on the physiological values in order to simulate the ACh hydrolysis in the synaptic cleft in compartment 2. The system in case of external disturbances such as the sudden change of feed choline concentration to the presynaptic neurons could be affected by the hysteresis with a sudden increase in ACh concentration in both compartments (especially in compartment 2 where ACh concentration increases 6 folds from 1.76155×10^{-6} to 9.1×10^{-6} kmol/m^3 near SB_1 as shown in Figure 3.3(b) with a small variation in the input conditions thus simulating the sudden neural transmission.

It is found that the feed acetate concentrations have less effect on the synthesis of ACh in comparison to the feed choline concentrations. The system is in rich with the dynamics at low concentration of s_{3f} where the feed acetate concentrations are too small to start the synthesis reaction catalyzed by ChAT. From these findings, it can be concluded that it not enough to increase the concentrations of acetate to obtain high levels of ACh, and choline supply is the most important substrate in the ACh synthesis and it seems that feed choline (s_{2f}) is limiting for the ACh synthesis. The disturbances and irregularities appearing in the system in the form of chaotic behavior may be a good indication for the cholinergic diseases such as Alzheimer's disease.

Chapter 4

Effect of Cholineacetyltransferase Activity and Choline Recycle Ratio on Modelling, Bifurcation and Chaotic Behavior of Acetylcholine Neurocycle and Their Relation to Alzheimer's and Parkinson's Diseases

This chapter is an extension of the previous two chapters on the modeling and analysis of bifurcation, dynamics, and chaotic characteristics of the acetylcholine (ACh) neurocycle. The two-compartment model that takes into consideration the physiological events of the choline uptake into the presynaptic neuron and choline release in the postsynaptic neuron is modified. The effects of cholineacetyltransferase (ChAT) activity and choline recycle ratio as bifurcation parameters, on the system performance are studied. It is found that as ChAT activity increases, ACh concentration in the model compartments increases continuously. The effect of choline recycle ratio shows that choline uptake plays an important role for supplying choline as a substrate for the synthesis reaction by ChAT in compartment 1. The concentrations of ACh, choline and acetate in the compartments are affected by the choline recycle ratio through a certain range of the choline recycle ratio then they become constant as the choline recycle ratio increases further. A detailed bifurcation analysis over a wide range of parameters is carried out in order to uncover some important features of the system, such as hysteresis, multiplicity, Hopf bifurcation, period doubling, chaotic characteristics, and other complex dynamics. These findings are related to the real phenomena occurring in the neurons, like periodic stimulation of neural cells and non-regular functioning of ACh receptors. The results of this model are compared to the results of physiological experiments and other published models. As there is strong evidence that cholinergic brain diseases like Alzheimer's disease and Parkinson's disease are related to the concentration of ACh, the present findings are useful for uncovering some of the characteristics of these diseases and encouraging more physiological research. It is concluded from our results that choline recycled is the most critical factor in ACh processes in comparison to ChAT activity.

Keywords: Bifurcation, Acetylcholinesterase, Cholineacetyltransferase, Acetylcholine, Choline, recycle ratio, Neurocycle, Parkinson's disease, Alzheimer's disease, Dynamic behavior, Chaos.

4.1 Introduction

Acetylcholine (ACh) as a neurotransmitter plays a central role in all mental and physical activities such as neuromuscular junction, memory excitation and thinking [Brandon et al., 2004]. The ACh neurocycle system is involved in the following main processes: Firstly, the biosynthesis of ACh occurring is performed in the presynaptic neurons and catalyzed by the enzyme Cholineacetyltransferase (ChAT); the required substrates are choline and acetyl coenzyme A (Acetyl-CoA). Secondly, ACh is released by fusion of the membranes of the presynaptic neurons with synaptic vesicles storing ACh, where ACh reacts with the receptors of the postsynaptic neurons to cause the electrochemical signals. Thirdly, ACh is hydrolyzed by the acetylcholinesterase (AChE) enzyme in the synaptic cleft to produce acetate and choline. Fourthly, the choline which is produced from the hydrolysis reaction is recycled from the synaptic cleft to the presynaptic neurons to be reused in the synthesis of ACh [Brandon et al., (2004)].

ChAT is the enzyme responsible for the biosynthesis of the neurotransmitter ACh which was described by Nachmansohn and Machado in 1943. ChAT is supplied from the cell bodies of cholinergic neurons by the mechanism of axonal transport [Tucek (1978)]. ChAT is a globular protein with a molecular weight of about 68000 daltons. ChAT catalyses the synthesize reaction of ACh [Tucek (1978)]: Choline + acetyl-CoA = ACh + CoA.

The disorders in ChAT activity may result in various cholinergic diseases like Huntington's disease, Alzheimer disease, and multiple sclerosis (Nunes-Tavares et al., 2000). Because ChAT has a great value in the peripheral and central nervous systems and because of its role in problems related to the cholinergic systems, a lot of investigations have been concerned about ChAT (Waser et al., 1989, Nunes-Tavares et al., 2000). Many researchers investigated ChAT from different views. Some of them like Salvaterra (1987), and Malthe et al., (1978) took it from the view of molecular biology; however, others were concerned from the dynamics point of view (Sakamoto et al., 1990) and others focused on were interested it from cellular localization of ChAT like Nunes-Tavares et al., (2000), Levey *et al., (*1998) and Docherty *et al. (*1987).

Leventer et al., (1982) investigated the effect of ChAT inhibitors on the levels of ACh in the placental tissues and the release of ACh into the medium. They found that the levels of ACh reduced by 61.3 % and 75% when BETA and 2- benzoylethyl trimethylammonium pyridine were used as inhibitors respectively. These results show the effect of ChAT activity inhibitors on ACh synthesis and reflect the importance of keeping the activity of the ChAT enzyme in the neurons.

The presynaptic neurons have ChAT enzyme with a high activity to supply the process of biosynthesis of ACh [Brandon et al (2004)]. ChAT normally exists in the neurons where other types of cells such as glial cells are free of ChAT. However, in abnormal pathologic conditions, glial cells can contain ChAT (Tucek 1978). Furthermore, ChAT does not exist in all nerve cells. There is a view showing that ChAT is specific for cholinergic neurons, however; some researchers think that ChAT may be accompanied by other neurotransmitter- synthesizing enzymes [Tucek (1978); Eckenstein and Sofroniew (1983); Blusztajn and Wurtman (1983)]. Most of nervous parts such as caudate nuclei, putamen, retina and the spinal cords contain ChAT in a great activity [Kish et al., 1999; Tucek, 1978; Takeshi and Kumiko (2006)]. There is no strong indications proving that the blood platelets and corneal epithelium contain ChAT [Tucek (1978); Pedata (2006); Koichiro and Takeshi (2000)]. According to Chapter 2, acetyl-CoA is the only component in the presynaptic neurons which is synthesized in the nerve terminals, whereas ChAT is synthesized in the cell body of the neurons and transported into the presynaptic terminal by the axonal transport mechanism; choline is obtained from the environment outside the presynaptic neurons.

Brains of Alzheimer's disease are characterized by loss of ChAT activity. Hence, there is an observable reduction in ACh synthesis in presynaptic and postsynaptic neurons and ACh release. In addition, the extent of reduction in ChAT activity determines the extent of cognitive weakness [Keverne and Ray (2008); Perry et al., (1999); Keverne and Ray (2008)]. Milos et al., (2005) indicated that the deficit in ChAT activity leading to cognitive impairment can be considered as a differentiation between clinical and preclinical forms of Alzheimer's disease.

As indicated in Chapter 3, the brain is unable to synthesize choline. Hence it can obtain choline from many sources other such as free choline in blood plasma and choline produced from the release of choline-containing compounds such as phospholipids, and choline recycled produced from the hydrolysis of ACh.

The free choline in the blood plasma share in a different fraction for supplying choline required for ACh synthesis based on the type of living beings. For example, Tucek (1978) showed that free choline contributes with 12% in rats, 50% in rabbits, and 80% in mice. Choline produced in synaptic gaps by the hydrolysis of ACh is re-utilized for the synthesis of ACh in presynaptic nerve endings (Tucek 1978). Therefore, choline recycled plays an important role in the synthesis of ACh and represent with around 50% of the choline utilized in the synthesis of ACh. Because the blood-brain barriers inhibit crossing plasma choline, the capillary endothelia of the brain overcomes this problem by choline carriers which work by facilitated diffusion similar to that for the neutral amino

acids [Carl Faingold and Gerhard (1991)]. Although choline transports from blood to brain after the consumption of high diet , the effluent of choline from brain to blood confirm the production of choline in brain by the hydrolysis of compounds containing choline such as phospholipids and ACh [Tucek (1985); Carl Faingold and Gerhard (1991)].

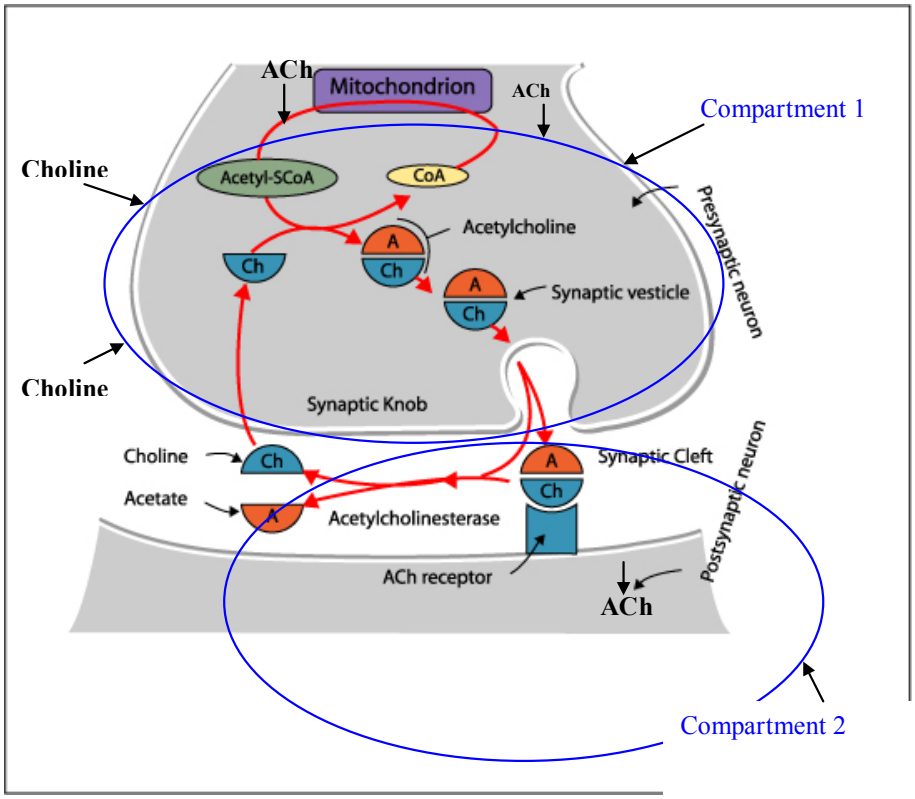

Figure 4-1: Schematic of synaptic neurons and cleft

"This image has been reproduced from AnaesthesiaUK with permission (www.AnaesthesiaUK.com)

Choline produced from the hydrolysis of ACh in the synaptic cleft is recycled to the presynaptic neurons. Approximately 50% of the choline utilized in the synthesis of ACh is believed to be recycled choline from ACh. Hence, choline uptake plays a significant role for supplying ChAT enzyme with the required amount of the substrate choline.

There are some researchers like Ehrenstein et al., (1997) and (2000) who investigated the relation between the deficient of the recycled choline supply to the presynaptic neurons and cholinergic diseases like Alzheimer's. They found that beta amyloid peptides aggregates can break

the membrane of the presyanptic membranes and cause leakage for choline outside. This leakage lead to a reduction of choline required for the enzyme ChAT resulting in a deficient of the synthesized ACh. There are other inhibitors such as hemicholinium-3 (HC-3) which inhibits choline transport (uptake) through the presynaptic membranes leading to reduction of the synthesized ACh levels in compartment 1 [Ferguson et al., (2004); Welsch (1976)].

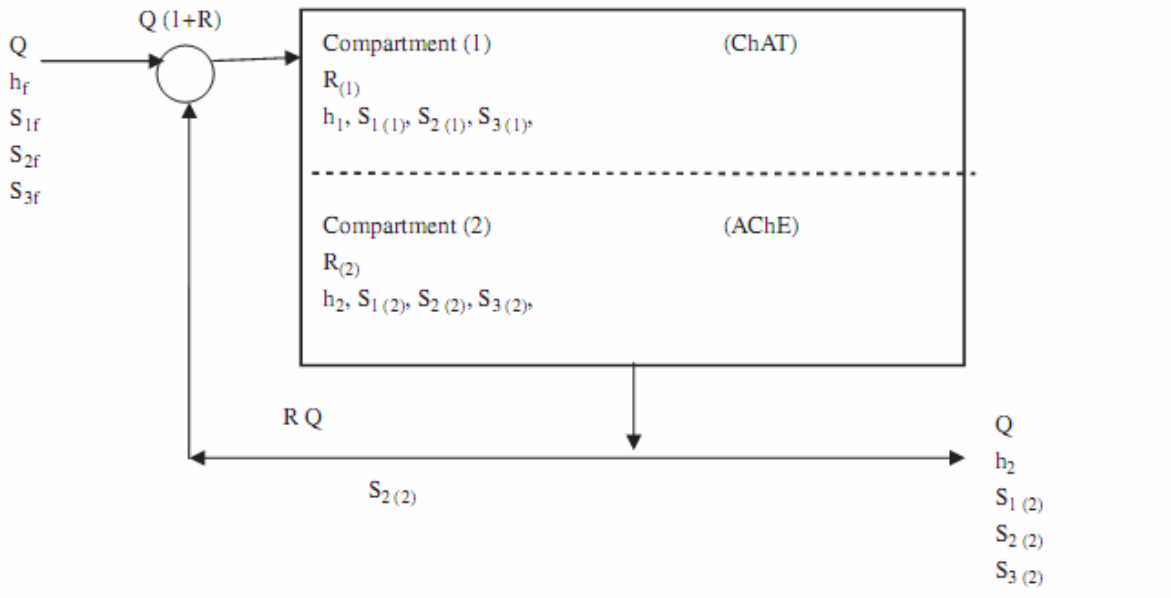

Figure 4-2: Two-enzyme/ two-compartment model

Elnashaie et al. (1995) studied the neurocycle of the ACh system utilizing with AChE as the only enzyme. They studied complexity phenomena including dynamic and static bifurcations and the different kinds of solutions existing in the system. Mahecha-Botero et al., (2004) investigated a simplified neurocycle for the ACh as a two compartment model in ChAT /AChE system and found that complex dynamic bifurcations, hysteresis, multiplicity, period doubling and period halving, as well as period adding and period subtracting dominated the dynamics of the system. Garhyan et al., (2006) built a mathematical model using kinetic data to investigate the nature of the ACh neurocycle system. They carried out a detailed bifurcation analysis over a wide range of parameters in order to uncover some important information related to the phenomena occurring in the physiological experiments, like periodic stimulation of neural cells and non-regular functioning of ACh receptors **[**Garhyan et al., (2006**),** Mahecha-Botero et al., (2004), Elnashaie et al. (1995), Elnashaie et al.

(2005))**.** However; they ignored the consideration of choline uptake in the system in addition to the importance of ChAT enzyme activity in the presynaptic neurons. Hence a lot of their results were out of the physiological range. It is not clear from these findings whether the rate-limiting step in the synthesis of ACh is the availability of choline or its transacetylation by ChAT. Therefore, an analysis of the uptake of choline from the synaptic cleft and its conversion to ACh is investigated to understand well the system of the ACh neurocycle [Steven et al., (1984); Hartmann et al., (2008)].

In previous chapters, we investigated the effect of feed choline, feed acetate (Mustafa et al., 2009b), and the effect of mobile ACh transport, feed hydrogen ions and AChE activity on the neurocycle effect (Mustafa et al., 2009a). We could determine the role of each parameter and the dynamics that each one behaves. It was concluded that the feed choline plays a more effective role than feed acetate concentrations. Furthermore, it was found that mobile feed ACh plays a vital role to reach the optimum levels of ACh in both compartments. The significant effect for hydrogen ions appeared at low concentration of feed hydrogen ions. A detailed study of complex static and dynamic behavior including bifurcation, instability, and chaos has been presented for each parameter.

In this chapter we investigate the effect of ChAT enzyme activity and choline recycle ratio on the ACh neurocycle based on the two kinetic mechanisms discussed in our previous work (Mustafa et al., 2009a). We analyze the synthesis of ACh at the level of single neuron cell, rather than the whole nervous system and investigate the role of ChAT enzyme activity and choline recycle ratio based on the choline uptake considerations. Our model extends up on two investigations (Mustafa et al., 2009 a, b) and the other investigations by Elnashaie and coworkers (Elnashaie et al., 1995; Mahecha-Botero et al., (2004) et al., 2004; Gahyran et al., 2006). Here we still employ a novel diffusion-reaction model but improve upon the previous investigations by considering realistic kinetic schemes and data for ChAT synthesis reaction, and account for the recycle effects of choline.

4.2 Formulation of the Diffusion-Reaction Two-Enzyme /Two-Compartment Model

The (ChAT/AChE) enzymes system inside the neural synaptic cleft can be schematically described in a simplified manner as shown in Figure 4.1. The complete neurocycle of the ACh as a neurotransmitter is simulated as a simplified two-enzyme/two-compartment model. As shown in Figure 4.1, compartment 1 refers to the presynaptic neuron, and compartment 2 refers to both the synaptic cleft and the postsynaptic neuron. The diagram shows that the choline is recycled from the synaptic cleft (compartment 2) into the presynaptic neuron terminal (compartment 1). Figure 4.1

shows that there is another stream of ACh entering compartment 1 coming by axonal transport. Also Figure 4.1 shows that there are two resources of choline. The first one is produced by the hydrolysis of ACh, and then a part of it is recycled to the first compartment. The second stream is synthesized outside presynaptic terminal where choline in the latter stream comes either directly from the free choline of the blood plasma, or from the brain cells, where it has been released from choline containing compounds (Tucek 1985). The choline produced in compartment 2 is the only component existing in the recycle stream. The physiological references such as Tucek et al., (1978) and (1985) confirm this point where they did not refer to recycling of any other components such as ACh and acetyl CoA. As explained before. Acetyl-CoA is synthesized in the mitochondria. The acetyl CoA should be plentiful since it is provided from pyruvate formed by the metabolism of glucose. All of these streams (the stream of axonal transport of ACh + the stream of choline synthesized in extracellular space of compartment 1 + the stream of Acetyl-CoA coming from mitochondria) are collected together in one feed stream which meets the recycle stream of choline coming from the hydrolysis of ACh to enter compartment 1 as shown in Figure 4.2. Figure 4.2 shows a simplified form of the feedback model of ACh neurocycle shown in Figure 4.1.

Figure 4.1 indicates that the ACh hydrolysis reaction, catalyzed by AChE, occurs on ACh receptors which are located on the top of the postsynaptic neurons. Then the products of hydrolysis (Choline and Acetate) go through the synaptic cleft. We lumped those two areas together into one homogeneously stirred compartment which is compartment 2 instead of 3 or 4 or 5 compartment model because both the synaptic cleft and the post-synaptic neurons are interactive ; in addition to avoid the expected complexity and difficulty to solve the model and analyze the results when the dimensionality is too high. The concentrations of components in compartment 2 represent the average concentrations in both the synaptic cleft and the post-synaptic neurons. Furthermore, we assumed that the flow rate of the feed stream to compartment 1 and that of the exit stream from compartment 2 are equal. In summary, each compartment is defined as a constant flow; constant volume, isothermal, continuous stirred tank reactor (CSTR) and the two compartments are separated by a permeable membrane.

The ionization of the acetic acid is assumed to be completely in order to simplify the solution of the model. The diffusion and reaction events occurring in two contacted cholinergic neurons are explained by the two-enzyme two-compartment model. We assume that all processes occurring in the presynaptic neurons are homogeneous. We neglect the internal mass transfer process occurring between the synaptic vesicles and the surrounding cytoplasm in the presynaptic neurons.

The following rate equations explain both synthesis and hydrolysis reactions catalyzed by ChAT and AChE respectively, where $R_{(1)}$ represents the rate of synthesis and $R_{(2)}$ represents the rate of hydrolysis(Tucek (1990), Garhyan et al., (2006)) as follows:

$R_{(1)}$: Choline + Acetyl - CA $\xrightarrow{ChAT}$ ACh + CoA (1)

ACh is destroyed in compartment 2 by AChE by the degradation reaction as follows:

$R_{(2)}$: ACh + Water $\xrightarrow{AChE}$ Choline + Acetate + H^+ (2)

Both $R_{(1)}$ and $R_{(2)}$ are considered to be substrate inhibited and pH-dependent. This leads to a non-monotonic dependence of the reaction rates on the substrates concentrations and pH. The rates can be formulated by employing certain assumptions and basic biokinetics knowledge as explained in the following section. The details of the derivation are given in our previous work (Mustafa et al., 2009)[a]. The final dimensionless forms of the ordinary differential equations of the eight state variables are summarized in Table 4.1. The model equations are in terms of eight state variables: $h_1, h_2, s_{1(1)}, s_{1(2)}, s_{2(1)}, s_{2(2)}, s_{3(1)}$ and $s_{3(2)}$ and twenty five parameters (Tables 4.2 and 4.3). All values of the parameters and rates and differential equations are in the dimensionless form. All values of the parameters (with respective references) used in this investigation are given in Table 4.3.

4.3 Solution Techniques and Numerical Tools

The results of bifurcation diagrams for the system were obtained using XPPAUT and AUTO 2000, a bifurcation and continuation software for ordinary differential equations package (Ermentrout 2002). The software AUTO 2000 is able to perform bifurcation analysis, determining the stability of the solutions, and drawing the different solution branches. It has a lot of applications in both mathematics and engineering research areas because of its flexibility, efficiency and its multiple facilities. Both static and dynamic bifurcations can be performed by this software package (Ermentrout 2002). The eigenvalues of the differential equations determine the stability of the system. If all eigenvalues have negative real parts, the system will be stable otherwise, it will be unstable. It will undergo bifurcation, if there is an eigenvalue with zero real part. The dynamics results such as phase planes and time traces were obtained via FORTRAN programme. For the chaotic behavior, we used one- dimensional Poincare map to investigate the intersections in one direction between a hyperplan surface (Which is chosen at certain value of a state variable) and trajectories. (Garhyan et al., 2006; and Strogatz 1994). From discrete points of intersections, we are able to construct the bifurcation diagram of Poincare. Then we can investigate the dynamics behavior of the chaotic

attractors. This is performed using IMSL libraries which contain DGEAR subroutine. Step size is chosen automatic based on the stiff differential equations during the investigations of the dynamics. Sometimes we used matlab to ensure the solution quality.

Table 4-1: Dimensionless forms of the ordinary differential equations of the eight state variables

Item	Compartment	Differential equation
Hydrogen protons	1	$\frac{dh_{(1)}}{dT} = h_f - \gamma_1 \left(\frac{1}{h_f}\right) - \alpha_H \left(h_{(1)} - h_{(2)}\right) + \alpha_{OH}\gamma_1 \left(\frac{1}{h_{(1)}} - \frac{1}{h_{(2)}}\right)$
	2	$\frac{dh_{(2)}}{dT} = V_R(\alpha_H \left(h_{(1)} - h_{(2)}\right) - \alpha_{OH}\gamma_1 \left(\frac{1}{h_{(1)}} - \frac{1}{h_{(2)}}\right) - \left(h_{(2)} - \frac{\gamma_1}{h_{(2)}}\right) + \frac{B_2}{k_{h1}} r(2))$
Acetylcholine	1	$\frac{ds_{1(1)}}{dT} = s_{1f} - \alpha_{s_1}\left(s_{1(1)} - s_{1(2)}\right) + \frac{B_1 r(1)}{K_{s1}}$
	2	$\frac{ds_{1(2)}}{dT} = V_R(\alpha_{s_1}\left(s_{1(1)} - s_{1(2)}\right) - s_{1(2)} - \frac{B_2 r(2)}{K_{s1}})$
Choline	1	$\frac{ds_{2(1)}}{dT} = s_{2f} + R * s_{2(2)} - \alpha_{s_2}\left(s_{2(1)} - s_{2(2)}\right) - \frac{B_1}{S_{2refernce}} r(1)$
	2	$\frac{ds_{2(2)}}{dT} = V_R(\alpha_{s_2}\left(s_{2(1)} - s_{2(2)}\right) - (1+R) * s_{2(2)} + \frac{B_2}{S_{2reference}} r(2))$
Acetate	1	$\frac{ds_{3(1)}}{dT} = s_{3f} - \alpha_{s_3}\left(s_{3(1)} - s_{3(2)}\right) - \frac{B_1}{S_{3refernce}} r(1)$
	2	$\frac{ds_{3(2)}}{dT} = V_R(\alpha_{s_3}\left(s_{3(1)} - s_{3(2)}\right) - s_{3(2)} + \frac{B_2}{S_{3refernce}} r(2))$
Rate of synthesis (r_1)	1	$r_{(1)} = \frac{\theta_1 s_{21} s_{31}}{\theta_2 / h_1 (h_1 + 1 + \delta h_1^2) + \theta_3 s_{31} + \theta_4 s_{21} + \theta_5 s_{21} s_{31}}$
Rate of hydrolysis (r_2)	2	$r_{(2)} = \frac{s_{12}}{s_{12} + 1/h_2 (h_2 + 1 + \delta h_2^2) + \alpha s_{12}^2}$

Table 4-2: Dimensionless state variables, parameters and other terms.

Dimensionless State Variables	
$h_j = \frac{[H^+]_j}{K_{h1}}$	Dimensionless hydrogen ion concentration in compartment j
$s_{1j} = \frac{[S_1]_j}{K_{s1}}$	Dimensionless acetylcholine concentration in compartment j
$s_{2j} = \frac{[S_2]_{(j)}}{[S_2]_{reference}}$	Dimensionless choline concentration in compartment j
$s_{3j} = \frac{[S_3]_j}{[S_3]_{reference}}$	Dimensionless acetate concentration in compartment j
Dimensionless Membrane Permeabilities	
$\alpha_{H^+} = \frac{\alpha'_{H^+} A_M}{q}$	$\alpha_{OH^-} = \frac{\alpha'_{OH^-} A_M}{q}$
$\alpha_{S_1} = \frac{\alpha'_{S_1} A_M}{q}$	$\alpha_{S_2} = \frac{\alpha'_{S_2} A_M}{q}$
$\alpha_{S_3} = \frac{\alpha'_{S_3} A_M}{q}$	
Dimensionless Kinetic Parameters for *AChE* Catalyzed Reaction	
$\gamma_1 = \frac{K_W}{K_{i1}}$	
Dimensionless Kinetic Parameters for *ChAT* Catalyzed Reaction	
$\theta_1 = Et(S_{2ref})S_{3ref}$	$\theta_2 = \frac{K_2 K_1}{K_2^{\backslash}}$
$\theta_3 = \frac{S_{3ref} K_1}{K_2^{\backslash}}$	$\theta_4 = \frac{S_{2ref}}{K_3 K_2^{\backslash}}$
$\theta_5 = \frac{(S_{2ref})S_{3ref}}{K_2^{\backslash}}$	

Other Terms Used in Dimensionless Form	
$V_R = \frac{V_{(1)}}{V_{(2)}}$	$T = \frac{q\,t}{V_{(1)}}$
$B_1 = \frac{V_1 V_{M1} \overline{ChAT}}{q}$	$B_2 = \frac{V_2 V_{M2} \overline{AChE}}{q}$

Table 4- 3: Values of the kinetic Parameters

:**Parameter**	**Value**	**Reference**
θ_1	5.2(0.1)	Hersh & Peet (1977)
θ_2	12	Hersh & Peet (1977)
θ_3	1000	Hersh & Peet (1977)
θ_4	5	Hersh & Peet (1977)
θ_5	1	Hersh & Peet (1977)
α	0.5	Garhyan et al., (2006), Elnashaie et al., 1983a; Elnashaie et al., 1983b; Elnashaie et al., 1984; Elnashaie et al., 1995; Ibrahim et al., 1997)
δ	1	Garhyan et al., (2006), Elnashaie et al., 1983a; Elnashaie et al., 1983b; Elnashaie et al., 1984; Elnashaie et al., 1995; Ibrahim et al., 1997)
$K_a(k_h)$	$1.066*10^{-6}$ kMole/m^3(μMole/mm^3)	Garhyan et al., (2006), Elnashaie et al., 1983a; Elnashaie et al., 1983b; Elnashaie et al., 1984; Elnashaie et al., 1995; Ibrahim et al., 1997)
K_{s1}	$5.033*10^{-7}$ kMole/m^3(μMole/mm^3)	Garhyan et al., (2006), Elnashaie et al., 1983a; Elnashaie et al., 1983b; Elnashaie et al., 1984; Elnashaie et al., 1995; Ibrahim et al., 1997)

S_{2ref}	1.0×10^{-4} kMole/m^3(μMole/mm^3)	Guyton and Hall (2000)
S_{3ref}	1.0×10^{-6} kMole/m^3(μMole/mm^3)	Guyton Hall (2000)
B_1	5.033×10^{-5} kMole/m^3(μMole/mm^3)	Garhyan et al., (2006)
B_2	5.033×10^{5} kMole/m^3(μMole/mm^3)	Garhyan et al., (2006)
α_{H^+}	2.25	Elnashaie et al., (1984)
α_{OH^-}	0.5	Elnashaie et al., (1984)
α_{S_1}	1	Elnashaie et al., (1984)
α_{S_2}	1	Elnashaie et al., (1984)
α_{S_3}	1	Elnashaie et al., (1984)
V_R	1.2	Elnashaie et al., (1984)
pH_f	8.2	Guyton (2000)
s_{1f}	15	Garhyan et al., (2006)
s_{2f}	1.15	Garhyan et al., (2006)
s_{3f}	3.9	Garhyan et al., (2006)
γ_1	0.01	Garhyan et al., (2006), Elnashaie et al., 1983a; Elnashaie et al., 1983b; Elnashaie et al., 1984; Elnashaie et al., 1995; Ibrahim et al., 1997)
R	0.8	Tucek (1978)

4.4 Physiological Values of the Parameters

To validate the results of the system with physiological and experimental results and with other models of previous investigators during the investigations of the change the system parameters, we should compare our system behavior with the following physiological values of ACh, choline, acetate, and pH. These values depend on experimental review and other models like that used by Garhyan et al., (2006) and Mahecha- Botero et al., (2004). The concentrations are given in (Kmol/m^3). Human brain pH in a feline model is found in the range of 6.95-7.35. (Zauner and Muizelaar, 1997), and pH in a human brain was found by (Rae et al., 1996) in the range 6.95 - 7.15.

Free ACh in rat brain was found around 0.22×10^{-5} kmol/m^3 and total ACh was in found around 1.77×10^{-5} kmol/m^3. Tucek, 1990 and Garhyan et al., 2006 showed that in guinea pig cerebral cortex the range was 0.31×10^{-5} (free ACh) to 1.67×10^{-5} kmol/m^3 (total ACh) [Garhyan et al., (2006)].

Wessler et al., (2001) Mahecha- Botero (2004) reported that ACh concentration in human placenta in the range of 3.0×10^{-5} to 55.5×10^{-5} kmol/m^3. Mahecha- Botero (2004) showed that in the isolated rings of rat pulmonary artery ACh was measured to be in the range of 0.001×10^{-5} to 3.0×10^{-5} as pointed to Kysela and Torok, (1996). Mahecha- Botero (2004) and Garhyan et al. (2006) reported that choline concentration in mouse rat brain is about 1.15×10^{-4} kmol/m^3. This range was confirmed by Tucek (1978) and choline concentration in human plasma is in the range of 0.01×10^{-4} to 0.7×10^{-4} kmol/m^3 (Chay and Rinzel, 1981; Mahecha – Botero (2004) and Garhyan et al., (2006)).

4.5 Results and Discussion

The behavior of the cholinergic ACh system is difficult to predict as it is related with cholinergic diseases such as Alzheimer's and Parkinson's diseases. Hence, it is very important to understand the system behavior. Now we investigate bifurcation and chaotic behavior extensively using two bifurcation parameters: (i) ChAT enzyme activity (B_1), and (ii) Choline recycle ratio (R). The effects of these parameters are explained below:

4.5.1 ChAT enzyme activity (B_1) as the bifurcation parameter

It is very important to study the effect of alterations in the activity of ChAT enzyme (B_1) as a bifurcation parameter catalyzing the ACh synthesis reactions occurring in compartment 1 on the behavior of the cholinergic ACh system in both compartment 1 and compartment 2 as well and to be able to predict their complex behavior. The bifurcation parameter ChAT enzyme activity (B_1) incorporates the following parameters (ChAT concentration in compartment 1, volume of compartment 1 and the flow rate): $B_1 = \frac{V_1 V_{M1} \overline{ChAT}}{q}$ where V_{M1} is the maximum rate of ACh synthesis that contains kinetic constants that dominate the synthesis reaction. Hence, changing the bifurcation parameter (B_1) gives the effect of the changing the enzymatic activity of the enzyme

ChAT. The disturbances in the activity of ChAT enzyme can cause cholinergic diseases like Alzheimer's and Parkinson's.

The effect of the bifurcation parameter (B_1) will be investigated through two cases: the first case investigates the static bifurcation including the hysteresis (or short term memory) phenomenon. This phenomenon is related to a big range of the activity ChAT enzyme. This case is taken at high value of the feed ACh concentrations s_{1f}=15 corresponding to 0.755 x10^{-5} kmol/m^3 as a medium value in the range of ACh in rat brain given by Tucek (1978). The second case discusses the dynamic bifurcation associated with variation of ChAT enzyme activity at s_{1f}=2.4 corresponding to 0.12 x10^{-5} kmol/m^3 which is the lowest value in the range given by Tucek 1978. The range given by Tucek (1978) is [0.12×10^{-5} to 1.77×10^{-5}] kmol/m^3. These cases are discussed in details below.

Case (1): Static Bifurcation **at s_{1f} =15**

Figure 4-3 illustrates the effect of B_1 (related to the activity of ChAT enzyme) as the bifurcation parameter for a certain range of values using a fixed value of $s_{1f}=15$ and other parameters values are kept constant as shown in Table 4-3. Generally it is observed that as B_1 increases, both s_{11} and s_{12} increase but s_{21} decreases due to the synthesis reactions catalyzed by the enzyme ChAT. It is clear that the state variables are characterized by hysteresis. As shown in Figure 4-3 ,there are various regions appearing in state variables due to changing the bifurcation parameter B_1 as below:

1) **Region 1**: High enzyme activity in the region $\left(9.78\times10^{-4}\le B_1\right)$ kmol/m^3

In this region the system is characterized by a unique stable steady state. It is clear that ChAT activity (B_1) which is involved in a wide range works with the highest efficiency leading to consumption of choline as a substrate in compartment (1) where the dimensionless (s_{21}) is less than 2.7 as shown in Figure 4-3 (c). Figures 4-3 (a) and (b) show that both (s_{11}) and (s_{12}) increase continuously more than 55 and 26 respectively corresponding to 27.682*10^{-6} and 18.11*10^{-6} kmol/m^3 respectively. Figure 4-3(d) shows that pH_2 increases more than 5.5. ACh in compartment (1) and (2), and choline concentration in compartment (2) are corresponding to the physiological range Kysela and Torok (1996). It is observed that pH_2 is involved a wide change because of the high ChAT enzyme activity. These results reflect the high efficiency of both synthesis reaction in compartment 1 and the transport of components from compartment 1 to compartment 2.

2) **Region 2**: $\left(7.53\times10^{-4} \le B_1 \le 9.78\times10^{-4}\right)$ kmol/m^3

As ChAT enzyme activity (B_1) decreases to $B_1 = 9.78\times10^{-4}$, the system is dominated by a hysteresis phenomenon occurring between the two static bifurcation points (SB_1 and SB_2). In this range there are two stable steady state solutions separated by unstable steady state solution (which is called saddle node).). The multiplicity dominates the system between the two static bifurcation points where the second static bifurcation appears at B_1=7.53x 10^{-4} kmol/m^3. Hysteresis causes the state variables to be very sensitive in the neighborhood of the static bifurcation points. For example, in Figure 4-3(b) the dimensionless (s_{12}) jumps from $s_{12} = 2.4$ to $s_{12} = 26.4$ with a slight increase in the enzyme activity near the static bifurcation point SB_1. However, as shown in Figure 4-3(a), when ChAT enzyme activity is decreased to less than $B_1 \prec 9.78\times10^{-4}$ kmol/m^3, s_{11} will decrease through a small range from 33 to 26 reflecting the ability of the pressynaptic neuron to keep the gradual synthesis reaction of ACh with a high efficiency even the reduction of ChAT enzyme activity. This will be more clarified if we compare the effect hysteresis behavior in s_{11} due to change of ChAT activity with the hysteresis behavior due to change in AChE activity (Mustafa et al., (2009)[b]). We will find there is a sudden change in s_{11} with AChE activity and gradual change in s_{11} with the reduction of ChAT activity in the range $B_1 \prec 7.53\times10^{-4}$ kmol/m^3.

This region fits reasonably well the expected physiological behavior. Figure 4-3(a) shows that s_{11} varies in the range 26 and 54.74 corresponding to 13×10^{-6} and 27.02×10^{-6} kmol/m^3 while the dimensionless s_{12} varies in the range 2 and 32 corresponding to 1×10^{-6} and 16×10^{-6} kmol/m^3. This region fits the expected physiological behavior where ACh in a rat brain was found to be in the range of (2.2×10^{-6} -17.7×10^{-6}) kmol/m^3 to (Tucek, 1978).

Figure 4-3(d) shows that pH_2 is out of the expected physiological range and it varies between 4.64 and 5.57 where pH was measured in the range of 6.95 - 7.15 human brain (Rae et al., 1996) and in a feline model pH was reported in the range of 6.95-7.35 (Zauner and Muizelaar, 1997), this is because of the assumption of the fully ionization of acetic acid. In reality, the acetic acid should be dissociated in a very small fraction, where 2-3% only of the original acetic acid as a product in the second compartment. In this case pH will change within a small range and can work as an accelerator or as an inhibitor and will control the transport process between both compartments. Figure 4-3(c) shows that s_{21} changes between 3.264×10^{-4} and 3.66×10^{-4} kmol/m^3. s_{21} is out of the expected physiological

range where choline concentration in mouse rat brain is about 1.15×10^{-4} kmol/m^3 (Tucek, 1978) and choline concentration in human plasma is in the range of 0.01×10^{-4} to 0.7×10^{-4} kmol/m^3 (Chay and Rinzel, 1981). This is due to that we started in the model with high feed choline concentrations s_{2f} = 1.15 corresponding to 1.15×10^{-4} kmol/m^3.

3) Region 3: Low enzyme activity in the region $\left(0 \prec B_1 \le 7.53\times10^{-4}\right)$ kmol/m^3. In this region there is only a unique stable steady state. Figure 4-3(a) shows that s_{11} varies between 1 and 20 corresponding to 0.5×10^{-6} and 10.07×10^{-6} kmol/m^3. Figure 4-3(b) shows that s_{12} varies between 0.1×10^{-6} and 1×10^{-6} kmol/m^3. The values of the variables in this region are out of the physiological values and do not follow the expected biological behavior where ACh in a rat brain was found to be in the range of 2.2×10^{-6} kmol/m^3 to 17.7×10^{-6} (Tucek, 1978). This region of B_1 shows that the low activity of ChAT leads to reduction of the synthesized ACh in compartment 1, s_{11} then the release of ACh will be decreased in terms of ACh concentration in compartment 2, s_{12}. The process of ACh release in synaptic cleft during the high activity of mammalian cholinergic neurons will be accompanied by a new synthesis of ACh by the enzyme ChAT in compartment 1 to compensate the released ACh [Nunes-Tavares (2000)].

These results showing an observable reduction in ACh synthesis in presynaptic and postsynaptic neurons and ACh release due to reduction of ChAT activity are considered as the main features of Alzheimer's disease. The results are in agreement with the results of Keverne and Ray (2008) who indicated the extent of reduction in ChAT activity determines the extent of cognitive weakness [Keverne and Ray (2008); Perry et al., (1999); Keverne and Ray (2008)]. Milos et al., (2005) indicated that the deficit in ChAT activity leading to cognitive loss can be considered as a differentiation between clinical and preclinical forms of Alzheimer's disease.

Figure 4-3(d) shows that pH_2 has a wide variation in the range 5.35 and 8.2. In this region, the hydrogen proton concentration is still high due to the low activity of ChAT enzyme. As mentioned earlier, a reasonable explanation of this big range of pH values is due to the assumption of fully ionization of acetic acid, i.e. one molecule of the acid gives a molecule of acetate ion and hydrogen ion

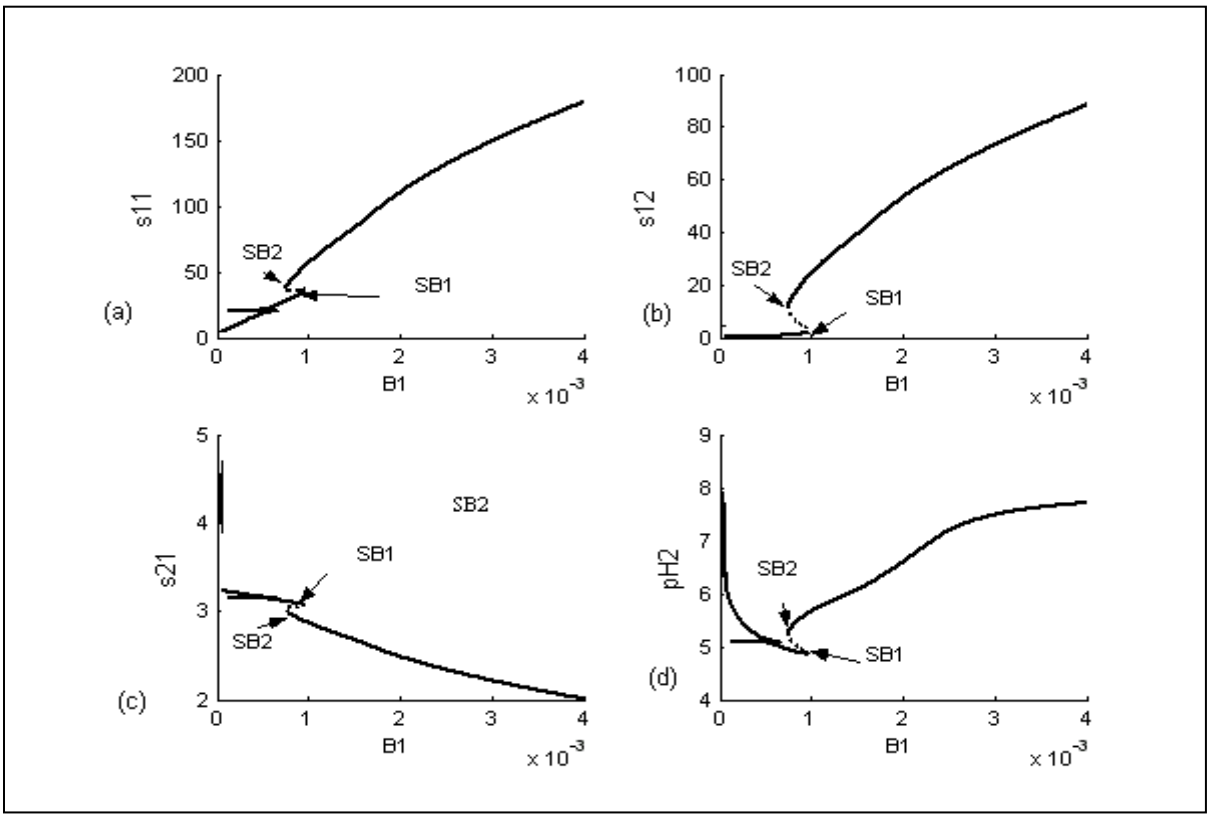

Figure 4-3: Bifurcation diagrams: ChAT activity (B_1) as the bifurcation parameter at $(s_{1f} = 15)$ dimensionless and rest of data as shown in Table 4-3:

(stable: —, unstable: -----), periodic branch (stable ●, unstable ○)

(a) Effect on ACh in compartment (1) (s_{11}); (b) Effect on ACh in compartment (2) (s_{12}), (c) Effect on choline concentration in compartment (1) (s_{21}), and (d) Effect on pH concentration in compartment (2) (pH_2).

whereas, from 1-2% only of the acetic acid goes through ionization process. Hence, acetic acid may go through partial ionization not fully ionization process. This region is close to the expected physiological range where pH was measured in the range of 6.95 - 7.15 human brain (Rae et al., 1996) and in a feline model pH was reported in the range of 6.95-7.35 (Zauner and Muizelaar, 1997).

The continuous increase of s_{11} and s_{12} as shown in Figure 4-3 (a) and Figure 4-3(b) respectively due to the increase of B_1 shows that there are other factors that can affect the ChAT activity and ACh processes and play an important role for controlling and regulating ACh concentrations in the both compartments.

One of the main factors is the increase of substrates concentrations of feed choline and feed acetate. Therefore, ChAT is not the most important factor in controlling and regulating the ACh neurocycle. According to Chapter 3 (Mustafa et al., 2009[b]) feed acetate concentrations does not play the crucial role and feed choline concentrations may play this role. The study of choline recycle ratio will highlight the importance of choline uptake for ACh synthesis.

Case (2): Dynamic Bifurcation at s_{1f} =2.4

Figure 4- 4 shows the dynamic bifurcation diagrams using the ChAT enzyme activity parameter B_1 as the bifurcation parameter but with a different value of feed ACh concentration $(s_{1f} = 2.4)$ which represent a very low feed mobile ACh concentrations coming by axonal transport mechanism. Figure 4- 4 illustrates that there are three main observed regions in the bifurcation diagram; each one has a determined qualitative behavior. There are two Hopf bifurcations (HBs). The first HB_1 appears at $B_1 = 4.99\times10^{-5}$ and the other HB_2 at $B_1 = 3.03\times10^{-5}$. Mathematically HB point appears when the real parts of a pair of complex conjugate eigenvalues become negative, causing the system to undergo a bifurcation. HB_2 is defined as a "subcritical Hopf bifurcation" because a branch of unstable periodic orbits (appeared as empty circles) appears with a stable stationery branch at this point forming a separatrix between the basins of the attraction of the stable steady states Figure 4.4 indicates that the system in the range of ($3\times10^{-5} \le B_1 \le 5.5\times10^{-5}$) complex behavior between the HB points. Hence, the periodic solution is the only solution available and the stationary points are not attractors, and the limit cycles are the only attractors (periodic attractors) as illustrated in Figure 4.4 in which the behavior of state variables describe oscillatory solutions.

The oscillatory behavior in the range of B_1 (range between HB_1 and HB_2) may play a vital role in the synthesis and release of ACh according to Santos et al., (2006). Solid bold curves represent stable steady state solutions and dashed lines represent the unstable steady states. Closed circles are used for stable orbits and the open circles for the unstable orbits. The qualitative behavior due to change of ChAT activity in the range ($3\times10^{-5} \le B_1 \le 5.5\times10^{-5}$) kmol/m^3 can be explained as shown in Figure 4-4 as follows:

1) **Region 1**: $\left(5\times10^{-5} \le B_1\right)$ kmol/m^3

In this region, Figure 4-4 shows that there is a unique stable steady state where ChAT activity operates with a high activity. Figure 4-4(a) indicates that s_{11} changes around 3.9 corresponding to 1.95×10^{-6} kmol/m^3 while Figure 4-4(b) illustrates that s_{12} changes around 0.3 corresponding to 0.15×10^{-6} kmol/m^3. It is clear that $s_{21} \ge 3.233$ as shown in Figure 4-4(c). In Figure 4-4(d), pH_2 changes around 6.5. On analyzing the physiological values, pH_2 is close to the physiological values varying between 6.95 and 7.15 in human brain (Rae et al., 1996). However, ACh does not agree with the physiological values because of the low ChAT activity according to Wessler et al., (2001) who reported that ACh concentration in human placenta is in the range of 3.0×10^{-5} to 55.5×10^{-5} kmol/m^3 and Kysela and Torok, (1996) who showed that ACh in the isolated rings of rat pulmonary artery was around 3.0×10^{-5} kmol/m^3.

2) Region 2: Enzyme activity in the range $\left(B_1 \le 3.03\times10^{-5}\right)$ kmol/m^3

Figure 4-4 shows that the ACh cholinergic system is dominated but a unique stable steady state (point attractor), where B_1 works with a very low activity, thus producing a small range of s_{12} which exists the range 1.2 to 1.35 corresponding to 0.6×10^{-6} and 0.675×10^{-6} kmol/m^3 as shown in Figure 4-4(b). Figure 4-4(a) shows that s_{11} is between 4.461 and 4.8 corresponding to 2.231×10^{-6} and 2.4×10^{-6} kmol/m^3. The choline concentrations has low values in this region as shown in Figure 4-4(c) where the dimensionless choline concentration in compartment 1 (s_{21}) is almost constant through (3.22623-3.22635) corresponding to $(3.22623\text{-}3.22635)\times10^{-4}$ kmol/m^3. In Figure 4-4(d) pH_2 has a high value pH_2 = 7.94 (low hydrogen protons concentration) in this region. On analyzing the physiological values, pH_2 does not agree with the physiological values varying between 7.14 and 7.16 (Rae et al., 1996; Zauner and Muizelaar, 1997). It is clear that as ChAT activity decreases, the values of state variables will decrease continuously. These results agree with the experimental results obtained by Nunes-Tavares 2002; Blusztajn and Wurtman, 1983 who showed that as ChAT is available in the cholinergic neurons, the levels of ACh will change clearly. Therefore, ChAT activity does not represent the rate-limiting factor for ACh biosynthesis. The results are in accordance with the results obtained by Brandon et al., (2004) who indicated that the loss of ChAT activity will cause a reduction in the rate of ACh synthesis in compartment 1. The reduction of ChAT activity needs other alternative effects to keep normal levels of ACh. According to Brandon et al., (2004), increased

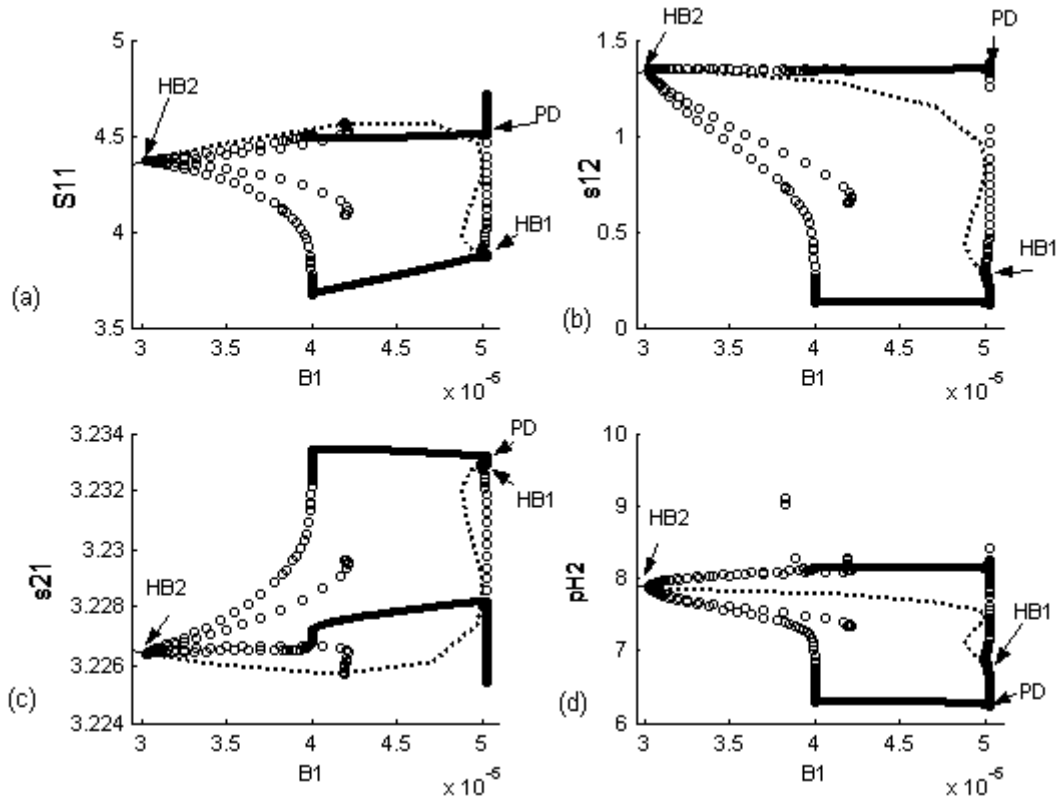

Figure 4-4: Bifurcation diagram: B_1 (ChAT activity) as the bifurcation parameter at $(s_{1f} = 2.4)$

(stable: —, unstable: ----------), periodic branch (stable ●, unstable ○):

(a) Effect on ACh in compartment (1) (s_{11}); (b) Effect on ACh in compartment (2) (s_{12}), (c) Effect on choline concentration in compartment (1) (s_{21}), and (d) Effect on pH concentration in compartment (2) (pH_2).

uptake of choline to ChAT in compartment 1 may be the alternative solution for keeping the high efficiency of ACh and the rate-limiting factor in the synthesis of ACh.

3) **Region 3**: $\left(3.03\times10^{-5} \le B_1 \le 5\times10^{-5}\right)$ kmol/m^3

This region is characterized by the complex behavior. The system demonstrates oscillatory behavior between HB_1 and HB_2. As the enzyme activity decreases to $B_1 = 4.98\times10^{-5}$, the first HB_1 occurs at $B_1 = 4.99\times10^{-5}$. In this region chaos may develop via the Feigenbaum (1980) PD route which appears at $B_2 = 4.983\times10^{-5}$ as shown in Figure 4-4. Mathematically HB_1 is called subcritical HB. **In**

the range of $\left(4.98.\times10^{-5} \le B_1 \le 4.99\times10^{-5}\right)$ kmol/m^3, the bistability behavior appears. It is observed that both point attractors and periodic attractors coexist with unstable periodic attractors (appeared as empty circles) separating them. The significance of the bistability is that the system can approach to both attractors (either point or periodic) at the same value of the bifurcation parameter B_1 if the initial conditions are different. In this small range, Figure 4-4 (a) shows that s_{11} oscillates between 3.68 and 4.5 corresponding to 1.84×10^{-6} and 2.25×10^{-6} kmol/m^3 respectively. pH_2 oscillates between 6.3 and 8.2, which is a region near to the expected physiological pH values (Figure 4-4(d)). Figure 4-4 (b) shows that s_{12} oscillates between 0.5×10^{-7} and 6.57×10^{-7} kmol/m^3 corresponding to a low ACh concentration. Figure 4-4(c) shows that s_{21} is close to the expected physiological range (Chay and Rinzel, 1981) with soft oscillations between 3.2265×10^{-4} and 3.233×10^{-4} kmol/m^3.

In the range of $\left(4\times10^{-5} \le B_1 \le 4.98\times10^{-5}\right)$ kmol/m^3, the system is characterized by unique stable periodic orbits showing sustained oscillations. This range shows that pH_2 changes between 6.3 and 8.1 as shown in Figure 4-4(d) and exists inside the expected physiological pH values **(**Rae et al., 1996**).** In Figure 4-4(b) s_{12} oscillates between 0.5×10^{-7} and 6.57×10^{-7} kmol/m^3 corresponding to very low ACh concentration. The choline concentration in compartment 1 is out of the expected physiological range (Chay and Rinzel, 1981) with soft oscillations around 3.223×10^{-4} and 3.233×10^{-4} kmol/m^3 as shown in Figure 4-4(c).

However, **in the range of** $\left(3.03\times10^{-5} \le B_1 \le 4\times10^{-5}\right)$ kmol/m^3, the system is characterized unique unstable periodic orbits as shown in Figure 4-4. As the enzyme activity decreases to $B_1 = 3.03\times10^{-5}$, the second Hopf bifurcation (HB_2) occurs.

The bistability behavior observed in the region $\left(4.98\times10^{-5} \le B_1 \le 4.9999\times10^{-5}\right)$ where periodic and point attractors coexist with an unstable periodic orbit as the separatrix separating the domains of attraction of the periodic and point attractors can more clarified when dynamic characteristics are investigated at different initial conditions as shown in Figure 4-5 and Figure 4-6.

Figure 4-5 illustrates that periodic solution is the only solution at the corresponding initial conditions and at B_1=4.999 x 10^{-5} and the rest of parameter values as shown in Table 4-3. Figure 4-5(a) shows the phase plane between s_{11} and s_{12} and Figure 4-5(b) shows the phase plane between s_{11} and pH_2. The phase planes are closed orbits indicating that the solutions are completely periodic. In

Figure 4-5 (c) pH_2 oscillates between 6.3 and 8.2, which is a region near to the expected physiological pH values (Rae et al., 1996; Zauner and Muizelaar, 1997). Figure 4-5(d) shows that s_{12} oscillates between 0.25 and 1.45 corresponding to a very low ACh concentration 1.25×10^{-7} and 7×10^{-7} kmol/m^3. Figure 4-5 (e) shows that s_{11} oscillates between 3.68 and 4.5 corresponding to 1.84×10^{-6} and 2.25×10^{-6} kmol/m^3. In addition, Figure 4-5(f) shows that s_{32} oscillates between 4.6 and 5.2 corresponding to 4.6×10^{-6} and 5.2×10^{-6} kmol/m^3.

Figure 4-6 shows the dynamics at the same value of ChAT activity like Figure 4-5 where B_1=4.999 x 10^{-5} but at different initial conditions. In Figure 4-6 the point attractor is the only solution. The amounts of choline and ACh associated with various times are also presented in Figure 4-6. The rate of decrease in acetate levels s_{32} is also the highest during the early portion of the period (Figure 4-6 (f)), but when $5 \le T$ (corresponding to $62.5\mu\text{sec} \le T$), s_{32} begins to plateau around 4.96. After $T = 40$ (corresponding to 500 μsec.) there was no further change in the intracellular levels of acetate s_{32}. In contrast to the levels of acetate, the amount of ACh ($s_{11}$and s_{12})as shown in Figure 4-6(e) and (d) increased in a high rate during the early portion of the incubation period then when $5 \le T$ it began to plateau. When $40 \le T$ there was no further change in the intracellular levels of s_{11}which stabilized around 3.898 (corresponding to 0.196 x 10^{-5} kmol/m^3) and s_{12} which stabilized around 0.299 (corresponding to 0.015 x 10^{-5} kmol /m^3). Figure 4- 6(c) shows that pH_2 increased rapidly during the early portion of the period, when $5 \le T$ pH_2 begins to plateau around 6.88. These results are in agreement with the results of Leventer et al., (1984) who found that the rate of choline consumption was very fast during the earlier portion of the reaction period and decreased as the reaction progressed. In addition, our results are in accordance with Wecker and Dettbarn (1978) who indicated that the steady state concentration of ACh in discrete brain regions seems to be kept within small physiological ranges and the contents of ACh will be unaltered even choline concentrations increased. The constancy concentrations of ACh in compartment 1 may refer to the inhibition of the synthesis reactions by the excess concentration of choline. The results are in agreement with the results obtained by Nunes-Tavares (2000) who pointed to the constancy of ACh levels in cholinergic cells. This because once ACh release is consumed due to high synaptic transmission, ACh is replaced by synthesizing new amount of ACh in compartment 1.

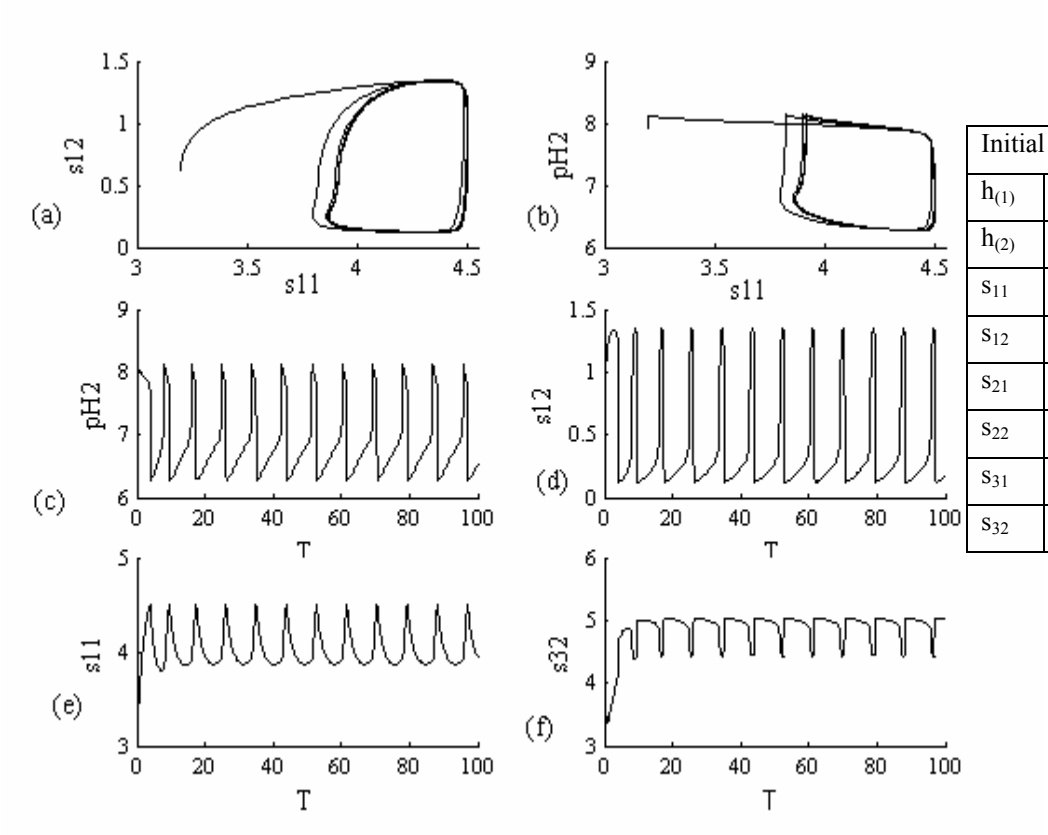

Initial conditions	
$h_{(1)}$	0.003796824
$h_{(2)}$	0.1405804
s_{11}	3.956
s_{12}	0.3
s_{21}	3.233
s_{22}	1.1606
s_{31}	8.2517318
s_{32}	4.9606

Figure 4- 5: Dynamic characteristics at B_1=4.999*10^{-5} and, s_{1f}=2.4, s_{3f}=3.9, s_{3f}=3.9, $h_f = 0.006268$: for the relevant initial conditions. Time trace (stable: —, unstable: ----------), phase plane (stable: •, unstable ◦)

(a) Phase plane for ACh in compartment 2 (s12) vs. the ACh in compartment 1 (s11)

(b) Phase plane for pH in compartment 2 (pH_2) vs. the ACh in compartment 1 (s_{11})

(c) Time traces of pH in compartment 2 (pH_2), (d) time traces of ACh in compartment 2 (s_{12}), (e) time traces of ACh in compartment 1 (s_{11}), and (f) Time traces of acetate in compartment 2(s_{32})

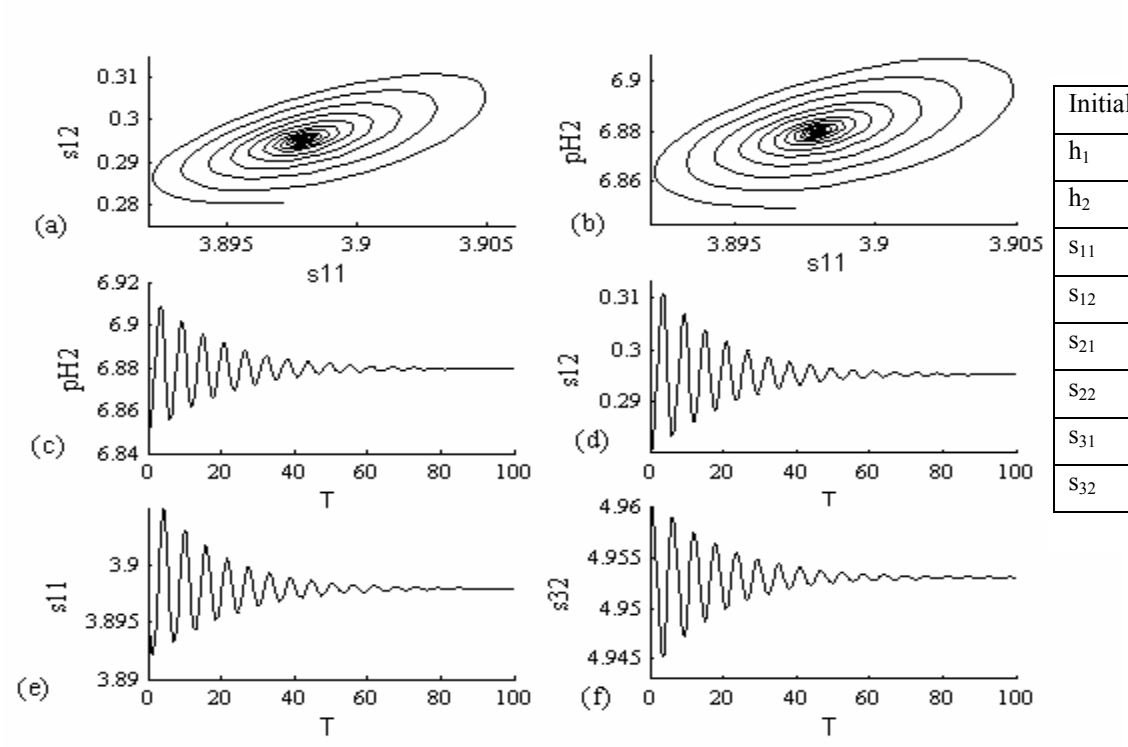

Initial conditions	
h_1	0.006268
h_2	0.0096807
s_{11}	3.1971322
s_{12}	0.628643
s_{21}	1.1557
s_{22}	1.614
s_{31}	4.4695
s_{32}	5.039

Figure 4- 6: Dynamic characteristics at B_1=4.999*10^{-5} and, s_{1f}=2.4, s_{3f}=3.9, $h_f = 0.006268$: for the relevant initial conditions. Time trace (stable: —, unstable: ---------), phase plane (stable: •, unstable**)**:

(a) phase plane for ACh in compartment 2 (s12) vs. the ACh in compartment 1 (s11)

(b) phase plane for pH in compartment 2 (pH_2) vs. the ACh in compartment 1 (s_{11})

(c) time traces of pH in compartment 2 (pH_2), (d) time traces of ACh in compartment 2 (s_{12}), (e) time traces of ACh in compartment 1 (s_{11}), and (f) Time traces of acetate in compartment 2(s_{32})

Figure 4-7 shows the static bifurcation diagram at $h_f = 0.002$ (pH = 8.69), $B_2 = 0.002$, $s_{1f} = 4.5$, s_{2f} = 2, and $s_{3f} = 2$ and the rest of the system parameters are given as shown in Table 4-3. The effect of B_1 as the bifurcation parameter on s_{11} is studied at the corresponding parameter values and initial conditions, in order to investigate the fully developed chaotic behavior. In Figure 4-7 there are two Hopf bifurcation points, the first HB_1 point is at B_1=5.68*10^{-5}, and the other is at B_1 = 0.0003707. It is clear as shown in Figure 4-7 the periodic branch loses its stability giving rise to chaotic behavior at B_1 = 0.000062487.

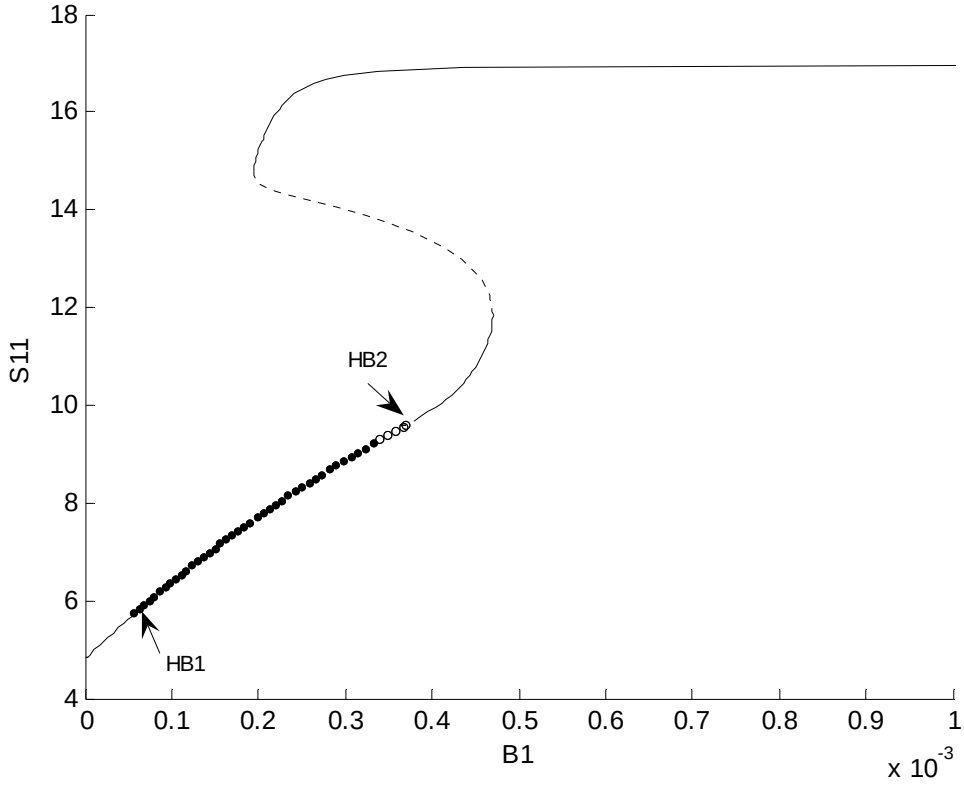

Figure 4-7: Bifurcation diagram at $s_{1f} = 4.5, s_{2f} = 2, s_{3f} = 2$, $h_f = 0.002$, $B_2 = 0.002$ and the rest of the system parameters a in Table 4-3, effect of B_1 on s_{11}

In addition, it is characterized by the presence of fully developed chaos as shown in Figure **4-**8(a). Chaos may develop via the well known Feigenbaum PD and period adding route (Feigenbaum, 1980). PD appears when $B_1 = 0.000066925$. In order to have a full picture about the evolution of the chaotic behavior, one-dimensional and one-directional Pioncare abstracted the time trace and phase plane representations to a comprehensive map where a hypothetical hyperplane surface is assumed to cross the trajectory in the phase space. Pioncare map describes the intersection between the hyper plan surface and the trajectories. Therefore, it converts the problem of orbits which are difficult to deal with to problems of points which are easier to handle. For example, a periodic solution (limit cycle) on the phase plane appears as one point on Poincaré map. When PD takes place, period 2 appears as two points on the map, period 4 as four points, and so on. When chaos takes place, a complicated collection of points appears on Poincare map. Figure 4-8(a) shows the Pioncare map of the region under consideration. It is clear that the evolution of chaotic behavior is via a period adding

sequence. This map of Figure 4-8(a) is constructed using a Pioncare plan at $s_{12} = 0.31$. The map is characterized also by wide regions of periodic windows of period two and period three. The periodic bifurcation sequence is characterized by period adding sequence to chaos and periods adding sequence of periodic windows; these are summarized below

Figure 4.8 shows that period one attractor appears at $B_1 = 6.8x10^{-5}$ then evolution of chaos via PD appears as B_1 decreases. When ChAT activity decreases to $B_1 = 6.58x10^{-5}$, window of period two appears then evolution of chaos via period adding sequence follows. Window of period three at $B_1 = 6.48x10^{-5}$ followed by evolution of chaos via period adding. Furthermore, when $B_1 = 6.43x10^{-5}$ window of period four followed by evolution of chaos via period adding and window of period five appears at $B_1 = 6.38x10^{-5}$ followed by evolution of chaos via period adding – window of period six at $B_1 = 6.35x10^{-5}$ and so on where a cascade of further period adding occurs as B_1 decreases until $B_1 = 0.000062444$ the map becomes chaotic and the attractor changes from a finite to an infinite set of points as infinite irregular windows.

Time traces and phase planes are shown in Figure 4-9 at $B_1 = 0.000062444$ as chaotic attractors where it is shown that after an initial transient, the solution settles into an irregular oscillation that persists as time approaches infinity. Figure 4-9(a) and (b) show phase planes where the orbits behave irregularly between s_{12} vs. s_{11} and between pH_2 vs. s_{11} respectively. The chaotic solutions are shown in Figures 4-9(c), (d), (e), and (f) where the chaotic attractors solutions repeat irregularly in an intermittency mechanism. In Figures 4-9(c), (d), (e), and (f) finite intervals of irregular oscillations are interrupted by intermittent bursts of irregular oscillations. The regular oscillations are similar to those seen in Figures 4-5(c), (d), (e), and (f) at the corresponding initial conditions. The bursts of irregular oscillations are more prominent in Figures 4-10(c), (d), (e), and (f) with the duration of regular oscillations decreasing in size and the bursts becoming more frequent as the initial conditions are different showing that the chaotic attractors are very sensitive to the initial conditions.

4.5.2 Choline Recycles Ratio (R) as the Bifurcation Parameter

We investigate static and dynamic bifurcations due to the variation of choline recycle ratio (R) which represents the ratio between the amount of choline recycled from compartment 2 (postsynaptic neuron), resulted from the hydrolysis of ACh by AChE, to the amount of feed choline

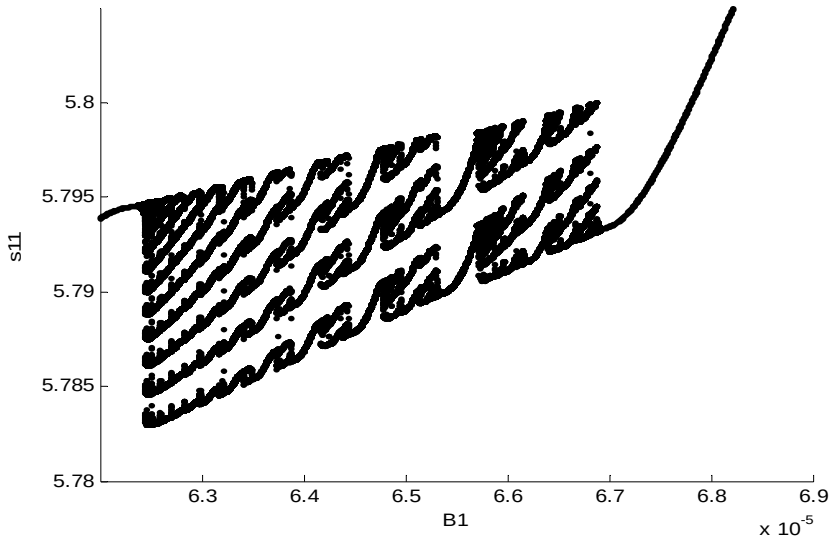

(a) Poincare diagram

(b)

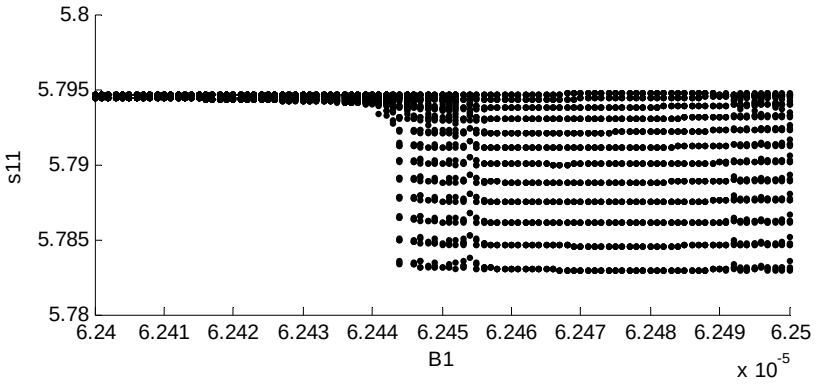

Figure 4-**8:** (a) One dimensional Poincaré bifurcation diagrams (Poincaré plane is located at $s_{12} = 0.31$, $s_{1f} = 4.5$, $s_{2f} = 2$, $s_{3f} = 2$, $h_f = 0.002$, $B_2 = 0.002$ and the rest of the system parameters a in Table 4-3 for the corresponding initial conditions

(b) Magnification of the box in Figure 4-8 a

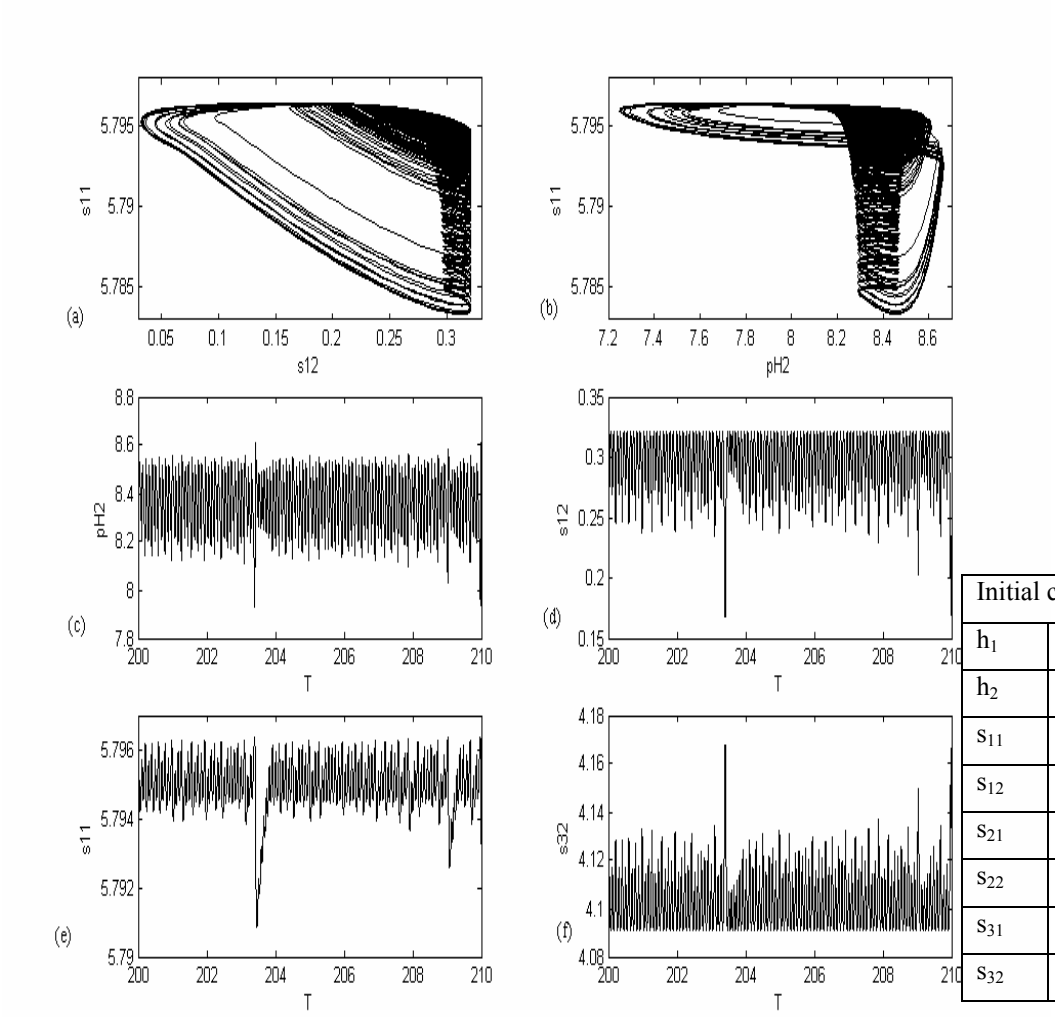

Initial conditions	
h_1	0.000805984
h_2	0.004122
s_{11}	5.74684
s_{12}	0.31
s_{21}	5.6255
s_{22}	2.018
s_{31}	5.09
s_{32}	3.833

Figure 4-9: Dynamic characteristics at B_1=0.000062444, $s_{1f} = 4.5, s_{2f} = 2, s_{3f} = 2, h_f = 0.002,$ $B_2 = 0.002$ **and the rest of the system parameters a in Table 4-3 for the corresponding initial conditions:**

(a) Phase plane for ACh in compartment 2 vs. the ACh in compartment 1.

(b) Phase plane for pH in compartment 2 vs. the ACh in compartment 1

(c) Time traces of pH in compartment 2 , (d) Time traces of ACh in compartment 2

(e) Time traces of ACh in compartment 1, and (f) Time traces of acetate in compartment 2

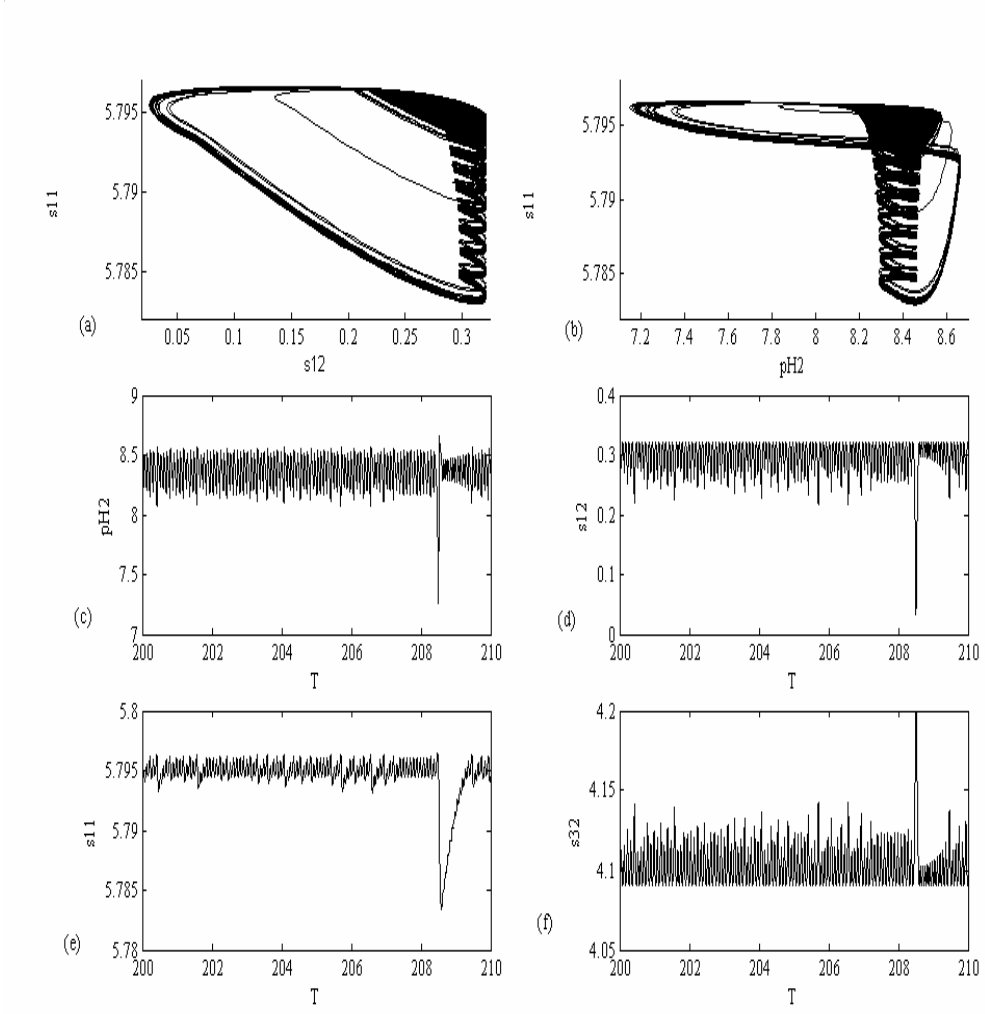

Initial conditions	
h_1	35
h_2	15.5
s_{11}	5.74684
s_{12}	0.9
s_{21}	5.6255
s_{22}	2.018
s_{31}	5.09
s_{32}	3.833

Figure 4-10: Dynamic characteristics at B_1=0.000062444, $s_{1f} = 4.5, s_{2f} = 2, s_{3f} = 2, h_f = 0.002$, $B_2 = 0.002$ and the rest of the system parameters a in Table 4-3 at the corresponding initial conditions

(a) Phase plane for ACh in compartment 2 vs. the ACh in compartment 1.

(b) Phase plane for pH in compartment 2 vs. the ACh in compartment 1

(c) Time traces of pH in compartment 2 , (d) Time traces of ACh in compartment 2

(e) Time traces of ACh in compartment 1, and (f) Time traces of acetate in compartment 2

(s_{2f}) coming from the blood and the environment outside compartments 1 and 2. The ratio (R) reflects the importance of the hydrolysis of ACh in compartment 2 to produce choline to be recycled to presynaptic neuron to provide the needed choline for the ACh synthesis reaction catalyzed by ChAT. It represents the role of choline uptake and its effect on the synthesis and release of ACh. It is very important to investigate the effect of choline uptake on the ACh system behavior. It will give us a clear picture about the role choline uptake which can play.

We study the static bifurcation at a high value of feed mobile ACh concentrations s_{1f} =15 corresponding to 0.755 x10^{-5} kmol/m^3 as a medium value in the range of ACh in rat brain given by Tucek (1978) and the dynamic bifurcation at s_{1f} =2.4 corresponding to 0.12 x10^{-5} kmol/m^3 which is the lowest value in the range given by Tucek (1978). The range given by Tucek (1978) is [0.12×10^{-5} to 1.77×10^{-5}] kmol/m^3.

Case (1): Static Bifurcation at s_{1f} =15 (corresponding to 0.755 x10^{-5} kmol/m^3**)**

Figure 4-11 shows the bifurcation diagrams with R as the bifurcation parameter at $s_{1f}=15$ and other parameter values are shown in Table 4-3. Figure 4-11 illustrates the static bifurcation through studying the effect of varying R on the state variable: s_{11}, s_{12}, s_{21}, $s_{32,}$ and pH_2 respectively. In Figure 4-11, it is clear that $s_{11}$and s_{12} increase as R increases until certain value then s_{11} and s_{12} remain constant with further increase of R. This is compatible with the experimental results done by (Tucek 1990 and Lefresne 1973) who indicated that the levels of ACh increase continuously until reaching plateau and then remain stable with further increase of choline substrate concentration. However; s_{21} increases linearly with increase of R. If we investigated the effect of R on s_{22}, we will find that s_{22} behaves the same like s_{21}. The ACh concentrations synthesized in both compartments 1 and 2 (s_{11}, s_{12}) are increasing with a high rate in the range of $(R\leq30)$, however; at high choline recycle ratio concentration $(30\leq R)$, ACh is synthesized less efficiently from the substrate choline concentration which accumulated in nervous tissue.

This is in agreement with the results obtained by Schwartz et al., (1975) who indicated that the rate of ACh synthesis depends on the concentration of the substrate choline. They found that the ratio of choline consumed for ACh synthesis was high around 60-75 % when the concentration of external choline was small, however; when the choline concentration increased, the ratio of choline consumption declined. Therefore, the levels of ACh in the presynaptic terminals are expected not be influenced by the high recycle ratio of choline. As the excess choline will contribute less efficiently in

the process of ACh synthesis because the enzyme ChAT may be inhibited by the excess choline in compartment 1. Furthermore, the results are compatible with the experimental results obtained by Weckler (1988) who indicated that the ACh content was not affected in the presence of high concentrations of free choline released from brain cells in rats although there was a high necessity for new synthesized ACh. In addition; Weckler (1988) indicated that the capability of the brain neurons to synthesize new ACh decreased highly in the conditions of lack of available choline, where the brain cells become unable to release free choline.

From the constancy of ACh levels in both compartments in the presence of choline concentrations higher than the critical value, $(30 \leq R)$, we can conclude that the process of ACh release from compartment 1 to compartment 2 proceeded in parallel to the incorporation of uptake of choline to compartment 1 to be catalyzed by the enzyme ChAT to produce ACh. In other words, the released ACh in compartment 2 is compensated by the synthesizing new ACh in compartment 1. Therefore, the rate of ACh release is in accordance with the rate of choline uptake. Another explanation is that this excess choline might be converted to an unknown material which is unable to be consumed to produce to ACh.

Figure 4-11 (d) shows that s_{32} decreases with increasing R until certain value of R then s_{32} remains constant with further increase of R. According to Figure 4-11 there are three main regions appearing as R increases while all other parameters maintained constant. These regions will be explained as follows:

1. **Region 1**: High choline recycle ratio in the region $(30 \leq R)$

In this region the system is characterized by a unique stable steady state and all the state variables except s_{21} reach plateau while s_{21} increases continuously as shown in Figure 4-11 where s_{12} approaches a value close to 45 corresponding to 2.26 x10^{-5} kmol/m^3 and s_{12} close to 18 (0.91x10^{-5} kmol/m^3) and s_{32} close to 3 corresponding to (3 x10^{-6} kmol/m^3). Figure 4-11(e) shows that pH_2 has its highest value of 5.45 which is close to the physiological values where Damsma et al., (1987) showed that the enzymatic conversion of choline and ACh was optimal between pH= 4 and pH= 5.5. However, Mexel et al., (2006) showed that cortical brain pH across ranged from 5.8 to 6.95.

2. **Region 2**: $(17.18 \leq R \leq 30)$

As R decreases to 17.18, a hysteresis phenomenon occurs and a multiplicity of steady states is observed between the two static bifurcation points (SB_1 and SB_2). In this range there are two stable steady state

solutions separated by unstable steady state solution (which is called saddle node). The multiplicity dominates the system between the two static bifurcation points. Hysteresis causes the state variables to be very sensitive in the neighborhood of the static bifurcation points. The hysteresis phenomenon has a vital significance where it reflects the flexibility of the system to external disturbances as the shortage or plentiful choline uptake for R values close to the static bifurcation points. For example, in Figure 4-11(b) the s_{12} jumps from 2.94345 to 18 corresponding to (0.15 and 0.91) x10^{-5} kmol/m^3 respectively with a slight increase in R near the static bifurcation point SB_1. This region fits reasonably well to the expected physiological behavior. Figure 4-11 (a) shows that s_{11} varies in the range 36 to 45 corresponding to 1.8×10^{-5} and 2.26×10^{-5} kmol/m^3. Figure 4-11(e) shows that pH_2 is out of the expected physiological range and it is varying between 4.64 and 5.57. A reasonable explanation of this unexpected pH values is due to the assumption of fully ionization of acetic acid, i.e. one molecule of the acid gives a molecule of acetate ion and hydrogen ion , whereas, from 1-2% only of the acetic acid goes through ionization process. Hence, acetic acid may go through partial ionization not fully ionization process.

3. **Region 3**: Low choline recycle ratio in the region $(0 \prec R \leq 17.18)$

In this region there is a unique stable steady state. The values of the variables in this region are close to the physiological values and follow the expected biological behavior Figure 4-11(a) shows that s_{11} varies between 15 and 27 corresponding to 7.5 x10^{-6} and 13.5 x10^{-6} kmol/m^3. Figure 4-11(b) shows that s_{12} varies between 0.002 and 2.98 corresponding to 0.0001x10^{-5} and 0.147x10^{-5} kmol/m^3. Figure 4-11 (e) shows that pH_2 varies from 4.75 to 5.23. These results except pH_2 are in agreement with the experimental results obtained by Schwartz et al., (1975) and Ismail et al., (1989) where Schwartz et al., (1975) indicated that the incorporation of choline to produce ACh was very high at small choline concentration. However, small choline concentration the incorporation of choline was low. Ismail et al., (1989) illustrated that the excess choline might not be ready for conversion into ACh.

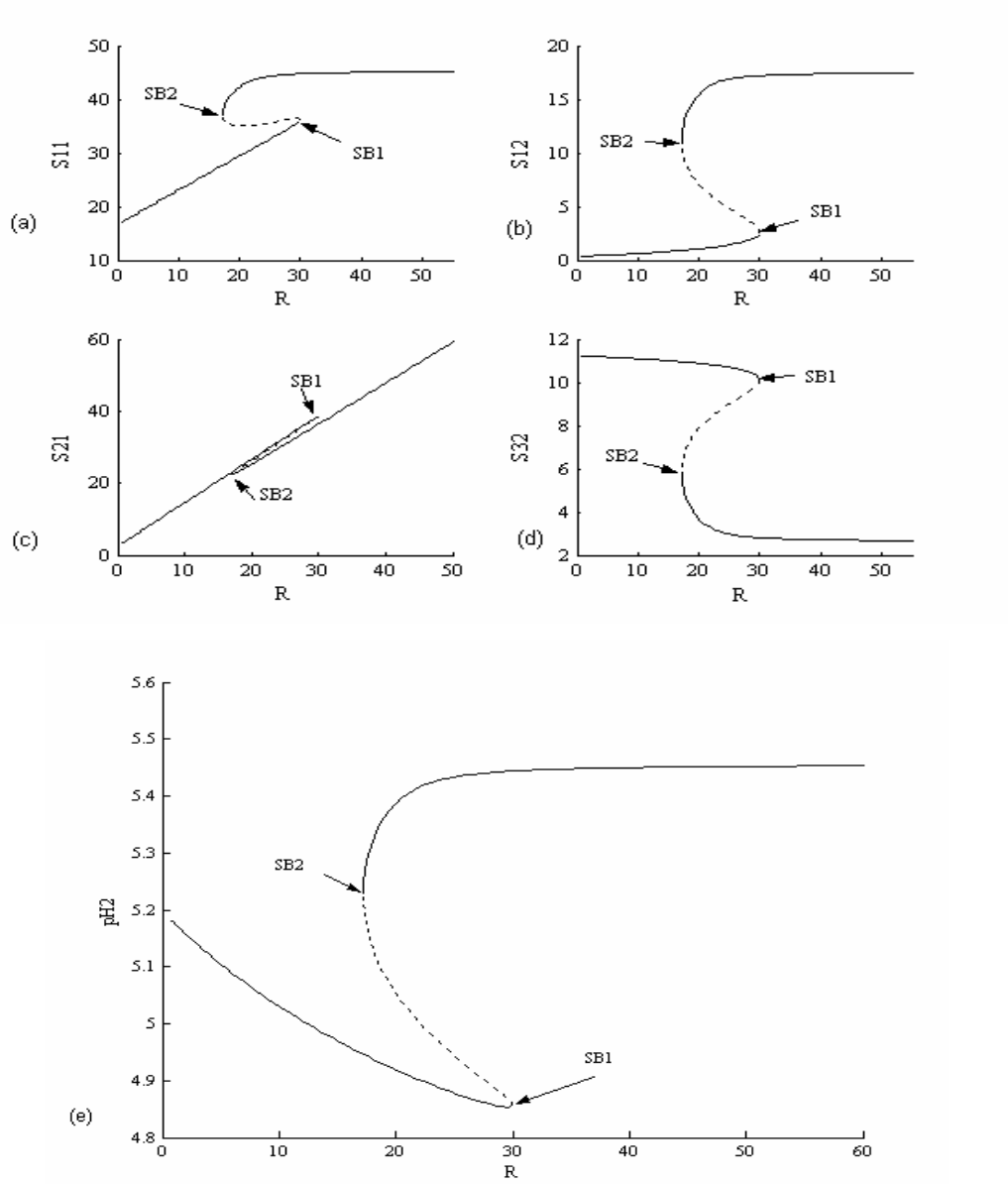

Figure 4-11: Bifurcation diagrams: Choline recycle ratio (R) as the bifurcation parameter at $(s_{1f} = 15)$ dimensionless and rest of data as shown in Table 4-3. stable: ——, unstable: ---------), periodic branch (stable ●, unstable ○):

(a)Effect on ACh in compartment (1) (s_{11}); (b) Effect on ACh in compartment (2) (s_{12}), (c) Effect on choline concentration in compartment (1) (s_{21}), (d) Effect on acetate concentration in compartment (2) (s_{32}), and (e) Effect on pH concentration in compartment (2) (pH_2).

Case (2): Dynamic Bifurcation at s_{1f}=2.4

Figure 4-12 illustrates the dynamic bifurcation diagrams using R as the bifurcation parameter but with a different value of feed ACh concentrations $\left(s_{1f} = 2.4\right)$ which represents a very low feed ACh concentration and the other parameter values are shown in Table 4-3. Figure 4-12 shows the complex behavior of the system through various stages in the neurocycle for a narrow range of the bifurcation parameter ($0 \prec R \leq 0.8$). It is clear that the system has rich dynamics phenomena at a very low range of R which is too small to start the synthesis reaction catalyzed by ChAT.

Three main regions in the bifurcation diagram are observed, each one corresponding to a different form of qualitative behavior. The HB appears at $R = 0.778$.

In the range of ($0 \leq R \leq 0.8$): The system demonstrates oscillatory behavior in the range ($0 \leq R \leq 0.8$). In this range, the equilibrium points are not attractors anymore but repellent, and the limit cycles are the only attractors (periodic attractors).

The first region: in the range of ($0.778 \leq R \leq 0.7945$), the bistability phenomena occurs where both periodic and point attractors coexist with an unstable periodic orbit as the separatrix separating the domains of attraction of the periodic and point attractors. This bistability leads to the condition that at the same value of R slightly different initial conditions lead to different types of attractors. It is noticed that after this range the periodic orbits cease to exist when ($0.7945 \leq$ R). The pH_2 is inside the physiological expected range where it is between 6.25 and 8.2. This region with low choline uptake is thus characterized by the presence of bistability. The PD point occurs at R=0.7948 where PD is one of the routes leading to chaos.

The **second region**: in the range of ($0.21 \leq R \leq 0.778$), the system oscillates periodically, where the periodic attractor are the only attractor in this range. However, in **the third region**: in the range of ($R \leq 0.21$), the system exhibits unstable periodic orbits. It is clear ACh concentrations in compartments 1 and 2: s_{11} , and s_{12} respectively is out of the physiologic range, because the range of the choline recycle ratio is very small, this means that choline uptake will be very low, hence the rate of ACh synthesis is very small.

There are many factors contributing to the rise of the complexity in the ACh system: the first factor is the competition between the diffusion and transport processes, from compartment 1 to compartment 2 and the enzymatic processes either the synthesis process catalyzed by ChAT and the hydrolysis process catalyzed by AChE. The high nonlinearity in the rate of reactions and their dependence on pH and their inhibition by substrates plays a role for giving rise for the oscillatory

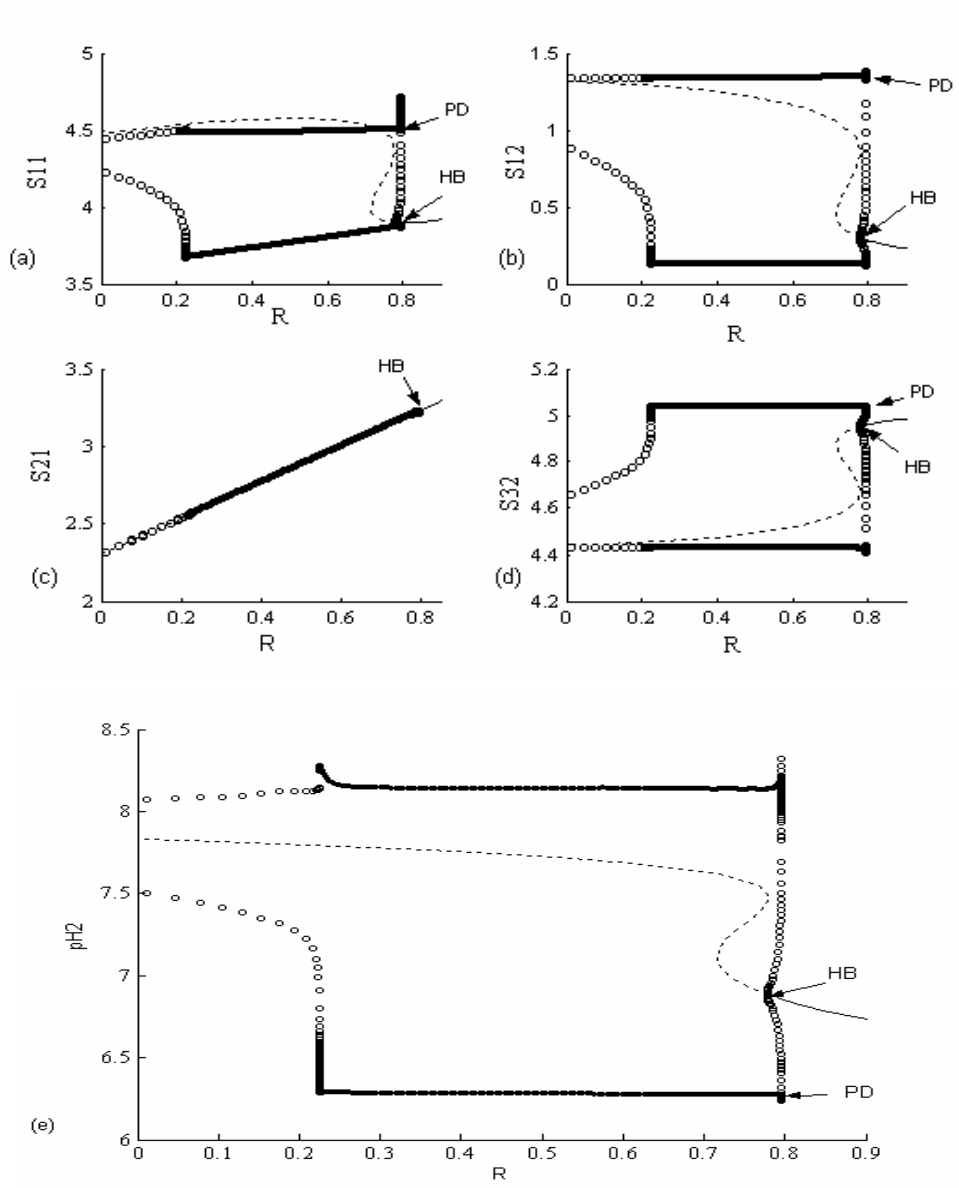

Figure 4- 12: Bifurcation diagram: Choline recycle ratio (R) as the bifurcation parameter at $(s_{1f} = 2.4)$

(stable: —, unstable: ----------), periodic branch (stable ●, unstable ○):

(a)Effect on ACh in compartment (1) (s_{11}); (b) Effect on ACh in compartment (2) (s_{12}), (c) Effect on choline concentration in compartment (1) (s_{21}), (d) Effect on acetate concentration in compartment (2) (s_{32}), and (e) Effect on pH concentration in compartment (2) (pH_2).

behavior. Finally, the choline recycle from compartment 2 to compartment 1 contributes the rise of complex behavior in the system.

The small levels of ACh in both compartments s_{11} and s_{12} as shown in Figure 4-12 because of the small values of the bifurcation parameter R confirm that choline stream produced from the hydrolysis of ACh in compartment 2 contributes with a significant portion of the choline used for ACh synthesis in compartment 1 (Wecker et al., (1979), Iwamoto (2006), Tucek et al., (1985))**.** Therefore, it is possible that under conditions of AChE inhibition, choline uptake in the recycle stream is diminished leading to lack of the synthesis of ACh [Wecker et al., (1979), Iwamoto (2006)]. The effect of choline recycle ratio shows that choline uptake plays an important role, for supplying the required choline as a substrate for the synthesis reaction catalyzed by ChAT in compartment 1. The concentrations of ACh, choline and acetate were affected by the choline recycle ratio through a certain range of R then they become constant as R increases. These results confirm the role of recycled choline produced from ACh hydrolysis and choline uptake in the ACh neurocycle. The results of this section resemble the results produced from studying the effect of feed choline concentrations in Chapter 3 (Mustafa et al., 2009[b]).

4.6 Summary and Conclusions

In this chapter, the effects of ChAT activity and choline uptake in terms of choline recycle ratio on a coupled ChAT/AChE enzyme system are investigated. It is found that as ChAT activity increases, ACh concentrations in compartments 1 and 2 increase continuously. In the range $\left(7.53\times10^{-4} \le B_1 \le 9.78\times10^{-4}\right)$ kmol/m^3; a hysteresis phenomenon is noticed between the two static bifurcation points (SB_1 and SB_2) in this range. Hysteresis generally expresses the capability of the system to respond for any sudden change in a range around the static bifurcation points of the bifurcation points as shown in Figure 4-3(b).

At the low values of ChAT activity, the system exhibits complex dynamics bifurcation including chaotic behavior via period doubling and period adding sequence in the range $\left(4.98\times10^{-5} \le B_1 \le 5\times10^{-5}\right)$ kmol/m^3. A bistability behavior is observed in a range close to the subcritical HB where periodic and point attractors coexist with an unstable periodic orbit as the separatrix separating the domains of attraction of the periodic and point attractors. This bistability leads to the condition, that at the same value of B_1 slightly different initial conditions lead to different

types of attractors. Both periodic orbits and steady stationery states co-exist together as shown in Figure 4-5 and Figure 4-6.

It can be concluded that ACh was synthesized considerably less efficiently at low values of B_1 which gives the opportunity for the system complexity. In addition, the increase of ChAT activity (B_1) can be considered satisfactory for fast synthesis of ACh in compartment 1 to compensate for the released ACh in compartment 2. Therefore, ChAT activity is a good key to cure the disturbances of ACh levels in cholinergic disorders such as Alzheimer's and Parkinson's diseases. It is found that the decline of ChAT activity will cause an observable reduction in the ACh synthesis s_{11} and ACh release s_{12} which represents one of the main symptoms of Alzheimer's disease.

The choline uptake in terms of choline recycle ratio affects greatly the ACh concentrations in both compartments which increase until a certain value of R=30 then they become constant in the range of $(R \geq 30)$. The system is dominated by the complexity and oscillatory behavior at low values of R where the reduction of R causes deficiency in choline supplied to the compartment 1. Therefore, choline uptake in terms of choline recycle ratio represents a limiting factor for controlling ACh cholinergic system and regulating the processes of ACh and adjusting the levels of the state variables in the system. ACh is synthesized less efficiently when $(R \geq 30)$. This is because the ChAT enzyme is inhibited by the excess of choline substrate which occur with the increase in choline uptake (R). This is in agreement with the results obtained by Schwartz et al., (1975). At the low values of choline recycle ratio, the system exhibits oscillatory behavior including chaotic behavior via a PD and period adding sequence in the range ($R \leq 0.8$).

From studying the effects of ChAT activity and R, our model results agree with the experimental results of Steven et al., 1982; Levnter et al., 1982; Krell and Goldberg, 1975 who observed that when ChAT inhibitors are injected into animals, a significant inhibition of brain ChAT activity is observed, but there is no significant reduction in the ACh levels in the brain. These experiments, coupled with others that investigated the effects of choline uptake inhibition (Yamamura and Snyder, 1973; Kuhar and Murrin, 1978) confirm that in the nervous tissue high-affinity choline uptake is the rate limiting for ACh synthesis. This is in agreement with our results that show that the choline is the most important factor in ACh processes and from the effect of choline recycle ratio, it is clear that choline uptake plays an important role, where it supplies choline as a substrate for the synthesis reaction catalyzed by ChAT in compartment 1.

Furthermore, the results are in accordance with the results obtained by Brandon et al., (2004) who indicated that the loss of ChAT activity will cause a decline in the rate of ACh synthesis in compartment 1. The reduction of ChAT activity needs other alternative effects to keep normal ACh concentrations. According to Brandon et al., (2004), increased uptake or recycle of choline to ChAT in compartment 1 may be the alternative solution for keeping the high efficiency of ACh and the rate-limiting factor in the synthesis of ACh.

Our results are also in accordance with the experimental results of other researchers who investigated both choline uptake coupled with ChAT in the presynaptic neurons [Sterling et al; 2006]. They found that inhibition ChAT activity did not block the synthesis of ACh in compartment 1. However, the inhibition of choline transport into compartment 1 blocked ACh synthesis completely in compartment 1 Barker and Mittag, 1973; Guynet et al, 1973; Yamamura and Snyder, 1973; Kuhar and Murrin, 1978, Sterling et al; 2006]. One of the explanations of these results is the existence of ChAT in the presynaptic terminals in a very higher activity than necessary for ACh synthesis [Trabucchi et al, I975; Haubrich, I976]. Finally, it can be concluded that choline recycled thereby choline uptake plays the role of rate limiting factor in the control of ACh synthesis.

Chapter 5
Application of Continuation Method and Bifurcation for the Acetylcholine Neurocycle Considering Partial Dissociation of Acetic Acid

In this chapter, bifurcation and chaotic behavior of the two-enzyme-two- compartment Acetylcholine (ACh) neurocycle model developed earlier (Mustafa et al., 2009 a, b) are investigated allowing for partial dissociation of acetic acid. The two-parameter continuation technique is used to investigate static and dynamic solutions of the ACh cholinergic neurocycle system based on feed choline concentration as the main bifurcation parameter. A detailed bifurcation analysis is carried out in order to uncover some important features of the system, such as static bifurcation, dynamic bifurcation and chaotic behavior. These findings are related to the real phenomena occurring in the neurons, like periodic stimulation of neural cells and non-regular functioning of ACh receptors. It is found that pH does exist in the range of [7.05- 7.75] which is inside the physiological range of pH of the brain associated with taking into consideration the partial dissociation of the acetic acid. The disturbances and irregularities (chaotic attractors) occurring in the ACh cholinergic system may be good indications to cholinergic diseases such as the Alzheimer's and Parkinson's diseases.

Keywords: Acetylcholine, Choline, Acetic acid, Hydrogen ions, period doubling, Dynamic behavior, Bifurcation, Chaos, Alzheimer's and Parkinson's diseases.

5.1 Introduction

Hydrogen ion (H^+) is a very simple element because it contains only one proton and its size is very small [Kaila and Ransom (1998)]. However, H^+ ions play an extremely vital role in all metabolic processes, and ion transport occurring in the living organisms. For example, the function of protein components can be altered from hydrophobicity to hydrophilicity because of its ability to release or bind H^+ ions [Karel and Milan (1997)]. It is observed that most pathological environments and ions diffusion are accompanied by observed pH alteration changes [Obara et al., (2008)]. Kaila and Ransom (1998) indicated that imbalance of neural excitability which occurs due to irregular changes in pH of neuronal environment and hence disturbances in action potentials generations, can cause some diseases such as epileptic seizures. Moreover, neural excitability can be increased during

alkalosis and decreased during acidosis. Scientists discovered that the response of cholinergic receptors can be reduced with the reduction of pH. Coma can be occurred due to improper response of nervous system. Any irregular alterations in induced pH of metabolic and nervous processes will affect the performance of receptors, transporters, and channels and will influence nervous excitability and communications and the performance of nervous functions of the brain [Kaila et al., (1998); Jaak (2007)]. H^+ ions play a vital role in signaling in the different parts of brain where the action potentials and the functions in both glial cells and neurons can be affected easily with any alterations in pH of the cells, so that transformation of information within the brain and between brain and other parts of the body will be affected [Kaila et al., (1998)]. According to Kaila et al.,(1998), based on pH regulations living organism cells keep their pH at a resting level which is more alkaline than acidic.

In the presynaptic neurons where ACh is synthesized by the enzyme ChAT, the internal organs such as the mitochondria and synaptic vesicles have the capability to keep pH gradient to regulate all the diffusion processes between the interior and exterior of the cells [Paulsen et al., (1996); Kaila et al., (1998); Diering et al., (2009)]. Because glial cells are very close to neurons and supply them with salts and nutrients, the extracellular pH of neurons will be affected by any slight change in the intracellular pH of glial cells [Claudia R. et al., (2007); Amato et al., 1994; Boron W.F (2004)]. Usually the extracellular pH of glial cells exists in the range 7.2-7.5, and their intracellular pH exists in the range of 6.9-7.6 [Christine et al., (1998)]. Walter (2004) showed that the mechanism of pH regulation via acid/base transport mechanisms is much complicated because there is a complex mutual effect between signal processing and pH effects [Walter (2004); Boron and Boulpaep (2002)]. Acetic acid as a weak acid and its conjugate as a weak base constitute a buffer pair. The components of this buffer power can bind and release ions and thereby affecting the functions of neurons and glial cells [Boron (2004); Zaniboni et al., (2003)].

H^+ may be stored in the vesicles and released with ACh leading to acidification of the synaptic cleft. This means that postsynaptic interactions between the ACh transmitters and the cholinergic receptors and synaptic transmission will be controlled and modulated by pH changes in the synaptic cleft [Abdrakhmanova et al., (2004); Mozrzymas et al., (2003)]. All the functions of the nervous system such as synaptic transmission, enzymatic processes, and all metabolic activities are influenced by any alterations in pH (Deitmer et al., 1996). So that pH changes represent a critical necessity for all biological functions (Deitmer et al., 1996).

5.2 Hydrogen Ions and Cholinergic Diseases

There is a lot of research proposing that there is a great relation between cholinergic diseases (such as Parkinson's disease and Alzheimer's disease) and pH disturbances in neurons and glial cells (Kaila et al., (1998); Claudia et al., (2007)). One of the main aspects for these diseases is that pH irregularities can cause changes in proliferation of glial cells. Glial cells are usually existent in plenty in nervous systems; hence, cellular proliferation can be affected by alterations in pH, thereby affecting neurons and transmitters. Therefore, it will helpful to control pH changes in glial and neurons to cure brain diseases (Kaila et al., (1998)).

Most of diseases (e.g., head injury, epilepsy, cancer, and stroke) are accompanied with severe pH alterations which cause imbalance in acid/base diffusion (Kaila et al., (1998)). According to Mario et al. (2005), brain afflicted by diseases is accompanied by disturbances in pH. For example, acute head injury is associated with chronic acidification causing neurological abnormalities such as lack of consciousness (Kaila et al., (1998)).; Mario et al., (2005)).

5.3 ACh Neurotransmitter and Partial Dissociation of Acetic Acid

ACh neurotransmitter can affect intracellular pH (pH of the presynaptic neurons) in several ways. ACh release is associated with opening of channels in asrtocytes can, therefore, lead to efflux of H^+ from the cells and cause an acidification of the postsynaptic neurons and synaptic cleft, however, it will cause alkalinization in the presynaptic neurons(Christine et al 1998; Boron (2004)). Neurons actively extrude acid to maintain intracellular pH at more alkaline levels than dictated by the H^+ equilibrium potential (Christine et al 1998; Gregory Zoppo 2009). Il'in et al., (1975) investigated how isolated neurons during the processes of ACh were influenced by changes in pH. They found that the sensitivity of the cholinergic receptor membrane reduced as pH reduced. In addition they found that the sensitivity to ACh inhibited in the acidic environment where pH in the range 5.8–6.0 and had not been responded even the pH increased to 10.6.

To simulate the hydrolysis and excitation processes of ACh, artificial membranes immobilized with the enzymes have been applied. Santos et al. (2006) found that an action potential difference in the form of hysteresis when they used artificial membranes immobilized with AChE and injected ACh in one side of the membrane. Because the enzymatic reactions were accompanied by production of H^+, an auto-catalytic behavior will be dominated in the system [Santos et al., (2006); Mustafa et al., a, b (2009)].

In the pervious three chapters the rate-limiting step in the ACh neurocycle was found to be the uptake of choline and that the feed choline is the most important substrate in ACh neurocycle. It was found that both acetyl-coA and ChAT activities are not the rate limiting factors in the neurocycle. However; we have found that the pH in compartments 1 and 2 are out of the physiological range in many cases. This is because of the fact that our previous model assumption considered that each mole of acetic acid produced during hydrolysis process gives one mole of hydrogen ions. In fact for the fully ionized acetic acid, this is not realistic. In this work we deal with this problem by considering the partial ionization of acetic acid. This will affect the H^+ protons concentration in both compartments leading to more realistic values of pH. In addition, we will consider the rate of formation of Acetyl CoA from acetate ions (A^-) and CoA, which will make the model more realistic. We will use the continuation method to investigate the dynamic bifurcation and chaotic behavior of the system based on these new considerations in addition to kinetic mechanisms for synthesis and hydrolysis reaction we considered earlier (Mustafa et al., 2009 a, b).

We will investigate the phenomena of complex dynamic and static behavior including bifurcation, period doubling (PD) instability, and chaos by developing the previous two-enzyme/two-compartment model considering partial dissociation of acetic acid and link these phenomena with the physiological behaviors relating to the cholinergic ACh neurocycle system.

5.4 Formulation of Diffusion-Reaction Two-Enzyme /Two-Compartment Model Based on Partial Dissociation of Acetic Acid

Figure 5-1 describes the ACh neurocyle system at the contact between two neurons. As illustrated by the figure, the presynaptic neuron represents compartment 1 and both the postsynaptic neuron and the synaptic cleft represent compartment 2. The choline is re-uptaken from the synaptic cleft into the presynaptic neuron terminal. Figure 5-1 shows that there is another stream of ACh which is called mobile ACh and enters compartment 1 coming by axonal transport. Also Figure 5-1 shows that there are two resources of choline. The first one is produced by the hydrolysis of ACh, and then a part of it is recycled to the first compartment. The other source is synthesized in the environment outside compartment 1 where choline in the latter stream comes either directly from the free choline of the blood plasma, or from the brain cells, where it has been released from choline-containing compounds (Tucek 1985, Mustafa et al., 2009 b). The choline produced in compartment 2 is the only component existing in the recycle stream. The physiological references such as Tucek et al. (1978) and (1985)

confirm this point where they do not refer to recycling of any other components such as ACh and acetyl CoA (Mustafa et al., 2009 b), as explained before. Acetyl-CoA is synthesized in the mitochondria with a certain rate ($r_{(3)}$) as will be explained. The acetyl CoA should be plentiful since it is provided from pyruvate formed by the metabolism of glucose. All of these streams (the stream of axonal transport of ACh, the stream of choline synthesized in extracellular space of compartment 1, the stream of Acetyl-CoA coming from mitochondria) are collected together in one feed stream which meets the recycle stream of choline coming from the hydrolysis of ACh to enter compartment 1 as shown in Figures 5-2 which shows a simplified form of the feedback model of ACh neurocycle shown in Figure 5-1.

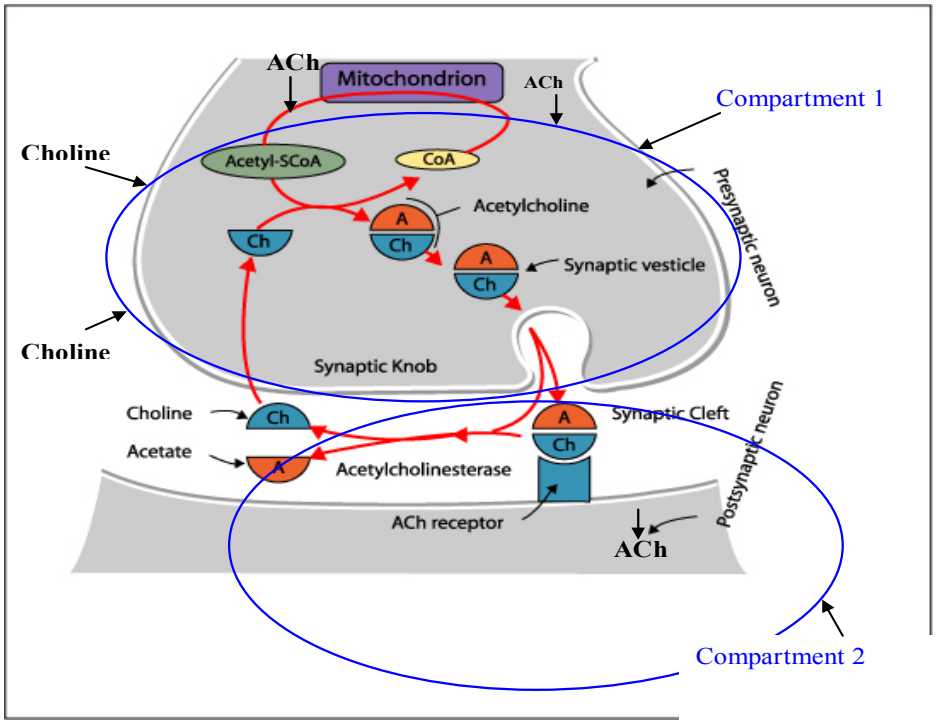

Figure 5-1 Schematic of synaptic neurons and cleft

"This image has been reproduced from Anesthesia with permission (www.AnaesthesiaUK.com)

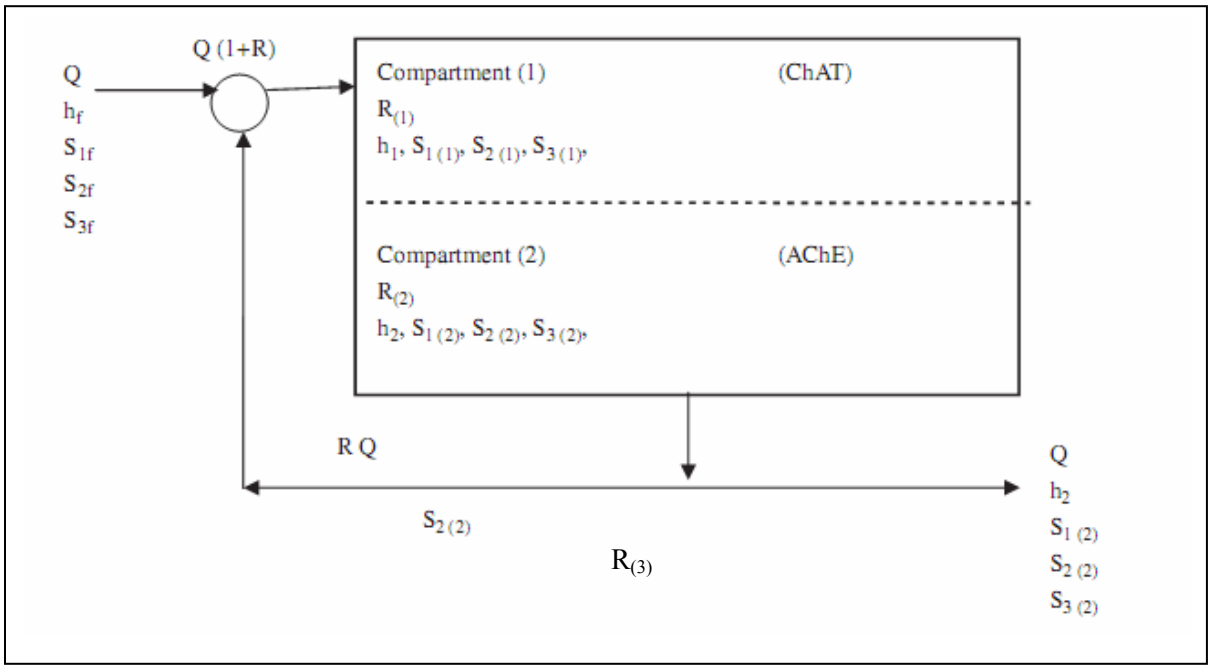

Figure 5-2: Two-enzyme/ two-compartment model

As shown in Figure 5-1 ACh hydrolysis reaction, catalyzed by acetylcholinesterase (AChE), occurs on ACh receptors which are located on the top of the postsynaptic neuron. Then the products of hydrolysis (choline and acetate) go through the synaptic cleft. As explained in Mustafa et al. (2009b), both regions of the synaptic cleft and postsynaptic neurons are unified together into one homogeneously stirred compartment (compartment 2) instead of more compartments because both the synaptic cleft and the postsynaptic neurons are homogeneous and interactive. In addition, this avoids the expected complexity and difficulty in solving the model and analyzing the results when the dimensionality of the system is too high. The concentrations of the components in compartment 2 represent the average concentrations in both the synaptic cleft and the postsynaptic neurons. Furthermore, we assumed that the flow rate of the feed stream to compartment 1 and that of the exit stream from compartment 2 are equal. In summary, each compartment is defined as a constant flow; constant volume, isothermal, continuous stirred tank reactor (CSTR) and the two compartments are separated by a permeable membrane. The behavior for a single synaptic vesicle is described by this

simple two-compartment model, assuming that all the events are homogeneous in all vesicles and using the proper dimensionless groups.

The rate of acetyl CoA synthesis from acetate and CoA catalyzed by the enzyme acetyl CoA synthase occurring in compartment (1) will be considered. The rate of dissociation of acetic acid (Ac) will be considered on the level of equilibrium. The acetate ion (Ac^-) produced from the ionization of Ac will contribute to the formation of Acetyl-CoA. In both compartments, there are two sources of hydrogen ions, the first one comes from the dissociation of Ac and the other comes from the ionization of water molecules. In order to illustrate the effect of partial hydrolysis of acetic acid in the model we can start with these proposed sets of chemical reactions in the two compartments as follows:

Compartment (1):

In compartment (1), acetyl CoA is synthesized by the Acetyl-CoA synthase and ACh is synthesized by the enzyme ChAT; acetic acid is hydrolyzed as follows (Tucek 1990**,** Mustafa et al., (2009) a, b):

$$R_{(1)}: \quad Ch + Acetyl - CoA \xrightarrow{ChAT} ACh + CoA \qquad (5.1)$$

$$R_{(3)}: \quad Ac^- + CoA \xrightarrow{AcetylCoA\ Synthase} Acetyl - CoA \qquad (5.2)$$

$$R_d: \quad Ac \xleftrightarrow{R_d} Ac^- + H^+ \qquad (5.3)$$

$$R_w: \quad H_2O \xleftrightarrow{R_W} H^+ + OH^- \qquad (5.4)$$

Where R_d is the rate of acetic acid dissociation, and R_w is the rate of water hydrolysis/formation.

Compartment (2):

After ACh causes the electrochemical (synaptic) signals by interaction with the postsynaptic receptors, ACh is destroyed in compartment 2 by AChE by the degradation reaction as follows:

$$R_{(2)}: ACh + Water \xrightarrow{AChE} Choline + [Ac] \ [acetic\ acid] \qquad (5.5)$$

$$R_d: \quad Ac \xleftrightarrow{R_d} Ac^- + H^+ \qquad (5.3)$$

$$R_w: \quad H_2O \xleftrightarrow{R_W} H^+ + OH^- \qquad (5.4)$$

The reactions $R_{(1)}$, and $R_{(2)}$ are considered to be substrate inhibited and in addition to $R_{(3)}$, all of them are hydrogen ions affected. This leads to a non-monotonic dependence of the reaction rates on the substrate concentrations and pH. The rates can be formulated by employing certain assumptions and basic biokinetics knowledge as explained in the following section. The details of the derivation are given in our chapters 2-4. The final dimensionless forms of the ordinary differential equations of the tenth – dimensional system are summarized in Table 5.1. The model equations are in

terms of ten state variables $h_{(1)}, h_{(2)}, a_{(1)}, a_{(2)}\ s_{1(1)}, s_{1(2)}, s_{2(1)}, s_{2(2)}, s_{3(1)}$ and $s_{3(2)}$ and 36 parameters (Tables 5.2 and 5.3). All values of the parameters (with respective references) used in this investigation are given in Table 5.3.

Table 5-1: Dimensionless forms of the ordinary differential equations of the eight state variables

Item	Compartment	Differential equations
Hydrogen protons	1	$\frac{dh_{(1)}}{dT} = F_1 + F_y * F_5$
	2	$\frac{dh_{(2)}}{dT} = V_R\left(F_3 + F_y * F_6\right)$
ACh	1	$\frac{ds_{1(1)}}{dT} = s_{1f} - \alpha_{s_1}\left(s_{1(1)} - s_{1(2)}\right) + \frac{B_1\, r(1)}{K_{s1}}$
	2	$\frac{ds_{1(2)}}{dT} = V_R\left(\alpha_{S_1}\left(s_{1(1)} - s_{1(2)}\right) - s_{1(2)} - \frac{B_2\, r(2)}{K_{s1}}\right)$
Choline	1	$\frac{ds_{2(1)}}{dT} = s_{2f} + R * s_{2(2)} - \alpha_{S2_1}\left(s_{2(1)} - s_{2(2)}\right) - \frac{B_1}{S_{2refernce}} r(1)$
	2	$\frac{ds_{2(2)}}{dT} = V_R\left(\alpha_{S2}\left(s_{2(1)} - s_{2(2)}\right) - (1+R) * s_{2(2)} + \frac{B_2}{S_{2reference}} r(2)\right)$
Acetyl CoA	1	$\frac{ds_{3(1)}}{dT} = s_{3f} - \alpha_{S3}\left(s_{3(1)} - s_{3(2)}\right) - \frac{B_1}{S_{3\,refernce}} r(1) + \frac{B_3}{S_{3\,refernce}} r(3)$
	2	$\frac{ds_{3(2)}}{dT} = V_R\left(\alpha_{S3}\left(s_{3(1)} - s_{3(2)}\right) - s_{3(2)}\right)$
Acetate	1	$\frac{da_{(1)}}{dT} = F_5$
	2	$\frac{da_{(2)}}{dT} = V_R * F_6$

Rate of ACh synthesis ($r_{(1)}$)	1	$r_{(1)} = \frac{c_1 s_{21} s_{31}}{(h_1 + 1 + \delta h_1^2) c_1 c_2 / h_1 + c_4 s_{31} + c_2 s_{21} + c_3 s_{21} s_{31}}$
Rate of hydrolysis ($r_{(2)}$)	2	$r_{(2)} = \frac{s_{12}}{s_{12} + 1/h_2 (h_2 + 1 + \delta h_2^2) + \alpha s_{12}^2}$
Rate of synthesis of Acetyl Co A ($r_{(3)}$)	1	$r_{(3)} = \frac{a_1}{a_1 + K_m (h_1 + 1 + \delta h_1^2)/h_1}$
F_{10}		$\alpha_{oH_{H^+}} \gamma_1 \left(\frac{1}{h_{(1)}} - \frac{1}{h_{(2)}} \right) - \alpha_{H_{H^+}} \left(h_{(1)} - h_{(2)} \right) + h_f - \frac{\gamma_1}{h_f} - Fy * a_f$
F_1		$F_{10} + R \left(h_2 - \frac{\gamma}{h} \right) - R F_y a_{(2)} + \alpha_A F_y \left(a_{(1)} - a_{(2)} \right) + \frac{B_3 r(3)}{Kh}$
F_{20}		$a_f \left(1 + \lambda h_f \right) - R a_{(2)} \left(1 + \lambda h_{(2)} \right) - \frac{B_3 r(3)}{A_{ref}}$
F_2		$F_{20} - \alpha_A \left(a_{(1)} - a_{(2)} \right) - \alpha_{AC} \lambda \left(a_{(1)} h_{(1)} - a_{(2)} h_{(2)} \right)$
F_{30}		$\alpha_H \left(h_{(1)} - h_{(2)} \right) - \alpha_A F_y \left(a_{(1)} - a_{(2)} \right) - \alpha_{OH} \gamma \left(\frac{1}{h_{(1)}} - \frac{1}{h_{(2)}} \right)$
F_3		$F_{30} - (1 + R) \left(h_{(2)} - \frac{\gamma}{h_{(2)}} - F_y * a_{(2)} \right)$
F_{40}		$\frac{V_R * B(2) r(2)}{A_{ref}} + \alpha_{AC} \lambda \left(a_{(1)} h_{(1)} - a_{(2)} h_{(2)} \right)$
F_4		$F_{40} - (1 + R) a_{(1)} (1 + \lambda h_{(2)}) + \alpha_A \left(a_{(1)} - a_{(2)} \right)$
F_5		$\frac{F_2 - \lambda F_1 a_{(1)}}{1 + \lambda a_{(1)}} + F_y \lambda a_{(1)}$
F_6		$\frac{F_4 - \lambda F_3 a_{(2)}}{1 + \lambda h_{(2)} + F_y \lambda a_{(2)}}$

Table 5-2: Dimensionless state variables, parameters and other terms.

Dimensionless State Variables			
$h_{(j)} = \frac{[H^+]_{(j)}}{K_{h1}}$	Dimensionless hydrogen ion concentration in compartment j		
$s_{1(j)} = \frac{[S_1]_{(j)}}{K_{s1}}$	Dimensionless ACh concentration in compartment j		
$s_{2(j)} = \frac{[S_2]_{(j)}}{[S_2]_{reference}}$	Dimensionless choline concentration in compartment j		
$s_{3(j)} = \frac{[S_3]_{(j)}}{[S_3]_{reference}}$	Dimensionless acetyl CoA concentration in compartment j		
$a_{(j)} = \frac{[A]_{(j)}}{[A]_{reference}}$	Dimensionless acetate concentration in compartment j		
Dimensionless Membrane Permeabilities			
$\alpha_{H^+} = \frac{\alpha'_{H^+} A_M}{q}$	$\alpha_{OH^-} = \frac{\alpha'_{OH^-} A_M}{q}$		$\alpha_{S_1} = \frac{\alpha'_{S_1} A_M}{q}$
$\alpha_{S_3} = \frac{\alpha'_{S_3} A_M}{q}$	$\alpha_{S_2} = \frac{\alpha'_{S_2} A_M}{q}$	$\alpha_{AC} = \frac{\alpha'_{AC} A_M}{q}$	$\alpha_A = \frac{\alpha'_A A_M}{q}$
Dimensionless Kinetic Parameters for ChAT Catalyzed Reaction			
$F_y = \frac{a_{ref}}{Kh}$	$\lambda = \frac{Kh}{Ka}$		
Other Terms Used in Dimensionless Form			
$V_R = \frac{V_{(1)}}{V_{(2)}}$	$\gamma_1 = \frac{K_W}{K_{i1}}$		$T = \frac{q\,t}{V_{(1)}}$
$B_1 = \frac{V_1 V_{M1} \overline{ChAT}}{q}$	$B_2 = \frac{V_2 V_{M2} \overline{AChE}}{q}$		$B_3 = \frac{V_1 V_{M3} \overline{ACoA\ Synthase}}{q}$

Table 5-3: Parameters Values:

Parameter	Value	Reference
C_5	5.2(0.1)	Hersh & Peet (1977)
C_1	2.4	Hersh & Peet (1977)
C_4	1000	Hersh & Peet (1977)
C_2	5	Hersh & Peet (1977)
C_3	1	Hersh & Peet (1977)
α	0.5	Garhyan et al., (2006), Elnashaie et al., 1983a; Elnashaie et al., 1983b; Elnashaie et al., 1984; Elnashaie et al., 1995; Ibrahim et al., 1997)
δ	1	Garhyan et al., (2006), Elnashaie et al., 1983a; Elnashaie et al., 1983b; Elnashaie et al., 1984; Elnashaie et al., 1995; Ibrahim et al., 1997)
$K_a(k_h)$	$1.0*10^{-6}$ kMole/m^3(μMole/mm^3)	Garhyan et al., (2006), Elnashaie et al., 1983a; Elnashaie et al., 1983b; Elnashaie et al., 1984; Elnashaie et al., 1995; Ibrahim et al., 1997)
K_{s1}	$4.5*10^{-7}$ kMole/m^3(μMole/mm^3	Garhyan et al., (2006), Elnashaie et al., 1983a; Elnashaie et al., 1983b; Elnashaie et al., 1984; Elnashaie et al., 1995; Ibrahim et al., 1997)
S_{2ref}	$1.4*10^{-5}$ kMole/m^3(μMole/mm^3)	Guyton and Hall (2000)
S_{3ref}	$1.5*10^{-6}$ kMole/m^3(μMole/mm^3)	Guyton and Hall (2000)
A_{ref}	$1.0*10^{-5}$ kMole/m^3(μMole/mm^3)	Tucek (1985)
AC_{ref}	$5.0*10^{-6}$ kMole/m^3(μMole/mm^3)	Tucek (1985)
B_1	$2.0*10^{-5}$ kMole/m^3(μMole/mm^3)	Garhyan et al., (2006)
B_2	$3.0*10^{-5}$ kMole/m^3(μMole/mm^3)	Garhyan et al., (2006)
B_3	$4.0*10^{-5}$ kMole/m^3(μMole/mm^3)	Assumed
α_{H^+}	2.	Elnashaie et al., (1984)
α_{OH^-}	0.5	Elnashaie et al., (1984)
α_{S_1}	2	Elnashaie et al., (1984)
α_{S_2}	2	Elnashaie et al., (1984)
α_A	0.6	Assumed

α_{AC}	2	Assumed
α_{S_3}	2	Elnashaie et al., (1984)
V_R	1.2	Elnashaie et al., (1984)
pH_f	8.0	Guyton and Hall (2000)
s_{1f}	1.11	Garhyan et al., (2006)
s_{2f}	4.6514	Garhyan et al., (2006)
s_{3f}	1.1	Garhyan et al., (2006)
a_f	3	Tucek (1985)
γ	0.01	Garhyan et al., (2006), Elnashaie et al., 1983a; Elnashaie et al., 1983b; Elnashaie et al., 1984; Elnashaie et al., 1995; Ibrahim et al., 1997)
K_d	0.000018	Golovanenko et al., (2006)
R	0.8	Tucek (1978)

5.5 Solution Techniques and Numerical Tools

The results of bifurcation diagrams for the system were obtained using XPPAUT and AUTO 2000, a bifurcation and continuation software for ordinary differential equations. Both static and dynamic bifurcations can be performed by this software package (Ermentrout 2002). The dynamics results such as phase planes and time traces were obtained via FORTRAN programme. For the chaotic behavior, we used one- dimensional Poincare map to investigate the intersections in one direction between a hyperplan surface (Which is chosen at certain value of a state variable) and trajectories [Garhyan et al. (2006); and Strogatz (1994)]. From discrete points of intersections, we are able to construct the bifurcation diagram of Poincare. Then we can investigate the dynamics behavior of the chaotic attractors. This is performed using IMSL libraries which contain DGEAR subroutine. Step size is chosen automatic based on the stiff differential equations during the investigations of the dynamics. Sometimes we used matlab to ensure the solution quality. The Poincare diagram is plotted using a program employed by Ibrahim et al., (2002) [Garhyan et al. (2006); Elnashaie et al. (1984)].

5.6 Physiological Values of the Parameters

To validate the results of the system with physiological and experimental results and with other models of previous investigators, we will compare our system behavior with the following physiological values of ACh, choline, acetate, and pH. These values depend on experimental results and other models like that used by Garhyan et al. (2006) and Mahecha- Botero et al. (2004). The concentrations are given in (Kmol/m^3). Human brain pH in a feline model is found to be in the range of 6.95-7.35 [Zauner and Muizelaar (1997)], and pH in a human brain was found by [Rae et al. (1996)] to be in the range 6.95 - 7.15. Free ACh in rat brain was found to be around 0.22×10^{-5} kmol/m^3 and total ACh was found to be around 1.77×10^{-5} kmol/m^3. Tucek (1990) and Garhyan et al. (2006) showed that in guinea pig cerebral cortex the range was from 0.31×10^{-5} (free ACh) to 1.67×10^{-5} kmol/m^3 (total ACh).

Wessler et al. (2001) and Mahecha- Botero et al. (2004) reported that ACh concentration in human placenta in the range of 3.0×10^{-5} to 55.5×10^{-5} kmol/m^3. Mahecha- Botero (2004) showed that in the isolated rings of rat pulmonary artery ACh was measured to be in the range of 0.001×10^{-5} to 3.0×10^{-5} see also [Kysela and Torok (1996)]. Mahecha- Botero et al. (2004) and Garhyan et al. (2006) reported that choline concentration in mouse rat brain is about 1.15×10^{-4} kmol/m^3. This range was confirmed by Tucek (1978) and choline concentration in human plasma is in the range of 0.01×10^{-4} to 0.7×10^{-4} kmol/m^3 [Chay and Rinzel (1981); Mahecha – Botero et al. (2004) and Garhyan et al. (2006)].

The real concentration of ACh in cholinergic neurons of the brain is not known [Tucek (1978) and (1990)]. The content of ACh in the rat brain will be taken as 1.2 x10^{-5} kmol/m^3 [Tucek et al. (1978)]. On the assumption that the neurons represent 1/3 of the weight of the brain (the rest being attributable to glial cells and extracellular fluid), that the ACh is confined to cholinergic neurons, and that cholinergic neurons represent 10% of the total volume of all neurons, the concentration of ACh in the cholinergic neurons will be equal to 1.2 x10^{-5} kmol/m^3 x 30=36 x10^{-5} kmol/m^3. Despite the uncertainties associated with these estimates (the main being the proportion of cholinergic neurons in the total neuronal population of the brain), it is evident that, in the light of the present knowledge, the estimated equilibrium concentration of ACh (12 x10^{-5} kmol/m^3) and the estimated concentrations of ACh in cholinergic neurons (36 x10^{-5} kmol/m^3) do not appear vastly different incompatible values. A higher concentration of ACh in presynaptic nerve endings might be achieved in two ways: by the

accumulation of ACh in synaptic vesicles, and by higher concentration of the substrates in this part of neuron. There is a wide range of H^+ and OH^- ions permeabilities; this range starts at 0.1 cm/s up to 0.0001 cm/s [Boron and Boulpaep (2002)]. The permeability of ACh is taken to be the same as the values used by Garhyan et al. (2006).

5.7 Results and Discussion

Because of the importance of the feed choline concentration s_{2f} as shown in chapters 3 and 4, it is selected as the main bifurcation parameter for a very narrow range ($4.4 \le s_{2f} \le 4.85$) in the dimensionless form corresponding to ($6.16\times10^{-5} \le s_{2f} \le 6.79\times10^{-5}$) kmol/m^3. Figure 5-3 shows the dynamic bifurcation diagrams at the set of system parameters as shown in Table 5-2 at the dimensionless feed acetate concentration A_f = 3 corresponding to 4.5x10^{-5} kmol/m^3. At low concentration of s_{2f} where the feed choline concentrations are in a very small range, the ACh cholinergic system is characterized by a lot of complexity.

As shown in Figure 5-3, the system demonstrates oscillatory behavior between the two Hopf bifurcation (HB) points where periodic or chaotic solutions appear. The first Hopf point is at s_{2f} = 4.442, the second Hopf point is at s_{2f} = 4.771 and the PD point is at s_{2f} = 4.674 where the periodic branch emanating loses its stability through period doubling cascade rout leading to chaos which will be analyzed in details later and the TR point exists at s_{2f} = 4.767. There are two static limit points (SLP).

The second HB point (s_{2f} = 4.771) is called a subcritical HB because a branch of unstable periodic orbits is extracted and separates the stable periodic orbits from the stable steady state. Hence, a bistability phenomenon exists around the second HB where both steady state and periodic solutions exist at the same values of the bifurcation parameter s_{2f} around a certain range of the second HB point. However, the first HB point at s_{2f} = 4.442 is called a supercritical HB. The dynamic bifurcation diagrams in Figure 5-3 can be divided into three main regions, each one corresponding to a different form of qualitative behavior and shown as follows:

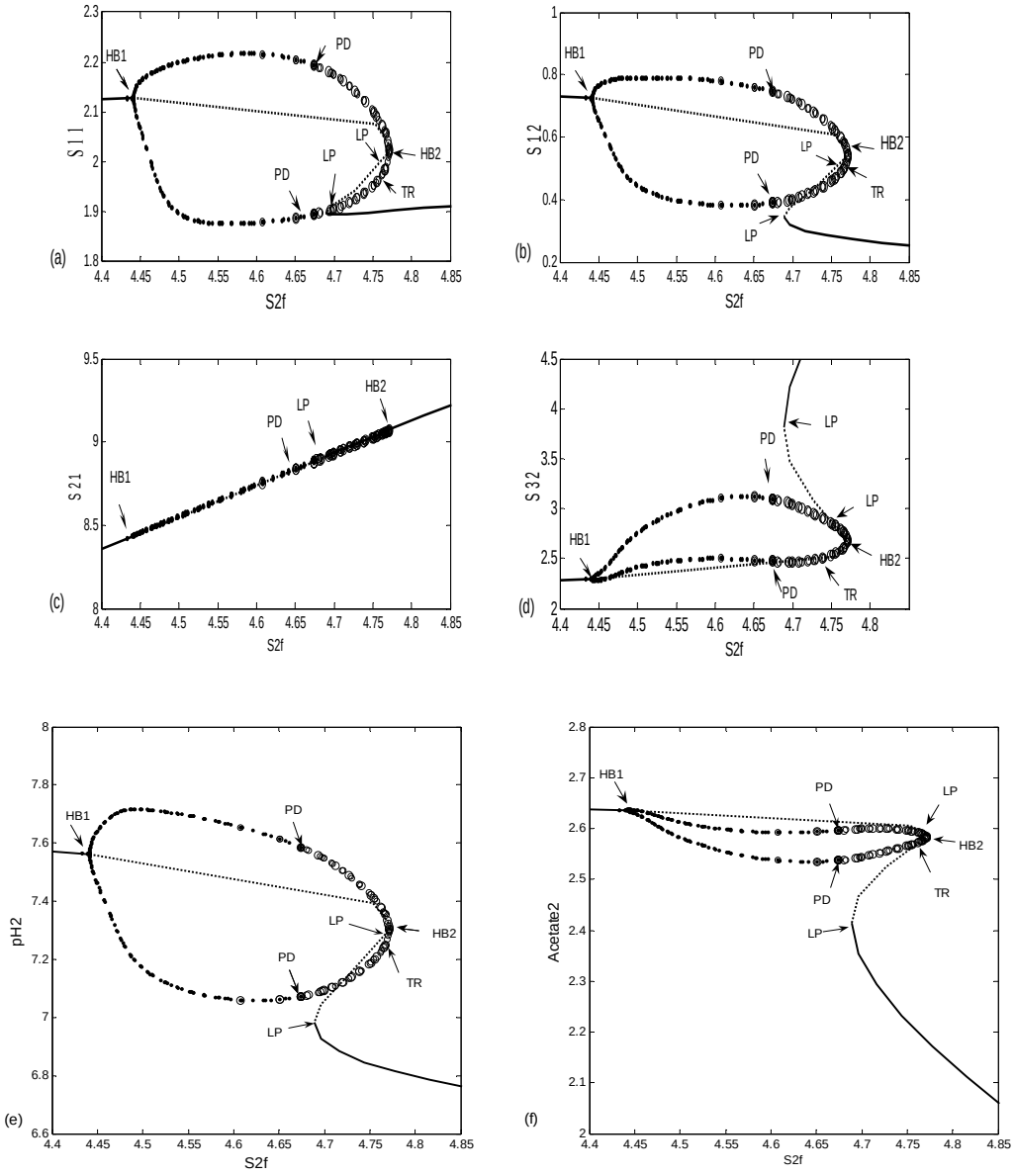

Figure 5-3: Bifurcation diagrams with choline feed concentration S_{2f} as the bifurcation parameter

(a) Bifurcation diagram for ACh concentration in compartment 1(S_{11}), (b) Bifurcation diagram for ACh concentration in compartment 2(S_{12}). (c)Bifurcation diagram for choline concentration in compartment 1(S_{21}), (d) Bifurcation diagram for Acetyl- CoA concentration in compartment 2(S_{32}), and (e) Bifurcation diagram for pH in compartment 2 (pH_2), and (f) Bifurcation diagram for Acetate concentration in compartment 2.

1) **Region 1**: $\left(0 \le s_{2f} \le 4.442\right)$

In this range which represents very low feed choline concentrations, the system is dominated by only a stable steady state (point) attractor. Figure 5-3(a) shows that s_{11} varies between 1.8 and 2.1 corresponding to 8.1×10^{-7} and 9.45×10^{-7} kmol/m3. Figure 5-3(b) shows that s_{12} varies between 0.63 and 0.73 corresponding to 2.835×10^{-7} and 3.825×10^{-7} kmol/m^3. Both of s_{11} and s_{12} are out of the physiological range. Figure 5-3 (d) shows that acetyl CoA (s_{32}) is around 2.25. Figure 5-3 (e) shows that pH_2 varies around 7.57 which is close to the physiological range due to consideration of the partial dissociation of acetic acid. Figure 5-3(f) shows that a_2 is around 2.63 which is close to the physiological range also.

2) **Region 2**: feed choline concentration in the region $\left(4.442 \le s_{2f} \le 4.771\right)$ corresponding to (6.22×10^{-5} and 6.68×10^{-5}) kmole/m^3. There are two Hopf bifurcations (HBs). The first HB_1 appears at $s_{2f} = 4.442$ and the other HB_2 at $s_{2f} = 4.771$ in which the behavior of state variables describes periodic solutions or oscillatory behavior. The unstable waves in the substrate make the system approach to either the periodic solutions on the right or the steady state solution to the left. Solid bold curves represent stable steady state solutions and dashed lines represent the unstable steady states. Closed circles are used for stable orbits and the open circles for the unstable orbits. The oscillatory behavior represented by the branch between HB_1 and HB_2 (unstable zone) is also easily visualized in Figure 5-3.

In the range ($4.442 \le s_{2f} \le 4.674$), the system is characterized only by stable periodic orbits; however, in the range $\left(4.674 \le s_{2f} \le 4.771\right)$ a bistability phenomenon is observed (periodic and point attractors coexisting with an unstable periodic orbit separating the domains of attraction of the periodic and point attractors). This bistability leads to the conditions that at the same value of s_{2f} slightly different initial conditions lead to different types of attractors. Also there is a sequence of PD which is one of the main ways leading to chaos. There are many PD points at s_{2f}=4.766 and 4.674 and there is a torous bifurcation (TR) point at s_{2f}=4.767.

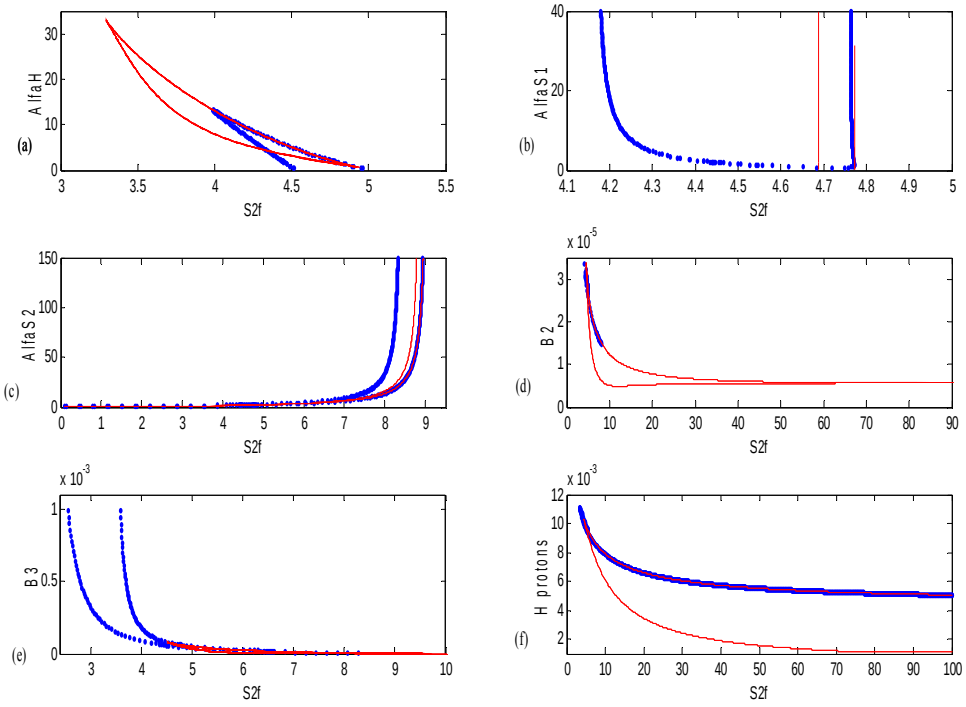

Figure 5-4: Two parameter continuation where Hopf is in blue color and SLP is in red. Feed choline (s_{2f}) is the horizontal in all figures vs. the following

(a) Feed choline concentrations (s_{2f}) vs. permeability of Hydrogen ions (α_H).

(b) Feed choline concentrations (s_{2f}) vs. permeability of ACh (α_{S1}).

(c) Feed choline concentrations (s_{2f}) vs. permeability of choline (α_{S2}).

(d) Feed choline concentrations (s_{2f}) vs. AChE activity (B_2).

(e) Feed choline concentrations (s_{2f}) vs. CoA activity (B_3), and

(f) Feed choline concentrations (s_{2f}) vs. Hydrogen ions concentrations

The bistability can be explained by the competition between the diffusion process from compartment 1 to compartment 2 and the enzymatic reaction catalyzed by the enzymes ChAT and AChE in compartments 1 and 2. Figure 5-3(e) shows that pH_2 exists in the range of [7.05- 7.75] between the two HB points. This range of pH_2 is inside the physiological range of the brain because of the partial dissociation of the acetic acid consideration.

3) Region 3: feed choline concentration in the region $\left(4.771 \le s_{2f} \le 4.85\right)$. In this region there is a unique stable steady state. The diagrams are characterized by steady state solutions where the point attractor is the only attractor as shown in Figure 5-3.

The two-parameter continuation technique has been used to investigate the influence of variation of the system parameters on the qualitative behavior of the system. By this technique both static and dynamic behavior can be elucidated with the changing of system parameters such as (s_{1f}, s_{3f}, v_r, A_f, α_H, α_{s1}, α_{s2}, α_{s3}, B_2, B_3, and H^+ ions), as shown in Figures 5-4(a)–(f) and Figures 5-5(a)–(e). In Figures 5-4(a)–(f) and Figures 5-5(a)–(e) the loci of the HB points (the blue color) and the loci of the static limit points (red color) have been shown as the system parameters vary with feed choline concentration (s_{2f}) as the main parameter. In these figures if a horizontal or vertical line is drawn inside the curves and if these lines cross the HB curves at two pints, oscillatory behavior will dominate between these HB points.

Figure 5-4(a) shows the two-parameter continuation diagram s_{2f} versus α_H. It is clear that at the given set of system parameters, all the qualitative changes in bifurcations are between the values of $\alpha_H = 0$ and 33. The diagram is characterized by the existence of two different loops, the first which is plotted using blue lines is HB points and the bigger one is the SLP points. The diagram shows that there are two regions of periodic or chaotic attractors, the lower region where $\alpha_H < 13.5$ is characterized by presence of Hopf and SLPs bifurcation points. In addition, it is characterized by a wider span of the Hopf points (on s_{2f} scale) as α_H approaches zero and a narrow span as α_H approaches 13.5. The upper region is characterized by existence of SLPs bifurcation points where the hopf bifurcation disappears completely when α_H is larger than 13.5. It is observed that both regions exist in the range of s_{2f} among 5 and 3.3.

Figure 5-4(b) illustrates the two-parameter continuation α_{s1} versus s_{2f}. The results are different from the results in Figure 5-4(a). The figure shows that there are no effects of changing s_{2f} on the qualitative behavior in bifurcations when ($\alpha_{s1} > 2$). Both SLP and HB changes vertically so that there are always two HB bifurcation points and two SLPs bifurcation points inside the same range of s_{2f} when ($\alpha_{s1} < 2$). The HB points disappear and only the two SLPs exist.

Figure 5-4(c) shows the two-parameter continuation diagram α_{s2} versus s_{2f}. There are two HB bifurcation points and two SLPs bifurcation points. All HB and SLP points exist in the range of s_{2f} between 0 and 9. As shown in the figure, the spans of HB and SLP points are very narrow in the range ($0 < s_{2f} < 7$) and these spans become wider in the range of ($7 < s_{2f} < 9$). In addition, both HB and SLP disappear as ($\alpha_{s2} < 2$). It is clear that there is no any influence of changing s_{2f} on the qualitative changes when ($s_{2f} > 9$).

Figure 5-4(d) illustrates the two-parameter continuation diagram B_2 versus s_{2f}. The figure shows that HB and SLP points lie in the range of B_2 between 0.5×10^{-5} and 4×10^{-5} kmol/m^3. Figure

5-4(d) illustrates that HB points exist only in a very narrow span of ($5 < s_{2f} < 8.5$) and ($B_2 > 1.5 \times 10^{-5}$) kmol/m^3. The HB points disappears in the range ($B_2 < 1.5 \times 10^{-5}$) kmol/m^3. The span of SLP becomes narrower as s_{2f} increases where B_2 changes in a very small range (0.6-0.7) x 10^{-5} kmol/m^3 as $s_{2f} > 40$.

Figure 5-4(e) shows the two-parameter continuation diagram B_3 versus s_{2f}. There are two HB bifurcation points and two SLPs bifurcation points. The figure illustrates that the SLP disappears completely in the range ($s_{2f} < 4.7$) and ($B_3 > 0.00006$). The span of HB points decreases as $s_{2f} > 4.7$ where B_3 exists in the range ($0.000001 < B_3 < 0.00006$).

Figure 5-4(f) illustrates the two-parameter continuation diagram feed H^+ versus s_{2f}. There are two HB bifurcation points in a very small range of ($3.4 < s_{2f} < 5.51$) and only one HB in the range of ($5.51 < s_{2f} < 15.4$). HB exists in the range of feed H^+ protons ($0.007 < H^+ < 11.03$) x10^{-3}. There is only one SLPs bifurcation point the range of ($4.41 < s_{2f} < 100$). As shown in the figure, both HB and SLP disappear ($s_{2f} < 3.4$).

Figure 5-5(a) represents the two-parameter continuation diagram A_f versus s_{2f}. According to the figure the range of HB and SLP exists in the range ($4.5 < s_{2f} < 8.6$) and ($A_f < 4.3$). The SLP exists only as ($4.7 < s_{2f} < 8.6$) and in the range of ($A_f < 3.7$). There are two HB points in the range of ($4.7 < s_{2f} < 5.3$) and only one HB point in the range of ($5.3 < s_{2f} < 8.6$).

Figure 5-5(b) illustrates the two-parameter continuation diagram s_{1f} versus s_{2f}. The figure shows that there are two HB bifurcation points and two SLPs bifurcation points. The range of HB and SLP exist in the range ($0 < s_{2f} < 9.5$) and ($0 < s_{1f} < 2.7$). The SLP exists only as ($4 < s_{2f} < 9.5$) and disappears in the range of ($0 < s_{2f} < 4$). The HB exists in the range of ($0 < s_{2f} < 8$) and disappears completely ($8 < s_{2f}$). The span of HB deceases as s_{2f} is less than 8 and the span of SLP increases in the range ($4 < s_{2f}$).

Figure 5-5(c) shows the two-parameter continuation diagram s_{3f} versus s_{2f}. There are two HB points and two SLPs points. The range of HB and SLP exist in the range ($2.5 < s_{2f} < 9$) and ($s_{3f} > 0$). The SLP exists only as ($4.7 < s_{2f} < 6.3$) and disappears in the range of ($s_{2f} < 4.7$). there are two HB points in the range of ($2.5 < s_{2f} < 4.7$) and HB disappears completely ($s_{2f} < 2.5$). The span of HB decreases as s_{2f} increases in the range ($2.5 < s_{2f}$) and the span of SLP increases in the range ($4.7 < s_{2f} < 6.3$).

Figure 5-5(d) illustrates the two-parameter continuation diagram V_R versus s_{2f}. There are two HB bifurcation points and two SLPs bifurcation points. The range of HB and SLP exists in the range ($2 < s_{2f} < 90$) and ($0.2 < V_R < 1.635$). The SLP exists only as ($2.5 < s_{2f} < 90$) and disappears in the range

of (s_{2f} < 2). The HB exists in the range of (2.5 < s_{2f} < 10) and disappears completely (s_{2f} > 10). The span of HB is very small where the range of V_R is (0.58 < V_R < 1.635).

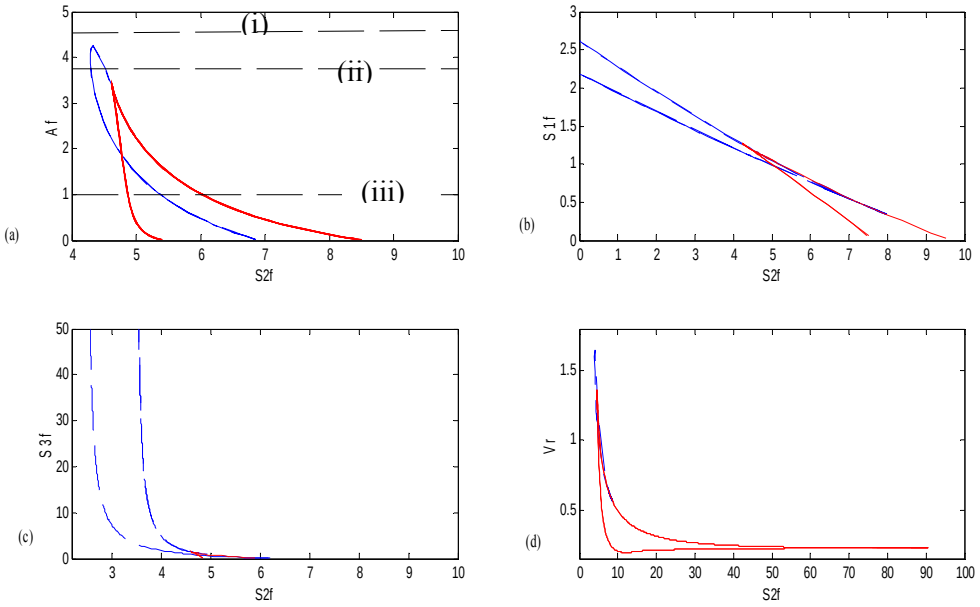

Figure 5-5: Two parameter continuation where Hopf in blue color and SLP in red. Feed choline (s_{2f}) is the horizontal in all figures vs. the following:

(a) Feed choline concentrations (s_{2f}) vs. feed acetate concentrations (A_f).

(b) Feed choline concentrations (s_{2f}) vs. feed ACh concentrations (s_{1f}).

(c) Feed choline concentrations (s_{2f}) vs. Acetyl CoA concentrations (s_{3f}).

(d) Feed choline concentrations (s_{2f}) vs. the ratio (V_r) and

The two-parameter continuation diagram which relates feed acetate concentration A_f to feed choline concentration s_{2f} is shown in Figure 5-5(a). To understand well the significance of the two-parameter continuation diagrams, Figure 5-5(a) showing the two-parameter continuation between A_f and s_{2f} is divided into 3 different regions according to the existence of SLPs and HB points. We will investigate the static and dynamic bifurcations based on the value of the parameter A_f in each region as follows:

Region (1):

This region extends above the value of A_f that corresponds to the end of the HB curve at about A_f = 4.5 as indicated by the horizontal dashed line (i) in Figure 5-5(a). It is observed that there is no any HB or SLP. It is more clarified when studying the dynamic bifurcation diagram as shown in Figure 5-6(a) at A_f=4.5. The bifurcation diagram illustrates that there is only one stable branch.

Region (2):

This region corresponds to a value of A_f = 3.3–4.258. It is characterized by the presence of two HB points as indicated by the horizontal dashed line (ii) in Figure 5-5(a). The presence of HB means that the system demonstrates oscillatory behavior and the periodic solution is the only available solution as shown in the dynamic bifurcation diagram as shown in Figure 5-6(b).

Region (2):

Figure 5-5(a) shows that at A_f=1 indicated by the dashed horizontal line (iii), there are only one HB point and two SLP points. Figure 5-6(c) shows the dynamic bifurcations where the HB exists at s_{2f} = 5.373 and the first SLP is at s_{2f} = 5.8 and the second SLP is at s_{2f} = 4.87. In this range, the system is characterized by multiplicity, where there are two stable steady states in the range ($4.87 < s_{2f} < 5.373$). In addition there is a periodic solution in the range of ($5.27<s_{2f}<5.4$).

To investigate the chaotic attractors of the system as the feed choline concentration as a bifurcation parameter, one-dimensional Poincare map is investigated. In Poincare map, we measure the intersections between a hypothetical hyperplan surface taken at certain value of a state variable and the trajectories in one direction. Poincare map has an advantage is that it converts the problems of closed orbits which is hard to deal with them into a problem of points which are easy to handle.

Figure 5-7(a) shows the Pioncare bifurcation map taken at A_f = 2.8 and the rest of the parameters as shown in Table 5-3. Poincare map measure the intersections between the trajectories and surface taken at s_{11} = 2.04. The feed choline concentration (s_{2f}) is the main bifurcation parameter taken in the range of ($4.665 < s_{2f} < 4.72$). Figure 5-7(a) shows that PD is the route leading to fully chaotic behavior. Figure 5-7(b) is a magnification for the zoom shown in Figure 5-7 (a).

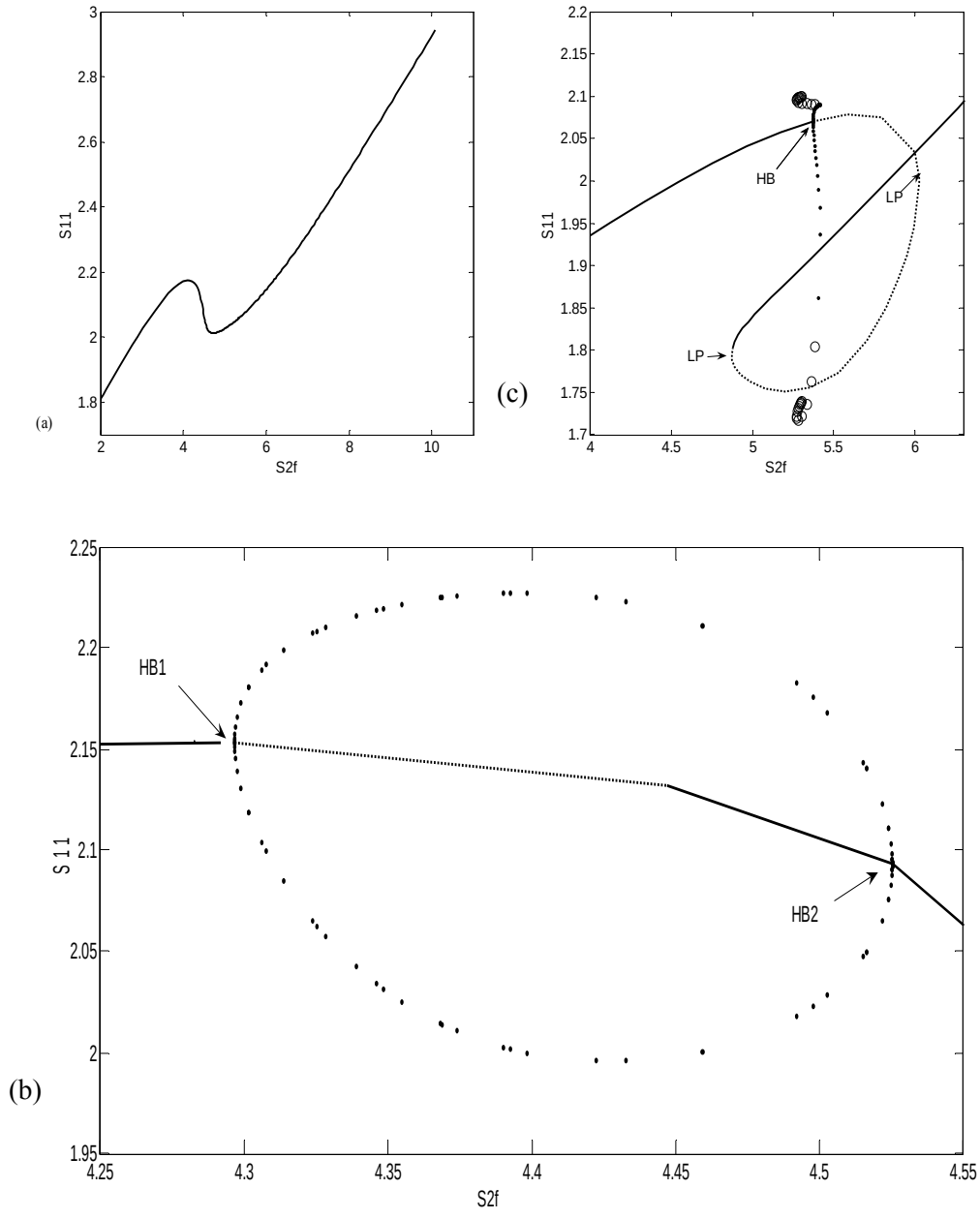

Figure 5-6: Bifurcation diagrams with choline feed concentration s_{2f} as the bifurcation parameter

(a) s_{2f} vs. s_{11} at A_f=4.5 (no HB no SLP)

(b) s_{2f} vs. s_{11} at A_f=3.75 (two HB points and no SLP)

(c) s_{2f} vs. s_{11} at A_f=1 (one HB and 2 SLP)

It is clear that the evolution of chaotic behavior is via PD sequence. This map of Figure 5-7(a) was constructed using Pioncare plan at $s_{11} = 2.04$ and $A_f = 2.8$. Figure 5-7(b) is a magnification for the zoom shown in Figure 5-7 (a). Figure 5-7(a) presents the period one bifurcation to chaos in the range of ($4.665<s_{2f}<4.72$). The hydrogen protons as state variable is in the range $\left(4.3x10^{-3} \le h \le 4.735x10^{-3}\right)$ corresponding to $\left(8.325 \le pH \le 8.398\right)$ which is close to the physiological range. The evolution of the chaotic behavior as shown in Figure 5-7(a) and Figure 5-7(b) is described by PD sequence and can be summarized as follows:

Period one attractor; window of period two; window of period four; window of period eight; window of period sixteen; evolution of chaos via PD route as shown in Figure 5-7(b). Then period one returns again $s_{2f} = 4.715$ where the chaotic behavior disappears. The torus bifurcation (TR) point appearing at $s_{2f} = 4.766$ as shown (Figure 5-3) may contribute the chaotic behavior of the system in the corresponding range of s_{2f} as the main bifurcation parameter.

Figures 5-8, 5-9 and 5-10 show the phase plans and the time traces of three kinds of attractors. Figures 5-8 (a)–(h) show the phase plans and the time traces of a chaotic attractors at $s_{2f} = 4.71$. Figures 5-9 (a)–(h) show period two attractor at $s_{2f} = 4.7014$. Figures 5-10 (a)–(h) show period four attractor at $s_{2f} = 4.7038$. It has been observed there are big disturbances in the ACh concentrations, choline, acetyl-coA in compartments as shown in Figures 5-8, 5-9, and 5-10. These disturbances and irregularities may be a good indication to the cholinergic diseases like Alzheimer's and Parkinson's diseases.

It is observed in Figures 5-8(g), 5-9(g) and 5-10(g) that pH_2 exists in the range 7.1 -7.55 which is a narrow range and exists in the physiological range. It is different from the value of pH in previous work done by (Mustafa et al., a, b, and c) because here the partial dissociation of acetic acid is considered. It is observed that the range of pH_1 [8.1-8.4] in compartment 1 is larger than that in compartment 2 (pH_2) which is in the range [7.1-7.55]. This is because of the higher concentration of hydrogen ions in compartment 2 due to the excess production of hydrogen ions due to the hydrolysis of ACh in addition to efflux of H^+ because of the partial dissociation of acetic acid.

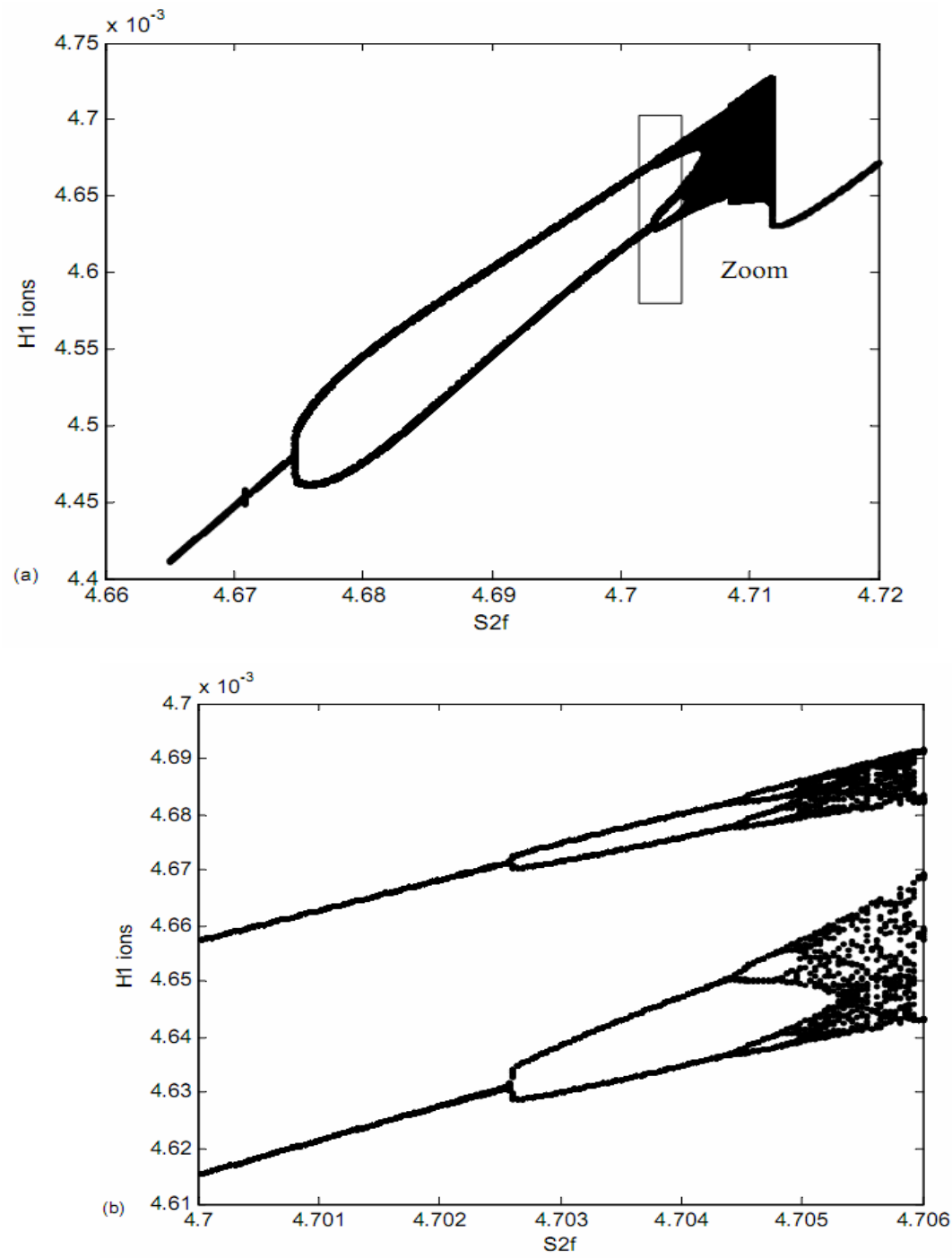

Figure 5-7: a) Poincare bifurcation diagram (Poincare plane is located at s_{12} =2.04, h_F=.01, s_{1F}=1.11, s_{3F}=1.1, A_F=2.8 and the rest of parameters as shown Table 5-3. (b) Enlargement for the zoom in (a)

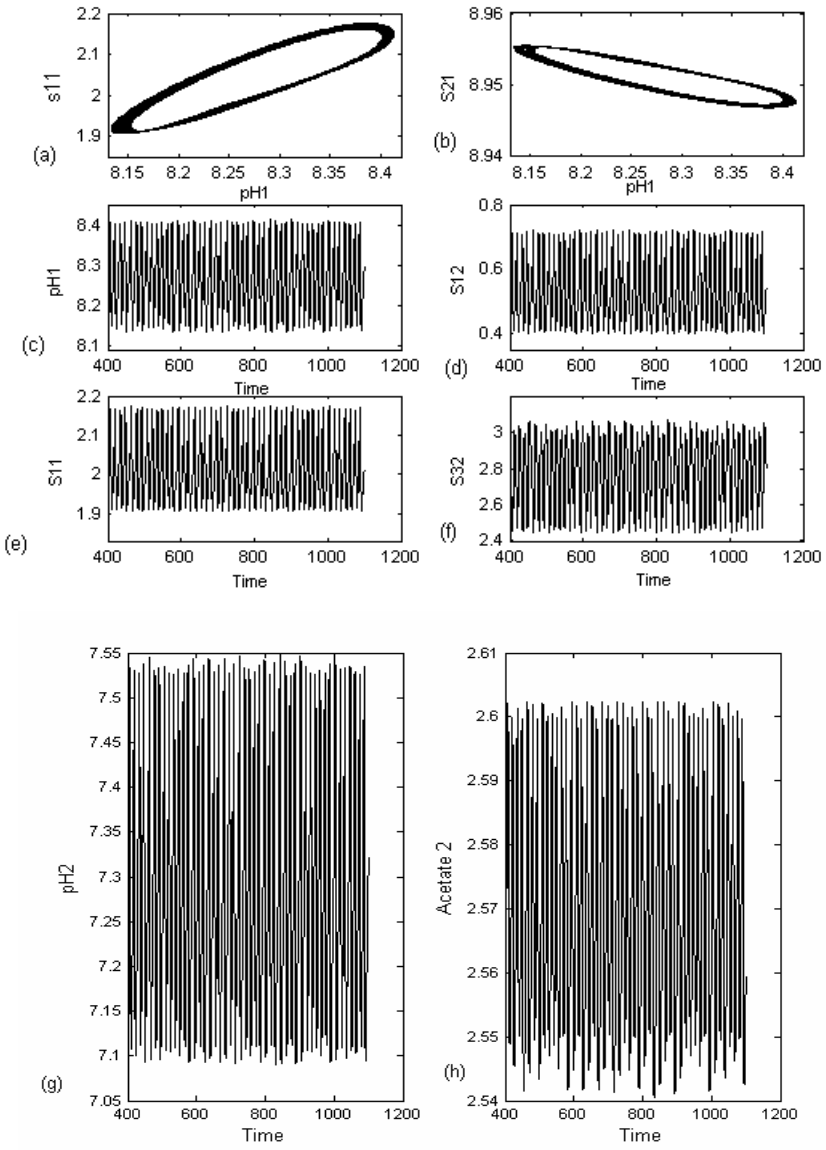

Figure 5-8: Dynamic characteristics at $s_{2f} = 4.71$ **, h_F =.01, s_{1F} =1.11, , s_{3F} =1.10, A_F=2.8 and the rest of the system parameters as shown Table** 5-3.

(a) Phase plane for ACh in compartment 2 vs. the ACh in compartment 1,

(b) Phase plane for pH in compartment 2 vs. the ACh in compartment 1 ,

(c) Time traces of pH in compartment 2 , (d) Time traces of ACh in compartment 2,

(e) Time traces of ACh in compartment 1 , (f) Time traces of acetyl CoA in compartment 2,

(g) Time traces of Phase plane for pH in compartment 2, and

(h) Time traces of acetate in compartment 2

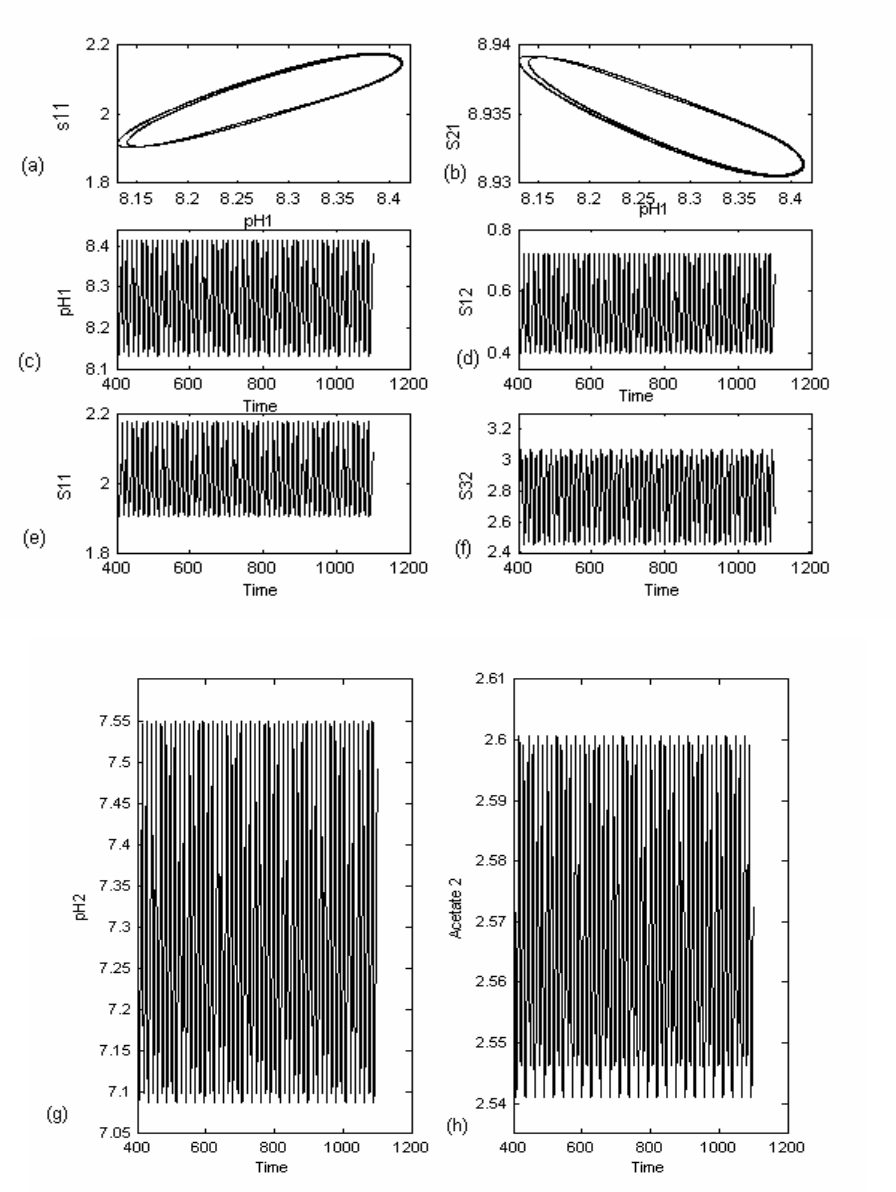

Figure 5-9: Dynamic characteristics at $S_{2f} = 4.7014$, h_F =0.01, s_{1F} =1.11, s_{3F} =1.10, A_F=2.8 and the rest of the system parameters as shown Table 5-3.

(a) Phase plane for ACh in compartment 2 vs. the ACh in compartment 1,

(b) Phase plane for pH in compartment 2 vs. the ACh in compartment 1 ,

(c) Time traces of pH in compartment 2 , (d) Time traces of ACh in compartment 2,

(e) Time traces of ACh in compartment 1 , (f) Time traces of acetyl CoA in compartment 2,

(g) Time traces of Phase plane for pH in compartment 2, and (h) Time traces of acetate in compartment 2

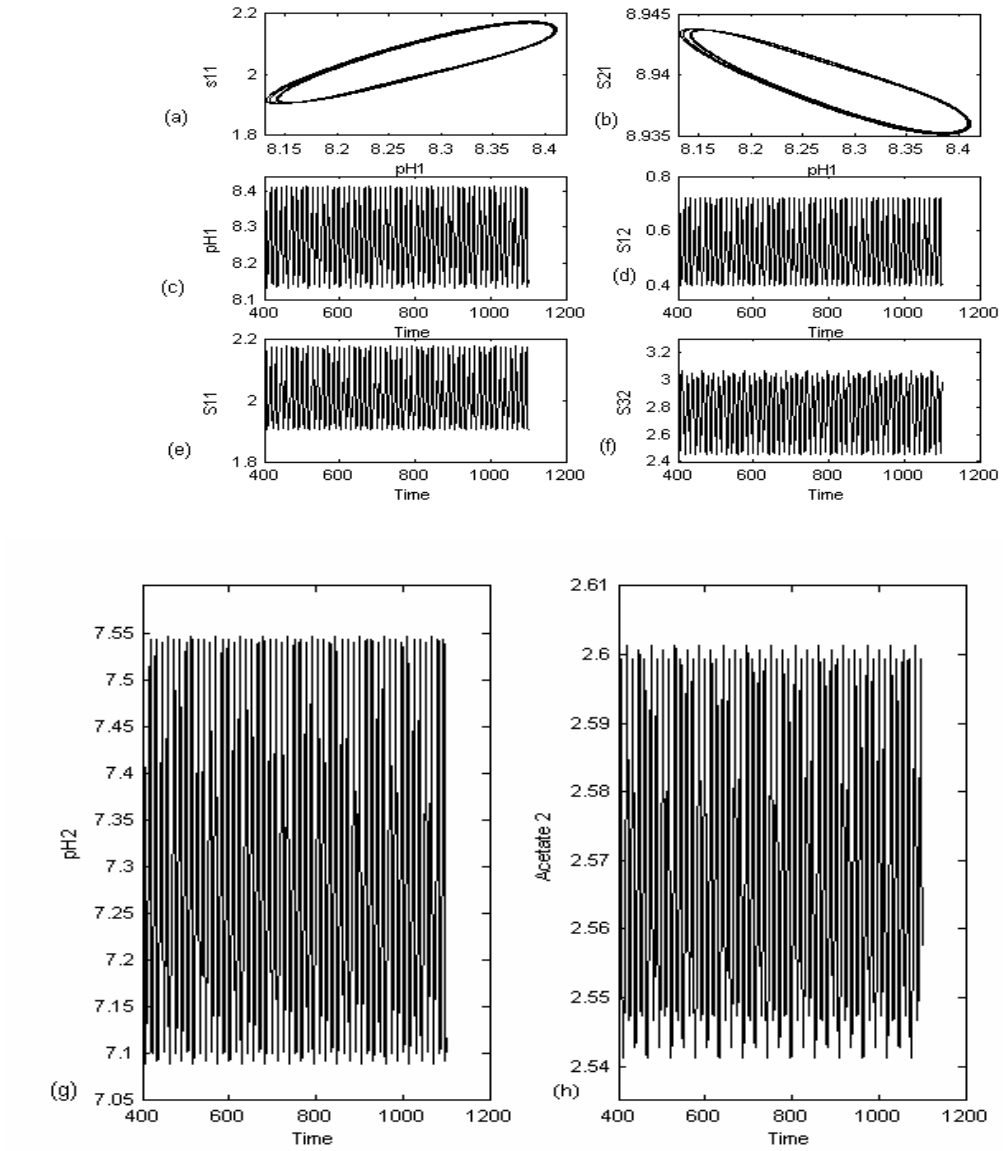

Figure 5-10: Dynamic characteristics at $s_{2f} = 4.709$, h_F =.01, s_{1F} =1.11, , s_{3F} =1.10, A_F=2.8 and the rest of the system parameters as shown Table 5-3.

(a) Phase plane for ACh in compartment 2 vs. the ACh in compartment 1,

(b) Phase plane for pH in compartment 2 vs. the ACh in compartment 1 ,

(c) Time traces of pH in compartment 2 , (d) Time traces of ACh in compartment 2,

(e) Time traces of ACh in compartment 1 , (f) Time traces of acetyl CoA in compartment 2,

(g) Time traces of Phase plane for pH in compartment 2, and

(h) Time traces of acetate in compartment 2

5.8 Summary and Conclusions

The complexity behavior of the ACh neurocycle system was investigated considering the partial dissociation of acetic acid in the presynaptic and postsynaptic. The two-parameter continuation technique enabled us to study the qualitative behavior of the system due to changing the system parameters. Based on the feed choline concentrations (s_{2f}) as the main bifurcation parameter and at different values of the feed acetate concentrations (A_f), we were able to study various static and dynamic bifurcation diagrams and obtain different solutions such as steady state, periodic and chaotic solutions. The results were compared to the results of physiological experiments and other published models. The pH values of both compartments were reasonable and were close to the physiological range. The chaotic behavior is obtained via PD sequence. The chaotic behavior expresses the disturbances and irregularities occurring in the cholinergic system and may be a good indication to the cholinergic disorders such as Alzheimer's and Parkinson's diseases. So considering the partial dissociation of acetic acid in this study enhanced the model prediction for the pH values and made it very close to the practical physiological range. In addition, it gives a reasonable explanation to such transients of pH in pre and postsynaptic regions. The competition between reactions and diffusion processes through the compartments, in addition to the three enzymatic processes, substrate inhibited and pH dependent, and finally the high nonlinearity in the rate of synthesis reaction catalyzed by ChAT and the rate of hydrolysis reaction catalyzed by AChE represent enough reasons for the complexity behavior appearing in the ACh system.

Chapter 6

Kinetic and Parameter Constants & Sensitivity Analysis

In this section, we present a detailed description of the kinetic parameter constants. We highlight the discrepancy in measuring the kinetic parameters and the different factors affecting the measurements. We focus on the molecular weight of ChAT, ACh, and choline concentrations. In addition, a sensitivity analysis is presented for some of the parameters used in this work.

6.1) Kinetic and Parameter Constants

Before explaining the kinetic and parameter constants, it is pointed out here that there are different ranges for the values of the kinetic parameters and even the state variables related to the ACh neurocycle. The observed discrepancy in measuring these values are due to different reasons: (1) the type of the tissue used for measurement, (2) the techniques used for measurement, and (3) the conditions of measurements such as temperature, pH and the type of experiment either in vitro or in vivo and type of animal, the tissues has been taken.

Three examples are given below to illustrate this point even though they are not discussed further in the thesis. The first example is the different ranges used in measuring the molecular weight of the enzyme ChAT; and the second one is related to the big range for the concentration of ACh. The last one is related to choline concentrations.

Molecular Weight of ChAT

If we look at the molecular weight of ChAT in Tucek (1987), we will find very large different ranges. Based on the tissue or the source and based on methods of measurements. Even if different methods of measurements are used for the same tissue, one will find different ranges of molecular weights. For example: The molecular weight of ChAT in rat brain by sedimentation analysis technique was 67,000 daltons; however, in human placenta by the same technique, it was 59,000 daltons. Another example, using gel filtration, the molecular weight of ChAT in the tissue of bovine caudate nuclei was found as 100,000 daltons or more in one measurement, and in another measurement, for the same tissue using the same method it was found as 65,000 daltons. There are two other measurements for

the same tissue and using the same gel filtration method, ChAT molecular weight was found as 12,000 daltons in one measurement, and in the range of 60,000-1,500,000 daltons in another measurement. However, using another method which is polyacrylamide gel electrophoresis, the molecular weight of ChAT was in a narrow range: 60 000-67000 daltons.

The observed discrepancy in measuring important properties such as the molecular weight of ChAT and ChAT activity reflects the differences in the methods of measurements and conditions of experiments in addition to the type of tissue. The reviewers accepted these discrepancies between these readings because there is no a strong evidence explaining the biophysical or biochemical aspects of these differences. The reason might be the existence of more than one form of the ChAT enzyme.

ACh concentrations:

Another example of discrepancies in the nervous systems is that of ACh concentrations. Free ACh in rat brain was found to be around 0.22×10^{-5} kmol/m^3 and total ACh was found to be around 1.77×10^{-5} kmol/m^3. Tucek, 1990 and Garhyan et al., 2006 showed that in guinea pig cerebral cortex the range was 0.31×10^{-5} (free ACh) to 1.67×10^{-5} kmol/m^3 (total ACh). However, Wessler et al., (2001) indicated that ACh concentration in human placenta is in the range (3.0×10^{-5} - 55.5×10^{-5}) kmol/m^3 which represents around 33 folds more than the concentration existing in cerebral cortex. Furthermore, Kysela and Torok (1996) illustrated that the concentration of ACh in rat pulmonary artery was in the range of 0.001×10^{-5} to 3.0×10^{-5} kmol/m^3. Bellier and Kimura (2007), in Table 2: showed that the concentration of ACh in ventral root intact around 16.3±2.4 pmol/mg which is equivalent to 1 (16.3±2.4) x10^{-6} $\frac{kmol}{m^3}$ which represents a different range[1].

Choline:

Llcol et al., (2005) indicated that a very big range exists for both serum free choline and serum phospholipids-bound choline. For serum free choline, the range was from 10.3 to 36.2 µmol/l corresponding to (10.3 to 36.2) x10^{-6} kmol/m^3 or (1.03 to 3.62) x10^{-4} kmol/m^3. For serum

[1] $\frac{1pmol}{mg}=\frac{10^{-12}mol}{10^{-3}gm}=\frac{10^{-9}mol}{gm}=\frac{10^{-9}mol}{mL}=\frac{10^{-9}mol}{10^{-3}L}=\frac{10^{-6}mol}{L}=10^{-6}\frac{kmol}{m^3}$

phospholipids-bound choline, the range 1927 to 2672 μmol/l corresponding to (1927 -2672) $x10^{-6}$ $kmol/m^3$ or (19.27 - 26.72) $x10^{-4}$ $kmol/m^3$. Furthermore, Persike et al. (2010) obtained a range of choline in microdialysis samples of 0.1−50 pmol/μl equivalent to 1-50 μmol/l or to 0.01-0.5 $x10^{-4}$ $kmol/m^3$.

Now, we will present the most important aspects for the kinetic constants and parameters we used in our system.

1) **Feed ACh concentration** used in our analysis is S_{1f} = 2.4 (in the dimensionless from) which is equivalent to 0.12* 10^{-5} $kmol/m^3$. This lies in the range of ACh in isolated rings of the rat pulmonary artery and was measured to be in the range of 0:001 × 10^{-5} to 3 × 10^{-5} $kmol/m^3$ according to (Kysela and Torok, 1996).

2) **Feed Choline concentration** the feed choline concentration we used is S_{2f}= 1.15 (in the dimensionless from) which is equivalent to 1.15* 10^{-4} $kmol/m^3$ in mouse brain. This range already should be higher than the range in human plasma which is in the range (0.01-0.7) * 10^{-4} $kmol/m^3$ according to Marriot (1994).

3) **Feed pH:** We used various ranges for the feed pH. Kaila and Ransom (1998) indicated that that "the physiologically relevant pH range (from 6.5 to 8) corresponding to a big H^+ activity range at very low absolute values from 10 to 300 nM", however, according to Rae et al., (1996), intracellular pH was measured in human brain using magnetic resonance spectroscopy and found to be in the range of 6.95–7.15. Oldendorf et al., (1979) did their experiments of brain uptake of nicotine and other components and found a very big range of pH in the range from 6.1 until 8.4. They found that nicotine uptake declined when pH reduced through a very big range of 8.3-4.2.

4) **Ks:** was used as a reference to convert ACh concentrations into the dimensionless form, it was also used for describing the dissociation constants for ACh hydrolysis. Radic and Taylor (2001) described the dependence of Ks on the pH values ($K_s = \frac{k_{-1}}{k_1}$). They found that in the pH range (5.5-11), K_s was in the range of (0.035-0.26) μM equivalent to (0.35-2.6) x 10^{-7} $Kmol/m^3$. Rosefeld and Sultatos (1986) found that K_s =0.339 μM which is equivalent to 3.39 $x10^{-7}$ $Kmol/m^3$ which includes our range. However, Ringdahl (1986) measured K_s for AChE and got a different range which was (1.7-2) μM equivalent to (17-20) $x10^{-7}$ $Kmol/m^3$. Our value of K_s of 5.033 $x10^{-7}$ $Kmol/m^3$ lies between the range of Radic and Taylor (2001) and the range of Ringdahl (1986).

5) **r_1 constants for the rate of ChAT synthesis:**

Most of the kinetic parameters used in describing the rate of ACh synthesis are based on the kinetic constants for choline acetyltransferase (ChAT) reaction used by Hersh and Peet (1977). However, they assumed that acetyl CoA is the main effective substrate. From our model and based on various physiological, biophysical, and chemical reviews, we found that choline is the most important substrate. Brain is unable to synthesize choline, however, acetyl CoA is synthesized in plenty in the mitochondria and available much in the presynaptic neurons. This leads to that there is a certain difference in our range for only θ_2 and θ_3. Other parameters exist in the same range of Hersh and Peet (1977). Even there are some other references mentioned by Hersh and Peet (1977) like Sastry and Henderson (1972) that have a very big difference in θ_3 and θ_4 as shown below:

	Constants in our model	Constants by Hersh and Peet (1977)	Constants by Sastry and Henderson (1972)
Θ_1	5.2	5.2(0.1)	
θ_2	12	16-28	
θ_3	1000	410(28)	3-5
Θ_4	5	11.9 (0.7)	113-150
Θ_5	1	1	

Sastry and Henderson (1972) and Hersh and Peet (1977) made their measurements based on human placenta. What I mean from the table is that I would like to point to the big discrepancy for measuring the kinetic parameter experimentally as shown between the Sastry and Henderson (1972) and Hersh and Peet (1977) although they used the same tissue which is human placenta. Hersh and Peet (1977) pointed to inconsistency of their measurements with others and explained in terms of what they called "random binding mechanism".

6) **K_i (inhibition constants for AChE)** This constant was found to be dependent on the concentration of inhibitor and operating conditions used in the experiments, so there was a very big range from (0.18 to 30) as shown by Rosenfeld and Sultatos (2006). It was found by Eastman et al. (1996) that the range of K_i is from 0.02 to 0.31 μM which is equivalent to (0.2 -3.1) $x10^{-7}$ Kmol/m^3.

Thus, our value is very close to this range. In our model, we got the value of Ki from the inhibition constant $\alpha_i = \frac{K_{s1}}{K_i}$ which was obtained from the continuation technique of Elnashaie et al., (1994).

7) **K_h.** This is a reference constant used to convert the concentration of hydrogen ions into the dimensionless form and was taken as $K_h = 1.0066 \times 10^{-6}$. We used $K_a = K_b = K_h$ Where each of the active enzyme species exists in equilibrium with inactive protonated and de-protonated forms. The equilibria are driven by the pH of the system. In the first of my study, I could not find reasonable values for K_a and K_b; where there are many different ranges used in ACh research. Like that used by Shen and Larter (1994) and because each of the active enzyme species exists in equilibrium with inactive protonated and de-protonated forms where the equilibria are driven by the pH of the system. We assumed that $K_a = K_b = K_h$ where $K_h = 1.0066 \times 10^{-6}$.

8) **Permeability Constants:**

We take the dimensionless permeability (α) for hydrogen, hydroxyl, ACh, choline, and acetate according to the following equation: $\alpha = \frac{\alpha' A_M}{q}$ Where α' is membrane permeability for substances (m/s), A_M is the area of membrane separating compartments 1 and 2 (m^2), and q is the volumetric flow rate (m^3/s).

We obtained the values of the dimensionless permeability based on the continuation technique by Elnashaie et al (1995). This is because the area of membrane, thickness of the membrane, and partition coefficients and volumetric flow rates are unknown. In addition, there is a big different rage for the diffusivity of components. For example, the diffusivity of ACh is in the range $(0.5\text{-}4) \times 10^{-4}$ cm^2/sec. This continuation method gives an overview for the effect of a big range for the permeability of each state variable in the system. Then the value of each permeability is chosen based on its effect on the system stability. Each substance of the system has a different mechanism for transport from one compartment to another as shown below:

1) The mechanism of transport of ACh from compartment 1 to compartment 2 is somewhat complex. It is called biologically "**kiss and run model**" where ACh in the cytoplasm of compartment 1 after the synthesis reaction is transported into the vesicles in unknown mechanism, then the vesicles are transported until they reach certain pores existing in the membrane of the presynaptic neuron by fusion. The value of the pore diameter is changed and accompanied by a change in the volume of synaptic vesicle during the fusion with membrane. The final result is that ACh is released into the

cleft. The mechanism of "**kiss and run model**" is regulated by Ca ions. We assumed that ACh is transported from compartment 1 to compartment 2 by "**kiss and run model"** and passive diffusion mechanism; this means the direction of transport down the concentration gradient from the high concentration in compartment 1 to the lower concentration region in compartment 2 (Hannah – 1999 and 2003). We assumed also choline, acetate, and hydrogen ions are transported by the same mechanism. There is another mechanism explaining the release of ACh. This mechanism is related to ion exchange where it is related to the diffusion of salts such as Na, H, K, Cl, and Ca in specific channels existing in the membrane of the presynaptic neurons to regulate the diffusion and reaction inside compartment 1. The unbalance in concentrations of these ions on both sides of the cell membrane causes potential difference leading to the release of substances. These channels are selective for these ions.

2) The mechanism of choline transport from compartment 2 to compartment 1 in the recycle stream is different. Choline is transported via a facilitated diffusion mechanism. In this mechanism choline is carried by transporters based on Na ions from the synaptic cleft to the presynaptic neuron. The transporter is called high affinity choline transporter (HACT). Finally, because the complicated mechanisms explaining the transport of the neurocycle components, and the uncertainty of most of the constants describing the dimensions of the compartments and flow rate either in or out of them, we depend on the continuation technique to select proper values of the permeability of each component.

9) **R:** This constant is taken to be 80% based on Tucek (1987) who explained the fraction of free choline in the plasma required for the biosynthesis of ACh in the brain. This fraction is estimated based on species where ACh is synthesized. For instances, in rats free choline represents 12%, in rabbits 50 %, and 80 % in mice (Tucek 1978). Choline produced in synaptic gaps by the hydrolysis of ACh is re-utilized for the synthesis of ACh in presynaptic nerve endings (Tucek 1978). Therefore, choline recycled plays an important role in the synthesis of ACh.

10) **AChE Activity**

According to Chuiko et al. (2003), Plasma AChE activity varies on average in the range 1.2 - 18.6 μmol/ml per h corresponding to (0.033 - 0.52) × 10^{-5} kmol/m^3sec. However, brain AChE activity varied among fish species approximately 15-fold, ranging from 138 to 2011 μmol/ml per h corresponding to (3.83 -55.86)× 10^{-5} kmol/m^3sec. We will find (2011 μmol/ml per h) equivalent to

(2011 × 10^{-6}× 10^{3} /3600 (mol/l sec). Hence, our AChE activity value 5.033 × 10^{-5} kmol/m^3 will be within the range [3.83-55.86] × 10^{-5} kmol/m^3.

11) **ChAT Activity:**

Bellier and Kimura (2007) showed very different ranges for total ChAT activity and AChE activity based on the type of tissue. For example, they showed that total ChAT activity in intact dorsal root ganglion was in the range (1.6-42.3) nmol/min/mg) which is equivalent to (2.67-70.5) x10^{-5}(kmol / (m^3 sec). Hence our ChAT activity values which 5.033 × 10^{-5} kmol/m^3 will be within this relevant range. Furthermore, Bellier and Kimura (2007) indicated that AChE activity in intact dorsal root ganglion was in the range (1.4-36.2) nmol/min/mg which is equivalent to (2.33-60.33) x10^{-5}(kmol / (m^3 sec)). Hence our AChE activity value which is 5.033 × 10^{-5} kmol/m^3 within this relevant range. Tucek (1978) showed that ChAT activity can be measured in terms of ACh synthesized concentrations (nmol Ach synthesized /mg) as follows: ChAT activity in Cerebral hemisphere in frontal lobe was 4.4, then it increased 3 times to be 18.6 in pyriform cortex, then it increased 6-fold to reach 26.2, and 18 times to be 72.8 in Caudate nucleus (head) in Extra-pyramidal area, and finally is multiplied around 26 times to be 111 in Putamen tissues.

12) **Dissociation of acetic acid:**

Partial dissociation of acetic acid plays a vital role in determining the pH values in both compartments. For example the channels existing in the membrane of the presynaptic neurons and the receptors of postsynaptic neurons can be opened and blocked based on the values of pH in both compartments. Landau and Nachsgen (1975) investigated that the influence of variation of acidic pH on the release of ACh. They found that H^+ protons interact with acidic sites of the presynaptic membranes to regulate the release of ACh. Therefore, there is a strong relation between the dissociation of the acid and the release of the ACh which is enhanced by protonation of the acetic acid which inhibits the release of Ca ions into the synaptic cleft. Acetic acid as a weak acid dissociates in a very low per cent when it dissolves in water. Hence the concentration of hydrogen ions as a product is very low.

6.2) Sensitivity Analysis of Parameters

In this section we present a sensitivity analysis study on certain parameters in order to investigate their effects on the state variables of the system. Although the bifurcation analysis presented in the previous chapters gives a good indication about the parametric sensitivity analysis, we highlight again the different influences of the system parameters. The most important parameters to be investigated are: Feed mobile ACh concentrations (S_{1f}), Feed choline concentration (S_{2f}), Feed acetate concentrations (S_{3f}), Feed hydrogen ions concentrations (h_f), ChAT activity (B_1), and AChE activity (B_2). We study the effects of these parameters on the state variables: ACh concentrations in compartments 1 and 2, acetate concentrations and pH. The compatibility of the results with the bifurcation diagrams of the previous chapters will be highlighted.

6.2.1) Effect of Mobile Feed ACh Concentrations (S_{1f})

Figure 6-1 shows the evolution of the ACh system as a function of time at different mobile feed ACh concentrations (S_{1f}) for a given initial conditions. All the parameters are taken constant as shown in Table (2-3) except S_{1f}. Figures 6-1 (a, b, c, and d) illustrate that all state variable approach steady state solutions (point attractors) at S_{1f} = 0, 4, and 10 in the dimensionless form. However, the oscillatory behavior is indicated at S_{1f} = 2.2. This is completely compatible with the dynamic bifurcation shown in Figure 2-8 of chapter 2 where we observed that the periodic orbits exist in the range ($1.99 < S_{1f} < 2.39$). This range is confirmed by the oscillatory behavior of Figure (6-1) at S_{1f} = 2.2. The oscillatory behavior ceases to exist outside this range ($1.99 < S_{1f} < 2.39$), where the system of ACh recovers its stability as shown in Figure 6-1 at S_{1f} = 0, 4, and 10. Figure 6-1a shows that the ACh concentration in compartment 1 (S_{11}) increases proportional to the increase of S_{1f}. However S_{12} does not take the same behavior reflecting the competition between the reaction of hydrolysis in compartment 2 catalyzed by the enzyme AChE and the diffusion of ACh from the presynaptic terminal to the synaptic cleft. It is clear that both acetate concentration in compartment 2 (Figure 6-1 c) and hydrogen ion concentration in terms of pH in compartment 2 (Figure 6-1 d) undergo the same kind of change with the ACh concentration in compartment 1.

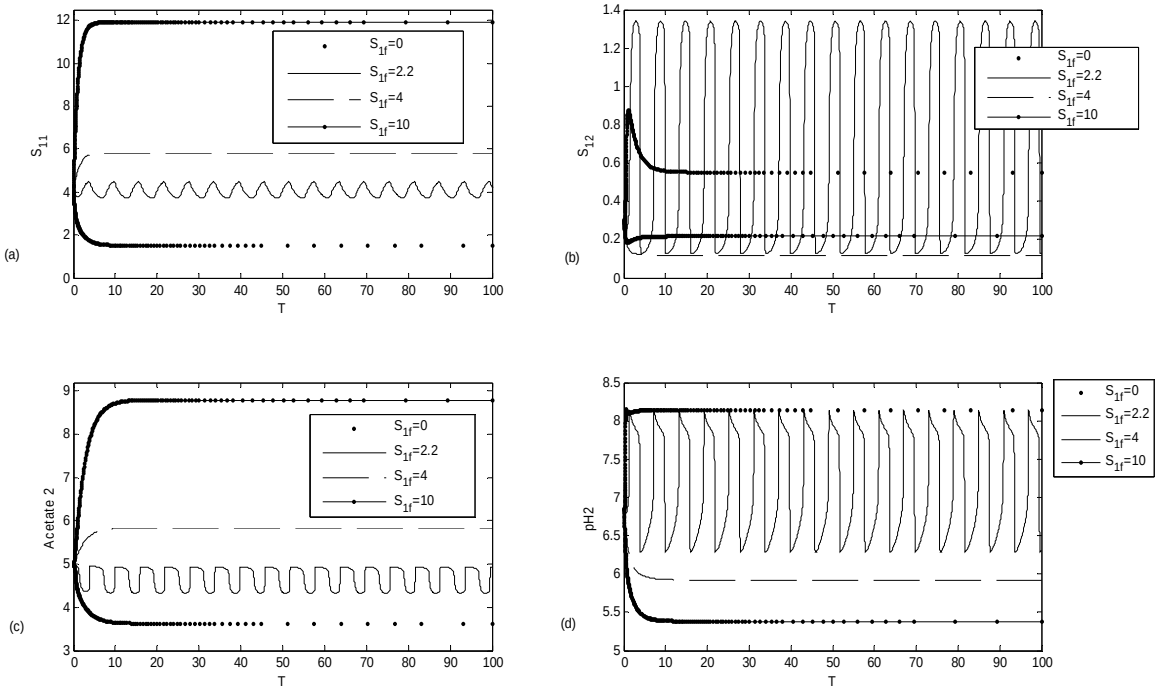

Figure 6-1: ACh system evolution as a function of time at different mobile feed ACh concentrations (S_{1f}):

a) Evolution of ACh concentration in compartment 1 (S_{11})

b) Evolution of ACh concentration in compartment 2 (S_{12})

c) Evolution of Acetate concentration in compartment 2 (S_{32}) or acetate 2

d) Evolution of pH in compartment 2 (pH_2)

Initial conditions	
$h_{(1)}$	.003796824
$h_{(2)}$	0.1405804
$s_{1(1)}$	3.956
$s_{1(21)}$	0.3
$s_{2(1)}$	3.233
$s_{2(2)}$	1.1606
$s_{3(1)}$	8.2517318
$s_{3(2)}$	4.9606

6.2.2) Effect of Feed Choline Concentrations (S_{2f})

In this section, we will investigate the effect of changing feed choline concentration (S_{2f}) on the evolution of ACh cholinergic system as a function of time as shown in Figure 6-2. All the parameters are taken constant as shown in Table 3.3 except S_{2f}. Figure 6-2 indicates that the system goes to steady state solution (point attractor) at $S_{2f} = 0$, 0.7, and 1.5 in the dimensionless form. However, the oscillatory behavior is clearly shown at $S_{2f} = 1$.

The results are completely compatible with the dynamic bifurcation results as shown in Figure 3-4 in Chapter 3 where we observed that the periodic orbits exist in the range ($0.69 < S_{2f} < 1.141$). This range is confirmed by the periodic orbits of Figure 6-2 at $S_{2f} = 1$. The oscillatory behavior ceases to exist outside this range ($0.69 < S_{2f} < 1.141$), where the system of ACh recovers its stability at $S_{2f} = 0$, 0.7, and 1.5.

Figure 6-2a shows that the ACh concentration in compartment 1 (S_{11}) increases proportional to the increase of S_{2f} as S_{2f} increases from 0 to 1.5.

However S_{12} does not take the same behavior reflecting the competition between the hydrolysis reaction in compartment 2 and the diffusion of ACh from the presynaptic terminal to the synaptic cleft. This competition is considered as one of the main reasons for the appeared complex phenomena such as bifurcation and oscillatory behavior. It is clear that acetate concentration in compartment 2 (Figure 6-2 c) is very small at $S_{2f} = 0$, however it increases as $S_{2f} = 0.7$, then it decreases again as S_{2f} increases to be 1.5, this reflects the mutual effects between the reactions in both compartments and the diffusion from compartment 1 to compartment 2.

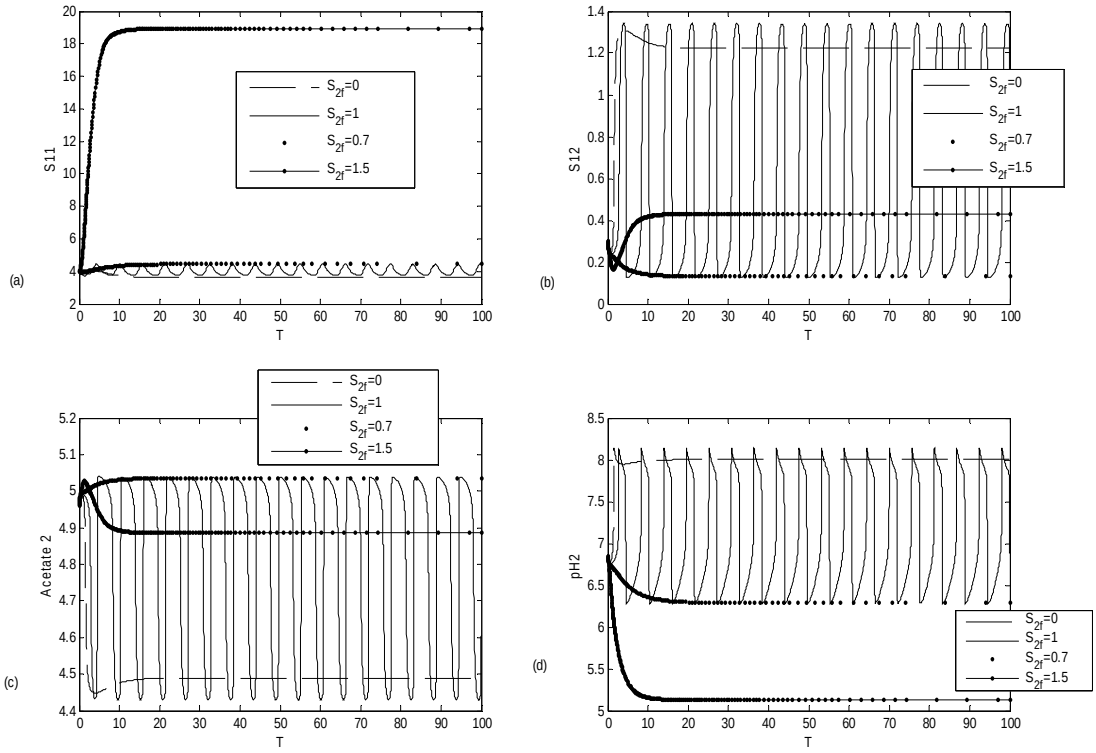

Figure 6-2: ACh system evolution as a function of time at different feed choline concentrations (S_{2f}):

a) Evolution of ACh concentration in compartment 1 (S_{11})

b) Evolution of ACh concentration in compartment 2 (S_{12})

c) Evolution of Acetate concentration in compartment 2 (S_{32}) or acetate 2

d) Evolution of pH in compartment 2 (pH_2)

Initial conditions	
$h_{(1)}$	.003796824
$h_{(2)}$	0.1405804
$s_{1(1)}$	3.956
$s_{1(21)}$	0.3
$s_{2(1)}$	3.233
$s_{2(2)}$	1.1606
$s_{3(1)}$	8.2517318
$s_{3(2)}$	4.9606

6.2.3) Effect of Feed Acetate Concentrations (S_{3f})

Figure 6-3 illustrates the evolution of ACh system as a function of time at different feed acetate concentrations (S_{3f}) at the corresponding initial conditions. All the parameters are taken constant as shown in Table 3-3 except S_{3f}. Figure 6-3 illustrates that the system approaches steady state solutions (point attractors) at $S_{3f} = 0$, 10, and 20 in the dimensionless form. However, the oscillatory behavior (periodic attractor) exists at $S_{3f} = 2.5$.

These results are completely compatible with the dynamic bifurcation as shown in Figure 3-12 in Chapter 3 which indicates that the oscillatory behavior exists in the feed acetate range of ($1.32 < S_{3f} < 3.79$). This range is confirmed by the periodic orbits of Figure 6-3 at $S_{3f} = 2.5$. Then the oscillatory behavior ceases to exist outside this range ($1.32 < S_{3f} < 3.79$), where the system of ACh recovers its stability as shown in Figure 6-3 for $S_{3f} = 0$, 10, and 20.

Figure 6-3 a shows that the ACh concentration I compartment 1 (S_{11}) increases at the fist transient at $S_{3f} = 0$ then it reaches a plateau where $S_{11} = 3.8$. However, as S_{3f} increases to 10 and 20, S_{11} will increase to the plateau to reach 4.07 and 4.15. If we compared these results with those of the effect of changing feed choline concentration (S_{2f}), we will find that S_{11} will increase from 4 to 19 (around 4-fold) as S_{2f} increases from 0 to 1.5. However, as S_{3f} increases from 0 to 20, the steady state plateau of S_{11} will increase only from 3.8 to 4.15. This confirms the limited effect of the feed acetate as a substrate on the system in comparison with the feed choline concentration as a substrate. These results agree with the bifurcation results of Chapter 3 and this confirms that S_{2f} is the most important substrate in comparison to feed acetate concentration (S_{3f}).

Figure 6-3a shows that the ACh concentration in compartment 1 (S_{11}) increases in parallel with the increase of S_{3f} where S_{11} increases as S_{3f} increases from 0 to 20. However, S_{12} does not take the same behavior reflecting the competition between the hydrolysis reaction in compartment 2 and the diffusion of ACh from the presynaptic terminal to the synaptic cleft. This competition is considered as one of the main reasons for giving rise to the bifurcation and oscillatory behavior. It is clear that acetate concentration in compartment 2 (Figure 6-3c) increases dramatically proportional to the feed acetate concentrations (S_{3f}). However, Figure (6-3 d) shows that pH in compartment 2 increases as S_{3f} decreases. pH_2 decreases from 7.9 at $S_{3f} = 0$ to 6.5 at $S_{3f} = 10$, then the decrease of pH_2 is very limited as it decreases to $pH_2 = 6.47$ at S_{3f} is doubled.

Initial conditions	
$h_{(1)}$	.003796824
$h_{(2)}$	0.1405804
$S_{1(1)}$	3.956
$S_{1(21)}$	0.3
$S_{2(1)}$	3.233
$S_{2(2)}$	1.1606
$S_{3(1)}$	8.2517318
$S_{3(2)}$	4.9606

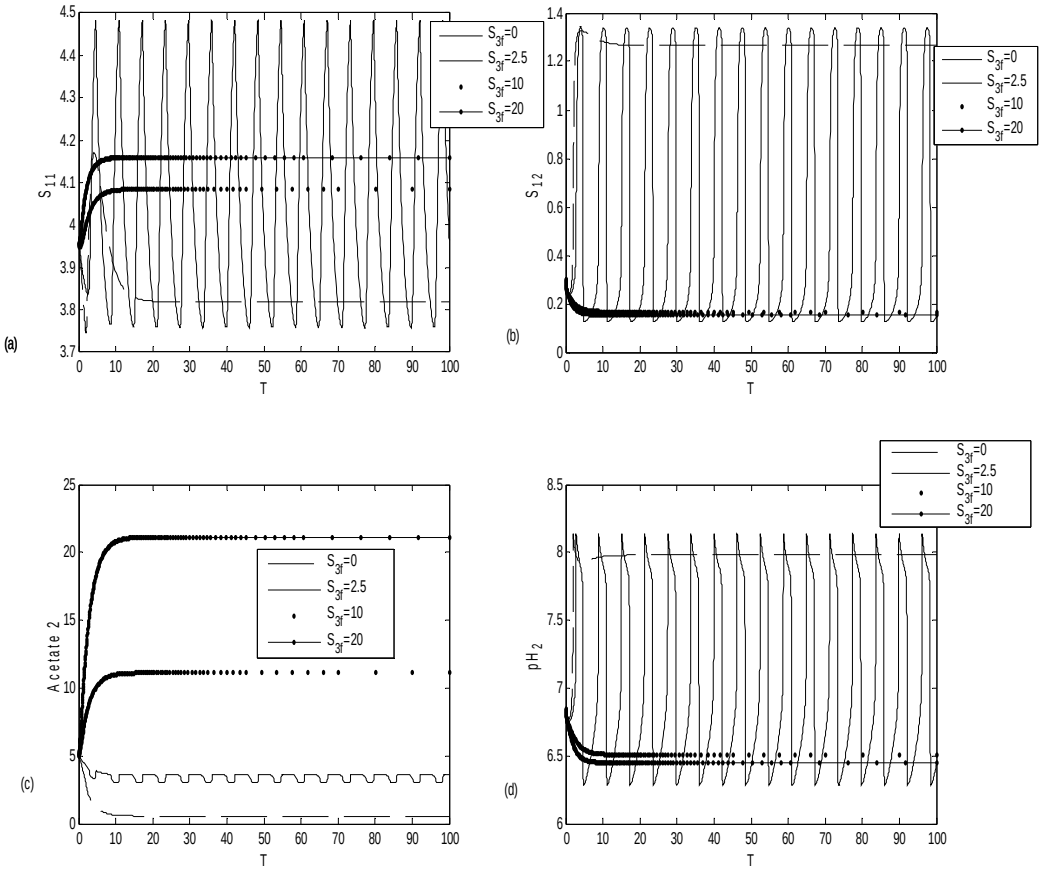

Figure 6-3: ACh system evolution as a function of time at different feed acetate concentrations (S_{3f}):

a) Evolution of ACh concentration in compartment 1 (S_{11})

b) Evolution of ACh concentration in compartment 2 (S_{12})

c) Evolution of Acetate concentration in compartment 2 (S_{32}) or acetate 2

d) Evolution of pH in compartment 2 (pH_2)

6.2.4) Effect of feed hydrogen ions concentrations (h_f)

Figure 6-4 shows the evolution of ACh system as a function of time at different feed hydrogen ions concentrations (h_f) at the corresponding initial conditions. All the parameters are taken constant as shown in Table 2-3 except h_f. Figure 6-4 illustrates that all state variables go to a steady state solution (point attractor) at pH_f = 6.65, 7.69, and 8.39 corresponding to h_f = 0.22, 0.02, and 0.004 respectively in the dimensionless form. However, the oscillatory behavior is clear at a pH_f = 8.2 corresponding to h_f = 0.006. This is completely compatible with the dynamic bifurcation results as shown in Figures 2-3 and 2-4 in Chapter 2 where we observed that the periodic orbits exist in the range ($0.00578 < h_f < 0.006263$) corresponding to ($8.2 < pH_f < 8.24$). This range is confirmed by the oscillatory behavior of Figure 6-4 at pH_f = 8.2, The oscillatory behavior ceases to exist outside this range ($8.2 < pH_f < 8.24$) where the system of ACh recovers its stability as shown in Figure 6-4 at pH_f = 6.65, 7.69, and 8.39.

Figure 6-4 shows that all the state variables in compartment 1 are constant even if pH_f changes from 6.65 to 7.69 (corresponding to an h_f from 0.22 to 0.02). This is in complete agreement with the dynamic bifurcations results shown in Figure 2-3. However, as pH_f increases to 8.39 (corresponding to h_f=0.004), both ACh concentration in compartment 1 (S_{11}), and compartment 2 (S_{12}) increases as shown in Figures 6-4 a and b respectively. However, Figure 6-4c indicates that acetate concentrations in compartment 2 decrease as pH_f increases since acetate is produced from the hydrolysis of ACh in compartment 2. Figure 6-4d shows that pH_2 increases proportional to pH_f. It is clear that both pH_f = 6.65 (corresponding to h_f = 0.22) and pH_f = 7.69 (corresponding to h_f = 0.02) have the same effect on the state variables of the system and this is again in agreement with the results shown in Figure 2-3.

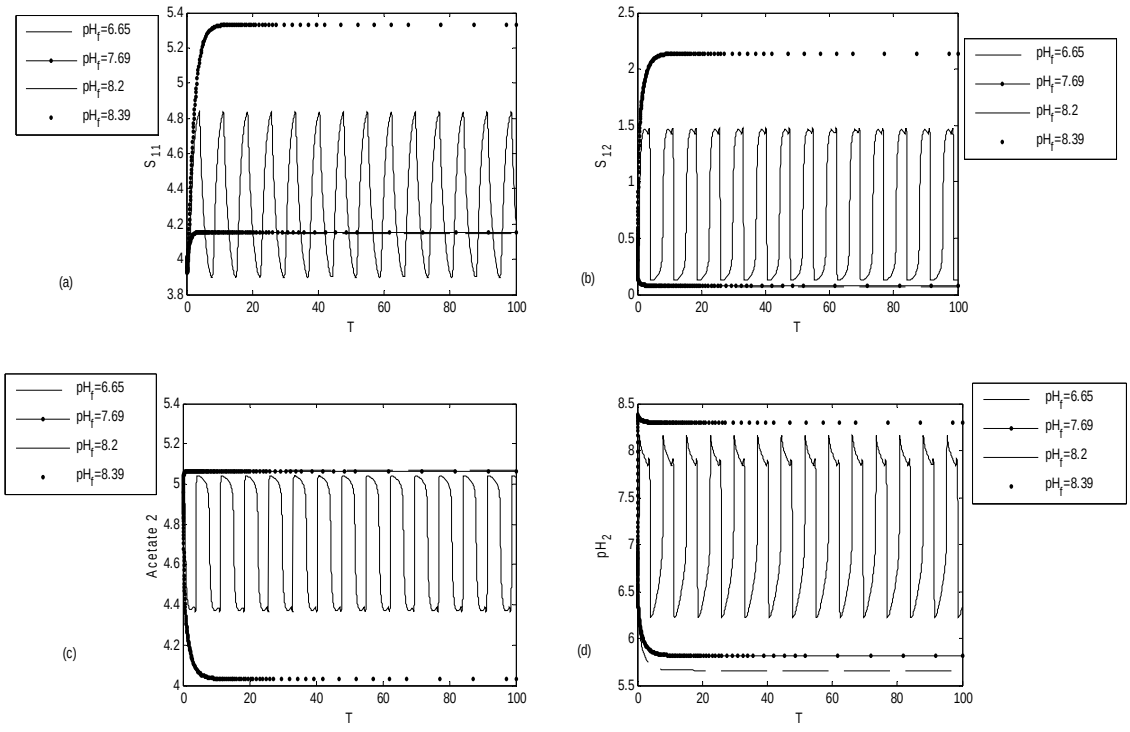

Figure 6-4: ACh system evolution as a function of time at feed hydrogen ions concentrations (h_f):

a) Evolution of ACh concentration in compartment 1 (S_{11})

b) Evolution of ACh concentration in compartment 2 (S_{12}),

c) Evolution of Acetate concentration in compartment 2 (S_{32}) or acetate 2

d) Evolution of pH in compartment 2 (pH_2)

According to the dimensionless form:

h_f=0.02 is corresponding to pH_f=7.69,

h_f=0.004 is corresponding to pH_f=8.39,

h_f=0.006 is corresponding to pH_f=8.2 , and

h_f=0.22 is corresponding to pH_f= 6.65

Initial conditions	
$h_{(1)}$	0.003796824
$h_{(2)}$	0.1405804
$s_{1(1)}$	3.956
$s_{1(21)}$	0.3
$s_{2(1)}$	3.233
$s_{2(2)}$	1.1606
$s_{3(1)}$	8.2517318
$s_{3(2)}$	4.9606

6.2.5) Effect of AChE Activity (B2)

In this section, the effect of varying the AChE activity (B_2) on the evolution of ACh cholinergic system as a function of time is investigated as shown in Figure 6-5. All the parameters are taken constant as shown in Table 2-3 except B_2.

Figure 6-5 indicates that the system approaches steady state solutions (point attractor) at B_2 = 0, $5.2x10^{-5}$, and $20x10^{-5}$ kmol/m^3. However, the oscillatory behavior is clearly indicated at $B_2 = 4.5\ x10^{-5}$ kmol/m^3. This is completely compatible with the dynamic bifurcation results as shown in Figure 2-6 of chapter 2 where we noticed that periodic orbits exist in the range ($3.93x\ 10^{-5} < B_2 < 4.99x10^{-5}$) kmol/m^3. This range is confirmed by the periodic orbits of Figure 6-5 at $B_2 = 4.5x10^{-5}$ kmol/m^3. Then the oscillatory behavior ceases to exist outside this range ($3.93x10^{-5} < B_2 < 4.99x10^{-5}$) kmol/m^3, where the system of ACh recovers its stability as shown in Figure 6-5 at B_2 = 0, $5.2x10^{-5}$, and $20x10^{-5}$ kmol/m^3.

Figure 6-5 a shows that the ACh concentration in compartment 1 (S_{11}) increases as B_2 decreases, where the highest value of S_{11} exists at B_2=0. Furthermore, S_{12} as shown in Figure 6-5b decreases as B_2 increases where S_{12} decreases to the lowest value at the highest value of $B_2 = 20x10^{-5}$ kmol/m^3. The results in Figures 6-5 a and b reflect the mutual effect between the diffusion and reaction. This can be explained as B_2 decreases, ACh concentration in compartment 2 (S_{12}) increases to a limit leading to decreasing the rate of diffusion of ACh from compartment 1 to compartment 2, thereby accumulating ACh concentration in compartment 1. Because acetate in compartment 2 is produced from the hydrolysis of ACh, it is clear from Figure 6-5(c) that acetate concentration increases as B_2 increases. The same happens with hydrogen ions which are produced from he hydrolysis of ACh, we find that pH_2 increases as B_2 decreases as shown in Figure 6-5 (b).

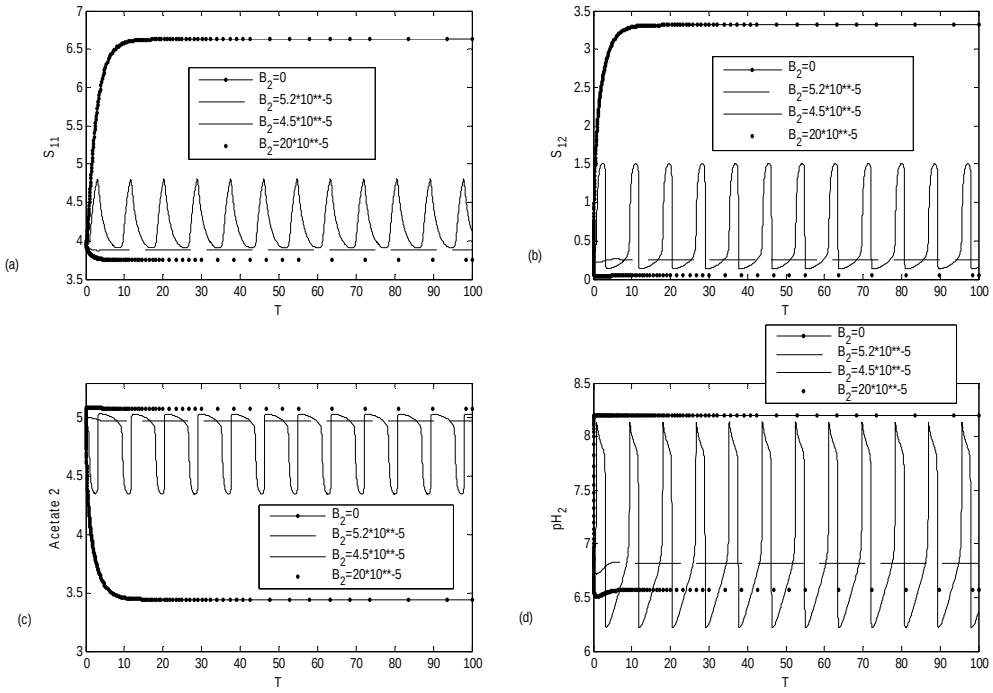

Figure 6-5: ACh system evolution as a function of time at different AChE activities (B_2):

a) Evolution of ACh concentration in compartment 1 (S_{11})

b) Evolution of ACh concentration in compartment 2 (S_{12}),

c) Evolution of Acetate concentration in compartment 2 (S_{32}) or acetate 2

d) Evolution of pH in compartment 2 (pH_2)

Initial conditions	
$h_{(1)}$	0.003796824
$h_{(2)}$	0.1405804
$s_{1(1)}$	3.956
$s_{1(21)}$	0.3
$s_{2(1)}$	3.233
$s_{2(2)}$	1.1606
$s_{3(1)}$	8.2517318
$s_{3(2)}$	4.9606

6.2.6) Effect of ChAT Activity (B1)

The influence of changing the ChAT activity (B_1) on the dynamics of the state variables as a function of time is studied as indicated in Figure 6-6. All the parameters are taken constant as shown in Table 4-3 except B_1.

It is clear from Figure 6-6 that at B_1 = 0, $3x10^{-5}$, $8x10^{-5}$ and $70x10^{-5}$) kmol/m^3, all state variables approach steady state solutions (point attractors), however; at $B_1 = 4x10^{-5}$ kmol/m^3, the oscillatory behavior dominates the system. These results are in complete agreement with the dynamic bifurcation results shown in Figure 4-4 of Chapter 4 where the periodic orbits exist in the range ($3.03x\ 10^{-5} < B_1 < 5x10^{-5}$) kmol/$m^3$. The periodic orbits in Figure 6-6 at $B_1 = 4x10^{-5}$ kmol/m^3 lie in the same range. It is observed that there is no periodic orbits outside this range ($3.03x\ 10^{-5} < B_1 < 5x10^{-5}$) kmol/$m^3$, where the stationary state behavior dominates all the state variables of the cholinergic system of ACh as indicated in Figure 6-6 at B_1 = 0, $3\ x10^{-5}$, $8x10^{-5}$ and $70x10^{-5}$ kmol/m^3.

As shown in Figure 6-6a, the ACh concentration in compartment 1 (S_{11}) increases as B_1 increases, where the highest value of S_{11} is at the highest value of B_1 which is $70x10^{-5}$ kmol/m^3.

Figure 6-6b indicates that S_{12} increases as B_1 increases from 0 to $3x10^{-5}$ kmol/m^3. However, S_{12} decreases as B_1 increases from $3x10^{-5}$ to $8x10^{-5}$ kmol/m^3. In addition, S_{12} increases again as B_1 increases from $8\ x10^{-5}$ to $70x10^{-5}$ kmol/m^3. These results reflect the competition between the diffusion and reaction terms. This coupling is considered as one of the main reasons leading to the appearance of the complex phenomena. Figure 6-6c shows that acetate concentration in compartment 2 behaves like S_{12}. However, Figure 6-6d shows that pH_2 takes the lowest values at the highest value of $B_1 = 70x10^{-5}$ kmol/m^3, and changes inversely with B_1.

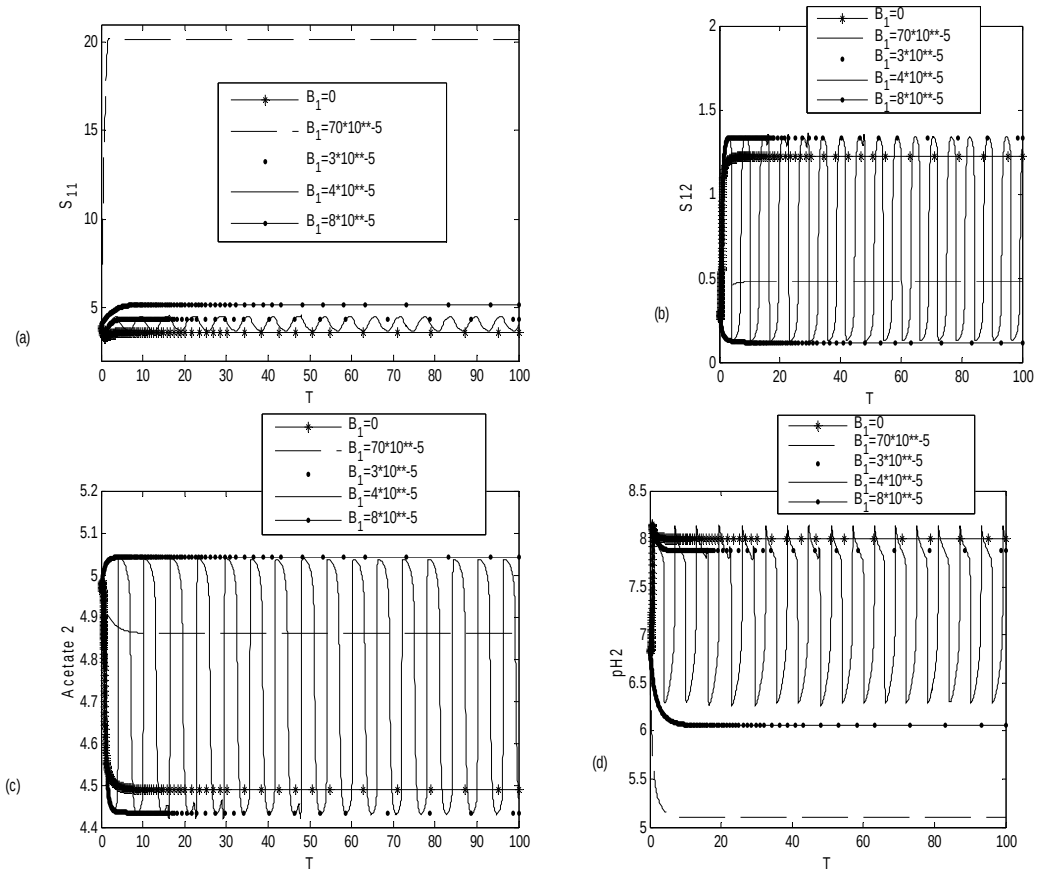

Figure 6-6: ACh system evolution as a function of time at different ChAT activities (B_1)

a) Evolution of ACh concentration in compartment 1 (S_{11})

b) Evolution of ACh concentration in compartment 2 (S_{12}),

c) Evolution of Acetate concentration in compartment 2 (S_{32}) or acetate 2

d) Evolution of pH in compartment 2 (pH_2

Initial conditions	
$h_{(1)}$	.003796824
$h_{(2)}$	0.1405804
$s_{1(1)}$	3.956
$s_{1(21)}$	0.3
$s_{2(1)}$	3.233
$s_{2(2)}$	1.1606
$s_{3(1)}$	8.2517318
$s_{3(2)}$	4.9606

Chapter 7
Conclusions and Future Work

The work described in this dissertation has concentrated on the synthesis, release, and hydrolysis processes of ACh neurocycle. These processes have been modeled mathematically and complex non-linear phenomena are discovered. These complex behaviors like (multiplicity, bifurcation, and chaotic behavior) are exploited to explain the abnormalities occurring in he cholinergic ACh neurocycle leading to cholinergic disorders such as Alzheimer's and Parkinson's diseases. The discussion that follows will summarize the main conclusions of this work and will compare the main results to what had been previously reported in the literature.

7.1 Conclusions

In Chapter 2 two kinetic mechanisms are proposed: the first is for AChE and the other is for ChAT to get more fundamental and reasonable rate equations pH-dependent and substrate inhibited for describing the synthesis and hydrolysis kinetics in the synapses and simulating the ACh neurocycle in the brain.

A novel eight-dimension non-linear mathematical (two-enzyme/two-compartment) model is developed for a coupled ChAT/AChE enzyme system where the physiological phenomena of the choline uptake from the synaptic cleft to the presynaptic neuron and fully ionization of acetic acid assumption are considered. In Chapter 2, the effect of three bifurcation parameters on the system performance have been investigated. These bifurcation parameters are: hydrogen ions feed concentrations, AChE activity, and mobile feed ACh concentrations. The complex static and dynamic phenomena such as bifurcation, oscillatory, instability and chaotic behavior of the system are extensively investigated with comparison to the actual physiological values to predict and control the system performance. The proposed model and kinetic mechanisms showed that they are important for understanding the behavior of the cholinergic ACh neurocycle.

It is found that the system is not influenced noticeably at high feed hydrogen ion concentration (low pH_f). The results are in accordance with the physiological and experimental and theoretical reviews. One of the main explanations is that the high concentrations of H^+ will inhibit choline uptake into presynaptic membrane, another explanation is that the high concentrations may inhibit the synthesis and hydrolysis reaction and finally will cause the state variables to approach the plateau as illustrated in Figure 2-3. The choline recycled from the postsynaptic neurons to be reused in the presynaptic neurons is taken into

consideration and will help the system to control and regulate the levels of the state variables in both compartments. Therefore, ACh and choline concentrations in compartment (1) are higher than that of Mahecha- Botero et al., (2004) because of the choline uptake considerations and the reasonable rate equation of synthesis of ACh. It was found that the system exhibit complex dynamics at low feed hydrogen ion concentrations.

From investigating the static bifurcation of the activity of AChE enzyme and mobile feed ACh concentrations as bifurcation parameters, it is observed that the hysteresis and multiplicity control the system. This hysteresis phenomenon reflects flexibility of the system and its capability to respond to any forcing disturbances affecting the cholinergic ACh system to be able to regulate its components to adapt to any sudden changes. The range of hysteresis for AChE enzyme activity is ($0.899\times10^{-4} \le B_2 \le 1.82\times10^{-4}$) which is larger than that of Mahecha – Botero et al., (2004). At relatively low mobile feed ACh concentrations and AChE enzyme activity, complex dynamic phenomena, and period adding to chaos to destroy chaos are observed. Fully developed chaos with multiple windows is also observed. It is found that ACh and choline concentrations in compartment (1) are higher than that of Mahecha – Botero et al., (2004) because the choline recycled from the postsynaptic neurons to be reused in the presynaptic neurons is taken into consideration in addition to the rate equation of synthesis of ACh which is concluded according to the enzymatic reactions. The mobile feed ACh concentrations play an important role for keeping ACh concentrations at high levels in both compartments 1 and 2 and for maintaining synaptic transmission efficiently. This means that the process of ACh synthesis in one neuron only without supply of mobile ACh from other neurons is not satisfactory to compensate for the released amount and mobile feed ACh coming from other neurons is necessary for performing the balance between the processes of release and synthesis of ACh.

The feed back mechanism of the system can work as a vital control device to control and regulate the transmission activity and the processes of the ACh in both compartments. The findings of this research can be useful to be able to understand the characteristics and the behavior of the ACh cholinergic system and discover the disturbances in the enzymatic processes occurring in the system. In addition, the relation between the neurological sicknesses like Alzheimer's and Parkinson's disease and the complex dynamics and chaotic behavior of the ACh system can be helpful for doing more research on other disorders in living organisms.

In Chapter 3, the effects of both feed choline and acetate substrates concentrations on ACh cholinergic system have been investigated where the physiological phenomena of the choline uptake from the synaptic cleft to the presynaptic neuron and fully ionization of acetic acid assumption have been taken

in consideration. It is found that the feed acetate concentrations have less effect on the synthesis of ACh in both compartments in comparison to the feed choline concentrations. The system is in rich with the dynamics at low concentration of s_{3f} where the feed acetate concentrations are too small to start the synthesis reaction catalyzed by ChAT.

It is found that as the feed choline concentrations increase, ACh levels in both compartments increase gradually until $(s_{2f} = 25.6)$ where ACh is synthesized less efficiently when $(s_{2f} \succ 25.6)$. Hence, the release of ACh in compartment 2 varies in parallel to the incorporation of the choline in compartment 1 to produce ACh. The released ACh can be compensated by synthesizing new ACh in compartment 1 (s_{11}). Therefore, the rate of ACh synthesis must be equal to the rate of transmitter release. This is in agreement with the results obtained by Schwartz et al., (1975). At low concentrations of the feed choline concentrations as shown in Figures 3.5 and 3.6, it was found that the system exhibits complex dynamics bifurcation including chaotic behavior via a PD and period adding sequence in the range ($1.14085 \le s_{2f} \le 1.14676$). A bistability behavior is observed where periodic and point attractors coexist with an unstable periodic orbit as the separatrix separating the domains of attraction of the periodic and point attractors. The system in case of external disturbances such as the sudden change of feed choline concentration to the presynaptic neurons could be affected by the hysteresis with a sudden increase in ACh concentration in both compartments (especially in compartment 2 where ACh concentration increases 6 folds from 1.76155×10^{-6} to 9.1×10^{-6} kmol/m^3 near SB_1 as shown in Figure 3.3(b) with a small variation in the input conditions thus simulating the sudden neural transmission.

From these results, it can be concluded that it not enough to increase the concentrations of acetate to obtain high levels of ACh, and choline supply is the most important substrate in the ACh synthesis and it seems that feed choline (s_{2f}) is limiting for the ACh synthesis. The disturbances and irregularities appearing in the system in the form of chaotic behavior may be a good indication for the cholinergic diseases such as Alzheimer's disease.

In Chapter 4, the effects of ChAT activity and choline uptake in terms of choline recycle ratio as bifurcation parameters, on the system performance have been studied. It is found that as ChAT activity increases, ACh concentrations in compartments 1 and 2 increase continuously. It is found in the range $\left(7.53\times10^{-4} \le B_1 \le 9.78\times10^{-4}\right)$ kmol/m^3; a hysteresis phenomenon is noticed between the two static bifurcation points (SB_1 and SB_2) in this range. Hysteresis generally expresses the capability of the system to respond for any sudden change in a range around the static bifurcation points of the bifurcation points as shown in Figure 4-3(b).

At the low values of ChAT activity, it is found that the system exhibits complex dynamics bifurcation including chaotic behavior via PD and period adding sequence in the range $\left(4.98\times10^{-5} \le B_1 \le 5\times10^{-5}\right)$ kmol/m^3. A bistability behavior is observed in a range close to the subcritical HB where periodic and point attractors coexist with an unstable periodic orbit as the separatrix separating the domains of attraction of the periodic and point attractors.

It is concluded that ACh was synthesized considerably less efficiently at low values of B_1 which giving the opportunity for the system complexity. In addition, the increase of ChAT activity (B_1) can be considered satisfactory for fast synthesis of ACh in compartment 1 to compensate for the released ACh in compartment 2. Therefore, ChAT activity is a good key to cure the disturbances of ACh levels in cholinergic disorders such as Alzheimer's and Parkinson's diseases. It is found that the decline of ChAT activity will cause an observable reduction in the ACh synthesis s_{11} and ACh release s_{12} which represents one of the main symptoms of Alzheimer's disease.

It is found that choline uptake in terms of choline recycle ratio affects greatly on ACh concentrations in both compartments which increase until certain value of R=30 then they become constant in the range of $\left(R \ge 30\right)$. The system is dominated by the complexity and oscillatory behavior at low values of R where the reduction of R causes deficient in choline supplied to the compartment 1. Therefore, choline uptake in terms of choline recycle ratio represents a limiting factor for controlling ACh cholinergic system and regulating the processes of ACh and adjusting the levels of the state variables in the system. ACh is synthesized less efficiently when $\left(R \ge 30\right)$. This is because that ChAT enzyme is inhibited by the excess of choline substrate which occurs with the increase in choline uptake (R). This is in agreement with the results obtained by Schwartz et al., (1975). At the low values of choline recycle ratio, it is found that the system exhibits oscillatory behavior including chaotic behavior via a PD and period adding sequence in the range ($R \le 0.8$).

From studying the effect of ChAT activity and R, our model results agree with the experimental results of Steven et al., 1982; Levnter et al., 1982; Krell and Goldberg, 1975 who illustrated that when ChAT inhibitors are injected into animals, a significant inhibition of brain ChAT activity is observed, but there is no significant reduction in the ACh levels in the brain was observed. These experiments, coupled with others who investigated the effects of choline uptake inhibition by Yamamura and Snyder, 1973; Kuhar and Murrin, 1978 who confirmed that, in nervous tissue, high-affinity choline uptake is the rate limiting for ACh synthesis. This is in agreement with our results that show that the choline is the most important factor in ACh processes and from the effect of choline recycle ratio, it is

clear that choline uptake plays an important role, where it supplies choline as a substrate for the synthesis reaction catalyzed by ChAT in compartment 1.

Furthermore, the results are in accordance with the results obtained by Brandon et al., (2004) who indicated that the loss of ChAT activity will cause a decline in the rate of ACh synthesis in compartment 1. The reduction of ChAT activity needs other alternative effects to keep normal ACh concentrations. According to Brandon et al., (2004), increased uptake or recycle of choline to ChAT in compartment 1 may be the alternative solution for keeping the high efficiency of ACh and the rate-limiting factor in the synthesis of ACh.

Our results are in accordance with the experimental results of other researchers who investigated both choline uptake coupled with ChAT in the presynaptic neurons [Sterling et al; 2006]. They found that inhibition ChAT activity did not block the synthesis of ACh in compartment 1. However, the inhibition of choline transport into compartment 1 blocked ACh synthesis completely in compartment 1 Barker and Mittag, 1973; Guynet et al, 1973; Yamamura and Snyder, 1973; Kuhar and Murrin, 1978, Sterling et al; 2006]. One of the explanations of these results is the existence of ChAT in the presynaptic terminals in a very higher activity than necessary for ACh synthesis [Trabucchi et al, I975; Haubrich, I976]. Finally, it is concluded that choline recycled thereby choline uptake plays the rate limiting factor in the control of ACh synthesis.

In Chapter 5, the complexity behavior of the ACh neurocycle system was investigated considering the partial dissociation of acetic acid in the presynaptic and postsynaptic. The two-parameter continuation technique enabled us to study the qualitative behavior of the system due to changing the system parameters. Based on the feed choline concentrations (s_{2f}) as the main bifurcation behavior and at different values of the feed acetate concentrations (A_f), we could study various static and dynamic bifurcation diagrams and obtain different solutions such as steady state, periodic and chaotic solutions. The results are compared to the results of physiological experiments and other published models. The pH values of both compartments were reasonable and were close to the physiological range. The chaotic behavior obtained via PD sequence. The chaotic behavior expresses the disturbances and irregularities occurring in the cholinergic system may be an indication to the cholinergic disorders such as Alzheimer's and Parkinson's diseases. Hence, considering the partial dissociation of acetic acid in this study enhanced the model prediction for the pH values and made it very close to the practical physiological range. In addition, it gives a reasonable explanation to such transients of pH in pre and postsynaptic regions. The competition between reactions and diffusion processes through the compartments, in addition to the three enzymatic processes, substrate inhibited

and pH dependent, and finally the high nonlinearity in the rate of synthesis reaction catalyzed by ChAT and the rate of hydrolysis reaction catalyzed by AChE represent enough reasons for the complexity behavior appearing in the ACh system.

This dissertation shows that the brain disorders such as Alzheimer's and Parkinson's diseases. are strongly related to the concentrations ACh in the brain. The compartments diffusion-reaction models are formulated to stimulate in-vivo experiments in ChAT and AChE system. These eight/ten dimensional models are used to investigate the complex bifurcation/chaotic behavior, effect of inhibitors/activators and external disturbances on the ACh neurocycle. The disturbances and irregularities in terms of (chaotic attractors) occurring the ACh cholinergic system may be a good indication to help new diagnostic and treatment techniques for the cholinergic diseases like Alzheimer's and Parkinson's diseases.

7.2 Contributions

1) On the level of **kinetics**, we modified two kinetic mechanisms in order to obtain reasonable rate equations for describing the rate of synthesis of ACh in the presynaptic neurons (compartment 1) catalyzed by the enzyme ChAT and the rate of ACh hydrolysis in the synaptic cleft catalyzed by the enzyme AChE. Both rate equations are characterized by non-monotonic kinetics due to pH dependence and substrate inhibition.
2) On the level of **modeling**, we improved previous models by considering new physiological phenomena such as choline uptake from the synaptic cleft to the presynaptic neurons in addition to the partial dissociation of acetic acid and the rate of formation of acetyl CoA (as shown in Chapter 5) which is synthesized inside the mitochondria synthesized by the enzyme acetyl CoA synthase to give us eight non-linear ordinary differential equations in the first part of the work (Chapters 2, 3, and 4) and 10 non-linear ordinary differential equations in the second part (Chapter 5) describing the diffusion-reaction processes in terms of a two-enzyme/ two compartment model.
3) On the level of **analysis**, we investigated bifurcation in the thesis to cover a wide range of static bifurcation (including multiplicity of point attractors) as well as dynamic bifurcation (including Hopf bifurcation for periodic attractors and also multiplicity of the periodic attractors and co-existence of periodic and point attractors). The work also includes chaotic attractors, with a different approach to chaos (e.g.: PD to chaos). The analysis also includes complex non-chaotic attractors discovered during this bifurcation investigation. Bifurcation analysis in this very general form is implicitly a

parametric study with the bifurcation parameter. The collection of all figures in the thesis is a very detailed parametric investigation. More than one model has been used to investigate certain phenomenon which is neglected in one model and included in the other model such as the phenomena of partial dissociation of acetic acid which is neglected in Chapters 2, 3, 4 and considered in Chapter 5. The work also includes relating the results to some published experimental and clinical results making a novel connection between bifurcation and chaos of this system and both Parkinson Disease and Alzheimer Disease From our bifurcation analysis, we could determine the role of each bifurcation parameter in the ACh neurocycle as follow:

a) The effect of mobile feed ACh concentration (S_{1f}) has been determined; we found that mobile feed ACh synthesized in other neurons and transported to the synaptic terminal by the axonal transport mechanism plays a very important role in obtaining the optimum levels of ACh. It contributes with the newly synthesized ACh in regulating and controlling the synaptic transmission and metabolic reaction and achieving the highest efficiency of the ACh neurocycle. The chaotic behavior appears due to the low concentrations of mobile feed ACh and contributes in arising irregularities and disturbances in the oscillation of ACh leading to cholinergic disorders particularly Alzheimer Disease.

b) The effect of feed choline (S2f) as a substrate coming from both the blood plasma and the release of phospholipids was studied. It is found that choline as substrate plays a vital role in the ACh neurocycle. In comparison with the effect of acetyl CoA, it is found that choline is the most important substrate although brain is unable to synthesize choline. At the high concentrations of choline substrate, it is found that the system will be affected very slightly. This is because choline will be converted to an unidentified material which cannot be consumed to produce ACh. In addition, the high concentration of feed choline will inhibit the enzyme of ChAT, so that the synthesis process will be inhibited completely in compartment 1. At low and medium concentrations of feed choline, it is found that the rate of choline conversion to ACh was high because the enzyme ChAT works efficiently. However, the very low concentrations of feed choline cause the appearance of chaotic behavior leading to oscillations and instability of the system. This is one of the main reasons leading to Alzheimer's and Parkinson's diseases.

c) The effect of feed acetyl CoA (S_{3f}) as a substrate was investigated extensively. It is found that feed acetyl CoA has a very limited effect on all state variables. This means that the change of feed acetyl CoA only is not enough to reach the optimum levels of ACh in both compartments. Acetyl CoA is

existent an excess amount because it is synthesized in the mitochondria of the presynaptic neurons. These results are completely compatible with the experimental and physiological results.

d) The effect of feed hydrogen ions (h_f) on the ACh neurocycle system was studied. It is found that the system is not influenced clearly at low pH_f. The results are in accordance with the physiological and experimental reviews. One of the main explanations is that the high concentrations of h_f will inhibit choline diffusion into presynaptic membrane; another explanation is that the high concentrations of h_f may inhibit the synthesis and hydrolysis reaction and finally will cause the state variables to approach the plateau as illustrated in Figure 2-3.

e) The effect of choline uptake in terms of choline recycle ratio (R) was investigated. It is found that choline uptake is the rate limiting step in the synthesis of ACh. It contributes to reaching optimum levels of ACh in both compartments. The impairments occurring in choline returning from the synaptic cleft to the presynaptic neuron because of hemicholinum or beta amyloid aggregates which inhibit choline transport thereby causing deficiency in choline content in the presynaptic neuron leading to shortage of ACh synthesized. The low value of R gives rise to the irregularities and disturbances in terms of chaotic attractor

f) The effect of ChAT activity on the system is studied. It is found that ChAT in a high activity is necessary to obtain high contents of ACh in the system. The low activity of the enzyme ChAT leads to disturbances and may lead to irregularity leading to instability of the system. Thus keeping the enzyme in a high activity is very necessary to obtain an efficient ACh system. However, in comparison with effect of choline uptake and choline substrate, it is found that ChAT activity is not the limiting factor.

g) For the effect of AChE activity, it is found that the high activity of AChE, the concentrations of ACh in both compartments reach the lowest range leading to lowest efficiency of synaptic transmission. However, the medium concentration causes the system to undergo hysteresis phenomena and the very low AChE activity results in the system instability and give the opportunity to the chaotic behavior.

h) It is found that the ACh concentrations in both compartments are compatible with the experimental results in the medium concentrations and the hysteresis concentrations of feed choline and during the medium range of the choline recycle ratio and through the hysteresis range of AChE and ChAT activity.

i) From our results of Chapters 3 and 4 the feed choline concentrations and choline recycle ratio should be kept in the medium range before reaching the plateau level to get the highest efficiency of the system.

4) On the level of **Pharmacology**, it is known that the principle of medications used for treating Alzheimer's disease is based on the inhibition of AChE in compartment (2), hence the concentration of ACh in compartment 2 increases and causes the synaptic transmission. However after some time, ACh in compartment 2 is decreased due to the diffusion with the post synaptic receptors. The drugs do not deal with the problem of deficient synthesis of ACh occurring in compartment 1. One of the main reasons leading to loss of ACh in compartment 1 is that the reduction of choline substrate from the recycle stream required for the ACh synthesis. The loss of choline occurred due to the inhibition of choline uptake. To deal with the deficiency in choline is the key role as mentioned previously choline uptake is the rate limiting step in the synthesis of ACh and choline substrate is the most important substrate in the system. Any medications that cannot treat the deficiency in choline content in compartment 1 will not be effective.

7.3 Future Work

The development of the present work can be extended as follows:

7.3.1 Future improvements in the developed model

1) In our model we assumed that the feed streams of the substrates of choline and acetyl CoA and the recycle stream of choline are all gathered in one feed stream and we assumed that the influx rates of the substrates of choline and acetyl- CoA are equal and constant with time. We found that the ACh concentrations in both compartments ($s_{(1(1)}$, and $s_{1(2)}$) reach a plateau after a transient period using appropriate initial conditions as was shown in chapters 2, 3, and 4 (see for example Figures 2.8 c, d, e, and f). However, one wonders what happens if a rapid synthesis of ACh is required as a response to the physiological functions such as neuromuscular junctions or memory excitations. For fast synthesis rates of ACh in the presynaptic terminals, it will be effective if we considered the influx rates of choline and acetyl CoA substrates changing with time to be able to replace released quantities of ACh and to meet needs for rapid ACh synthesis and keeping synaptic transmission [Kacser and Burns (1973); Sakamoto (1990); Gerald et al., (1996); Fadel et al., (2005)].

2) ACh neurotransmitters after being released from the presynaptic neurons interact with the postsynaptic neurons to cause electric and chemical messages. Then they are hydrolyzed by the enzyme AChE. It is a valuable addition if the interaction with postsynaptic receptors is taken as additional compartment.

3) Since ACh neurons are lost in Alzheimer's disease, it has been of interest to increase ACh synthesis in brains of the effected patients. It is important to study the effect of the inhibitors such as hemicholinium concentrations (HC-3) and β-amyloid aggregates as bifurcation parameters on the system performance and investigating the complex behavior, the dynamics, and chaos behaviors in the system. A mathematical approximation for the interaction between β-amyloid protein and choline uptake can be created.

7.3.2 Characterizing β-amyloid protein aggregates

1) It is observed that the brains of patients with Alzheimer's disease are characterized by β-amyloid protein, tangles, plaques, death of neurons, and lack of ACh. Some researchers proposed that amyloid plaques play a central role due to interaction with neurons leading to tangles and loss of neurons [Ariel et al., (2004), Hardy and Higgins, 1992)]. Furthermore, it has been proposed that β-amyloid protein aggregated causes leakage in the membranes of the presynaptic neurons leading to the loss of choline required for ACh synthesis [Wurtman, (1992), Laura et al., (2004)]. It is very important to investigate the factors affecting β-amyloid protein aggregation such as protein concentration, ionic strength, pH, and temperature in order to understand the aggregation phenomena and to determine the most important factor leading to Alzheimer's disease. The mechanisms involved the aggregation of amyloid β peptide represent an important challenge in the comprehension of inhibition of aggregation. Therefore, a better understanding of the nature of peptide aggregation and the interaction between β-amyloid protein and ACh neurocycle forming complexes is mandatory.

2) Designing artificial membranes immobilized with ChAT and AChE enzymes is important to simulate ACh neurocycle and investigate the effect of changing pH, concentration of ACh and concentration of enzymes, and other factors on excitability and oscillations in artificial membranes. The effect of the same parameters on the action potential difference of the membranes can be investigated. This investigation can be carried out theoretically and experimentally as well.

Appendices

Appendix (A): Proposed Mechanisms for Enzymatic Processes of ACh

A.1 Mechanism of hydrolysis of ACh in compartment (2)

S_1=ACh concentration, E_1= AChE, and P=Ch +AcCo-A

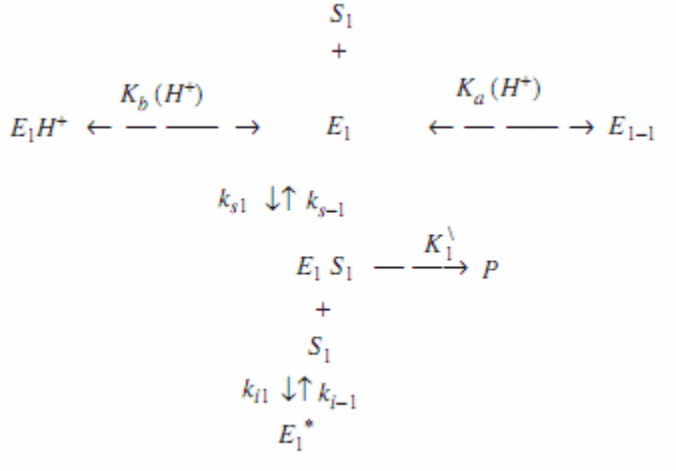

Figure A-1: Hydrolysis reaction model

The full mechanism for the pH dependent AChE kinetics is shown in Figure A-1. The vertical direction represents the main reaction path. The active enzyme species presents in equilibrium with inactive protonated and de-protonated forms. The pH controls the system. E_1 is the active form of the enzyme; E_1H^* and E_1^- are the protonated and de-protonated inactive enzyme forms. E_1S_1 and E_1* are enzyme intermediate complexes. The substrate can combine with E_1S_1 to form another complex E_1* that cannot react further to give product. Hence, the reaction mechanism is inhibited by substrate.

E_1, S_1, and E_1S_1 are related by:

$$S_1 E_1 (K_{s1}) = ks_{-1}(E_1 S_1) \qquad A(1)$$

or

$$E_1 = \frac{K_{S1} E_1 S_1}{S_1} \qquad A(2)$$

where $K_{s1} = \frac{ks_{-1}}{k_{s1}}$, E_1 and E^- related by :

$$k_a(E_1) = k_{-a}E_1^-(H^+), \qquad A\ (3)$$

$$\therefore or\ E_1^- = \frac{K_a}{H^+}(E_1) \qquad A(4)$$

where $K_a = \frac{k_a}{k_{-a}}$, E_1 and $EH_1^{*:}$ are related by:

$$k_b(E_1H^+) = k_{-b}(H^+)(E_1) \qquad A(5)$$

$$E_1H^+ = \frac{k_{-b}}{k_b}(H^+)(E_1) = \frac{H^+}{K_b}(E_1) \qquad A(6)$$

Where $, K_b = \frac{k_b}{k_{-b}},$ *and*

$$E_{t1} = E_1 + E^- + E_1H_1^+ = E_1(1 + \frac{K_a}{H^+} + \frac{H^+}{K_b}) = \frac{K_{s1}}{S_1}(1 + \frac{K_a}{H^+} + \frac{H^+}{K_b})E_1S_1 \qquad A(7)$$

E_1^* is produced due to the inhibition by S_1 , i.e.

$$k_{i1}(E_1S_1)S_1 = E_1^*(k_{i-1}) \qquad A\ (8)$$

$$E_1^* = \frac{(E_1S_1)S_1}{k_{i-1}}(k_{i1}) = \frac{S_1}{K_{i1}}E_1S_1 \qquad A(9)$$

letting $S_1=S_{12}$ and $H^+=H^+_2$ refer to ACh and hydrogen ions concentrations in compartment (2), respectively, give

$$Et = E_{t1} + E_1S_1 + E_1^* = (E_1S_1)\left(\frac{K_{s1}}{S_{12}}(1 + \frac{K_a}{H_2^+} + \frac{H_2^+}{K_b}) + 1 + \frac{S_{12}}{K_{i1}}\right)$$

$$or\ E_1S_1 = \frac{Et\ (S_{12})}{S_{12} + K_{s1}(1 + \frac{K_a}{H_2^+} + \frac{H_2^+}{K_b}) + \frac{S_{12}^2}{K_{i1}}} \qquad A(10)$$

Therefore:

$$R_2 = K_1^{\backslash}(E_1S_1) = \frac{K_1^{\backslash}Et\ (S_{12})}{S_{12} + K_{s1}(1 + \frac{K_a}{H_2^+} + \frac{H_2^+}{K_b}) + \frac{S_{12}^2}{K_{i1}}} \qquad A(11)$$

By dividing through by (K_{s1}), and after some algebraic manipulations, we get:

$$R_2 = \frac{VM_2(s_{12})}{s_{12} + 1/h_2(h_2 + 1 + \delta h_2^2) + \alpha s_{12}^2}$$

$$Where\ \ \delta = \frac{K_a}{K_b}, K_a = \frac{k_a}{k_{-a}}, K_b = \frac{k_b}{k_{-b}}, h = \frac{H^+}{K_a}, s_{12} = \frac{S_{12}}{K_{s1}}, \alpha = \frac{K_{s1}}{K_{i1}} \qquad A(12)$$

$$Therefor;\ r_2 = \frac{s_{12}}{s_{12} + 1/h_2(h_2 + 1 + \delta h_2^2) + \alpha s_{12}^2} \qquad A(13)$$

A.2 Mechanism of synthesis of ACh in compartment (1)

Figure A_2 shows a full mechanism for the pH-dependent enzyme synthesis reaction model.

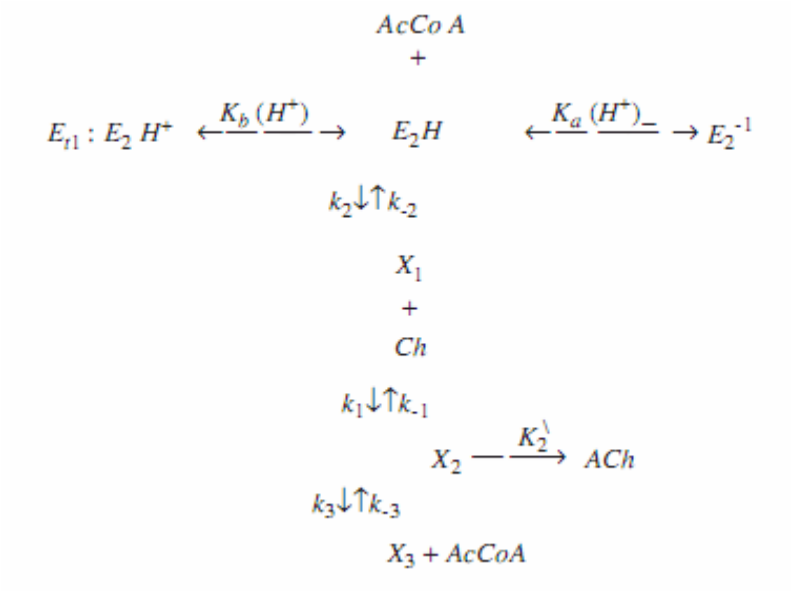

Figure A-2: Synthesis reaction model

The full mechanism for the pH dependent ChAT kinetics is shown in Figure A-2. The main reaction route occurs in the vertical direction. The active enzyme species exists in equilibrium with inactive protonated and de-protonated forms. The equilibria are driven by the pH of the system. E_2H, is the active form of the enzyme; E_2H^* and E_2^- are the protonated and de-protonated inactive enzyme forms.X_1, X_2, and X_3 are enzyme intermediate complexes.

The rate of synthesis can be written as:

$$E_{t2} = E_2H + E_2^- + E_2H_2^+ = E_2H\left(1 + \frac{K_a}{H_1^+} + \frac{H_1^+}{K_b}\right) \qquad A(14)$$

X_1 and X_2 are related through the following expressions:

$$X_1(Ch)\,k_1 = X_2\,k_{-1}\ ,\ or\ X_1 = \frac{k_{-1}}{k_1}\frac{1}{Ch}X_2 = \frac{K_1}{Ch}X_2 \qquad A(15)$$

where $K_1 = \frac{k_{-1}}{k_1}$, E_2H and X_1 are related by:

$$k_2(AcCoA)\,E_2H = k_{-2}X_1(Ch)\ ,or\ E_2H = \frac{K_2K_1}{AcCoA\ Ch}X_2 \qquad A(16)$$

where,: $K_2 = \frac{k_{-2}}{k_2}$. From equations A(13) and A(15) we get:

$$E_{t2} = E_2H + E_2^{-} + E_2H_1^{*} = \frac{K_2K_1}{AcCoA\ Ch}\left(1 + \frac{K_a}{H_1^{+}} + \frac{H_1^{+}}{K_b}\right)X_2 \qquad A(17)$$

X_2 and X_3 are related by

$$X_2(k_3) = k_{-3}(X_3)(AcCoA) \qquad A(18)$$

$$or\ X_3 = \frac{1}{K_3(AcCoA)}X_2 \qquad A(19)$$

Where: $K_3 = \frac{k_{-3}}{k_3}$, Since $E_t = E_{t2} + X_1 + X_2 + X_3$ We get :

$$E_t = X2\left(\frac{K_2K_1}{AcCoA\ Ch}\left(1 + \frac{K_a}{H_1^{+}} + \frac{H_1^{+}}{K_b}\right) + \frac{K_1}{Ch} + 1 + \frac{1}{K_3(AcCoA)}\right) \qquad A(20)$$

or

$$X2 = \frac{Et\ (Ch)(AcCoA)}{K_2K_1\left(1 + \frac{K_a}{H_1^{+}} + \frac{H_1^{+}}{K_b}\right) + K_1(AcCoA) + Ch(AcCoA) + \frac{Ch}{K_3}} \qquad A(21)$$

Since $R_1 = K_2^{\backslash}X_2$, therefore:

$$r1 = \frac{\theta_1\,s_{31}\,s_{21}}{\theta_2 / h_1\,(h_1 + 1 + \delta h_1^2) + \theta_3\,s_{31} + \theta_4 s_{21} + \theta_5\,s_{31}\,s_{21}} \qquad A(22)$$

Appendix (B): Dynamic Model Equations

Figure 2-2 illustrates a simplified description for the two-enzyme/two-compartment system. It is clear that the recycle stream of choline is from compartment 2 to compartment 1. the outflow of compartment 1 represent the inflow of compartment 1 and via the diffusion. The derivation of dynamic model equations is performed via component unsteady state mole balance of all substances leading to eight ordinary differential equations as shown below. The reaction rates are as formulated in Appendix A.

Hydrogen ions

For compartment (1):

$$V_{(1)}\frac{d\left[H^+\right]_{(1)}}{dt} = q\left(\left[H^+\right]_f\right) - \alpha'_{H^+}\,A_M\left(\left[H^+\right]_{(1)} - \left[H^+\right]_{(2)}\right) - V_{(1)}\,R_{W(1)} \qquad B(1)$$

Where

$\left[H^+\right]_f$ is the concentration of hydrogen ions in the feed

For compartment 2

$$V_{(2)}\frac{d\left[H^+\right]_{(2)}}{dt} = \alpha'_{H^+}\,A_M\left(\left[H^+\right]_{(1)} - \left[H^+\right]_{(2)}\right) - q\left(\left[H^+\right]_{(2)}\right) - V_{(2)}\,R_{W(2)} + V_{(2)}\left(R_{(2)}\,\overline{AChE}\right) \qquad B(2)$$

Hydroxyl ions

For compartment (1):

$$V_{(1)}\frac{d\left[OH^-\right]_{(1)}}{dt} = q\left(\left[OH^-\right]_f\right) - \alpha'_{OH}\,A_M\left(\left[OH^-\right]_{(1)} - \left[OH^-\right]_{(2)}\right) - V_{(1)}\,R_{W(1)} \qquad B(3)$$

Where

$\left[OH^-\right]_f$ is the concentration of hydroxyl ions in the feed

For compartment (2):

$$V_{(2)}\frac{d\left[OH^-\right]_{(2)}}{dt} = \alpha'_{OH}\,A_M\left(\left[OH^-\right]_{(1)} - \left[OH^-\right]_{(2)}\right) - q\left(\left[OH\right]\right)_{(2)} - V_{(2)}\,R_{W(2)} \qquad B(4)$$

ACh:

For compartment (1)

$$V_{(1)}\frac{d[S_1]_{(1)}}{dt} = q\left([S_1]_f\right) - \alpha'_{S_1} A_M \left([S_1]_{(1)} - [S_1]_{(2)}\right) + V_{(1)}\left(R_{(1)}\overline{ChAT}\right) \qquad B(5)$$

For compartment2

$$V_{(2)}\frac{d[S_1]_{(2)}}{dt} = \alpha'_{S_1} A_M \left([S_1]_{(1)} - [S_1]_{(2)}\right) - Q\,[S_1]_{(2)} - V_2\left(R_{(2)}\overline{AChE}\right) \qquad B(6)$$

$[S_1]_f$ is the feed acetylcholine concentration

Choline

For compartment 1:

$$V_{(1)}\frac{d[S_2]_{(1)}}{dt} = q\left([S_2]_f + R*[S_2]_{(2)}\right) - \alpha'_{S2} A_M \left([S_2]_{(1)} - [S_2]_{(2)}\right) - V_{(1)}\left(R_{(1)}\overline{ChAT}\right) \qquad B(7)$$

For compartment (2)

$$V_{(2)}\frac{d[S_2]_{(2)}}{dt} = \alpha'_{S2} A_M \left([S_2]_{(1)} - [S_2]_{(2)}\right) - q\left(R*[S_2]_{(2)}\right) + V_{(2)}\left(R_{(2)}\overline{AChE}\right) \qquad B(8)$$

Where: $[S_2]_f$ is the concentration of feed choline.

Acetate

For compartment 1:

$$V_{(1)}\frac{d[S_3]_{(1)}}{dt} = q\left([S_2]_f\right) - \alpha'_{S_1} A_M \left([S_2]_{(1)} - [S_2]_{(2)}\right) - V_{(1)}\left(R_{(1)}\overline{ChAT}\right) \qquad B(9)$$

Where $[S_3]_f$ is the concentration of acetate in the feed

For compartment (2)

$$V_{(2)}\frac{d[S_3]_{(2)}}{dt} = \alpha'_{S3} A_M \left([S_3]_{(1)} - [S_3]_{(2)}\right) - q\left([S_3]_{(2)}\right) + V_{(2)}\left(R_{(2)}\overline{AChE}\right) \qquad B(10)$$

The pseudo-steady state assumption for hydroxyl ions gives,

$$\frac{d[OH^-]}{dt} = 0 \qquad \text{B(11)}$$

Assuming that the hydrogen and hydroxyl ions are at equilibrium gives,

$$K_W = [H^+][OH^-] \qquad \text{B(12)}$$

K_W is the equilibrium constant for water reversible dissociation.

Using the differential equations for $[H^+]$ and $[OH^-]$ together with relations (B (1)) and (B (3)) gives the following differential equations.

For compartment 1, it becomes

$$V_{(1)}\frac{d[H^+]_{(1)}}{dt} = q\left\langle \left([H^+]_f\right) - K_w\left(\frac{1}{[H^+]_f}\right)\right\rangle - A_M\,\alpha'_{H^+}\,\left([H^+]_{(1)} - [H^+]_{(2)}\right)$$

$$+ A_M\,\alpha'_{OH^-}K_w\left(\frac{1}{[H^+]_{(1)}} - \frac{1}{[H^+]_{(2)}}\right) \qquad B(13)$$

We proceed in a similar fashion for compartment 2 to get:

$$V_{(2)}\frac{d[H^+]_{(2)}}{dt} = \alpha'_{H^+}\,A_M\left([H^+]_{(1)} - [H^+]_{(2)}\right) - \alpha'_{OH}\,A_M K_W\left(\frac{1}{[H^+]_{(1)}} - \frac{1}{[H^+]_{(2)}}\right)$$

$$- q\left(\left([H^+]_{(2)} - \frac{K_W}{[H^+]_{(2)}}\right)\right) + V_{(2)}\left(R_{(2)}\,\overline{AChE}\right) \qquad B(14)$$

$$V_{(1)}\frac{d[H^+]_{(1)}}{dt} = q\left([H^+]_f\right) - \alpha'_{H^+}\,A_M\left([H^+]_{(1)} - [H^+]_{(2)}\right)$$

$$- V_{(1)}\,R_{W(1)} \qquad B(15)$$

The pseudo-steady state assumption for hydroxyl ions is employed here also

$$\frac{d[OH^-]}{dt} = 0$$

The assumption that the hydrogen and hydroxyl ions are at equilibrium still holds, i.e.

$$K_W = [H^+][OH^-]$$

Using the differential equations (B (1) and B (3) for $[H^+]$ and $[OH^-]$ together with relations B (1) and B (3) give the rise to the following additional differential equations.

$$V_{(1)}\frac{d\left[H^+\right]_{(1)}}{dt} = q\left\langle\left(\left[H^+\right]_f\right) - K_w\left(\frac{1}{\left[H^+\right]_f}\right)\right\rangle - A_M\ \alpha'_{H^+}\ \left(\left[H^+\right]_{(1)} - \left[H^+\right]_{(2)}\right)$$

$$+ A_M\ \alpha'_{OH^+} K_w\left(\frac{1}{\left[H^+\right]_1}\right) \qquad B(16)$$

$$V_{(2)}\frac{d\left[H^+\right]_{(2)}}{dt} = \alpha'_{H^+}\ A_M\left(\left[H^+\right]_{(1)} - \left[H^+\right]_{(2)}\right) - q\left(\left[H^+\right]_{(2)}\right) - V_{(2)}\ R_{W(2)} + V_{(2)}\left(R_{(2)}\ \overline{AChE}\right) \qquad B(17)$$

$$V\left(_2\right)\frac{d\left[OH^-\right]_{(2)}}{dt} = \alpha'_{OH}\ A_M\left(\left[OH^-\right]_{(1)} - \left[OH^-\right]_{(2)}\right) - q\left(\left[OH^+\right]_{(2)}\right) - V_{(2)}\ R_{W(2)} \qquad B(18)$$

$$V_{(2)}\frac{d\left[H^+\right]_{(2)}}{dt} = \alpha'_{H^+}\ A_M\left(\left[H^+\right]_{(1)} - \left[H^+\right]_{(2)}\right) - \alpha'_{OH} A_M K_W\left(\frac{1}{\left[H^+\right]_{(1)}} - \frac{1}{\left[H^+\right]_{(2)}}\right) -$$

$$q\left(\left(\left[H^+\right]_{(2)} - \frac{K_W}{\left[H^+\right]_{(2)}}\right)\right) + V_{(2)}\left(R_{(2)}\ \overline{AChE}\right) \qquad B(19)$$

References

Chapter 1:

1) Alzheimer, A., (1906), Uber einen eigenartigen schweren Erkrankungsprozeb der Hirnrinde. Neurologisches Centralblatt (Lecture presented at the 37th meeting of the southwest German psychiatrists in Tubingen). 23, 1129.
2) Ana Castro and Ana Martinez, (2001), Peripheral and Dual Binding Site Acetyl cholinesterase Inhibitors: Implications in treatment of Alzheimer's disease, Mini Reviews in Medicinal Chemistry, 1, 267-272
3) Anctil M., (2009); Chemical transmission in the sea anemone Nematostella vectensis: A genomic perspective; Comparative Biochemistry and Physiology Part D: Genomics and Proteomics; 4(4); 268-289
4) Angela De Iuliis, Jessica Grigoletto, Alessandra Recchia, Pietro Giusti and Paola Arslan, (2005), A proteomic approach in the study of an animal model of Parkinson's disease , Clinica Chimica Acta , Volume 357, Issue 2, 24, 202-209
5) Ariel E. Reyes, Marcelo A. Chacón, Margarita C. Dinamarca, Waldo Cerpa, Carlos Morgan and Nibaldo C. Inestrosa, (2004), Acetylcholinesterase-Aß Complexes Are More Toxic than Aß Fibrils in Rat Hippocampus Effect on Rat ß-Amyloid Aggregation, Laminin Expression, Reactive Astrocytosis, and Neuronal Cell Loss , (American Journal of Pathology. 164:2163-2174.)
6) Ashwani V., (1992), Biochemical Adaption of Brain AChE during temperature acclimmation of fish Tilapia massambica Peters. Wilson College, University of Mumbai
7) Balasubramanian, A.S.; Bhanumathy, C.D. FASEB J., 1993, 7, 1354-1358.
8) Ballivet, M., Alliod, C., Bertrand, S., and Bertrand, D. (1996), Nicotinic acetylcholine receptors in the nematode Caenorhabditis elegans. J. Mol. Biol. 258, 261–269.
9) Berl S., Clarke, D.D. and Schneider, D. (eds.), (1975), Metabolic Compartmentation and Neurotransmission (Plenum Press, New York).
10) Collier, B., A. Tandon, M. A. M. Prado, and M. Bachoo (1993), Storage and release of acetylcholine in a sympathetic ganglion. Prog. Brain Res. 98, 183.
11) Collier, B. (1988), About the coupling of acetylcholine hydrolysis and choline uptake at cholinergic nerve terminals. J. Neurochem. 50, 323–324

12) Combes D, Fedon Y, Toutant JP, (2003), Arpagaus M in "Multiple ace genes encoding AChE of Caenorhabditis elegans have distinct tissue expression." Eur J Neurosci. ;18(3):497-512

13) Cooper, J. R. (1994), unsolved problems in the cholinergic nervous system. J. Neurochem. 63, 395.

14) Cooper, J. R., Floyd E. Bloom, and Robert H. Roth, (2003), The Biochemical Basis of Neuropharmacology, 8th Ed.; Oxford New York

15) Cordell, B. (1994), b-Amyloid formation as a potential therapeutic target for Alzheimer's disease. Annu. Rev. Pharmacol. Toxicol. 34, 69.

16) Dale, H.H. (1914), The action of certain esters and ethers of choline, and their relation to muscarine., J. Pharm. Exp. Ther., 6: 147–190.

17) Dale, H.H. (1938), Acetylcholine as chemical transmitter of the effects of nerve impulses. J. Mt. Sinai Hosp., 5: 401–429.

18) David A Bateman, JoAnne McLaurin, and Avijit Chakrabartty, (2007), Requirement of aggregation propensity of Alzheimer amyloid peptides for neuronal cell surface binding, BMC Neurosci. 8: 29.

19) Dobransky, T., W. L. Davis, and F. J. Rylett (2001), Functional characterization of phosphorylation of 69-kDa human 440 by protein kinase C. J. Biol. Chem. 276, 222

20) Dorothea Kominos, (1995), Toward understanding Aggregation , Biophysical Journal 69: 739-740

21) Dowdall, M.J., (1975), Synthesis and storage of acetylcholine in cholinergic nerve terminals, in: Metabolic Compartmen- tation and Neurotransmission, S. Berl, D.D. Clarke and D. Schneider (eds.) (Plenum Press, New York) pp. 585--607.

22) Dunning B B and Xenia Machne; pH optimum for the Rate of Acetylcholine action in neurons; Agents and actions 2/3(1971).

23) Eccles, J.C., Fatt, P. and Koketsu, K. (1954), Cholinergic and inhibitory synapses in a pathway from motor axon-collaterals to motorneurones. J. Physiol., 126: 524–562.

24) Edith Hamel (2004), Cholinergic modulation of the cortical microvascular bed, 145: 171-178

25) Ericson, J. P., H. Varoqui, M. K. H. Schafer, W. Modi, M. F. Diebler, E. Weihe, J. Rand, L. Eiden, T. I. Bonner, and T. B. Usdin (1994), Functional identification of a vesicular

acetylcholine transporter and its expression from a cholinergic gene locus. J. Biol. Chem. 269, 21929.

26) Friboulet, R.; David, A.; Thomas, D., (1981), Excitability memory and oscillation in artificial acetyl cholinesterase membranes. J. Membr. Sci. 8, 33.

27) Friboulet A, (1989), Propriétés structurales et dynamiques d'une enzyme: l'acétylcholinestérase, PHD thesis, Université de Technologie de Compiègne. Compiègne-France.

28) Friboulet A. and Thomas D., (1982), Electrical excitability of artificial enzyme membranes. Biophysical Cheministry, vol 16, pp 153-157.

29) Gaffey, G. T and Mullins L. J., (1958), ion fluxes during the action potential in Chara . J Physiol.., Lond. 144 , 505-24

30) Galdzicki, Z., R. Fukuyama, K. C. Wadhwani, S. I. Rapoport, and G. Ehrenstein (1994), β-Amyloid increases choline conductance of PC12 cells: possible mechanism of toxicity in Alzheimer's disease. Brain Res. 646:332-336.

31) Games, D., D. Adams, R. Alessandrini, R. Barbour, et al. (1995), Alzheimer-type neuropathology in transgenic mice overexpressing V717F 3-amyloid precursor protein. Nature. 373:523-527.

32) Garfinkel, D., (1975), Introduction to simulation techniques in neurochemistry, in: Metabolic Compartmentation and Neurotransmission, S. Berl, D.D. Clarke and D. Schneider (eds.) (Plenum Press, New York), 327--336.

33) Garhyan Parag, Mahecha A Botero; Elnashaie, S.S.E.H.; (2006), Complex Bifurcation/ Chaotic Behavior of Acetyl cholinesterase and choline Acetyltransferase Enzymes system; Mathematical and computer Modeling; 30 824-853

34) Gerald Ehrenstein, Zygmunt Galdzicki, and G. David Lange, (1997), The Choline Leakage Hypothesis for the loss of Acetylcholine in Alzheimer's disease, Biophysical Journal (730: 1276-1280.

35) Gouri, Anahita (2004), Acetylcholinesterase Activity and Isozyme Pattern in Normal and Lithium-treated Developing Chick Brain, University of Mumbai, Department of Life Sciences, Sophia College.

36) Inouye, H., P. E. Fraser, and D. A. Kirschner, (1993), Structure of β - crystallite assemblies formed by Alzheimer, β -amyloid protein analogues: analysis by x-ray diffraction. Biophys. J. 64:502-519.

37) Inestrosa, N.C.; Alarcon, R. J. Physiol. Paris, (1998), 92 341-344.

38) Israel, H., Mitsuo, Y., Abraham, F., Advances in Behavioral Biology. Volume 44, Alzheimer's and Parkinson's Diseases-Recent Developments, Kluver Scientific. 1995.

39) Israel, M. and Y. Dunant (1998), Acetylcholine release and the cholinergic genomic locus. Mol. Neurobiol. 16, 1.

40) Israel, M. and B. Lesbats (1981), Chemiluminescent determination of acetylcholine and continuous detection of its release from Torpedo electric organ synapses and synaptosomes. Neurochem. Int. 3, 81.

41) Jarrett, J. T., and P. T. Lansbury, Jr. (1993), Seeding "one-dimensional crystallization" of amyloid: a pathogenic mechanism in Alzheimer's disease and scrapie Cell. 763: 1055-1058

42) Jean-Pierre Bellier and Hiroshi Kimura (2007), Acetylcholine synthesis by choline acetyltransferase of a peripheral type as demonstrated in adult rat dorsal root ganglion, Journal of Neurochemistry Volume 101 Issue 6 1607-1618.

43) Jenden, D. J., M. Roch, and R. A. Booth (1973), Simultaneous measurement of endogenous and deuterium-labeled tracer variants of choline and acetylcholine in subpicomole quantities by gas chromatography/mass spectrometry. Anal. Biochem. 55, 438.

44) Jian-Zhong Guo, Yingbing Liu, Eva M. Sorenson and Vincent A. Chiappinelli, (2005), Synaptically Released and Exogenous ACh Activates Different Nicotinic Receptors to Enhance Evoked Glutamatergic Transmission in the Lateral Geniculate Nucleus, Neurophysiol 94: 2549-2560.

45) Jones AK, Bentley GN, Oliveros Parra WG, Agnew A. in "Molecular characterization of an acetylcholinesterase implicated in the regulation of glucose scavenging by the parasite Schistosoma." FASEB J. 2002 Mar;16(3):441-3.

46) Mahecha- Botero, Andres, Garhyan, Parag, Elnashaie S. S. E. H., (2004), Bifurcation and chaotic of a coupled acetylcholinesterase/choline acetyltransferase diffusion-reaction enzymes system. Chemical Engineering Science 59,581-597.

47) Mustafa[a] I H, G. Ibrahim, A. Elkamel, S.S.E.H. Elnashaie, P. Chen, (2009), Non Linear Feedback Modeling and Bifurcation of the Acetylcholine Neurocycle and its Relation to Alzheimer's and Parkinson's Diseases; accepted by Journal of chemical engineering science 64(1), 69-90.

48) Mustafa[b] I H, G. Ibrahim, A. Elkamel, S.S.E.H. Elnashaie, P. Chen, (2009), Effect of Choline and Acetate Substrates on Bifurcation and Chaotic Behavior of Acetylcholine

49) Rand, J.B. Acetylcholine (2007), WormBook, ed. The C. elegans Research Community, WormBook, doi/10.1895/wormbook. 1.131.1, http://www.wormbook.org

50) Rand, J.B. and Russell, R.L. (1984), Choline acetyltransferase-deficient mutants of the nematode Caenorhabditis elegans. Genetics 106, 227–248.

Chapter 2:

1) Alvarez, A.; Opazo, C.; Alarcon, R.; Garrido, J.; Inestrosa, N.C. J. Mol. Biol., 1997, 272, 348-361.

2) Alvarez, A.; Alarcon, R.; Opazo, C.; Campos, E.; Muñoz, F.J.; Calderon, F.H.; Dajas, F.; Gentry, M.K.; Doctor, B.P.; DeMello, F.G.; Inestrosa, N.C. J. Neurosci., 1998, 18, 3213-3223.

3) Alzheimer, A. Uber einen eigenartigen schweren Erkrankungsprozeb der Hirnrinde. Neurologisches Centralblatt (Lecture presented at the 37th meeting of the southwest German psychiatrists in Tubingen). 1906, 23, 1129.

4) Ana Castro and Ana Martinez, Peripheral and Dual Binding Site Acetyl cholinesterase Inhibitors: Implications in treatment of Alzheimer's disease, Mini Reviews in Medicinal Chemistry, 2001, 1, 267-272

5) Anctil M., (2009); Chemical transmission in the sea anemone *Nematostella vectensis*: A genomic perspective; Comparative Biochemistry and Physiology Part D: Genomics and Proteomics; 4(4); 268-289

6) Angela De Iuliis, Jessica Grigoletto, Alessandra Recchia, Pietro Giusti and Paola Arslan, (2005), A proteomic approach in the study of an animal model of Parkinson's disease , Clinica Chimica Acta , Volume 357, Issue 2, 24, 202-209

7) Ariel E. Reyes, Marcelo A. Chacón, Margarita C. Dinamarca, Waldo Cerpa, Carlos Morgan and Nibaldo C. Inestrosa, (2004), Acetylcholinesterase-Aß Complexes Are More Toxic than Aß Fibrils in Rat Hippocampus Effect on Rat ß-Amyloid Aggregation, Laminin Expression, Reactive Astrocytosis, and Neuronal Cell Loss , (American Journal of Pathology. 164:2163-2174.)

8) Ashwani V: Biochemical Adaption of Brain AChE during temperature acclimmation of fish Tilapia massambica Peters. Wilson College, University of Mumbai (1992)

9) Chay, R.R.; Rinzel, J. Bursting, beating and chaos in an excitable membrane model. *Biophys. J.* 1985, 47, 357

10) Doedel, E.J.; Champneys, A.R.; Fairgrieve, T.F.; Kuznetsov, Y.A.; Sandstede, B.; Wang, X.J. *AUTO97: Continuation and bifurcation software for ordinary differential equations*. Department of Computer Science, Concordia University, Montreal, Canada, 1997.

11) Elnashaie, S.S.E.H.; El-Rifai, M.A.; Ibrahim, G. (1983) The effect of hydrogen ion production on the steady-state multiplicity of substrate inhibited enzymatic reactions steady-state considerations. Applied Biochemistry and Biotechnology, 8, 275.

12) Elnashaie, S.S.E.H.; El-Rifai, M.A.; Ibrahim, G. (1983). The effect of hydrogen ion production on the steady-state multiplicity of substrate inhibited enzymatic reactions. II: Transient behavior. Applied Biochemistry and Biotechnology, 8, 467.

13) Elnashaie, S.S.E.H.; El-Rifai, M.A.; Ibrahim, G. (1984) The effect of hydrogen ion production on the steady-state multiplicity of substrate inhibited enzymatic reactions. III: asymmetrical steady-states in enzyme membranes. Applied Biochemistry and Biotechnology, 9, 455.

14) Elnashaie, S.S.E.H.; Ibrahim, G.; Teymour, F. A (1995). Chaotic behavior of an acetyl cholinesterase enzyme system. Chaos, Solitons & Fractals. 5, 933.

15) Ermentrout, B. (2002.). Simulating, Analyzing, and Animating Dynamical Systems: A Guide to Xppaut for Researchers and Students; SIAM: New York

16) Fan, Y.S. and Holden, A.V., (1993).. Bifurcation, bursting, chaos and crisis in the Rose-Hindmarsh model for neuronal activity, Chaos, Solitons & Fractals, 3(4), 439

17) Feigenbaum, M.L. (1980). Universal behavior in nonlinear systems. Los Alamos Sci., 1, 4-36

18) Fitzhugh, R. Impulses and physiological states in theoretical models of nerve membranes. *Biophys. J.* 1985, 1, 445.

19) Friboulet, R.; David, A.; Thomas, D. (1981). Excitability memory and oscillation in artificial acetyl cholinesterase membranes. Journal of Membrane Science 8, 33.

20) Garhyan P., Mahecha A Botero ; Elnashaie, S.S.E.H.; (2006). Complex Bifurcation/ Chaotic Behavior of Acetylcholinesterase and Cholineacetyltransferase Enzymes system; Mathematical and Computer Modeling; 30 824-853

21) Guyton, C.A.; Hall, J.E. (2000.). Textbook of Medical Physiology, 10th Ed.; W. B. Saunders Company: Amsterdam

22) Hersh LB, Peet M. Re-evaluation of the kinetic mechanism of the choline acetyltransferase reaction.(1977) Journal Biological Chemistry, 25;252(14):4796–4802.

23) Hindmarsh, J. L. and Rose, R. M., (1984). A model of neuronal bursting using three coupled first order differential equations, Proceedings of the Royal Society Series, B 221 (1222), 87

24) Hindmarsh, J. L. and Rose, R. M., (1982). A model of the nerve impulse using two first-order differential equations, Nature, 296(5853), 162

25) Hindmarsh, J. L and R. M. Rose , (1984). Model of Neuronal Bursting Using Three Coupled First Order Differential Equations , Proceedings of the Royal Society of London Series , Biological Sciences, 221 (1222), 87-102

26) Holden AV, Fan YS (1992c) Crisis-induced chaos in the Rose-Hindmarsh model for neuronal activity. Chaos Solitons &Fractals 2:583–595

27) Holden, A.V. and Fan, Y.S., From simple to complex oscillatory behaviour via intermittent chaos in the Rose - Hindmarsh model for neuronal activity, Chaos, Solitons & Fractals, 2(4), 349–369 (1992b).

28) Holden, A.V. and Fan, Y.S., (1992a). From simple to simple bursting oscillatory behavior via chaos in the Rose - Hindmarsh model for neuronal activity. Chaos Solitons &Fractals 221–236.

29) Ibrahim, G; Elnashaie, S.S.E.H. 1997, Hyperchaos in acetylcholinesterase enzyme systems. Chaos, Solitons & Fractals, 8, 1977-2007

30) Iwamoto H, Randy D. Blakely, and Louis J. De Felice, (2006) ; Na^+, Cl^-, and pH Dependence of the Human Choline Transporter (hCHT) in Xenopus oocytes: The Proton Inactivation Hypothesis of hCHT in Synaptic Vesicles ; The Journal of Neuroscience, September 27, , 26(39):9851-9859

31) Just, W.,Kantz,H.,2000.Some considerations on Poincare maps for chaotic flows Journal of Physics A: Mathematical and General 33, 163–170

32) Koch, A.L., (1986). The pH in the neighborhood of membranes generating a protomotive force, Journal of Theoretical Biology, 120

33) Kysela, S.; Torok, J. Histamine H_1-receptor antagonists do not prevent the appearance of endothelium-dependant relaxation to acetylcholine in rat pulmonary artery. *Physiological Research,* 1996, 45(4), 345.

34) Mahecha- Botero A., Garhyan, Elnashaie S. S. E. H., (2004). Bifurcation and chaotic of a coupled acetyl cholinesterase/choline acetyltransferase diffusion-reaction enzymes system. Chemical Engineering Science 59,581-597.

35) Mustafa I H, G. Ibrahim, A. Elkamel, S.S.E.H. Elnashaie, P. Chen, (2009), Non Linear Feedback Modeling and Bifurcation of the Acetylcholine Neurocycle and its Relation to Alzheimer's and Parkinson's Diseases; accepted by Journal of chemical engineering science 64(1), 69-90.

36) Naparrstek, A.; Romette, J.L.; Kernevez, J.P.; Thomas, D. Memory in enzyme membranes. *Nature*. 1974, 249, 490-491.

37) Quinn, D.M. (1995.); Balasubremanian, A.S.; Doctor, B.P.; Taylor, P. Enzymes of the Cholinestrase Family; Plenum Press: London

38) Rae, C.; Scott, R.; Thompson, C.H.; Dumughn, I.; Kemp, G; Styles, P.; Tracey, I.M.; Radda, G.K. Is brain pH a biochemical marker of IQ? Proceedings Biological Sciences. 1996, 262, 1061-1064

39) Santos J., Lozano R., Friboulet A., Mondie S., (2006), Prediction of unstable behavior in enzymatic diffusion-reaction Processes; Proceedings of the 45th IEEE Conference on Decision & ControlManchester Grand Hyatt Hotel; San Diego, CA, USA, December 13-15, 2006.

40) Shen P and Larter R; (1994). Role of substrate inhibition kinetics in enzymatic chemical oscillations. Biophysical J. ; 67(4): 1414–1428

41) Tucek, S., (1978). Acetylcholine Synthesis in Neurons; Champan & Hall, London. 1978.

42) Tucek, S. (1985). Regulation of acetylcholine synthesis in the brain. Journal of Neurochemistry, 44:11-24.

43) Wessler, I.; Roth, E.; Schwarze, S.; Weikel, W.; Bittinger, F.; Kirkpatrick, C.J.; Kilbindger, H.(2001). Release of non-neural acetylcholine from the human placenta: difference to neural acetylcholine. Naunyn- Schmiedeberg's Archieves of Pharmacology , 364, 205.

44) Wecker L., Dettbarn W. D., and Schmidt D. E. (1978) Choline administration: Modification of the central actions of atropine.Science 199, 86-87.

45) Zauner, A.; Muizelaar, J.P.; Brain metabolism and cerebral blood flow. Head Injury: Pathophysiology and Management of Severe Closed Injury, Eds. Reilly, P; Bullock, R; Chapman & Hall: London 1997

Chapter 3:

1) Ballivet, M., Alliod, C., Bertrand, S., and Bertrand, D. (1996). Nicotinic ACh receptors in the nematode Caenorhabditis elegans. J. Mol. Biol. 258, 261–269.

2) Bielarczyk H and Szutowicz A., (1989), Evidence for the regulatory function of synaptoplasmic acetyl- CoA in ACh synthesis in nerve endings, Biochem. J. 262, 377-380

3) Birks R. I. (1985), Activation of ACh synthesis in cat sympathetic Ganglia: dependence on external choline and sodium- pump rate. J. Physiol. (367) 401-417

4) Blusztajn JK and Wurtman RJ, (1983), Choline and cholinergic neurons, Science 12 August 1983: 614-620, DOI: 10.1126/science.6867732

5) Brandon E. P., Tiffany Mellott, Donald P. Pizzo, Nicole CoufalKevin A. D'Amour, Kevin Gobeske, Mark Lortie, Ignacio Lopez-Coviella, Brygida BerseLeon J. Thal, Fred H. Gage, and Jan Krzysztof Blusztajn; (2004) ; The Journal of Neuroscience, 24(24):5459-5466;

6) Bussiere, M., Vance, J.E., Campenot, R.B., and Vance, D.E. (2001). Compartmentalization of choline and ACh metabolism in cultured sympathetic neurons. J. Biochem. (Tokyo) 130, 561–568.

7) Carl Faingold and Gerhard H. Fromm, (1991), Drugs for the Control of Epilepsy: Actions on Neuonal Networks Involved in Seizure Networks, CRC Press.

8) Carmichael Israel V., Crawford M, Minhas K., Saldivia, Sandrin S., Campisi and Orrego H. (1991), Central Nervous System Effects of Acetate: Contribution to the Central Effects of Ethanol. The Journal of pharmacology and Experimental Therapeutics, 259(1), 403-408

9) Chay, T.R., Rinzel, J., 1985. Bursting, Beating and chaos in an excitable membrane model. Biophysical Journal 47, 357–366

10) Chiao-Kang Chao, Elizabeth A. Pomfret and Steven Zeisel. (1988), Uptake of choline by rat mammary-gland epithelial cells. Biochem. J. (1988) 254, 33-38.

11) Collier B. and Katz H. S. (1974), ACh synthesis from recaptured choline by a sympathetic ganglion, Physiol Vol 238, Issue 3 pp 639-655

12) Collier B, Ilson D (1977) The effect of preganglionic nerve stimulation on the accumulation of certain analogues of choline by a sympathetic ganglion. J Physiol (Lond) 264: 489-509

13) Cooper Jack R., (1994), Unsolved Problems in the Cholinergic Nervous System, Journal of Neurochemistry, 63 (2), 395 - 399

14) Damsma G. , D. Lammerts van Bueren, B. H. C. Westerink I , A. S. Horn (1987) , Determination of ACh and Choline in the Femtornole Range by Means of HPLC, a Post-Column Enzyme Reactor, and Electrochemical Detection, Chromatographia Vol. 24, 827-831

15) Dawn Signor Matthies, Paul A. Fleming, Don M. Wilkes, and Randy D. Blakely , (2006), The Caenorhabditis elegans Choline Transporter CHO-1 Sustains ACh Synthesis and Motor Function in an Activity-Dependent Manner , The Journal of Neuroscience, 2006, 26(23):6200-6212

16) Doedel, E.J.; Champneys, A.R.; Fairgrieve, T.F.; Kuznetsov, Y.A.; Sandstede, B.; Wang, X.J. AUTO97: Continuation and bifurcation software for ordinary differential equations. Department of Computer Science, Concordia University, Montreal, Canada, 1997.

17) Elnashaie, S.S.E.H.; El-Rifai, M.A.; Ibrahim, G.(1983) The effect of hydrogen ion production on the steady-state multiplicity of substrate inhibited enzymatic reactions. I. Steady-state considerations. Applied. Biochemistry and Biotechnology 8, 275.

18) Elnashaie, S.S.E.H.; El-Rifai, M.A.; Ibrahim, G. (1983). The effect of hydrogen ion production on the steady-state multiplicity of substrate inhibited enzymatic reactions. II. Transient behavior. Applied. Biochemistry and Biotechnology 8, 467.

19) Elnashaie, S.S.E.H.; El-Rifai, M.A.; Ibrahim, G. (1984) The effect of hydrogen ion production on the steady-state multiplicity of substrate inhibited enzymatic reactions. III. Asymmetrical steady-states in enzyme membranes. Applied. Biochemistry and Biotechnology 9, 455.

20) Elnashaie, S.S.E.H.; Ibrahim, G.; Teymour, F. A (1995). Chaotic behavior of an acetyl cholinesterase enzyme system. Chaos, Solitons & Fractals. 5, 933.

21) Elnashaie S. S.E., Uhlig F., and Affane C.b , 2005, Numerical techniques for chemical and biological engineers using MATLAB : a simple bifurcation approach, New York : Springer, 2007.

22) Ermentrout, B. (2002.). Simulating, Analyzing, and Animating Dynamical Systems: A Guide to Xppaut for Researchers and Students; SIAM: New York

23) Eugene P. Brandon, Tiffany Mellott, Donald Pizzo, Nicole Coulfal, Kevin D'Amour, Kevin Gobeske, Mark Lortie , Ignacio lopez- Covielle , Brygide Berse, Leon Thal , Fred Gage, Jan Blusztan, (2004). Choline transporter 1 maintains cholinergic function in choline acetyltransferase haploinsufficiency. The journal of Neuroscience , 24 (24), 5459-5466

24) Fan, Y.S. and Holden, A.V., (1993).. Bifurcation, bursting, chaos and crisis in the Rose-Hindmarsh model for neuronal activity, Chaos, Solitons & Fractals, 3(4), 439

25) Feigenbaum, M.L. (1980). Universal behavior in nonlinear systems. Los Alamos Science, 1, 4-36.

26) Fitzhugh, R. Impulses and physiological states in theoretical models of nerve membranes. Biophysical Journal. 1985, 1, 445.

27) Friboulet A and D. Thomas, 1985, Electrical excitability of artificial enzyme membranes III. Hysteresis and oscillations observed with immobilized acetylcholinesterase membranes, Biophysical Chemistry,16(2):153-7.

28) Friboulet, R.; David, A.; Thomas, D. (1981). Excitability memory and oscillation in artificial acetyl cholinesterase membranes. Journal of Membrane Science 8, 33.

29) Friboulet A and D. Thomas, 1982, Electrical excitability of artificial enzyme membranes II. Electrochemical and enzyme properties of immobilized acetylcholinesterase membranes, Biophysical Chemistry 16 145-151

30) Garhyan Parag, Mahecha A Botero; Elnashaie, S.S.E.H.; (2006). Complex Bifurcation/ Chaotic Behavior of Acetyl cholinesterase and choline Acetyltransferase Enzymes system; Mathematical and computer Modeling; 30 824-853

31) Glenn Wetzel and Joan Heller Brown, (1983), Relationship between Choline uptake ACh synthesis and ACh release in isolated rat atria. Journal of pharmacology and Experimental Therapeutics 226(2).

32) Guyton, C.A.; Hall, J.E. (2000.). Textbook of Medical Physiology, 10th Ed.; W. B. Saunders Company: Amsterdam

33) Hindmarsh, J. L. and Rose, R. M., (1982). A model of the nerve impulse using two first-order differential equations, Nature, 296(5853), 162

34) Hindmarsh, J. L and R. M. Rose , (1984). Model of Neuronal Bursting Using Three Coupled First Order Differential Equations , Proceedings of the Royal Society of London. Series B, Biological Sciences, Vol. 221, No. 1222 , 87-102

35) Holden, A.V. and Fan, Y.S., (1992a). From simple to simple bursting oscillatory behavior via chaos in the Rose-Hindmarsh model for neuronal activity. Chaos, Solitons & Fractals, 221–236.

36) Holden, A.V. and Fan, Y.S., From simple to complex oscillatory behaviour via intermittent chaos in the Rose-Hindmarsh model for neuronal activity, Chaos, Solitons & Fractals, 2(4), 349–369 (1992b).

37) Holden AV, Fan YS (1992c) Crisis-induced chaos in the Rose-Hindmarsh model for neuronal activity. Chaos, Solitons & Fractals, 2:583–595

38) Jan K, Blusztajn, Richard J. Wurtman, (1981), Choline biosynthesis by a preparation enriched in synaptosomes from rat brain, Nature 290, 417 - 418 , doi:10.1038/290417a

39) Javier Chavarriga, Isaac A. García and Jordi Sorolla, (2005), Resolution of the Poincaré problem and nonexistence of algebraic limit cycles in family (I) of Chinese classification , Chaos, Solitons & Fractals, 24(2), ,491-499.

40) Just, W.,Kantz,H.,2000.Some considerations on Poincare maps for chaotic flows Journal of Physics A: Mathematical and General 33, 163–170.

41) Ibrahim, G; Elnashaie, S.S.E.H. Hyperchaos in acetyl cholinesterase enzyme systems. Chaos, Solitons & Fractals.(1997), 8, 1977.

42) Ismail H. Ulus, Richard J. Wurtman , Charlotte Mauron and Jan Krzysztof Blusztajn, (1989), Choline increases acetylcholine release and protects against the stimulation-induced decrease in phosphatide levels within membranes of rat corpus striatum, Brain Research. 484 (1989) 217-227

43) Iwamoto H, Randy D. Blakely, and Louis J. De Felice, (2006) ; Na^+, Cl^-, and pH Dependence of the Human Choline Transporter (hCHT) in Xenopus Oocytes: The Proton Inactivation Hypothesis of hCHT in Synaptic Vesicles ; The Journal of Neuroscience, September 27, , 26(39):9851-9859.

44) Kwok Y. N. and, Collier, (1982) Synthesis of acetylcholine from acetate in a sympathetic Ganglion. Neurochemistry (39) 16-26.

45) Kysela, S.; Torok, J. Histamine H_1-receptor antagonists do not prevent the appearance of endothelium-dependant relaxation to acetylcholine in rat pulmonary artery. Physiological Research, 1996, 45(4), 345.

46) Lee H-C, Fellenz-Maloney M-P, Liscovitch M, Blusztajn JK (1993) Phospholipase D-catalyzed hydrolysis of phosphatidylcholine provides the choline precursor for acetylcholine synthesis in a human neuronal cell line. Proc Natural Academy Science USA 90: 10086-10090

47) Lefresne P., Guyenet P and Glowinski J. (1973), Acetylcholine synthesis from [2^{14}C] pyruvate in rat striatal slices. The Journal of Neurochemistry 20, 1083-1097

48) Lynn Wecker, and Wolf Dettbarn, (1979), Relationship between Choline availability and acetylcholine synthesis in discrete regions of rat brain, The Journal of Neurochemistry (33) 961-967

49) Mahecha Andres - Botero, Parag Garhyan, Elnashaie S. S. E. H., (2004). Bifurcation and chaotic of a coupled acetylcholinesterase/choline acetyltransferase diffusion-reaction enzymes system, Chemical Engineering Science 59,581-597.

50) Matthies, D.S., Fleming, P.A., Wilkes, D.M., and Blakely, R.D. (2006). The Caenorhabditis elegans choline transporter CHO-1 sustains acetylcholine synthesis and motor function in an activity-dependent manner. Journal of Neuroscience 26, 6200–6212.

51) Michel, Z. Yuan, S. Ramsubir, and M. Bakovic (2006), Choline Transport for Phospholipid Synthesis. Experimental Biology and Medicine, 231(5): 490 - 504 Michel, Z. Yuan, S. Ramsubir, and M. Bakovic (2006), Choline Transport for Phospholipid Synthesis. Experimental Biology and Medicine, 231(5): 490 - 504

52) Morel N.(1976). Effect of Choline on the rates of synthesis and of release of acetylcholine in the electric organ of torpedo.; The Journal of Neurochemistry 1976 (27) 779-784.

53) Mullen G. P., E. A. Mathews, M. H. Vu, J. W. Hunter, D. L. Frisby, A. Duke, K. Grundahl, J. D. Osborne, J. A. Crowell, and J. B. Rand, (2007), Choline Transport and de novo Choline Synthesis Support Acetylcholine Biosynthesis in Caenorhabditis elegans Cholinergic Neurons , Genetics; 177(1): 195 - 204.

54) Mustafa[a] I H, G. Ibrahim, A. Elkamel, S.S.E.H. Elnashaie, P. Chen, (2009), Non Linear Feedback Modeling and Bifurcation of the Acetylcholine Neurocycle and its Relation to Alzheimer's and Parkinson's Diseases; accepted by Journal of chemical engineering science 64(1), 69-90.

55) Mustafa[b] I H, G. Ibrahim, A. Elkamel, S.S.E.H. Elnashaie, P. Chen, (2009), Effect of Choline and Acetate Substrates on Bifurcation and Chaotic Behavior of Acetylcholine Neurocycle and Alzheimer's and Parkinson's Diseases; Journal of chemical engineering science. 64(9), 2096-2112.

56) Pinthong M, S. A. G. Black, F. M. Ribeiro, C. Pholpramool, S. S. G. Ferguson, and R. J. Rylett, (2008), Activity and Subcellular Trafficking of the Sodium-Coupled Choline Transporter CHT Is Regulated Acutely by Peroxynitrite. Molecular Pharmacology., 73(3): 801 – 812

57) Rae, C.; Scott, R.; Thompson, C.H.; Dumughn, I.; Kemp, G; Styles, P.; Tracey, I.M.; Radda, G.K. Is brain pH a biochemical marker of IQ? Proceedings Biological Sciences. 1996, 262, 1061-1064

58) Santos, J. Friboulet, A.; Lozano (2006), Modeling of acetylcholinesterase immobilized into artificial membrane; Annual International Conference of the IEEE Engineering in Medicine and Biology - Proceedings, 28th Annual International Conference of the IEEE Engineering in Medicine and Biology Society, EMBS'06, 2006, p 4187-4191

59) Schwartz James, Michael L. Eisentadt, and Howard Cedar, (1975), Metabolism of Acetylcholine in the Nervous system of Aplysia californica 1. Source of choline and its uptake in intact tissue. The Journal of General Physiology (65), 255-273.

60) Shawn M. Ferguson, and Randy D. Blakely, (2004), The Choline Transporter Resurfaces: New Roles for Synaptic Vesicles, Molecular Interventions 4:22-37

61) Schwartz James, Michael Eisenstadt, and Howard Cedar, (1975), Metabolism of ACh in the nervous system of Aplysia californica. The Journal of General Physiology, (65), 255-273.

62) Steven Leventer, Peter Rowell, and Mary Clark, (1982) The effect of choline acetyltransferase inhibition on Acetylcholine synthesis and release in term humanplacenta, The journal of pharmacology and experimental therapeutics , 222(2)

63) Steven Leventer, Peter Rowell, (1984), Investigation of the rate limiting stepin the synthesis of acetylcholine by human placenta. Placenta, 5, 261-270

64) Strogatz S. (1994), Nonlinear dynamics and chaos, second printing,

65) Tucek, S., (1978). Acetylcholine Synthesis in Neurons; Champan &hall, London. 1978.

66) Tucek, S. (1985). Regulation of acetylcholine synthesis in the brain. The Journal of Neurochemistry 44:11-24.

67) Tucek S. (1988) Choline acetyltransferase and the synthesis of acetylcholine, in Handbook of Experimental Pharmacology, Vol. 86 (Whittaker V. P., ed), 125-165. Springer-Verlag, Berlin.

68) Tucek S (1990), The synthesis of acetylcholine: twenty years of progress. Prog Brain Research 84: 467-477

69) Wecker L., Dettbarn W. D., and Schmidt D. E. (1978) Choline administration: Modification of the central actions of atropine. Science 199, 86-87.

70) Wecker,: L, 1988, Influence of dietary choline availability and neuronal demand on acetylcholine synthesis by rat brain, The Journal of Neurochemistry. 1988 Aug; 51(2): 497-504

71) Wessler, I.; Roth, E.; Schwarze, S.; Weikel, W.; Bittinger, F.; Kirkpatrick, C.J.; Kilbindger, H.(2001). Release of non-neural acetylcholine from the human placenta: difference to neural acetylcholine. Naunyn-Schmiedeberg's Archives of Pharmacology 364, 205.

72) Yuri Kiselevski , Nicholas Oganesian, Sergey Zimatkin, Andrzej Szutowicz, Stefan Angielski, Pavel Niezabitowski, Wojciech Uracz, Ryszard Gryglewski, (2003), Acetate metabolism in brain mechanisms of adaptation to ethanol. Med Sci Monit, 9(5): BR218-222

73) Zauner, A., Muizelaar, P., 1997. Brain metabolism and cerebral blood fow. In: Reilly, P., Bullock, R. (Eds.), Head Injury. Pathophysiology and Management of Severe Closed Injury. Chapman & Hall Medical, London, p. 92

74) Zhao D, Frohman MA, Blusztajn JK (2001) Generation of choline for acetylcholine synthesis by phospholipase D isoforms. BMC Neuroscience 2: 16.

Chapter 4:

1) Alvarez, A.; Opazo, C.; Alarcon, R.; Garrido, J.; Inestrosa, N.C. J. Mol. Biol., 1997, 272, 348-361.

2) Alvarez, A.; Alarcon, R.; Opazo, C.; Campos, E.; Muñoz, F.J.; Calderon, F.H.; Dajas, F.; Gentry, M.K.; Doctor, B.P.; DeMello, F.G.; Inestrosa, N.C. J. Neurosci., 1998, 18, 3213-3223.

3) Alzheimer, A. Uber einen eigenartigen schweren Erkrankungsprozeb der Hirnrinde. Neurologisches Centralblatt (Lecture presented at the 37th meeting of the southwest German psychiatrists in Tubingen). 1906, 23, 1129.

4) Ana Castro and Ana Martinez, Peripheral and Dual Binding Site Acetyl cholinesterase Inhibitors: Implications in treatment of Alzheimer's disease, Mini Reviews in Medicinal Chemistry, 2001, 1, 267-272

5) Anctil M., (2009); Chemical transmission in the sea anemone *Nematostella vectensis*: A genomic perspective; Comparative Biochemistry and Physiology Part D: Genomics and Proteomics; 4(4); 268-289

6) Angela De Iuliis, Jessica Grigoletto, Alessandra Recchia, Pietro Giusti and Paola Arslan, (2005), A proteomic approach in the study of an animal model of Parkinson's disease , Clinica Chimica Acta , Volume 357, Issue 2, 24, 202-209

7) Ariel E. Reyes, Marcelo A. Chacón, Margarita C. Dinamarca, Waldo Cerpa, Carlos Morgan and Nibaldo C. Inestrosa, (2004), Acetylcholinesterase-Aß Complexes Are More Toxic than Aß Fibrils in Rat Hippocampus Effect on Rat ß-Amyloid Aggregation, Laminin Expression, Reactive Astrocytosis, and Neuronal Cell Loss , (American Journal of Pathology. 164:2163-2174.)

8) Ashwani V: Biochemical Adaption of Brain AChE during temperature acclimmation of fish Tilapia massambica Peters. Wilson College, University of Mumbai (1992)

9) Birks R. I. (1985), Activation of Acetylcholine synthesis in cat sympathetic Ganglia: dependence on external choline and sodium- pump rate. J. Physiol. (367) 401-417.

10) Brandon E. P., Tiffany Mellott, Donald Pizzo, Nicole Coulfal, Kevin D'Amour, Kevin Gobeske, Mark Lortie , Ignacio lopez- Covielle , Brygide Berse, Leon Thal , Fred Gage, Jan Blusztan, (2004). Choline transporter 1 maintains cholinergic function in choline acetyltransferase haploinsufficiency. The journal of Neuroscience , 24 (24), 5459-5466

11) Carl L. Faingold and Gerhard H. Fromm, 1991, Drugs for the Control of Epilepsy: Actions on Neuonal Networks Involved in Seizure Networks, CRC Press.

12) Chay, R.R.; Rinzel, J. Bursting, beating and chaos in an excitable membrane model. *Biophysical Journal,* 1985, 47, 357.

13) Chiao-Kang Chao, Elizabeth A. Pomfret and Steven Zeisel. (1988), Uptake of choline by rat mammary-gland epithelial cells. Biochem. J. (1988) 254, 33-38.

14) Docherty M & Bradford HF. 1986. A cell-surface antigen of cholinergic nerve terminals recognized by antisera to choline acetyltransferase. *Neurosci Lett* 70: 234-238.

15) Doedel, E.J.; Champneys, A.R.; Fairgrieve, T.F.; Kuznetsov, Y.A.; Sandstede, B.; Wang, X.J. *AUTO97: Continuation and bifurcation software for ordinary differential equations*. Department of Computer Science, Concordia University, Montreal, Canada, 1997.

16) Eckenstein Flix and Sofroniew Michael, 1983; Identification of central cholinergic neurons containing both choline acetytransferase and acetylcholinesterase and of central neurons containing only acetylcholinesterase. ; The Journal of Neuroscience, 3(11) 2286-2291

17) Ehrenstein G, Z Galdzicki, and G D Lange; (1997); The choline-leakage hypothesis for the loss of acetylcholine in Alzheimer's disease; Biophys J. 73(3): 1276–1280.

18) Ehrenstein G, Z Galdzicki, and G D Lange; (2000); positive-feedback model for the loss of acetylcholine in Alzheimer's disease; Ann N Y Acad Sci.; 899:283-91.

19) Elnashaie, S.S.E.H.; El-Rifai, M.A.; Ibrahim, G.(1983) The effect of hydrogen ion production on the steady-state multiplicity of substrate inhibited enzymatic reactions. I. Steady-state considerations. *Appl.Biochem. Biotechnol.*, 8, 275.

20) Elnashaie, S.S.E.H.; El-Rifai, M.A.; Ibrahim, G. (1983) . The effect of hydrogen ion production on the steady-state multiplicity of substrate inhibited enzymatic reactions. II. Transient behavior. *Appl. Biochem. Biotechnol.*, 8, 467.

21) Elnashaie, S.S.E.H.; El-Rifai, M.A.; Ibrahim, G. (1984) The effect of hydrogen ion production on the steady-state multiplicity of substrate inhibited enzymatic reactions. III. Asymmetrical steady-states in enzyme membranes. *Appl. Biochem. Biotechnol.*, 9, 455.

22) Elnashaie, S.S.E.H.; Ibrahim, G.; Teymour, F. A (1995). Chaotic behavior of an acetyl cholinesterase enzyme system. *Chaos, Solitons & Fractals*. 5, 933.

23) Ermentrout, B. (2002.). *Simulating, Analyzing, and Animating Dynamical Systems: A Guide to Xppaut for Researchers and Students*; SIAM: New York

24) Fan, Y.S. and Holden, A.V., (1993).. Bifurcation, bursting, chaos and crisis in the Rose-Hindmarsh model for neuronal activity, *Chaos, Solitons & Fractals*, 3(4), 439

25) Feigenbaum, M.L. (1980). Universal behavior in nonlinear systems. *Los Alamos Sci.*, 1, 4-36
Ferguson Shawn M., Mihaela Bazalakova, Valentina Savchenko, Juan Carlos Tapia, Jane Wright†, and Randy D. Blakely; (2004); Lethal impairment of cholinergic neurotransmission in hemicholinium-3-sensitive choline transporter knockout mice; PNAS 2004 101:8762-8767.

26) Fitzhugh, R. Impulses and physiological states in theoretical models of nerve membranes. *Biophysical Journal,* 1985, 1, 445.

27) Friboulet, R.; David, A.; Thomas, D. (1981). Excitability memory and oscillation in artificial acetyl cholinesterase membranes. *J. Membr. Sci.* 8, 33.

28) Garhyan Parag, Mahecha A Botero ; Elnashaie, S.S.E.H.; (2006). Complex Bifurcation/ Chaotic Behavior of Acetyl cholinesterase and choline Acetyltransferase Enzymes system; Mathematical and computer Modeling; 30 824-853

29) Glenn Wetzel and Joan Heller Brown , (1983) , Relationship between Choline uptake acetylcholine synthesis and acetylcholine release in isolated rat atria. J pharmacology and Experimental Therapeutics 226(2).

30) Guyton, C.A.; Hall, J.E. (2000.). *Textbook of Medical Physiology, 10th Ed.*; W. B. Saunders Company: Amsterdam

31) Hartmann J., Cornelia Kiewert, Ellen G. Duysen, Oksana Lockridge and Jochen Klein; (2008); Choline availability and acetylcholine synthesis in the hippocampus of acetylcholinesterase-deficient mice ; Neurochemistry International; 52(6, 972-978

32) Hersh LB, Peet M. Re-evaluation of the kinetic mechanism of the choline acetyltransferase reaction. *J Biol Chem.* 1977 Jul 25;252(14):4796–4802.

33) Hindmarsh, J. L. and Rose, R. M., (1984). A model of neuronal bursting using three coupled first order differential equations, *Proc. Roy. Soc.*, B221 (1222), 87

34) Hindmarsh, J. L. and Rose, R. M., (1982). A model of the nerve impulse using two first-order differential equations, Nature, 296(5853), 162

35) Hindmarsh, J. L and R. M. Rose , (1984). Model of Neuronal Bursting Using Three Coupled First Order Differential Equations, *Proceedings of the Royal Society of London. Series B, Biological Sciences*, Vol. 221, No. 1222 pp. 87-102

36) Holden AV, Fan YS (1992c) Crisis-induced chaos in the Rose-Hindmarsh model for neuronal activity. Chaos Solitons Fractals 2:583–595

37) Holden, A.V. and Fan, Y.S., From simple to complex oscillatory behaviour via intermittent chaos in the Rose-Hindmarsh model for neuronal activity, *Chaos, Solitons & Fractals*, 2(4), 349–369 (1992b).

38) Holden, A.V. and Fan, Y.S., (1992a). From simple to simple bursting oscillatory behavior via chaos in the Rose-Hindmarsh model for neuronal activity. Chaos Solitons Fractals 221–236.

39) Ibrahim, G; Elnashaie, S.S.E.H. Hyperchaos in acetyl cholinesterase enzyme systems. *Chaos, Solitons & Fractals*.(1997), 8, 1977.

40) Iwamoto H, Randy D. Blakely, and Louis J. De Felice, (2006) ; Na^+, Cl^-, and pH Dependence of the Human Choline Transporter (hCHT) in Xenopus Oocytes: The Proton Inactivation Hypothesis of hCHT in Synaptic Vesicles ; The Journal of Neuroscience, September 27, , 26(39):9851-9859.

41) James Schwartz, Michael Eisenstadt, and Howard Cedar, (1975), Metabolism of Acetylcholine in the nervous system of Aplysia californica. The J. of General physiology, (65), 255-273.

42) Just, W., Kantz, H., 2000. Some considerations on Poincare maps for chaotic flows Journal of Physics A: Mathematical and General 33, 163–170.

43) Kato T. 1989. Choline Acetyltransferase activities in single spinal motor neurons from patients with Amyotrophic Lateral Sclerosis. *J Neurochem* 52: 636- 640.

44) Keverne Jessica and Ray Melissa; 2008; Neurochemistry of Alzheimer's disease, Psychiatry, 7(1) 6-8

45) Koch, A.L., (1986). The pH in the neighborhood of membranes generating a protomotive force, Journal of Theoretical Biology, 120.

46) Kwork Y. N. and, Collier, (1982) Synthesis of acetylcholine from acetate in a sympathetic Ganglion. Neurochem (39) 16-26.

47) Kysela, S.; Torok, J. Histamine H_1-receptor antagonists do not prevent the appearance of endothelium-dependant relaxation to acetylcholine in rat pulmonary artery. *Physiological Research,* 1996, 45(4), 345.

48) Leventer S M, P P Rowell and M J Clark, (1982) The effect of choline acetyltransferase inhibition on Acetylcholine synthesis and release in term human placenta, The journal of pharmacology and experimental therapeutics , 222(2)

49) Leventer S M, P P Rowell, (1984), Investigation of the rate limiting step in the synthesis of acetylcholine by human placenta. Placenta, 5, 261-270

50) Levey AI, Gilmor ML, Count SE &Wiley RG. 1998. Coordinate expression of the vesicular acetycholine transporter and choline acetyltransferase following septohippocampal pathway lesions. *J Neurochem* 71: 2411-2420.

51) Lynn Wecker, and Wolf Dettbarn, (1979), Relationship between Choline availability and acetylcholine synthesis in discrete regions of rat brain, J Neurochemistry (33) 961-967.

52) Mahecha- Botero Andres, Garhyan Parag, Elnashaie S. S. E. H., (2004). Bifurcation and chaotic of a coupled acetylcholinesterase/choline acetyltransferase diffusion-reaction enzymes system. Chemical Engineering Science 59,581-597.

53) Malthe-Sørenssen D & Fonnun F. 1972. Multiple forms of Choline Acetyltransferase in several species demonstrated by Isoelectric Focusing. *Biochem J* 127: 229-236.

54) Malthe Sosrenssen D, Lea T. , Fonnum F, Eskeland T., (1978), Molecular characterization of cholineacetyltransferase from bovine brain caudate nucleus and some immunological properties of the highly purified enzyme, Journal of Neurochemistry , 30(1) 35 – 46.

55) Milos D. Ikonomovic, MD; Elliott J. Mufson,; Joanne Wuu, ScM; David A. Bennett, MD; Steven T. DeKosky, MD ; 2005; Reduction of Choline Acetyltransferase Activity in Primary Visual Cortex in Mild to Moderate Alzheimer's Disease; *Achieves of Neurology.* 2005; 62:425-430.

56) Morel N.(1976). Effect of Choline on the rates of synthesis and of release of acetylcholine in the electric organ of torpedo; The Journal of Neurochemistry 1976 (27) 779-784.

57) Mustafa[a] I H, G. Ibrahim, A. Elkamel, S.S.E.H. Elnashaie, P. Chen, (2009), Non Linear Feedback Modeling and Bifurcation of the Acetylcholine Neurocycle and its Relation to

Alzheimer's and Parkinson's Diseases; accepted by Journal of chemical engineering science 64(1), 69-90.

58) Mustafa[b] I H, G. Ibrahim, A. Elkamel, S.S.E.H. Elnashaie, P. Chen, (2009), Effect of Choline and Acetate Substrates on Bifurcation and Chaotic Behavior of Acetylcholine Neurocycle and Alzheimer's and Parkinson's Diseases; Journal of chemical engineering science. 64(9), 2096-2112.

59) NachmansohnD&Machado AL. 1943. The formation of acetylcholine. A new enzyme choline acetylase. *J Neurophysiol* 6: 397-403.

60) Naparrstek, A.; Romette, J.L.; Kernevez, J.P.; Thomas, D. Memory in enzyme membranes. *Nature*. 1974, 249, 490-491

61) Nayfeh Ali H. and Balakumar Balachandran (1995), Applied Nonlinear Dynamics: Analytical, Computational, and Experimental Methods; pp 290-313. Printed in the Federal Republic of Germany, John Wiley & Sons, lnc. ISBN-13: 978-0-47 1-59348-5

62) Nunes-Tavares Nilson, Narcisa Leal, Cunha Silva, and Aida Hasson – Voloch. , (2002) , Choline acetyltransferase detection in normal and enervated elecrtocyte from Electrophorus electricus (gl.) using a confocal scanning optical microscopy analysis ,An . Acad Bras Ci, 72 (3).

63) Perry E., M. Walker, J. Grace and R. Perry, (1999), Acetylcholine in mind: a neurotransmitter correlate of consciousness, Trends Neurosci 22 , 273–280

64) Polsky R & Shuster L. 1976. Preparation and characterization of two isozymes of Choline Acetyltransferase from Squid Head Ganglia. (II- Self- Association, Molecular weight determinations and Studies with inactivating antisera. *Biochem Biophys Acta* 445: 43-66.

65) Quinn, D.M. (1995.); Balasubremanian, A.S.; Doctor, B.P.; Taylor, P. Enzymes of the Cholinestrase Family; Plenum Press: London

66) Rae, C.; Scott, R.; Thompson, C.H.; Dumughn, I.; Kemp, G; Styles, P.; Tracey, I.M.; Radda, G.K. Is brain pH a biochemical marker of IQ? Proceedings Biological Sciences. 1996, 262, 1061-1064.

67) Salvaterra Paul, 1987, Molecular biology and neurobiology of choline acetyltransferase, *Molecular Neurobiology, 1(3) 247-280*

68) Shen P and Larter R; (1994). Role of substrate inhibition kinetics in enzymatic chemical oscillations. Biophysical J. ; 67(4): 1414–1428

69) Sterling G. H, Peter H. Doukas, Fiori J. Ricciardi Jr., Diane W. Biedrzycka John J. O'Neill; (2006); Inhibition of High-Affinity Choline Uptake and Acetylcholine Synthesis by Quinuclidinyl and Hemicholinium Derivatives; Journal of Neurochemistry; 46 (4), 1170 - 1175

70) Tucek, S., (1978). Acetylcholine Synthesis in Neurons; Champan &hall, London. 1978.

71) Tucek, S. (1985). Regulation of acetylcholine synthesis in the brain. *J. Neurochem. 44:11-24.*

72) Uyeda CT, Eng LF, Chao LP & Wolfgran F. 1974. Antibody to bovine choline acetyltransferase and immunofluorescent localisation of the enzyme in neurons. *Nature* 250: 243-245.

73) Waser G, Riggio G & Raeber AJ. 1989. Purification and isolation of choline acetyltransferase from the electric organ of *Torpedo marmorata* by affinity chromatography. *Eur J Biochem* 186: 487-492.

74) Wecker L., Dettbarn W. D., and Schmidt D. E. (1978) Choline administration: Modification of the central actions of atropine Science 199, 86-87.

75) Wessler, I.; Roth, E.; Schwarze, S.; Weikel, W.; Bittinger, F.; Kirkpatrick, C.J.; Kilbindger, H.(2001). Release of non-neural acetylcholine from the human placenta: difference to neural acetylcholine. Naunyn- Schmiedeberg's Arch. Pharmacol., 364, 205.

76) Wurtman RJ, Blusztajn JK, Ulus IH, Coviella IL, Buyukuysal RL, Growdon JH&Slack BE. 1990. Choline metabolism in cholinergic neurons: implications for the pathogenesis of neurodegenerative diseases. *Adv Neurol* 51: 117-125.

77) Zauner, A.; Muizelaar, J.P.; Brain metabolism and cerebral blood flow. Head Injury: Pathophysiology and Management of Severe Closed Injury, Eds. Reilly, P; Bullock, R; Chapman & Hall: London 1997.

Chapter 5:

1) Alvarez, A.; Opazo, C.; Alarcon, R.; Garrido, J.; Inestrosa, N.C. J. Mol. Biol., 1997, 272, 348-361.

2) Alvarez, A.; Alarcon, R.; Opazo, C.; Campos, E.; Muñoz, F.J.; Calderon, F.H.; Dajas, F.; Gentry, M.K.; Doctor, B.P.; DeMello, F.G.; Inestrosa, N.C. J. Neurosci., 1998, 18, 3213-3223.

3) Alzheimer, A. Uber einen eigenartigen schweren Erkrankungsprozeb der Hirnrinde. Neurologisches Centralblatt (Lecture presented at the 37th meeting of the southwest German psychiatrists in Tubingen). 1906, 23, 1129.

4) Ana Castro and Ana Martinez, Peripheral and Dual Binding Site Acetyl cholinesterase Inhibitors: Implications in treatment of Alzheimer's disease, Mini Reviews in Medicinal Chemistry, 2001, 1, 267-272

5) Anctil M., (2009); Chemical transmission in the sea anemone Nematostella vectensis: A genomic perspective; Comparative Biochemistry and Physiology Part D: Genomics and Proteomics; 4(4); 268-289

6) Angela De Iuliis, Jessica Grigoletto, Alessandra Recchia, Pietro Giusti and Paola Arslan, (2005), A proteomic approach in the study of an animal model of Parkinson's disease , Clinica Chimica Acta , Volume 357, Issue 2, 24, 202-209

7) Ariel E. Reyes, Marcelo A. Chacón, Margarita C. Dinamarca, Waldo Cerpa, Carlos Morgan and Nibaldo C. Inestrosa, (2004), Acetylcholinesterase-Aß Complexes Are More Toxic than Aß Fibrils in Rat Hippocampus Effect on Rat ß-Amyloid Aggregation, Laminin Expression, Reactive Astrocytosis, and Neuronal Cell Loss , (American Journal of Pathology. 164:2163-2174.)

8) Ashwani V: Biochemical Adaption of Brain AChE during temperature acclimmation of fish Tilapia massambica Peters. Wilson College, University of Mumbai (1992)

9) Abdrakhmanova Galya, Lars Cleemann, Jon Lindstrom, and Martin Morad, (2004), Differential Modulation of β2 and β4 Subunits of Human Neuronal Nicotinic Acetylcholine Receptors by Acidification Molecular Pharmacology 66: 347-355

10) Amato, A., Ballerini, L. and Attweil, D. (1994) Intracellular pH changes produced by glutamate uptake in rat hippocampus slices. J. Neurophysiology. 72, 1686-1696.

11) Antosdiewicz J. McCammon JA, Gilson MK (1994); Prediction of pH-dependent properties of proteins. J. mol Biol. 238:415-436.

12) Ansell G. B.and Spannesr (1975) The metabolism of choline in regions of rat brain and the effect of hemicholinium- 3. Biochemical. Pharmacology. 24, 1719-1 723

13) Ballivet. M., Alliod, C., Bertrand, S., and Bertrand, D. (1996). Nicotinic ACh receptors in the nematode Caenorhabditis elegans. Journal of Molecular Biology 2 258, 261–269.

14) Bielarczyk H and Szutowicz A., (1989), Evidence for the regulatory function of synaptoplasmic acetyl- CoA in ACh synthesis in nerve endings, Biochemical journal. 262, 377-380

15) Bartolini M., V. Cavrini, V. and Andrisano O., (2005), Batchwise covalent immobilization of human acetylcholinesterase: Kinetic and inhibition spectrophotometric studies. Analytical Biochemistry 342 163–166

16) Birks R. I. (1985), Activation of ACh synthesis in cat sympathetic Ganglia: dependence on external choline and sodium- pump rate. journal of Physiology (367) 401-417

17) Blusztajn JK and Wurtman RJ, (1983), Choline and cholinergic neurons, Science Science.614 - 620 , DOI: 10.1126

18) Boron W.F. and Boulpaep E.L. (2002), Medical Physiology, WB Saunders Eds. SBN:0721632564

19) Boron W.F (2004), Regulation of intracellular pH; Advanced Physiol. Edu. 28 160-179

20) Bussiere, M., Vance, J.E., Campenot, R.B., and Vance, D.E. (2001). Compartmentalization of choline and ACh metabolism in cultured sympathetic neurons. Journal of biochemistry (Tokyo) 130, 561–568.

21) Carl L. Faingold and Gerhard H. Fromm, 1991, Drugs for the Control of Epilepsy: Actions on Neuronal Networks Involved in Seizure Networks, CRC Press.

22) Casoux H. , Blackledge MJ, Rajagopalan B, Taylor DJ, Redda GK (1989): Human primary brain tumor metabolism in vivo- a phosphorous Magnetic resonance spectroscopy study. British journal of cancer 60: 430-436

23) Carmichael F. J, Israel V., Crawford M, Minhas K., Saldivia, Sandrin S., Campisi and Orrego H. (1991), Central Nervous System Effects of Acetate: Contribution to the Central Effects of Ethanol. The Journal of Pharmacology and Experimental Therapeutics, 259(1), 403-408

24) Chay, T.R., Rinzel, J., 1985. Bursting, Beating and chaos in an excitable membrane model. Biophysical Journal 47, 357–366

25) Chiao-Kang, Elizabeth A. Pomfret and Steven Zeisel. ,1988, Uptake of choline by rat mammary-gland epithelial cells. Biochemical Journal 254, 33-38.

26) Chen C.-H., Y.-T. Hsu, C.-C. Chen and R.-C. Huang; (2009); Acid-sensing ion channels in neurons of the rat suprachiasmatic nucleus; J. Physiology.; 587 (8): 1727-1737.

27) Chesler M. (2003) ,Regulation and Modulation of pH in the Brain , Physiological Reviews , 83,1183-1221

28) Claudia Rohl, Ralph Lucius and Jobst Sievers, (2007), The effect of activated microglia on astrogliosis parameters in astrocyte cultures; Brain Research 1129, 43-52

29) Collier B. and Katz H. S. (1974), ACh synthesis from recaptured choline by a sympathetic ganglion, Physiology 238 (3) 639-655

30) Collier B, Ilson D (1977) The effect of preganglionic nerve stimulation on the accumulation of certain analogues of choline by a sympathetic ganglion. Journal of Physiology (London) 264: 489-509

31) Cooper Jack R., (1994), Unsolved Problems in the Cholinergic Nervous System, Journal of Neurochemistry, 63 (2), 395 - 399

32) Damsma G. , D. Lammerts van Bueren, B. H. C. Westerink I , A. S. Horn (1987) , Determination of ACh and choline femtomole range by means of HPLC, a post-column enzyme reactor, and electrochemical detection, Chromatographia. 24, 827-831

33) Dawn Signor Matthies, Paul A. Fleming, Don M. Wilkes, and Randy D. Blakely ,(2006), The Caenorhabditis elegans Choline Transporter CHO-1 Sustains ACh Synthesis and Motor Function in an Activity-Dependent Manner , The Journal of Neuroscience, 2006, 26(23):6200-6212

34) Deitmer W.J. and Rose C.R. (1996), pH regulation and proton signaling by glial cells Progress in Neurobiology, 48(2), 73-103.

35) Denton, J.S., F.V. McCann and J.C. Leiter.(2007), CO_2 chemosensitivity in /Helix aspersa/: Three K^+ currents mediate pH-sensitive neuronal activity. Am. J. Physiology. Cell. 292:C292-C304.

36) Diering G. H, J. Church and M. Numata ; 2009; Secretory Carrier Membrane Protein 2 Regulates Cell-surface Targeting of Brain-enriched Na+/H+ Exchanger NHE5; J. Biol. Chem. 284 (20): 13892-13903.

37) Doedel, E.J.; Champneys, A.R.; Fairgrieve, T.F.; Kuznetsov, Y.A.; Sandstede, B.; Wang, X.J. AUTO97: Continuation and bifurcation software for ordinary differential equations. Department of Computer Science, Concordia University, Montreal, Canada, 1997.

38) Elnashaie, S.S.E.H.; El-Rifai, M.A.; Ibrahim, G.(1983) The effect of hydrogen ion production on the steady-state multiplicity of substrate inhibited enzymatic reactions. I. Steady-state considerations. Applied Biochemistry and Biotechnology 8, 275.

39) Elnashaie, S.S.E.H.; El-Rifai, M.A.; Ibrahim, G. (1983). The effect of hydrogen ion production on the steady-state multiplicity of substrate inhibited enzymatic reactions. II. Transient behavior. Applied Biochemistry and Biotechnology 8, 467.

40) Elnashaie, S.S.E.H.; El-Rifai, M.A.; Ibrahim, G. (1984) The effect of hydrogen ion production on the steady-state multiplicity of substrate inhibited enzymatic reactions. III. Asymmetrical steady-states in enzyme membranes. Applied Biochemistry and Biotechnology 9, 455.

41) Elnashaie, S.S.E.H.; Ibrahim, G.; Teymour, F. A (1995). Chaotic behavior of an acetyl cholinesterase enzyme system. Chaos, Solitons & Fractals 5, 933.

42) Elnashaie S. S.E., Uhlig F., and Affane C.b , 2007, Numerical techniques for chemical and biological engineers using MATLAB: a simple bifurcation approach, Springer., New York.

43) Ermentrout, B. (2002.). Simulating, Analyzing, and Animating Dynamical Systems: A Guide to Xppaut for Researchers and Students; SIAM: New York

44) Eugene P. Brandon, Tiffany Mellott, Donald Pizzo, Nicole Coulfal, Kevin D'Amour, Kevin Gobeske, Mark Lortie , Ignacio lopez- Covielle , Brygide Berse, Leon Thal , Fred Gage, Jan Blusztan, (2004). Choline transporter 1 maintains cholinergic function in choline acetyltransferase haploinsufficiency. The Journal of Neuroscience , 24 (24), 5459-5466

45) Fan, Y.S. and Holden, A.V., (1993).. Bifurcation, bursting, chaos and crisis in the Rose-Hindmarsh model for neuronal activity, Chaos, Solitons & Fractals, 3(4), 439.

46) Feigenbaum, M.L. (1980). Universal behavior in nonlinear systems. Los Alamos Science, 1, 4-36.

47) Friboulet A and D. Thomas, 1985, Electrical excitability of artificial enzyme membranes III. Hysteresis and oscillations observed with immobilized acetylcholinesterase membranes, Biophysical Chemistry, 16(2):153-157.

48) Friboulet, R.; David, A.; Thomas, D. (1981). Excitability memory and oscillation in artificial acetyl cholinesterase membranes. Journal of Membrane Science 8, 33.

49) Friboulet A and D. Thomas, 1982, Electrical excitability of artificial enzyme membranes II. Electrochemical and enzyme properties of immobilized acetylcholinesterase membranes, Biophysical Chemistry 16 145-151

50) Garhyan Parag, Mahecha A Botero; Elnashaie, S.S.E.H.; (2006). Complex Bifurcation/ Chaotic Behavior of Acetyl cholinesterase and cholineacetyltransferase Enzymes system; Mathematical and computer Modeling; 30 824-853

51) Glenn Wetzel and Joan Heller Brown, (1983), Relationship between Choline uptake ACh synthesis and ACh release in isolated rat atria. Journal of pharmacology and Experimental Therapeutics 226(2).

52) Golovanenko A. L. , R. V. Kirillova, T. F. Odegova and G. A. Pavlova; (2006); Standardization of gel for the treatment of deep caries; Pharmaceutical Chemistry Journal; 40 (4); 231-233

53) Gregory J. ,Zoppo, (2009), Relationship of Neurovascular Elements to Neuron Injury during Ischemia; *Cerebrovascular Diseases* 2009; 27 (1):65-76 (DOI: 10.1159/000200442)

54) Guyton, C.A.; Hall, J.E. (2000.). Textbook of Medical Physiology. tenth ed.; W. B. Saunders Company: Amsterdam

55) Hindmarsh, J. L. and Rose, R. M., (1982). A model of the nerve impulse using two first-order differential equations, Nature, 296(5853), 162

56) Hindmarsh, J. L and R. M. Rose, (1984). Model of neuronal bursting using three coupled first order differential equations, Proceedings of the Royal Society of London. Series B, Biological Sciences, 221, (1222) , 87-102.

57) Holden, A.V. and Fan, Y.S., (1992a). From simple to simple bursting oscillatory behavior via chaos in the Rose- Hindmarsh model for neuronal activity. Chaos, Solitons & Fractals, 221–236.

58) Holden, A.V. and Fan, Y.S., From simple to complex oscillatory behavior via intermittent chaos in the Rose-Hindmarsh model for neuronal activity, Chaos, Solitons & Fractals, 2(4), 349–369 (1992b).

59) Holden AV, Fan YS (1992c) Crisis-induced chaos in the Rose-Hindmarsh model for neuronal activity. Chaos, Solitons & Fractals, 2:583–595

60) Il'in V., P. D. Brezhestovskii, and E. A. Vulfius (1976), Effect of pH on Properties of the cholinergic Receptor Membrane of Limnaea Stagnalis Neurons. Translated from Neirofiziologiya, 8(6) 640-644

61) Ibrahim, G; Elnashaie, S.S.E.H. Hyperchaos in acetylcholinesterase enzyme systems. Chaos, Solitons & Fractals.(1997), 8, 1977.

62) Ismail H. Ulus, Richard J. Wurtman , Charlotte Mauron and Jan Krzysztof Blusztajn, (1989), Choline increases acetylcholine release and protects against the stimulation-induced decrease in phosphatide levels within membranes of rat corpus striatum, Brain Research. 484 (1989) 217-227

63) Iwamoto H, Randy D. Blakely, and Louis J. De Felice, (2006) ; Na^+, Cl^-, and pH Dependence of the Human Choline Transporter (hCHT) in Xenopus Oocytes: The Proton Inactivation Hypothesis of hCHT in Synaptic Vesicles ; The Journal of Neuroscience, September 27, , 26(39):9851-9859.

64) Jaak Panksepp (2007), Neuroevolutionary sources of laughter and social joy: Modeling primal human laughter in laboratory rats, Behavioural Brain Research, 182 (2), 231-244

65) Jan K, Blusztajn, Richard J. Wurtman, (1981), Choline biosynthesis by a preparation enriched in synaptosomes from rat brain, Nature 290, 417 - 418 , doi:10.1038/290417a

66) Javier Chavarriga, Isaac A. García and Jordi Sorolla, (2005), Resolution of the Poincaré problem and nonexistence of algebraic limit cycles in family (I) of Chinese classification , Chaos, Solitons & Fractals, 24(2), ,491-499.

67) Joachim W. Deitmer, and Christine R. Rose (1996), pH regulation and proton signaling by glial cells , Progress in Neurobiology, 48(2)73-103

68) Just. W., Kantz, H., (2000), Some considerations on Poincare maps for chaotic flows Journal of Physics A: Mathematical and General 33, 163–170.

69) Kaila K., Bruce R. Ransom (1998); pH and Brain Function; Edition: Published by Wiley-IEEE, 1998 ISBN 0471118389, 9780471118381

70) Karel Sigler and Milan Hofer, 1997, Biotechnological Aspects of Membrane Function, Critical Reviews in Biotechnology, 17(2), 69-86

71) Kewitzh, Pleulo, D Ross K. & Schwartzkopff T. (1975) in Cholinergic Mechanisms (WASER P. G., ed.) pp. 131-135. Raven Press. New York.

72) Kwok Y. N. and, Collier, (1982) Synthesis of acetylcholine from acetate in a sympathetic Ganglion. Neurochemistry (39) 16-26.

73) Kysela, S.; Torok, J. Histamine H_1-receptor antagonists do not prevent the appearance of endothelium-dependant relaxation to acetylcholine in rat pulmonary artery. Physiological Research, 1996, 45(4), 345.

74) Laurie Kelly; (2005), Essentials of Human Physiology for Pharmacy, Crc press
Boca Raton London New York Washington, D.C.

75) Lee H-C, Fellenz-Maloney M-P, Liscovitch M, Blusztajn JK (1993) Phospholipase D-catalyzed hydrolysis of phosphatidylcholine provides the choline precursor for acetylcholine synthesis in a human neuronal cell line. Proceedings of the Natural Academy of Sciences USA 90: 10086-10090

76) Lefresne P., Guyenet P and Glowinski J. (1973), Acetylcholine synthesis from [2^{14}C] pyruvate in rat striatal slices. The Journal of Neurochemistry 20, 1083-1097

77) Lynn Wecker, and Wolf Dettbarn, (1979), Relationship between Choline availability and acetylcholine synthesis in discrete regions of rat brain, The Journal of Neurochemistry (33) 961-967

78) Mahecha Andres - Botero, Parag Garhyan, Elnashaie S. S. E. H., (2004). Bifurcation and chaotic of a coupled acetylcholinesterase/choline acetyltransferase diffusion-reaction enzymes system, Chemical Engineering Science 59,581-597.

79) Mario Carvi Nievas MD, Selim Toktamis MD, Hans-Georg Höllerhage MD and Eberhard Haas MD (2005), Hyperacute measurement of brain-tissue oxygen, carbon dioxide, pH, and

intracranial pressure before, during, and after cerebral angiography in patients with aneurysmatic subarachnoid hemorrhage in poor condition, Surgical Neurology 64(4) 362-367

80) Matthies, D.S., Fleming, P.A., Wilkes, D.M., and Blakely, R.D. (2006). The Caenorhabditis elegans choline transporter CHO-1 sustains acetylcholine synthesis and motor function in an activity-dependent manner. Journal of Neuroscience 26, 6200–6212.

81) Mexel S, M Frank, R Berger, CE Adams, RG Ross, R Freedman and S Leonard (2005) Differential modulation of gene expression in the NMDA postsynaptic density of schizophrenic and control smokers. . Molecular Brain Research 139 (2), 317-332.

82) Michel, Z. Yuan, S. Ramsubir, and M. Bakovic (2006), Choline Transport for Phospholipids Synthesis. Experimental Biology and Medicine, 231(5): 490 - 504 Michel, Z. Yuan, S. Ramsubir, and M. Bakovic (2006), Choline Transport for Phospholipids Synthesis. Experimental Biology and Medicine, 231(5): 490 - 504

83) Morel N.(1976). Effect of choline on the rates of synthesis and of release of acetylcholine in the electric organ of torpedo.; The Journal of Neurochemistry 1976 (27) 779-784.

84) Mullen G. P., E. A. Mathews, M. H. Vu, J. W. Hunter, D. L. Frisby, A. Duke, K. Grundahl, J. D. Osborne, J. A. Crowell, and J. B. Rand, (2007), Choline Transport and de novo Choline Synthesis Support Acetylcholine Biosynthesis in Caenorhabditis elegans Cholinergic Neurons , Genetics; 177(1): 195 - 204.

85) Mustafa[a] I H, G. Ibrahim, A. Elkamel, S.S.E.H. Elnashaie, P. Chen, (2009), Non Linear Feedback Modeling and Bifurcation of the Acetylcholine Neurocycle and its Relation to Alzheimer's and Parkinson's Diseases; Journal of chemical engineering science 64(1), 69-90.

86) Mustafa[b] I H, A. Elkamel, G. Ibrahim, S.S.E.H. Elnashaie, P. Chen, (2009), Effect of Choline and Acetate Substrates on Bifurcation and Chaotic Behavior of Acetylcholine Neurocycle and Alzheimer's and Parkinson's Diseases; Journal of chemical engineering science. 64(9), 2096-2112.

87) Mustafa[c] I H, G. Ibrahim, A. Elkamel, S.S.E.H. Elnashaie, P. Chen, (2009), Effect of Cholineacetyltransferase Activity and Choline Recycle Ratio, submitted to Journal of inter. Process Eng,

88) Obara M., Monika Szeliga and Jan Albrecht, (2008), Regulation of pH in the mammalian central nervous system under normal and pathological conditions: Facts and hypotheses , Neurochemistry International 52 (6) 905-919

89) Paulsen IT, Brown MH and Skurray RA (1996), Proton-dependent multidrug efflux systems, Microbiological Reviews, 60(4), 575-608.

90) Pinthong M, S. A. G. Black, F. M. Ribeiro, C. Pholpramool, S. S. G. Ferguson, and R. J. Rylett, (2008), Activity and subcellular trafficking of the sodium-coupled choline transporter CHT is regulated Acutely by peroxynitrite. molecular pharmacology., 73(3): 801 – 812

91) Rae, C.; Scott, R.; Thompson, C.H.; Dumughn, I.; Kemp, G; Styles, P.; Tracey, I.M.; Radda, G.K. 1996, Is brain pH a biochemical marker of IQ? Proceedings of Biological Sciences. 262, 1061-1064

92) Risto A, Kauooinen and Stephen Williams (1998), Use of NMR Spectroscopy in Mointoring Cerebral pH and Metaboilism During systemic and focal acid-base disturbances, pH and brain Function 605-619

93) Santos, J. Friboulet, A.; Lozano (2006), Modeling of acetylcholinesterase immobilized into artificial membrane; Annual International Conference of the IEEE Engineering in Medicine and Biology - Proceedings, 28th Annual International Conference of the IEEE Engineering in Medicine and Biology Society, EMBS'06, 2006, p 4187-4191

94) Schwartz James, Michael L. Eisentadt, and Howard Cedar, (1975), Metabolism of Acetylcholine in the Nervous system of Aplysia californica 1. Source of choline and its uptake in intact tissue. The Journal of General Physiology (65), 255-273.

95) Shawn M. Ferguson, and Randy D. Blakely, (2004), The choline transporter resurfaces: new roles for synaptic vesicles, Molecular Interventions 4:22-37

96) Schwartz James, Michael Eisenstadt, and Howard Cedar, (1975), Metabolism of ACh in the nervous system of Aplysia californica. The Journal of General Physiology, (65), 255-273.

97) Steven Leventer, Peter Rowell, (1984), Investigation of the rate limiting step in the synthesis of acetylcholine by human placenta. Placenta, 5, 261-270

98) Strogatz S. (1994), Nonlinear dynamics and chaos, second printing,

99) Sungchul Ji (1997), Isomorphism between cell and human languages: molecular biological, bioinformatic and linguistic implications, Biosystems, 44 (1)17-39

100) Sykova E., (2004); Extrasynaptic volume transmission and diffusion parameters of the extracellular space, Neuroscience 129 (4), 861-876

101) Takeshi Fujii, Y. Watanabe, K. Fujimoto and K. Kawashima: Expression of acetylcholine in lymphocytes and modulation of an independent lymphocytic cholinergic activity by immunological stimulation. Biogenic amines 17, 373-386 (2003)

102) Tucek, S., (1978). Acetylcholine Synthesis in Neurons; Champan &hall, London. 1978.

103) Tucek S. (1983), The synthesis of acetylcholine, in Handbook of Neurochemistry, 2nd ed., Vol. 4 (Lajtha A., ed), pp. 219- 249. Plenum Press, New York.

104) Tucek, S. (1985). Regulation of acetylcholine synthesis in the brain. The Journal of Neurochemistry 44:11-24.

105) Tucek S. (1988) Choline acetyltransferase and the synthesis of acetylcholine, in Handbook of Experimental Pharmacology, vol. 86. Springer, Berlin 125-165.

106) Tucek S (1990), The synthesis of acetylcholine: twenty years of progress. Progress in Brain Research 84: 467-477

107) Zheng J., S. Lee, Z. Zhou, (2004), A Developmental Switch in the Excitability and Function of the Starburst Network in the Mammalian Retina, Neuron, 44 (5), 851-864

Chapter 6:

1) Oldendorf, L Braun and E Cornford (1979); pH dependence of blood-brain barrier permeability to lactate and nicotine; Stroke, 10, 577-581.

2) Chuiko G. M., V. A. Podgornaya and Y. Y. Zhelnin (2003); Acetylcholinesterase and butyrylcholinesterase activities in brain and plasma of freshwater teleosts: cross-species and cross-family differences ; Comparative Biochemistry and Physiology Part B: Biochemistry and Molecular Biology; 135 (1), Issue 1, 55-6.

3) llcol Yo, Resul Ozbek, Emre Hamurtekin, Ismail H. Ulus, (2005); Choline status in newborns, infants, children, breast-feeding women, breast-fed infants and human breast milk; The journal of Nutritional biochemistry ; 16 (8), 489-499.

4) Persike, Martina Zimmermann, Jochen Klein and Michael Karas, (2010); Quantitative Determination of Acetylcholine and Choline in Microdialysis Samples by MALDI-TOF MS, *Anal. Chem.*, Article ASAP.

Chapter 7:

1) Ariel E. Reyes, Marcelo A. Chacon, Margarita C. Dinamarca, Waldo Cerpa, Carlos Morgan and Nibaldo C. Inestrosa, (2004), Acetylcholinesterase-Aß Complexes Are More Toxic than Aβ Fibrils in Rat Hippocampus Effect on Rat ß-Amyloid Aggregation, Laminin Expression, Reactive Astrocytosis, and Neuronal Cell Loss, (*American Journal of Pathology.* 164:2163-2174)

2) Birks R. I. (1985), Activation of ACh synthesis in cat sympathetic Ganglia: dependence on external choline and sodium- pump rate. J. Physiol. (367) 401-417.
3) Callahan, L. M., and P. D. Coleman. 1995. Neurons bearing neurofibrillary tangles are responsible for selected synaptic deficits in Alzheimer's disease. Neurobiol. Aging. 16:311-4.
4) Carl L. Faingold and Gerhard H. Fromm, (1991), Drugs for the Control of Epilepsy: Actions on Neuonal Networks Involved in Seizure Networks, CRC Press.
5) Carpenter, J.F., Kendrick, B.S., et al., 1999. Inhibition of stress induced aggregation of protein therapeutics. Methods Enzymol. 309, 236–255.
6) David A Bateman, JoAnne McLaurin, and Avijit Chakrabartty, (2007), Requirement of aggregation propensity of Alzheimer amyloid peptides for neuronal cell surface binding, BMC Neurosci. 8:29.
7) Fadel J., R. Pasumarthi and L.R. Reznikov, (2005), Stimulation of cortical acetylcholine release by orexin A , Neuroscience , 130 (2), 541-547.
8) Garhyan Parag, Mahecha A Botero; Elnashaie, S.S.E.H.; (2006). Complex Bifurcation/ Chaotic Behavior of Acetyl cholinesterase and choline Acetyltransferase Enzymes system; Mathematical and computer Modeling; 30 824-853.
9) Gerald Ehrenstein, Zygmunt Galdzicki, and G. David Lange, 1997, The Choline Leakage Hypothesis for the loss of Acetylcholine in Alzheimer's disease, Biophysical Journal 730: 1276-1280.
10) Gupta, P., Hall, C.K., et al., 1998. Effect of denaturant and protein concentrations upon protein refolding and aggregation: a simple lattice model. Protein Sci. 7, 2642–2652.
11) Hardy, J. A., and G. A. Higgins. 1992. Alzheimer's disease: the amyloid cascade hypothesis. Science. 256:184-185.
12) Jack R. cooper ;(1994), Unsolved problems in the cholinergic Nervous system; Journal of Neurochemistry 395-399.
13) Kacser, H. and Burns, J.A., (1973), The control of flux, in: Rate Control of Biological Processes, D.D. Davies (ed.) (Cambridge University Press, London), 65-104.
14) Kwok Y. N. and, Collier, (1982) Synthesis of acetylcholine from acetate in a sympathetic Ganglion. Neurochemistry (39) 16-26.
15) Laura A. Robertson , Kenneth L. Moya , Kieran C. Breen, (2004), the potential role of tau protein O-glycosylation in Alzheimer's disease, Volume 6, 489 – 495.

16) Laura A. Volpicelli-Daley, Anna Hrabovska, Ellen G. Duysen, Shawn M. Ferguson, Randy D. Blakely, Oksana Lockridge, and Allan I. Levey, (2003), Altered Striatal Function and Muscarinic Cholinergic Receptors in Acetylcholinesterase Knockout Mice, Mol Pharmacol 64:1309-1316.

17) Mahecha Andres - Botero, Parag Garhyan, Elnashaie S. S. E. H., (2004). Bifurcation and chaotic of a coupled acetylcholinesterase/choline acetyltransferase diffusion-reaction enzymes system, Chemical Engineering Science 59,581-597.

18) Sakamoto, Naoto, 1987, A transfer-function representation for regulatory responses of a controlled metabolic pathway. BioSystems 20, 317-327.

19) Sakamoto Naoto; (1990), linear feedback control of acetylcholine level in the presynaptic terminal; Biosystems, 17(7); 2257-2266.

20) Schwartz James, Michael Eisenstadt, and Howard Cedar, (1975), Metabolism of ACh in the nervous system of Aplysia californica. The Journal of General Physiology, (65), 255-273.

21) Wurtman, R. J. 1992, Choline metabolism as a basis for the selective vulnerability of cholinergic neurons. Trends Neurosci. 15:117-122.